

are presented in a general way. Custom-designed modifications of these types can significantly alter the specific duties.

8.3 DESIGN OF A SINGLE-EFFECT EVAPORATOR

In a single-effect evaporator, as shown in Figure 8.11, dilute liquid feed is pumped into the heating chamber, where it is heated indirectly with steam. Steam is introduced into the heat exchanger, where it condenses to give up its heat of vaporization to the feed, and exits the system as condensate.

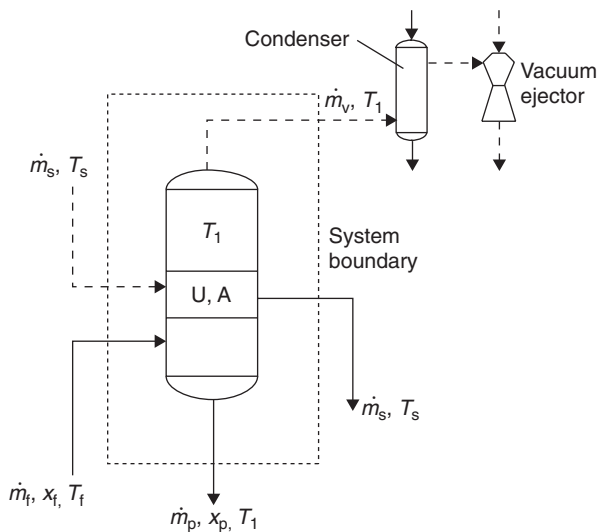
The temperature of evaporation, T_1 , is controlled by maintaining vacuum inside the heating chamber. The vapors leaving the product are conveyed through a condenser to a vacuum system, usually a steam ejector or a vacuum pump. In a batch system, the feed is heated until the desired concentration is obtained. The concentrated product is then pumped out of the evaporator system.

Heat and mass balances conducted on the evaporator system allow determination of various design and operating variables. Such variables may include mass flow rates, final concentration of product, and heat-exchanger area.

The following expressions can be obtained by conducting a mass balance on flow streams and product solids, respectively.

$$\dot{m}_f = \dot{m}_v + \dot{m}_p \quad (8.1)$$

■ **Figure 8.11** Schematic diagram of a single-effect evaporator.



where \dot{m}_f is the mass flow rate of dilute liquid feed (kg/s), \dot{m}_v is the mass flow rate of vapor (kg/s), and \dot{m}_p is the mass flow rate of concentrated product (kg/s),

$$x_f \dot{m}_f = x_p \dot{m}_p \quad (8.2)$$

where x_f is the solid fraction in the feed stream (dimensionless) and x_p is the solid fraction in the product stream (dimensionless).

An enthalpy balance conducted on the evaporator system gives the following expression:

$$\dot{m}_f H_f + \dot{m}_s H_{vs} = \dot{m}_v H_{v1} + \dot{m}_p H_{p1} + \dot{m}_s H_{cs} \quad (8.3)$$

where \dot{m}_s is the mass flow rate of steam (kg/s); H_f is enthalpy of dilute liquid feed (kJ/kg); H_{p1} is enthalpy of concentrated product (kJ/kg); H_{vs} is enthalpy of saturated vapor at temperature T_s (kJ/kg); H_{v1} is enthalpy of saturated vapor at temperature T_1 (kJ/kg); H_{cs} is enthalpy of condensate (kJ/kg); T_s is temperature of steam ($^{\circ}\text{C}$); T_1 is the boiling temperature maintained inside the evaporator chamber ($^{\circ}\text{C}$); and T_f is the temperature of dilute liquid feed ($^{\circ}\text{C}$).

The first term in Equation (8.3), $\dot{m}_f H_f$, represents the total enthalpy associated with the incoming dilute liquid feed, where H_f is a function of T_f and x_f . The enthalpy content H_f can be computed from

$$H_f = c_{pf}(T_f - 0^{\circ}\text{C}) \quad (8.4)$$

The specific heat may be obtained either from Table A.2.1 or by using Equation (4.3) or Equation (4.4).

The second term, $\dot{m}_s H_{vs}$, gives the total heat content of steam. It is assumed that saturated steam is being used. The enthalpy, H_{vs} , is obtained from the steam table (Table A.4.2) as enthalpy of saturated vapors evaluated at the steam temperature T_s .

On the right-hand side of Equation (8.3), the first term, $\dot{m}_v H_{v1}$, represents total enthalpy content of the vapors leaving the system. The enthalpy H_{v1} is obtained from the steam table (Table A.4.2) as the enthalpy of saturated vapors evaluated at temperature T_1 .

The second term, $\dot{m}_p H_{p1}$, is the total enthalpy associated with the concentrated product stream leaving the evaporator. The enthalpy content H_{p1} is obtained using the following equation:

$$H_{p1} = c_{pp}(T_1 - 0^{\circ}\text{C}) \quad (8.5)$$

where c_{pp} is the specific heat content of concentrated product (kJ/[kg $^{\circ}\text{C}$]).

Again, c_{pp} is obtained from Table A.2.1 or by using Equation (4.3) or Equation (4.4).

The last term, $\dot{m}_s H_{cs}$, represents the total enthalpy associated with the condensate leaving the evaporator. Since an indirect type of heat exchanger is used in evaporator systems, the rate of mass flow of incoming steam is the same as the rate of mass flow of condensate leaving the evaporator. The enthalpy H_{cs} is obtained from the steam table (Table A.4.2) as enthalpy of saturated liquid evaluated at temperature T_s . If the condensate leaves at a temperature lower than T_s , then the lower temperature should be used to determine the enthalpy of the saturated liquid.

In addition to the mass and enthalpy balances given previously, the following two equations are also used in computing design and operating variables of an evaporator system.

For the heat exchanger, the following expression gives the rate of heat transfer:

$$q = UA(T_s - T_1) = \dot{m}_s H_{vs} - \dot{m}_s H_{cs} \quad (8.6)$$

where q is the rate of heat transfer (W), U is the overall heat transfer coefficient (W/[m² K]), and A is the area of the heat exchanger (m²).

The overall heat-transfer coefficient decreases as the product becomes concentrated, due to increased resistance of heat transfer on the product side of the heat exchanger. In addition, the boiling point of the product rises as the product becomes concentrated. In Equation (8.6), a constant value of the overall heat-transfer coefficient is used and would result in some “overdesign” of the equipment.

Steam economy is a term often used in expressing the operating performance of an evaporator system. This term is a ratio of rate of mass of water vapor produced from the liquid feed per unit rate of steam consumed.

$$\text{Steam economy} = \dot{m}_v / \dot{m}_s \quad (8.7)$$

A typical value for steam economy of a single-effect evaporator system is close to 1.

Example 8.2

Apple juice is being concentrated in a natural-circulation single-effect evaporator. At steady-state conditions, dilute juice is the feed introduced at a rate of 0.67 kg/s. The concentration of the dilute juice is 11% total solids. The juice

is concentrated to 75% total solids. The specific heats of dilute apple juice and concentrate are 3.9 and 2.3 kJ/(kg °C), respectively. The steam pressure is measured to be 304.42 kPa. The inlet feed temperature is 43.3°C. The product inside the evaporator boils at 62.2°C. The overall heat-transfer coefficient is assumed to be 943 W/(m² °C). Assume negligible boiling-point elevation. Calculate the mass flow rate of concentrated product, steam requirements, steam economy, and the heat-transfer area. The system is sketched in Figure E8.1.

Given

Mass flow rate of feed $\dot{m}_f = 0.67$ kg/s

Concentration of food $x_f = 0.11$

Concentration of product $x_p = 0.75$

Steam pressure = 304.42 kPa

Feed temperature $T_f = 43.3^\circ\text{C}$

Boiling temperature T_1 in evaporator = 62.2°C

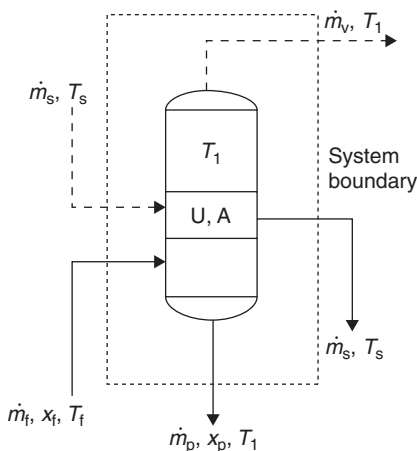
Overall heat transfer coefficient $U = 943$ W/(m² K)

Specific heat of dilute feed $c_{pf} = 3.9$ kJ/(kg °C)

Specific heat of concentrated product $c_{pp} = 2.3$ kJ/(kg °C)

Approach

We will use the heat and mass balances given in Equations (8.1), (8.2), and (8.3) to determine the unknowns. Appropriate values of enthalpy for steam and vapors will be obtained from steam tables.



■ **Figure E8.1** Schematic diagram of a single-effect evaporator.

Solution

1. From Equation (8.2),

$$(0.11)(0.67 \text{ kg/s}) = (0.75)\dot{m}_p$$

$$\dot{m}_p = 0.098 \text{ kg/s}$$

Thus, mass flow rate of concentrated product is 0.098 kg/s.

2. From Equation (8.1),

$$\dot{m}_v = (0.67 \text{ kg/s}) - (0.098 \text{ kg/s})$$

$$\dot{m}_v = 0.57 \text{ kg/s}$$

Thus, mass flow rate of vapors is 0.57 kg/s.

3. To use the enthalpy balance of Equation (8.3), the following quantities are first determined:

From Equation (8.4),

$$H_f = (3.9 \text{ kJ/kg } ^\circ\text{C})(43.3^\circ\text{C} - 0^\circ\text{C}) = 168.9 \text{ kJ/kg}$$

From Equation (8.5),

$$H_{p1} = (2.3 \text{ kJ/kg } ^\circ\text{C})(62.2^\circ\text{C} - 0^\circ\text{C}) = 143.1 \text{ kJ/kg}$$

From the steam table (Table A.4.2),

Temperature of steam at 304.42 kPa = 134°C

Enthalpy for saturated vapor H_{vs} (at $T_s = 134^\circ\text{C}$) = 2725.9 kJ/kg

Enthalpy for saturated liquid H_{cs} (at $T_s = 134^\circ\text{C}$) = 563.41 kJ/kg

Enthalpy for saturated vapor H_{v1} (at $T_1 = 62.2^\circ\text{C}$) = 2613.4 kJ/kg

$$(0.67 \text{ kg/s})(168.9 \text{ kJ/kg}) + (\dot{m}_s \text{ kg/s})(2725.9 \text{ kJ/kg})$$

$$= (0.57 \text{ kg/s})(2613.4 \text{ kJ/kg}) + (0.098 \text{ kg/s})(143.1 \text{ kJ/kg})$$

$$+ (\dot{m}_s \text{ kg/s})(563.41 \text{ kJ/kg})$$

$$2162.49 \dot{m}_s = 1390.5$$

$$\dot{m}_s = 0.64 \text{ kg/s}$$

4. To calculate steam economy, we use Equation (8.7).

$$\text{Steam economy} = \frac{\dot{m}_v}{\dot{m}_s} = \frac{0.57}{0.67} = 0.85 \text{ kg water evaporated/kg steam}$$

5. To compute area of heat transfer, we use Equation (8.6).

$$A(943 \text{ W/m}^2\text{ } ^\circ\text{C})(134^\circ\text{C} - 62.2^\circ\text{C})$$

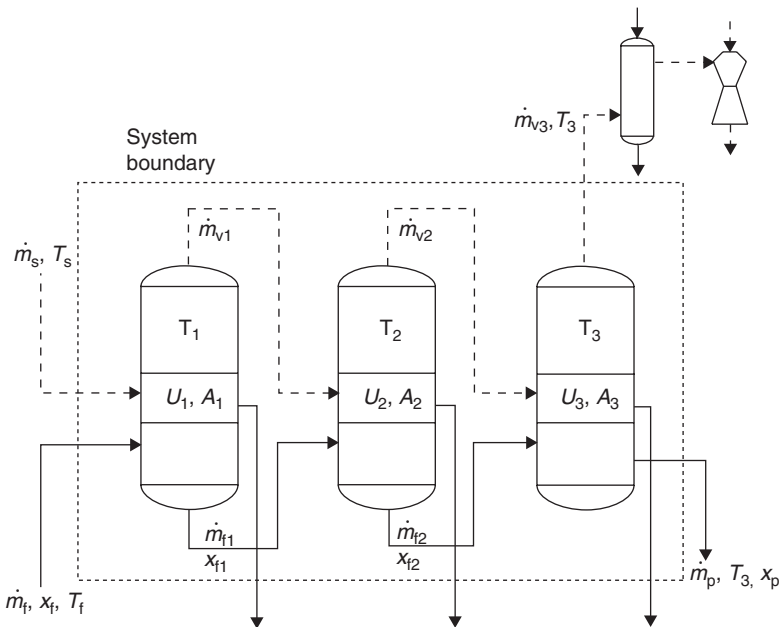
$$= (0.64 \text{ kg/s})(2725.9 - 563.41 \text{ kJ/kg})(1000 \text{ J/kJ})$$

$$A = 20.4 \text{ m}^2$$

8.4 DESIGN OF A MULTIPLE-EFFECT EVAPORATOR

In a triple-effect evaporator, shown in Figure 8.12, dilute liquid feed is pumped into the evaporator chamber of the first effect. Steam enters the heat exchanger and condenses, thus discharging its heat to the product. The condensate is discarded. The vapors produced from the first effect are used as the heating medium in the second effect, where the feed is the partially concentrated product from the first effect. The vapors produced from the second effect are used in the third effect as heating medium, and the final product with the desired final concentration is pumped out of the evaporator chamber of the third effect. The vapors produced in the third effect are conveyed to a condenser and a vacuum system. In the forward feed system shown, partially concentrated product from the first effect is fed to the second effect. After additional concentration, product leaving the second effect is introduced into the third effect. Finally, product with the desired concentration leaves the third effect.

Design expressions for multiple-effect evaporators can be obtained in the same manner as for a single-effect evaporator, discussed in Section 8.3.



■ **Figure 8.12** Schematic diagram of a triple-effect evaporator.

Conducting mass balance analysis on the flow streams,

$$\dot{m}_f = \dot{m}_{v1} + \dot{m}_{v2} + \dot{m}_{v3} + \dot{m}_p \quad (8.8)$$

where \dot{m}_f is the mass flow rate of dilute liquid feed to the first effect (kg/s); \dot{m}_{v1} , \dot{m}_{v2} , and \dot{m}_{v3} are the mass flow rates of vapor from the first, second, and third effect, respectively (kg/s); and \dot{m}_p is the mass flow rate of concentrated product from the third effect (kg/s).

Using mass balance on the solids fraction in the flow streams,

$$x_f \dot{m} = x_p \dot{m}_p \quad (8.9)$$

where x_f is the solid fraction in the feed stream to be consistent with the first effect (dimensionless) and x_p is the solid fraction in the product stream from the third effect (dimensionless).

We write enthalpy balances around each effect separately.

$$\dot{m}_f H_f + \dot{m}_s H_{vs} = \dot{m}_{v1} H_{v1} + \dot{m}_{f1} H_{f1} + \dot{m}_s H_{cs} \quad (8.10)$$

$$\dot{m}_{f1} H_{f1} + \dot{m}_{v1} H_{v1} = \dot{m}_{v2} H_{v2} + \dot{m}_{f2} H_{f2} + \dot{m}_{v1} H_{c1} \quad (8.11)$$

$$\dot{m}_{f2} H_{f2} + \dot{m}_{v2} H_{v2} = \dot{m}_{v3} H_{v3} + \dot{m}_p H_{p3} + \dot{m}_{v2} H_{c2} \quad (8.12)$$

where the subscripts 1, 2, and 3 refer to the first, second, and third effect, respectively. The other symbols are the same as defined previously for a single-effect evaporator.

The heat transfer across heat exchangers of various effects can be expressed by the following three expressions:

$$q_1 = U_1 A_1 (T_s - T_1) = \dot{m}_s H_{vs} - \dot{m}_s H_{cs} \quad (8.13)$$

$$q_2 = U_2 A_2 (T_1 - T_2) = \dot{m}_{v1} H_{v1} - \dot{m}_{v1} H_{c1} \quad (8.14)$$

$$q_3 = U_3 A_3 (T_2 - T_3) = \dot{m}_{v2} H_{v2} - \dot{m}_{v2} H_{c2} \quad (8.15)$$

The steam economy for a triple-effect evaporator as shown in Figure 8.12 is given by

$$\text{Steam economy} = \frac{\dot{m}_{v1} + \dot{m}_{v2} + \dot{m}_{v3}}{\dot{m}_s} \quad (8.16)$$

Example 8.3 illustrates the use of these expressions in evaluating the performance of multiple-effect evaporators.

Calculate the steam requirements of a double-effect forward-feed evaporator (Fig. E8.2) to concentrate a liquid food from 11% total solids to 50% total solids concentrate. The feed rate is 10,000 kg/h at 20°C. The boiling of liquid inside the second effect takes place under vacuum at 70°C. The steam is being supplied to the first effect at 198.5 kPa. The condensate from the first effect is discarded at 95°C and from the second effect at 70°C. The overall heat-transfer coefficient in the first effect is 1000 W/(m² °C); in the second effect it is 800 W/(m² °C). The specific heats of the liquid food are 3.8, 3.0, and 2.5 kJ/(kg °C) at initial, intermediate, and final concentrations. Assume the areas and temperature gradients are equal in each effect.

Example 8.3

Given

Mass flow rate of feed $\dot{m}_f = 10,000 \text{ kg/h} = 2.78 \text{ kg/s}$

Concentration of feed $x_f = 0.11$

Concentration of product $x_p = 0.5$

Steam pressure = 198.5 kPa

Feed temperature = 20°C

Boiling temperature T_2 in second effect = 70°C

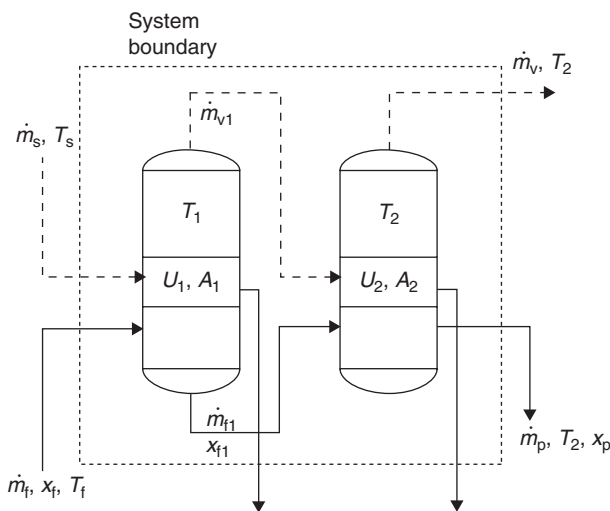
Overall heat-transfer coefficient U_1 in first effect = 1000 W/(m² °C)

Overall heat-transfer coefficient U_2 in second effect = 800 W/(m² °C)

Specific heat of dilute feed $c_{pf} = 3.8 \text{ kJ/(kg °C)}$

Specific heat of feed at intermediate concentration $c'_{pf} = 3.0 \text{ kJ/(kg °C)}$

Specific heat of concentrated food product $c_{pp} = 2.5 \text{ kJ/(kg °C)}$



■ **Figure E8.2** Schematic diagram of a double-effect evaporator.

Approach

Since this is a double-effect evaporator, we will use modified forms of Equations (8.8), (8.9), (8.10), (8.11), (8.13), and (8.14). Enthalpy values of steam and vapors will be obtained from steam tables.

Solution

1. From Equation (8.9),

$$(0.11)(2.78 \text{ kg/s}) = (0.75)\dot{m}_p$$

$$\dot{m}_p = 0.61 \text{ kg/s}$$

2. From Equation (8.8),

$$2.78 = \dot{m}_{v1} + \dot{m}_{v2} + 0.61$$

Thus, the total amount of water evaporating is

$$\dot{m}_{v1} + \dot{m}_{v2} = 2.17 \text{ kg/s}$$

3. Steam is being supplied at 198.5 kPa or 120°C, the temperature in the second effect is 70°C, and thus the total temperature gradient is 50°C.

$$\Delta T_1 + \Delta T_2 = 50^\circ\text{C}$$

Assuming equal temperature gradient in each evaporator effect,

$$\Delta T_1 = \Delta T_2 = 25^\circ\text{C}$$

4. The area of heat transfer in the first and second effects are the same. Thus, from Equations (8.13) and (8.14),

$$\frac{q_1}{U_1(T_s - T_1)} = \frac{q_2}{U_2(T_1 - T_2)}$$

or

$$\frac{\dot{m}_s H_{vs} - \dot{m}_s H_{cs}}{U_1(T_s - T_1)} = \frac{\dot{m}_{v1} H_{v1} - \dot{m}_{v1} H_{c1}}{U_2(T_1 - T_2)}$$

5. To use Equations (8.10) and (8.11), we need values for enthalpy of product.

$$H_f = c_{pf}(T_f - 0) = (3.8 \text{ kJ/kg}^\circ\text{C})(20^\circ\text{C} - 0^\circ\text{C}) = 76 \text{ kJ/kg}$$

$$H_{f1} = c'_{pf}(T_1 - 0) = (3.0 \text{ kJ/kg}^\circ\text{C})(95^\circ\text{C} - 0^\circ\text{C}) = 285 \text{ kJ/kg}$$

$$H_{f2} = c_{pp}(T_2 - 0) = (2.5 \text{ kJ/kg}^\circ\text{C})(70^\circ\text{C} - 0^\circ\text{C}) = 175 \text{ kJ/kg}$$

In addition, from steam tables,

$$\begin{aligned} \text{At } T_s = 120^\circ\text{C} \quad & H_{vs} = 2706.3 \text{ kJ/kg} \\ & H_{cs} = 503.71 \text{ kJ/kg} \\ \text{At } T_1 = 95^\circ\text{C} \quad & H_{v1} = 2668.1 \text{ kJ/kg} \\ & H_{c1} = 397.96 \text{ kJ/kg} \\ \text{At } T_2 = 70^\circ\text{C} \quad & H_{v2} = 2626.8 \text{ kJ/kg} \\ & H_{c2} = 292.98 \text{ kJ/kg} \end{aligned}$$

6. Thus, substituting enthalpy values from step (5) in the equation given in step (4),

$$\begin{aligned} & \frac{[(\dot{m}_s \text{ kg/s})(2706.3 \text{ kJ/kg}) - (\dot{m}_s \text{ kg/s})(503.71 \text{ kJ/kg})](1000 \text{ J/kJ})}{(1000 \text{ W/[m}^2\text{C]})(120^\circ\text{C} - 95^\circ\text{C})} \\ &= \frac{[(\dot{m}_{v1} \text{ kg/s})(2668.1 \text{ kJ/kg}) - (\dot{m}_{v1} \text{ kg/s})(397.96 \text{ kJ/kg})](1000 \text{ J/kJ})}{(800 \text{ W/[m}^2\text{C]})(95^\circ\text{C} - 70^\circ\text{C})} \end{aligned}$$

or

$$\frac{2205.59\dot{m}_s}{25,000} = \frac{2270.14\dot{m}_{v1}}{20,000}$$

7. Using Equations (8.10) and (8.11),

$$\begin{aligned} & (2.78)(76) + (\dot{m}_s)(2706.3) \\ &= (\dot{m}_{v1})(2668.1) + (\dot{m}_{f1})(285) + (\dot{m}_s)(503.71) \\ & (\dot{m}_{f1})(285) + (\dot{m}_{v1})(2668.1) \\ &= (\dot{m}_{v2})(2626.8) + (\dot{m}_p)(175) + (\dot{m}_{v1})(397.96) \end{aligned}$$

8. Let us assemble all equations representing mass flow rates of product, feed, vapor, and steam.

From step (1): $\dot{m}_p = 0.61$

From step (2): $\dot{m}_{v1} + \dot{m}_{v2} = 2.17$

From step (6): $0.088\dot{m}_s = 0.114\dot{m}_{v1}$

From step (7):

$$\begin{aligned} 2202.59\dot{m}_s &= 2668.1\dot{m}_{v1} + 285\dot{m}_{f1} - 211.28 \\ 2270.14\dot{m}_{v1} &= 2626.8\dot{m}_{v2} + 175\dot{m}_p - 285\dot{m}_{f1} \end{aligned}$$

9. In step (8), we have five equations with five unknowns, namely, \dot{m}_p , \dot{m}_{v1} , \dot{m}_{v2} , \dot{m}_s , and \dot{m}_{f1} . We will solve these equations using a spreadsheet procedure to solve simultaneous equations. The method described in the following was executed on Excel™.
10. The simultaneous equations are rewritten so that all unknown variables are collected on the right-hand side. The equations are rewritten so that the

■ **Figure E8.3** A spreadsheet to solve simultaneous equations.

	A	B	C	D	E	F	G	H
1								
2		1.000	0.000	0.000	0.000	0.000		0.61
3		0.000	0.000	1.000	1.000	0.000		2.17
4		0.000	0.088	-0.114	0.000	0.000		0
5		0.000	2202.590	-2668.100	0.000	-285.000		-211.28
6		-175.000	0.000	2270.140	-2626.800	285.000		0
7		=+MINVERSE(B2:F6)					=+MMULT(B9:F13,H2:H6)	
8								
9		1.000	0.000	0.000	0.000	0.000		0.61
10		0.045	0.670	4.984	0.000	0.000		1.43
11		0.034	0.517	-4.925	0.000	0.000		1.10
12		-0.034	0.483	4.925	0.000	0.000		1.07
13		0.022	0.336	84.621	-0.003	0.000		1.46
14								

coefficients can easily be arranged in a matrix. The spreadsheet method will use a matrix inversion process to solve the simultaneous equations.

$$\dot{m}_p + 0\dot{m}_s + 0\dot{m}_{v1} + 0\dot{m}_{v2} + 0\dot{m}_{f1} = 0.61$$

$$0\dot{m}_p + 0\dot{m}_s + \dot{m}_{v1} + \dot{m}_{v2} + 0\dot{m}_{f1} = 2.17$$

$$0\dot{m}_p + 0.088\dot{m}_s - 0.114\dot{m}_{v1} + 0\dot{m}_{v2} + 0\dot{m}_{f1} = 0$$

$$0\dot{m}_p + 2202.59\dot{m}_s - 2668.1\dot{m}_{v1} + 0\dot{m}_{v2} - 285\dot{m}_{f1} = -211.28$$

$$-175\dot{m}_p + 0\dot{m}_s + 2270.14\dot{m}_{v1} - 2626.8\dot{m}_{v2} + 285\dot{m}_{f1} = 0$$

11. As shown in Figure E8.3, enter the coefficients of the left-hand side of the preceding equations in array B2:F6; enter the right-hand side coefficients in a column vector H2:H6.
12. Select another array B9:F13 (by dragging the cursor starting from cell B9). Type + MINVERSE(B2:F6) in cell B9 and press the CTRL, SHIFT, and ENTER keys simultaneously. This procedure will invert the matrix B2:F6 and give the coefficients of the inverted matrix in array B9:F13.
13. Highlight cells H9:H13 by dragging the cursor starting from cell H9. Type + MMULT(B9:F13,H2:H6) into cell H9; press the CTRL, SHIFT, and ENTER keys simultaneously. The answers are displayed in the column vector H9:H13. Thus,

$$\dot{m}_p = 0.61 \text{ kg/s}$$

$$\dot{m}_s = 1.43 \text{ kg/s}$$

$$\dot{m}_{v1} = 1.10 \text{ kg/s}$$

$$\dot{m}_{v2} = 1.07 \text{ kg/s}$$

$$\dot{m}_{f1} = 1.46 \text{ kg/s}$$

14. The steam requirements are computed to be 1.43 kg/s.
15. The steam economy can be computed as

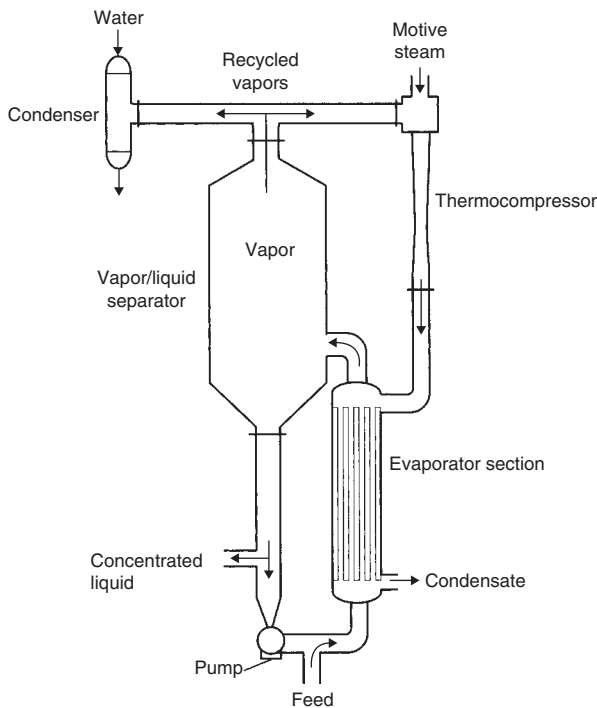
$$\frac{\dot{m}_{v1} + \dot{m}_{v2}}{\dot{m}_s} = \frac{1.10 + 1.07}{1.43} = 1.5 \text{ kg water vapor/kg steam}$$

8.5 VAPOR RECOMPRESSION SYSTEMS

The preceding discussion on multiple-effect evaporators has shown how energy requirements of the total system are decreased by using exit vapors as the heating medium in subsequent effects. Two additional systems that employ vapor recompression assist in reduction of energy requirements. These systems are thermal recompression and mechanical vapor recompression. A brief introduction to these two systems follows.

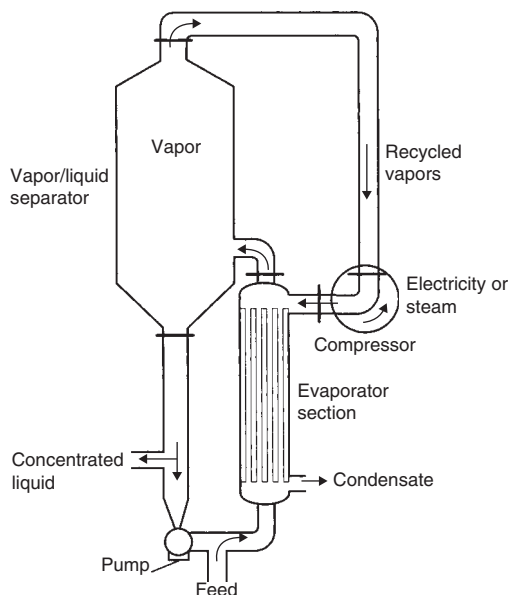
8.5.1 Thermal Recompression

Thermal recompression involves the use of a steam jet booster to recompress part of the exit vapors, as shown in Figure 8.13. Through recompression, the pressure and temperature of exit vapors are increased. These systems are usually applied to single-effect evaporators or to the first effect of multiple-effect evaporators. Application of this system requires that steam be available at high pressure, and low-pressure steam is needed for the evaporation process.



■ **Figure 8.13** Schematic diagram of a thermal recompression system.

■ **Figure 8.14** Schematic diagram of a mechanical vapor recompression system.



8.5.2 Mechanical Vapor Recompression

Mechanical vapor recompression involves compression of all vapors leaving the evaporator, as shown in Figure 8.14. Vapor compression is accomplished mechanically, using a compressor driven by an electric motor, a steam turbine, or a gas engine. A steam-turbine-driven compressor is most suitable for mechanical recompression if high-pressure steam is available. Availability of electricity at low cost would favor the use of an electric motor.

Mechanical vapor recompression systems are very effective in reducing energy demands. Under optimum conditions, these systems can lower the energy requirements by an amount equivalent to adding 15 effects. These systems can be very noisy to operate due to the use of large compressors.

Mathematical procedures useful in designing vapor recompression systems are beyond the scope of this text. Students could consult Heldman and Singh (1981) for more information on these procedures.

PROBLEMS

- 8.1** A fruit juice at 20°C with 5% total solids is being concentrated in a single-effect evaporator. The evaporator is being operated at a sufficient vacuum to allow the product moisture to

evaporate at 80°C , and steam with 85% quality is being supplied at 169.06 kPa. The desired concentration of the final product is 40% total solids. The concentrated product exits the evaporator at a rate of 3000 kg/h. Calculate the (a) steam requirements and (b) steam economy for the process, when condensate is released at 90°C . The specific heat of liquid feed is $4.05\text{ kJ}/(\text{kg}^{\circ}\text{C})$, and of concentrated product is $3.175\text{ kJ}/(\text{kg}^{\circ}\text{C})$.

8.2 A single-effect evaporator is being used to concentrate 10,000 kg/h of tomato juice from 5% total solids to 30% total solids. The juice enters the evaporator at 15°C . The evaporator is operated with steam (80% quality) at 143.27 kPa. The vacuum inside the evaporator allows the juice to boil at 75°C . Calculate (a) the steam requirements and (b) steam economy for the process. Assume the condensate is discharged at 75°C . The specific heat of the liquid feed is $4.1\text{ kJ}/(\text{kg}^{\circ}\text{C})$ and the concentrated product is $3.1\text{ kJ}/(\text{kg}^{\circ}\text{C})$.¹

***8.3** A four-effect evaporator is being considered for concentrating a fruit juice that has no appreciable boiling-point elevation. Steam is available at 143.27 kPa, and the boiling point of the product in the fourth effect is 45°C . The overall heat-transfer coefficients are $3000\text{ W}/(\text{m}^2^{\circ}\text{C})$ in the first effect, $2500\text{ W}/(\text{m}^2^{\circ}\text{C})$ in the second effect, $2100\text{ W}/(\text{m}^2^{\circ}\text{C})$ in the third effect, and $1800\text{ W}/(\text{m}^2^{\circ}\text{C})$ in the fourth effect. Calculate the boiling-point temperatures of the product in the first, second, and third effects. Assume the heating areas in all the effects are equal to 50 m^2 each. The mass flow rate of steam to the first effect is 2400 kg/h, the feed rate to the first effect of 5% total solids fluid is 15,000 kg/h, the concentrated product from the first effect leaves at 6.25% total solids, and the concentration of product leaving the second effect is 8.82% total solids.

***8.4** A double-effect evaporator is being used to concentrate fruit juice at 25,000 kg/h. The juice is 10% total solid at 80°C . The juice must be concentrated to 50% total solids. Saturated steam at 1.668 atm is available. The condensing temperature of the vapor in the second effect is 40°C . The overall heat-transfer coefficient in the first effect is $1000\text{ W}/(\text{m}^2^{\circ}\text{C})$, and in the second effect it is $800\text{ W}/(\text{m}^2^{\circ}\text{C})$. Calculate the steam

*Indicates an advanced level of difficulty.

economy and area required in each effect, assuming the areas are equal in each effect. (Hint: Assume $(\Delta T)_2 = 1.3 \times (\Delta T)_1$.)

- *8.5** A double-effect evaporator is being used to concentrate a liquid food from 5 to 35% total solids. The concentrated product leaves the second effect at a rate of 1000 kg/h. The juice enters the first effect at 60°C. Saturated steam at 169.06 kPa is available. Assume the areas in each effect are equal and the evaporation temperature inside the second effect is 40°C. The overall heat-transfer coefficient inside the first effect is 850 W/(m² °C) and inside the second effect is 600 W/(m² °C). Calculate the steam economy and the area required in each effect. (Hint: Assume $(\Delta T)_{1st\ effect} = (\Delta T)_{2nd\ effect}$ and do at least one iteration.)
- *8.6** Solve Problem 8.5 using MATLAB®. For a tutorial on using MATLAB® see www.rpaulsingh.com.
- *8.7** A single effect evaporator is being used to concentrate tomato paste. The outlet concentration, x_1 , is controlled by regulating the product flow out, \dot{m}_p , and the feed flow in, \dot{m}_f , is used to maintain the level of the product in the evaporator. Measurements show that:

$$\begin{array}{lll} T_s = 130\text{ C} & T_1 = 48\text{ C} & T_f = 25\text{ C} \\ x_f = 0.05 & x_1 = 0.30 & A = 28\text{ m}^2 \\ U = 1705\text{ W/(m}^2\text{ C)} \end{array}$$

- Using MATLAB® calculate the feed rate, \dot{m}_f , steam consumption, \dot{m}_s , and the steam economy.
 - If the concentration of the feed is increased to $x_f = 0.10$ by a preprocessing step, calculate the new values for \dot{m}_f , \dot{m}_s and steam economy. Assume no boiling point elevation and steady state. Use the Irvine and Liley (1984) equations to obtain steam properties and the ASHRAE model to calculate the enthalpy of the juice.
- 8.8** The overall heat transfer coefficient in a single effect tomato paste evaporator is related to product temperature and concentration by the empirical equation:

$$U = (4.086 \cdot T_1 + 72.6)/x_1 \quad (\text{W/m}^2\text{ °C})$$

*Indicates an advanced level of difficulty.

Given the following information:

$$\begin{aligned} \dot{m}_f &= 2.58 \text{ kg/s} & x_f &= 0.05 & T_f &= 71.1^\circ\text{C} \\ A &= 46.5 \text{ m}^2 & T_1 &= 93.3^\circ\text{C} & T_s &= 126.7^\circ\text{C} \end{aligned}$$

Find \dot{m}_p , \dot{m}_v , \dot{m}_s , x_1 and the economy using MATLAB® function called *fsolve* nonlinear equation solver. Assume steady state, and there is no boiling point elevation. Use the Irvine and Liley (1984) equations to obtain steam properties and the ASHRAE model to calculate the enthalpy of the juice.

LIST OF SYMBOLS

A	area of heat exchanger (m^2)
c_{pf}	specific heat content of dilute liquid feed ($\text{kJ}/[\text{kg } ^\circ\text{C}]$)
c_{pp}	specific heat content of concentrated product ($\text{kJ}/[\text{kg } ^\circ\text{C}]$)
ΔT	temperature gradient inside an evaporator; temperature of steam—temperature of boiling liquid inside the evaporator chamber ($^\circ\text{C}$)
H_{cs}	enthalpy of condensate at temperature T_s (kJ/kg)
H_f	enthalpy of liquid feed (kJ/kg)
H_p	enthalpy of concentrated product (kJ/kg)
H_{v1}	enthalpy of saturated vapor at temperature T_1 (kJ/kg)
H_{vs}	enthalpy of saturated vapor at temperature T_s (kJ/kg)
\dot{m}_f	mass flow rate of dilute liquid feed (kg/s)
\dot{m}_p	mass flow rate of concentrated product (kg/s)
\dot{m}_s	mass flow rate of steam or condensate (kg/s)
\dot{m}_v	mass flow rate of vapor (kg/s)
q	rate of heat transfer (W)
T_1	boiling temperature maintained inside the evaporator chamber ($^\circ\text{C}$)
T_f	temperature of dilute liquid feed ($^\circ\text{C}$)
T_s	temperature of steam ($^\circ\text{C}$)
T	temperature ($^\circ\text{C}$)
U	overall heat transfer coefficient ($\text{W}/[\text{m}^2 \text{ K}]$)
x_f	solid fraction in feed stream, dimensionless
x_p	solid fraction in product stream, dimensionless

■ BIBLIOGRAPHY

American Society of Heating, Refrigerating and Air Conditioning Engineers, Inc (2005). *2005 ASHRAE Handbook of Fundamentals*. ASHRAE, Atlanta, Georgia.

- Anonymous (1977). *Upgrading Existing Evaporators to Reduce Energy Consumption*. Technical Information Center, Department of Energy, Oak Ridge, Tennessee.
- Blakebrough, N. (1968). *Biochemical and Biological Engineering Science*. Academic Press, New York.
- Charm, S. E. (1978). *The Fundamentals of Food Engineering*, 3rd ed. AVI Publ. Co, Westport, Connecticut.
- Coulson, J. M. and Richardson, J. F. (1978). *Chemical Engineering*, 3rd ed., Vol. II. Pergamon Press, New York.
- Geankoplis, C. J. (2003). *Transport Processes and Separation Process Principles*, 4th ed. Pearson Education Inc, New Jersey.
- Heldman, D. R. and Singh, R. P. (1981). *Food Process Engineering*, 2nd ed. AVI Publ. Co, Westport, Connecticut.
- Irvine, T. F. and Liley, P. E. (1984). *Steam and Gas Tables with Computer Equations*, Appendix I, 23. Academic Press, Inc, Orlando.
- Kern, D. W. (1950). *Process Heat Transfer*. McGraw-Hill, New York.
- McCabe, W. L., Smith, J. C., and Harriott, P. (1985). *Unit Operations of Chemical Engineering*, 4th ed. McGraw-Hill, New York.

Psychrometrics

The subject of psychrometrics involves determination of thermodynamic properties of gas–vapor mixtures. The most common applications are associated with the air–water vapor system.

An understanding of the procedures used in computations involving psychrometric properties is useful in design and analysis of various food processing and storage systems. Knowledge of properties of air–water vapor mixture is imperative in design of systems such as air-conditioning equipment for storage of fresh produce, dryers for drying cereal grains, and cooling towers in food processing plants.

In this chapter, important thermodynamic properties used in psychrometric computations are defined. Psychrometric charts useful in determining such properties are presented. In addition, procedures to evaluate certain air-conditioning processes are discussed.

9.1 PROPERTIES OF DRY AIR

9.1.1 Composition of Air

Air is a mixture of several constituent gases. The composition of air varies slightly, depending on the geographical location and altitude. For scientific purposes, the commonly accepted composition is referred to as standard air. The composition of standard air is given in Table 9.1.

The apparent molecular weight of standard dry air is 28.9645. The gas constant for dry air, R_a , is computed as

$$\frac{8314.41}{28.9645} = 287.055 \text{ (m}^3 \text{ Pa)/(kg K)}$$

All icons in this chapter refer to the author's web site, which is independently owned and operated. Academic Press is not responsible for the content or operation of the author's web site. Please direct your web site comments and questions to the author: Professor R. Paul Singh, Department of Biological and Agricultural Engineering, University of California, Davis, CA 95616, USA. Email: rps@rpaulsingh.com

Table 9.1 Composition of Standard Air

Constituent	Percentage by volume
Nitrogen	78.084000
Oxygen	20.947600
Argon	0.934000
Carbon dioxide	0.031400
Neon	0.001818
Helium	0.000524
Other gases (traces of methane, sulfur dioxide, hydrogen, krypton, and xenon)	0.000658
	100.000000

9.1.2 Specific Volume of Dry Air

Ideal gas laws can be used to determine the specific volume of dry air. Therefore,

$$V'_a = \frac{R_a T_a}{p_a} \quad (9.1)$$

where V'_a is the specific volume of dry air (m^3/kg); T_a is the absolute temperature (K); p_a is partial pressure of dry air (kPa); and R_a is the gas constant ($[\text{m}^3 \text{ Pa}]/[\text{kg K}]$).

9.1.3 Specific Heat of Dry Air

At 1 atm (101.325 kPa), the specific heat of dry air c_{pa} in a temperature range of -40 to 60°C varying from 0.997 to 1.022 kJ/(kg K) can be used. For most calculations, an average value of 1.005 kJ/(kg K) may be used.

9.1.4 Enthalpy of Dry Air

Enthalpy, the heat content of dry air, is a relative term and requires selection of a reference point. In psychrometric calculations the reference pressure is selected as the atmospheric pressure and the reference temperature is 0°C . Use of atmospheric pressure as the reference allows the use of the following equation to determine the specific enthalpy:

$$H_a = 1.005(T_a - T_0) \quad (9.2)$$

where H_a is enthalpy of dry air (kJ/kg); T_a is the dry bulb temperature ($^{\circ}\text{C}$); and T_0 is the reference temperature, usually selected as 0°C .

9.1.5 Dry Bulb Temperature

Dry bulb temperature is the temperature indicated by an unmodified temperature sensor. This is in contrast to the wet bulb temperature (described in Section 9.3.8) where the sensor is kept covered with a layer of water. Whenever the term temperature is used without any prefix in this book, dry bulb temperature is implied.

9.2 PROPERTIES OF WATER VAPOR

In Section 9.1, constituents of standard dry air were given. However, atmospheric air always contains some moisture. Moist air is a binary mixture of dry air and vapor. The vapor in the air is essentially superheated steam at low partial pressure and temperature. Air containing superheated vapor is clear; however, under certain conditions the air may contain suspended water droplets leading to the condition commonly referred to as “foggy.”

The molecular weight of water is 18.01534. The gas constant for water vapor can be determined as

$$R_w = \frac{8314.41}{18.01534} = 461.52 \text{ (m}^3 \text{ Pa)/(kg mol K)}$$

9.2.1 Specific Volume of Water Vapor

Below temperatures of 66°C , the saturated or superheated vapor follows ideal gas laws. Thus, the characteristic state equation can be used to determine its properties.

$$V'_w = \frac{R_w T_A}{p_w} \quad (9.3)$$

where p_w is the partial pressure of water vapor (kPa), V'_w is the specific volume of water vapor (m^3/kg), R_w is the gas constant for water vapor ($[\text{m}^3 \text{ Pa}/[\text{kg K}]]$), and T_A is the absolute temperature (K).

9.2.2 Specific Heat of Water Vapor

Experiments indicate that within a temperature range of -71 to 124°C , the specific heat of both saturated and superheated vapor changes only slightly. For convenience, a specific-heat value of $1.88 \text{ kJ}/(\text{kg K})$ can be selected.

9.2.3 Enthalpy of Water Vapor

The following expression can be used to determine the enthalpy of water vapor:

$$H_w = 2501.4 + 1.88(T_a - T_0) \quad (9.4)$$

where H_w is enthalpy of saturated or superheated water vapor (kJ/kg); T_a is the dry bulk temperature (°C); and T_0 is the reference temperature (°C).

9.3 PROPERTIES OF AIR–VAPOR MIXTURES

Similar to gas molecules, the water molecules present in an air–vapor mixture exert pressure on the surroundings. Air–vapor mixtures do not exactly follow the perfect gas laws, but for total pressures up to about 3 atm these laws can be used with sufficient accuracy.

9.3.1 Gibbs–Dalton Law

In atmospheric air–steam mixtures, the Gibbs–Dalton law is followed closely. Thus, the total pressure exerted by a mixture of perfect gases is the same as that exerted by the constituent gases independently. Atmospheric air exists at a total pressure equal to the barometric pressure. From the Gibbs–Dalton law,

$$p_B = p_a + p_w \quad (9.5)$$

where p_B is the barometric or total pressure of moist air (kPa), p_a is the partial pressure exerted by dry air (kPa), and p_w is the partial pressure exerted by water vapor (kPa).

9.3.2 Dew-Point Temperature

Water vapors present in the air can be considered steam at low pressure. The water vapor in the air will be saturated when air is at a temperature equal to the saturation temperature corresponding to the partial pressure exerted by the water vapor. This temperature of air is called the dew-point temperature. The dew-point temperature can be obtained from the steam table; for example, if the partial pressure of water vapor is 2.064 kPa, then the dew-point temperature can be directly obtained as the corresponding saturation temperature, 18°C.

A conceptual description of the dew-point temperature is as follows. When an air–vapor mixture is cooled at constant pressure and constant humidity ratio, a temperature is reached when the mixture

becomes saturated. Further lowering of temperature results in condensation of moisture. The temperature at which this condensation process begins is called the dew-point temperature.

9.3.3 Humidity Ratio (or Moisture Content)

The humidity ratio W (sometimes called moisture content or specific humidity) is defined as the mass of water vapor per unit mass of dry air. The common unit for the humidity ratio is kg water/kg dry air. Thus,

$$W = \frac{m_w}{m_a} \quad (9.6)$$

or

$$W = \left(\frac{18.01534}{28.9645} \right) \frac{x_w}{x_a} = 0.622 \frac{x_w}{x_a} \quad (9.7)$$

where x_w is the mole fraction for water vapor and x_a is the mole fraction for dry air.

The mole fractions x_w and x_a can be expressed in terms of partial pressure as follows. From the perfect gas equations for dry air, water vapor, and mixture, respectively,

$$p_a V = n_a RT \quad (9.8)$$

$$p_w V = n_w RT \quad (9.9)$$

$$pV = nRT \quad (9.10)$$

Equation (9.10) can be written as

$$(p_a + p_w)V = (n_a + n_w)RT \quad (9.11)$$

Dividing Equation (9.8) by Equation (9.11),

$$\frac{p_a}{p_a + p_w} = \frac{n_a}{n_a + n_w} = x_a \quad (9.12)$$

and, dividing Equation (9.9) by Equation (9.11),

$$\frac{p_w}{p_a + p_w} = \frac{n_w}{n_a + n_w} = x_w \quad (9.13)$$

Thus, from Equations (9.7), (9.12), and (9.13),

$$W = 0.622 \frac{p_w}{p_a}$$

Since $p_a = p_B - p_w$,

$$W = 0.622 \frac{p_w}{p_B - p_w} \quad (9.14)$$

9.3.4 Relative Humidity

Relative humidity ϕ is the ratio of mole fraction of water vapor in a given moist air sample to the mole fraction in an air sample saturated at the same temperature and pressure. Thus,

$$\phi = \frac{x_w}{x_{ws}} \times 100 \quad (9.15)$$

From Equation (9.13),

$$\phi = \frac{p_w}{p_{ws}} \times 100$$

where p_{ws} is the saturation pressure of water vapor.

For conditions where the perfect gas laws hold, the relative humidity can also be expressed as a ratio of the density of water vapor in the air to the density of saturated water vapor at the dry bulb temperature of air. Thus,

$$\phi = \frac{\rho_w}{\rho_s} \times 100 \quad (9.16)$$

where ρ_w is the density of water vapor in the air (kg/m^3) and ρ_s is the density of saturated water vapor at the dry bulb temperature of air (kg/m^3). As the name suggests, relative humidity is not a measure of the absolute amount of moisture in the air. Instead, it provides a measure of the amount of moisture in the air relative to the maximum amount of moisture in air saturated at the dry bulb temperature. Since the maximum amount of moisture in the air increases as the temperature increases, it is important to express the temperature of the air whenever relative humidity is expressed.

9.3.5 Humid Heat of an Air–Water Vapor Mixture

The humid heat c_s is defined as the amount of heat (kJ) required to raise the temperature of 1 kg dry air plus the water vapor present by 1 K. Since the specific heat of dry air is $1.005 \text{ kJ}/(\text{kg dry air K})$ and $1.88 \text{ kJ}/(\text{kg water K})$ for water vapor, humid heat of the air–vapor mixture is given by

$$c_s = 1.005 + 1.88 W \quad (9.17)$$

where c_s is the humid heat of moist air ($\text{kJ}/[\text{kg dry air K}]$) and W is the humidity ratio ($\text{kg water}/\text{kg dry air}$).

9.3.6 Specific Volume

The volume of 1 kg dry air plus the water vapor in the air is called specific volume. The commonly used units are cubic meter per kilogram (m^3/kg) of dry air.

$$V'_m = \left(\frac{22.4 \text{ m}^3}{1 \text{ kg mol}} \right) \left(\frac{1 \text{ kg mol air}}{29 \text{ kg air}} \right) \left(\frac{T_a + 273}{0 + 273} \right) + \left(\frac{22.4 \text{ m}^3}{1 \text{ kg mol}} \right) \left(\frac{1 \text{ kg mol water}}{18 \text{ kg water}} \right) \left(\frac{T_a + 273}{0 + 273} \right) \frac{W \text{ kg water}}{\text{kg air}} \quad (9.18)$$

$$V'_m = (0.082T_a + 22.4) \left(\frac{1}{29} + \frac{W}{18} \right) \quad (9.19)$$

Calculate the specific volume of air at 92°C and a humidity ratio of 0.01 kg water/kg dry air.

Example 9.1

Given

Dry bulb temperature = 92°C

Humidity ratio = 0.01 kg water/kg dry air

Solution

Using Equation (9.19),

$$\begin{aligned} V'_m &= (0.082 \times 92 + 22.4) \left(\frac{1}{29} + \frac{0.01}{18} \right) \\ &= 1.049 \text{ m}^3/\text{kg dry air} \end{aligned}$$

9.3.7 Adiabatic Saturation of Air

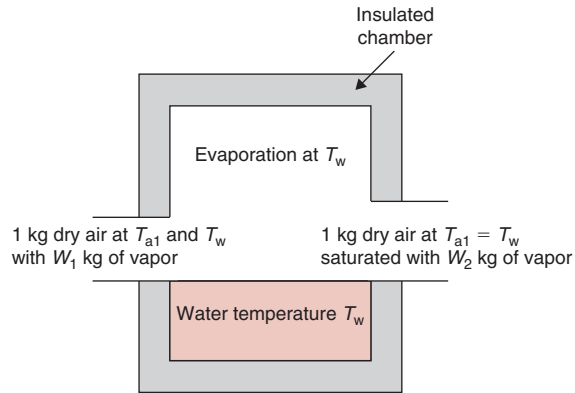
The phenomenon of adiabatic saturation of air is applicable to the convective drying of food materials.

The adiabatic saturation process can be visualized by the following experiment. In a well-insulated chamber as shown in Figure 9.1, air is allowed to contact a large surface area of water. The insulated chamber assures no gain or loss of heat to the surroundings (adiabatic conditions). In this process, part of the sensible heat of entering air is transformed into latent heat.

For the conditions just described, the process of evaporating water into the air results in saturation by converting part of the sensible heat of the entering air into latent heat and is defined as adiabatic saturation.



■ **Figure 9.1** Adiabatic saturation of air in an insulated chamber. (From Jennings, 1970. Copyright © 1970 by Harper and Row, Publishers. Reprinted with permission of the publisher.)



The equation for adiabatic saturation is

$$T_{a1} = H_L \frac{(W_2 - W_1)}{(1.005 + 1.88W_1)} + T_{a2} \quad (9.20)$$

Equation (9.20) can be written as

$$\frac{W_2 - W_1}{T_{a1} - T_{a2}} = \frac{\bar{c}_s}{H_L} \quad (9.21)$$

where $\bar{c}_s = 1.005 + 1.88(W_1 + W_2)/2$.

Example 9.2

Air at 60°C dry bulb temperature and 27.5°C wet bulb temperature, and a humidity ratio of 0.01 kg water/kg dry air is mixed with water adiabatically and is cooled and humidified to a humidity ratio of 0.02 kg water/kg dry air. What is the final temperature of the conditioned air?

Given

Inlet: dry bulb temperature = 60°C

wet bulb temperature = 27.5°C

Initial humidity ratio $W_1 = 0.01$ kg water/kg dry air

Final humidity ratio $W_2 = 0.02$ kg water/kg dry air

Solution

1. From Table A.4.2, latent heat of vaporization at 27.5°C = 2436.37 kJ/kg
2. Using Equation (9.20),

$$\begin{aligned} T_{\text{exit}} &= 60 - \frac{2436.37(0.02 - 0.01)}{[1.005 + (1.88)(0.015)]} \\ &= 36.4^\circ\text{C} \end{aligned}$$

9.3.8 Wet Bulb Temperature

In describing air–vapor mixtures, two wet bulb temperatures are commonly used: the psychrometric wet bulb temperature and the thermodynamic wet bulb temperature. For moist air, the numerical values of these two temperatures are approximately the same. However, in other gas–vapor systems, the difference between the two temperatures can be substantial.

The psychrometric wet bulb temperature is obtained when the bulb of a mercury thermometer is covered with a wet wick and exposed to unsaturated air flowing past the bulb at high velocity (about 5 m/s). Alternatively, the bulb covered with a wet wick can be moved through unsaturated air. When the wick is exposed to unsaturated air, moisture evaporates due to the vapor pressure of saturated wet wick being higher than that of the unsaturated air.

The evaporation process requires latent heat from the wick and causes the temperature of the covered bulb to decrease. As the temperature of the wick decreases below the dry bulb temperature of air, the sensible heat flows from the air to the wick and tends to raise its temperature. A steady state is achieved when the heat flow from air to wick is equal to the latent heat of vaporization required to evaporate the moisture from the wick. This equilibrium temperature indicated by a wet bulb thermometer or similarly modified temperature sensor is called the wet bulb temperature.

As mentioned previously, the movement of air past the wet wick is essential, otherwise the wick will attain an equilibrium temperature between T_a and T_w .

In contrast to the psychrometric wet bulb temperature, the thermodynamic wet bulb temperature is reached by moist air when it is adiabatically saturated by the evaporating water. The thermodynamic wet bulb temperature is nearly equal to the psychrometric wet bulb temperature for moist air.

A mathematical equation that relates partial pressures and temperatures of air–vapor mixtures, developed by Carrier, has been used widely in calculations to determine psychrometric properties. The equation is

$$p_w = p_{wb} - \frac{(p_B - p_{wb})(T_a - T_w)}{1555.56 - 0.722T_w} \quad (9.22)$$

where p_w is the partial pressure of water vapor at dew-point temperature (kPa); p_B is the barometric pressure (kPa); p_{wb} is the saturation pressure of water vapor at the wet bulb temperature (kPa); T_a is the dry bulb temperature ($^{\circ}\text{C}$); and T_w is the wet bulb temperature ($^{\circ}\text{C}$).

Example 9.3

Find the dew-point temperature, humidity ratio, humid volume, and relative humidity of air having a dry bulb temperature of 40°C and a wet bulb temperature of 30°C .

Given

Dry bulb temperature = 40°C

Wet bulb temperature = 30°C

Solution

1. From Table A.4.2,

Vapor pressure at 40°C = 7.384 kPa

Vapor pressure at 30°C = 4.246 kPa

2. From Equation (9.22),

$$\begin{aligned} p_w &= 4.246 - \frac{(101.325 - 4.246)(40 - 30)}{1555.56 - (0.722 \times 30)} \\ &= 3.613 \text{ kPa} \end{aligned}$$

From Table A.4.2, the corresponding temperature for 3.613 kPa vapor pressure is 27.2°C . Thus, the dew-point temperature = 27.2°C .

3. Humidity ratio, from Equation (9.14),

$$W = \frac{(0.622)(3.613)}{(101.325 - 3.613)} = 0.023 \text{ kg water/kg dry air}$$

4. Humid volume, from Equation (9.19),

$$\begin{aligned} V'_m &= (0.082 \times 40 + 22.4) \left(\frac{1}{29} + \frac{0.023}{18} \right) \\ &= 0.918 \text{ m}^3/\text{kg dry air} \end{aligned}$$

5. Relative humidity: Based on Equation (9.15), the relative humidity is the ratio of the partial pressure of water vapor in the air (3.613 kPa) to the vapor pressure at dry bulb temperature (7.384 kPa), or

$$\phi = \frac{3.613}{7.384} \times 100 = 48.9\%$$

Develop a spreadsheet that can be used to determine psychrometric properties such as dew-point temperature, humidity ratio, humid volume, and relative humidity for air with a dry bulb temperature of 35°C and a wet bulb temperature of 25°C.

Example 9.4

Given

Dry bulb temperature = 35°C

Wet bulb temperature = 25°C

Solution

1. The spreadsheet is developed using Excel™. To determine, under saturation conditions, temperature when pressure is known or pressure when temperature is known, empirical expressions developed for a steam table by Martin (1961) and Steltz et al. (1958) are used. The equations used for this spreadsheet are valid between 10° and 93°C, and 0.029 and 65.26 kPa.
2. The spreadsheet formulas and results are shown in Figure E9.1. The procedure for calculation of psychrometric properties is the same as that used in Example 9.3.

	A	B	C	D	E
1	Dry bulb temperature	35	C	7.46908269	-7.50675994E-03
2	Wet bulb temperature	25	C	-4.6203229E-09	-1.215470111E-03
3	x1	-610.398			
4	x2	-628.398			35.15789
5	vapor pressure (at dbt)	5.622	kPa		24.592588
6	vapor pressure (at wbt)	3.167	kPa		2.1182069
7	pw (SI units)	2.529	kPa		-0.3414474
8	pw (English units)	0.367	psia		0.15741642
9	pw_inter	1.299			-0.031329585
10	Dew-point temperature	21.27	C		0.003865828
11	Humidity ratio	0.016	kg water/kg dry air		-2.49018E-05
12	Specific volume	0.904	m³/kg dry air		6.8401559E-06
13	Relative humidity	44.98	%		
14					
15	B3	= (B1*1.8+32)-705.398			
16					
17	B4	= (B2*1.8+32)-705.398			
18					
19	B5	= 6.895*EXP(8.0728362+(B3*(D1+E1*B3+D2*B3^3)/((1+E2*B3)*((B1*1.8+32)+459.688))))			
20					
21	B6	= 6.895*EXP(8.0728362+(B4*(D1+E1*B4+D2*B4^3)/((1+E2*B4)*((B2*1.8+32)+459.688))))			
22					
23	B7	= B6-(((101.325-B6)*(B1-B2)/(1555.56-(0.722*B2))))			
24	B8	= B7/6.895			
25					
26	B9	= LN(10*B8)			
27					
28	B10	= ((E4+E5*B9+E6*(B9)^2+E7*(B9)^3+E8*(B9)^4+E9*(B9)^5+E10*(B9)^6+E11*(B9)^7+E12*(B9)^8)-32)/1.8			
29					
30	B11	= 0.622*B7/(101.325-B7)			
31					
32	B12	= (0.082*B1+22.4)*(1/29+0.023/18)			
33					
34	B13	= B7/B5*100			
35					
36					

■ **Figure E9.1** Calculation of the psychrometric properties for Example 9.4.

Steps:
 1) Enter equations for cells B3 to B13 as shown
 2) Enter coefficients in cells D1, D2, E1, E2, E4 to E12 as shown above. These coefficients are from Martin (1961)
 3) Enter temperature values in cells B1 and B2, results are calculated in B10 to B13

3. Enter empirical coefficients in cells D1:E2 and E4:E12; these coefficients are obtained from Martin (1961) and Steltz et al. (1958).
4. Enter mathematical expressions for calculating various psychrometric properties in cells B3:B13.
5. Enter 35 in cell B1 and 25 in cell B2. The results are calculated in the spreadsheet.

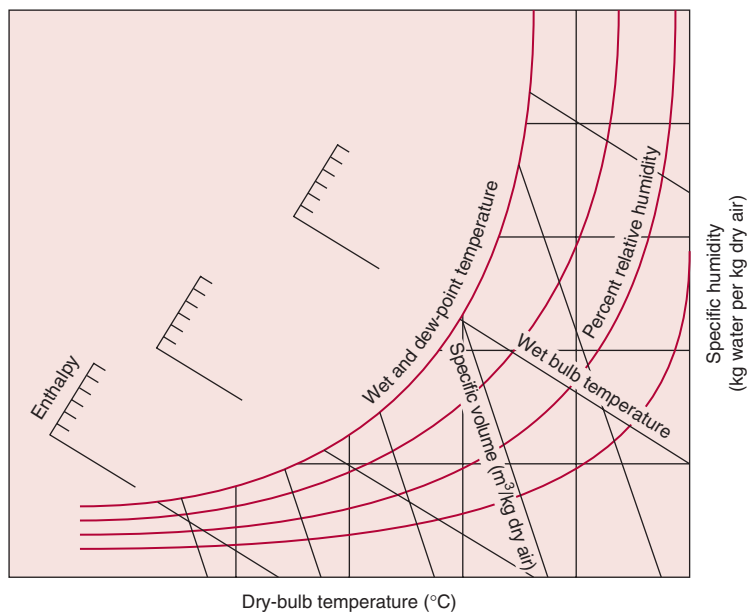
9.4 THE PSYCHROMETRIC CHART

9.4.1 Construction of the Chart

From the preceding sections, it should be clear that the various properties of air–vapor mixtures are interrelated, and such properties can be computed using appropriate mathematical expressions. Another method to determine such properties is the use of a psychrometric chart drawn for a given barometric pressure. If two independent property values are known, the chart allows rapid determination of all psychrometric properties.

The construction of a psychrometric chart can be understood from Figure 9.2. The basic coordinates of the chart are dry bulb temperature plotted as the abscissa and humidity ratio (or specific humidity) as the ordinate. The wet bulb and dew-point temperatures are plotted

■ **Figure 9.2** A skeleton psychrometric chart.



on the curve that swings upward to the right. The constant wet bulb temperature lines drawn obliquely are shown on Figure 9.2. The constant enthalpy lines coincide with the wet bulb temperature lines. The relative humidity curves also swing upward to the right. Note that the saturation curve represents 100% relative humidity. The constant specific volume lines are drawn obliquely; however, they have a different slope than the wet bulb temperature lines.

The psychrometric chart with all the thermodynamic data is shown in Appendix A.5. To use this chart, any two independent psychrometric properties are required. This allows location of a point on the psychrometric chart. The remaining property values can then be read from the chart. As an example, in Figure E9.2, a point A is located for known dry bulb and wet bulb temperatures. The various property values such as relative humidity, humidity ratio, specific volume, and enthalpy can then be read from the chart. It may be necessary to interpolate a property value, depending on the location of the point.

It should be noted that the psychrometric chart given in Appendix A.5 is for a barometric pressure of 101.325 kPa. All example problems discussed in this book assume a barometric pressure of 101.325 kPa. For other pressure values, charts drawn specifically for those pressures would be required.

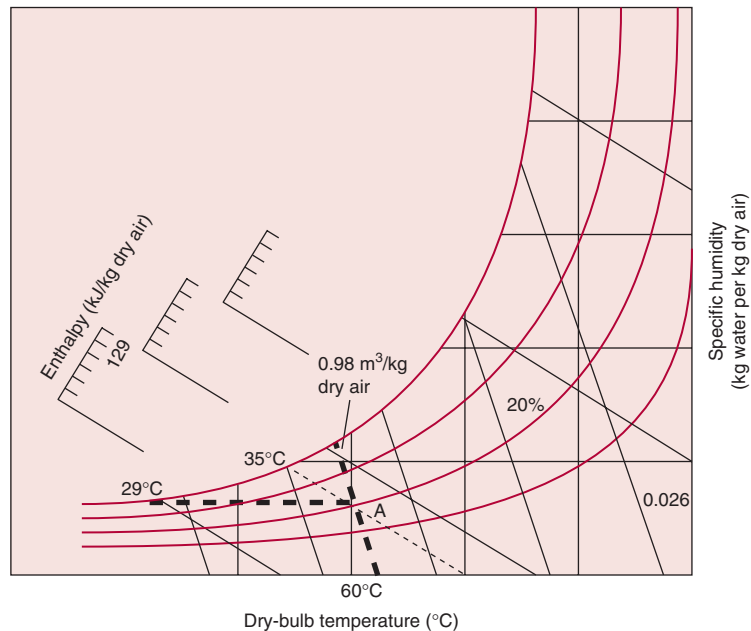
An air–vapor mixture is at 60°C dry bulb temperature and 35°C wet bulb temperature. Using the psychrometric chart (Appendix A.5), determine the relative humidity, humidity ratio, specific volume, enthalpy, and dew-point temperature.

Example 9.5

Solution

1. From the two given independent property values, identify a point on the psychrometric chart. As shown in the skeleton chart (Fig. E9.2), the following steps illustrate the procedure.
2. Location of point A: Move up on the 60°C dry bulb line until it intersects with the 35°C wet bulb temperature line.
3. Relative humidity: Read the relative humidity curve passing through A; $\phi = 20\%$.
4. Specific humidity: Move horizontally to the right of the ordinate to read $W = 0.026$ kg water/kg dry air.
5. Enthalpy: Move left on the oblique line for constant enthalpy (same as constant wet bulb temperature) to read $H_w = 129$ kJ/kg dry air.
6. Specific volume: By interpolation between specific volume lines, read $V'_m = 0.98$ m³/kg dry air.

■ **Figure E9.2** A psychrometric chart with conditions of air given in Example 9.5.



7. Dew-point temperature: Move horizontally to the left to intersect the 100% relative humidity (saturation curve). The temperature at the intersection is the dew-point temperature, or 29°C.

9.4.2 Use of Psychrometric Chart to Evaluate Complex Air-Conditioning Processes

Several air-conditioning processes can be evaluated using the psychrometric chart. Usually, it is possible to describe an entire process by locating certain points as well as drawing lines on the chart that describe the psychrometric changes occurring during the given process. The value of such analysis is in relatively quick estimation of information useful in the design of equipment used in several food storage and processing plants, including air-conditioning, heating, drying, evaporative cooling, and humidification, as well as dehumidification of air. The following are some processes with important applications to food processing.

9.4.2.1 Heating (or Cooling) of Air

Heating (or cooling) of air is accomplished without addition or removal of moisture. Thus, the humidity ratio remains constant. Consequently, a straight horizontal line on the psychrometric chart exhibits a heating (or cooling) process.

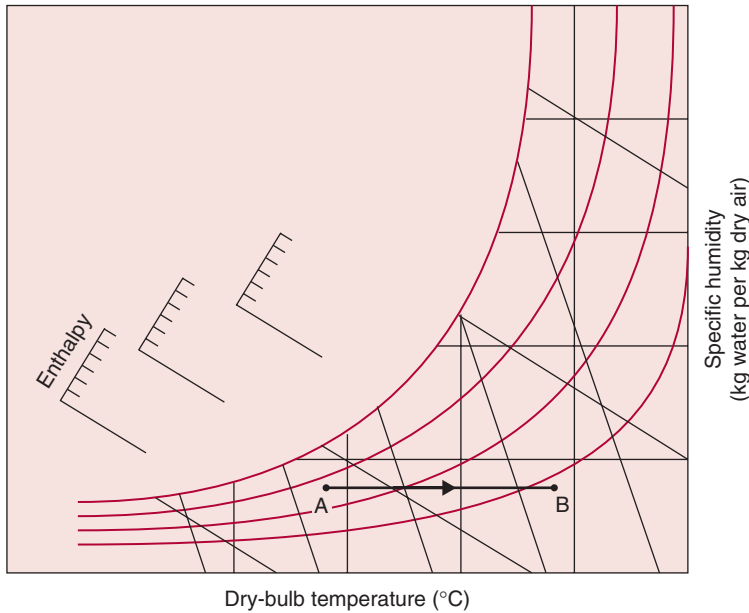


Figure 9.3 A heating process A–B shown on a psychrometric chart.

As shown in Figure 9.3, the process identified by line AB indicates a heating/cooling process. It should be obvious that if the air–vapor mixture is heated, the dry bulb temperature would increase; thus the process conditions will change from A to B. Conversely, the cooling process will change from B to A.

To calculate the amount of thermal energy necessary to heat moist air from state A to state B, the following equation can be used:

$$q = \dot{m}(H_B - H_A) \quad (9.23)$$

where H_B and H_A are enthalpy values read from the chart.

Calculate the rate of thermal energy required to heat $10 \text{ m}^3/\text{s}$ of outside air at 30°C dry bulb temperature and 80% relative humidity to a dry bulb temperature of 80°C .

Example 9.6

Solution

1. Using the psychrometric chart, we find at 30°C dry bulb temperature and 80% relative humidity, the enthalpy $H_1 = 85.2 \text{ kJ/kg dry air}$, humidity ratio $W_1 = 0.0215 \text{ kg water/kg dry air}$, and specific volume $V'_1 = 0.89 \text{ m}^3/\text{kg dry air}$. At the end of the heating process, the dry bulb temperature is 80°C with a humidity ratio of $0.0215 \text{ kg water/kg dry air}$. The remaining values are read

from the chart as follows: enthalpy $H_2 = 140 \text{ kJ/kg dry air}$; relative humidity $\phi_2 = 7\%$.

2. Using Equation (9.23),

$$\begin{aligned} q &= \frac{10}{0.89} (140 - 85.2) \\ &= 615.7 \text{ kJ/s} \\ &= 615.7 \text{ kW} \end{aligned}$$

3. The rate of heat required to accomplish the given process is 615.7 kW

4. In these calculations, it is assumed that during the heating process there is no gain of moisture. This will not be true if a directly fired gas or oil combustion system is used, since in such processes small amounts of water are produced as part of the combustion reaction (see Section 3.2.2).

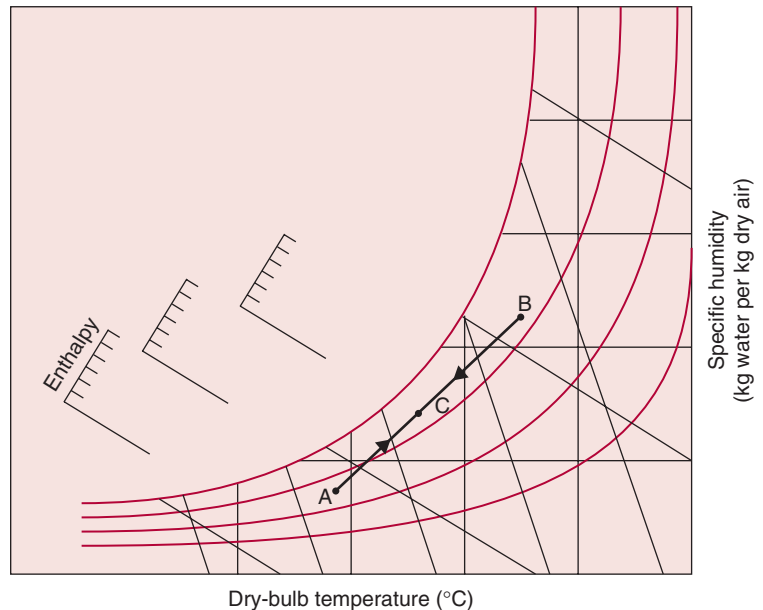
9.4.2.2 Mixing of Air

It is often necessary to mix two streams of air of different psychrometric properties. Again, the psychrometric chart can easily be used to determine the state of the mixed air.

The procedure involves first locating the conditions of the two air masses on the chart, as shown in Figure 9.4, points A and B. Next, the two points are joined with a straight line. This straight line is then



Figure 9.4 Mixing of air in equal parts shown on a psychrometric chart.



divided in inverse proportion to the weights of the individual air quantities. If the two air quantities are equal in weight, the air mixture will be denoted by point C (midpoint of line AB), as shown in Figure 9.4.

In efforts to conserve energy, a food dryer is being modified to reuse part of the exhaust air along with ambient air. The exhaust airflow of $10 \text{ m}^3/\text{s}$ at 70°C and 30% relative humidity is mixed with $20 \text{ m}^3/\text{s}$ of ambient air at 30°C and 60% relative humidity. Using the psychrometric chart (Appendix A.5), determine the dry bulb temperature and humidity ratio of the mixed air.

Example 9.7

Solution

1. From the given data, locate the state points A and B, identifying the exit and ambient air as shown on the skeleton chart (Fig. E9.3).
2. Join points A and B with a straight line.
3. The division of line AB is done according to the relative influence of the particular air mass. Since the mixed air contains 2 parts ambient air and 1 part exhaust air, line AB is divided in 1:2 proportion to locate point C. Thus, the shorter length of line AC corresponds to larger air mass.
4. The mixed air, represented by point C, will have a dry bulb temperature of 44°C and a humidity ratio of $0.032 \text{ kg water/kg dry air}$.

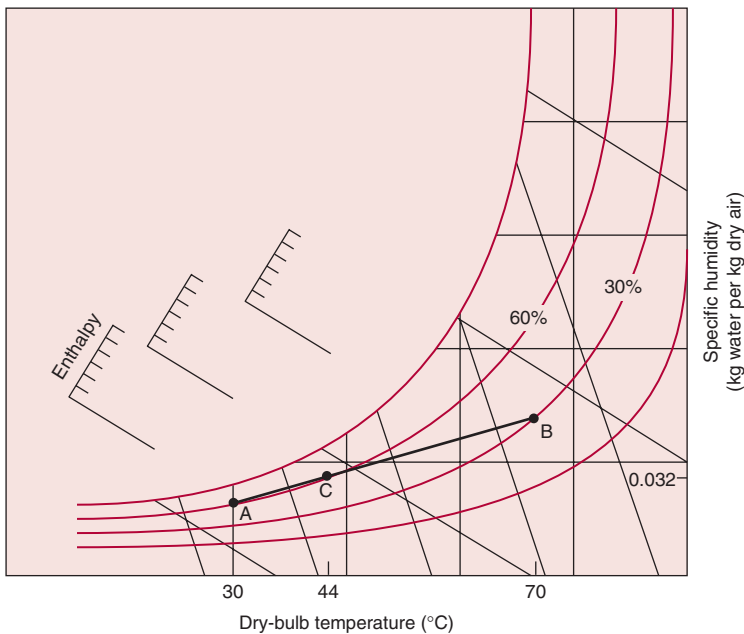
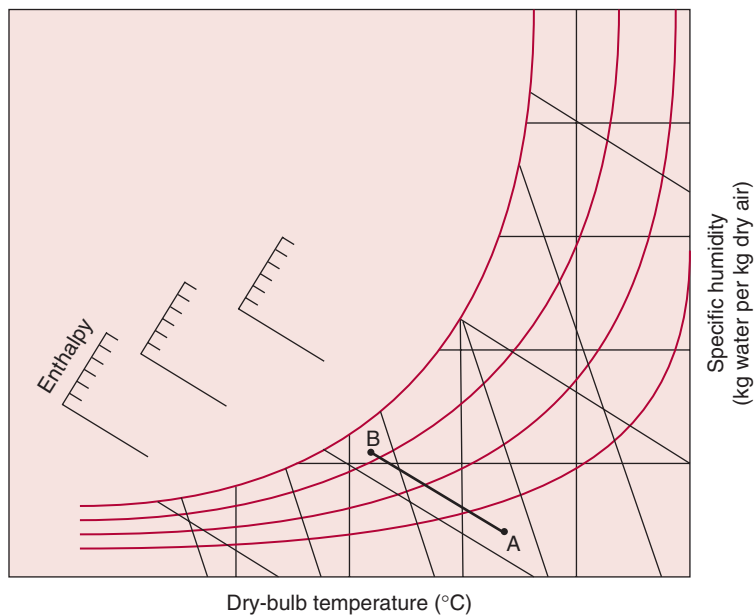


Figure E9.3 Mixing of air in unequal parts for data given in Example 9.7.



Figure 9.5 Drying (or adiabatic saturation) process shown on a psychrometric chart.



9.4.2.3 Drying

When heated air is forced through a bed of moist granular food, the drying process can be described on the psychrometric chart as an adiabatic saturation process. The heat of evaporation required to dry the product is supplied only by the drying air; no transfer of heat occurs due to conduction or radiation from the surroundings. As air passes through the granular mass, a major part of the sensible heat of air is converted to latent heat, as more water is held in the air in vapor state.

As shown in Figure 9.5, during the adiabatic saturation process the dry bulb temperature decreases and the enthalpy remains constant, which also implies a practically constant wet bulb temperature. As air gains moisture from the product, the humidity ratio increases.

Example 9.8

Heated air at 50°C and 10% relative humidity is used to dry rice in a bin dryer. The air exits the bin under saturated conditions. Determine the amount of water removed per kg of dry air.

Solution

1. Locate point A on the psychrometric chart, as shown in Figure E9.4. Read humidity ratio = 0.0078 kg water/kg dry air.
2. Follow the constant enthalpy line to the saturation curve, point B.

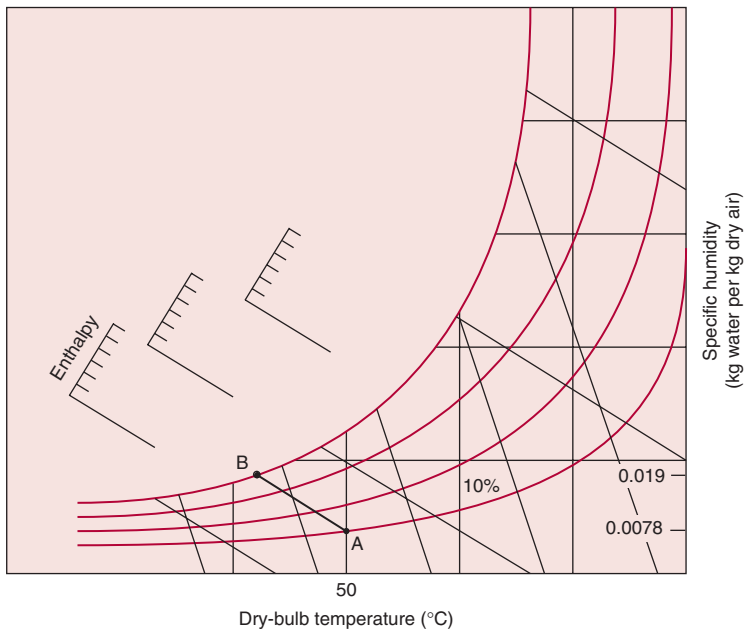


Figure E9.4 Drying process for conditions given in Example 9.8.

3. At point B, read the humidity ratio = 0.019 kg water/kg dry air.
4. The amount of moisture removed from rice = $0.019 - 0.0078 = 0.0112$ kg water/kg dry air.

PROBLEMS

- 9.1 The barometer for atmospheric air reads 750 mm Hg; the dry bulb temperature is 30°C; wet bulb temperature is 20°C. Determine:
 - a. The relative humidity.
 - b. The humidity ratio.
 - c. The dew-point temperature.
- 9.2 The humidity ratio of moist air at atmospheric pressure and at 27°C is 0.015 kg water/kg dry air. Determine
 - a. The partial pressure of water vapor.
 - b. The relative humidity.
 - c. The dew-point temperature.
- 9.3 Calculate (a) specific volume, (b) enthalpy, and (c) humidity ratio for moist air at 21°C and relative humidity of 30%, at a barometric pressure of 755 mm Hg.

- *9.4** Atmospheric air at 750 mm Hg has an 11°C wet bulb depression from 36°C dry bulb temperature, during an adiabatic saturation process. Determine:
- Humidity ratio from adiabatic saturation equation.
 - Vapor pressure and relative humidity at 36°C.
 - Dew-point temperature.
- 9.5** Atmospheric air at 760 mm Hg is at 22°C dry bulb temperature and 20°C wet bulb temperature. Using the psychrometric chart, determine:
- Relative humidity.
 - Humidity ratio.
 - Dew-point temperature.
 - Enthalpy of air per kg dry air.
 - Volume of moist air/kg dry air.
- 9.6** Moist air flowing at 2 kg/s and a dry bulb temperature of 46°C and wet bulb temperature of 20°C mixes with another stream of moist air flowing at 3 kg/s at 25°C and relative humidity of 60%. Using a psychrometric chart, determine the (a) humidity ratio, (b) enthalpy, and (c) dry bulb temperature of the two streams mixed together.
- *9.7** Air at a dry bulb temperature of 20°C and relative humidity of 80% is to be heated and humidified to 40°C and 40% relative humidity. The following options are available for this objective: (a) by passing air through a heated water-spray air washer; (b) by preheating sensibly, and then passing through a water-spray washer with recirculated water until relative humidity rises to 95% and then again heating sensibly to the final required state. Determine for (a) and (b) the total heating required, the make-up water required in water-spray air washer, and the humidifying efficiency of the recirculated spray water.
- 9.8** Moist air at 35°C and 55% relative humidity is heated using a common furnace to 70°C. From the psychrometric chart, determine how much heat is added per m³ initial moist air and what the final dew-point temperature is.
- *9.9** A water-cooling tower is to be designed with a blower capacity of 75 m³/s. The moist air enters at 25°C and wet bulb temperature of 20°C. The exit air leaves at 30°C and relative humidity of 80%. Determine the flow rate of water, in kg/s, that can be

* Indicates an advanced level of difficulty in solving.

cooled if the cooled water is not recycled. The water enters the tower at 40°C and leaves the tower at 25°C.

- *9.10** Ambient air with a dew point of 1°C and a relative humidity of 60% is conveyed at a rate of 1.5 m³/s through an electric heater. The air is heated to a dry bulb temperature of 50°C. The heated air is then allowed to pass through a tray drier that contains 200 kg of apple slices with an initial moisture content of 80% wet basis. The air exits the dryer with a dew-point temperature of 21.2°C.
- If the electrical energy costs 5¢/(kW h), calculate the electrical costs for heating the air per hour of operation.
 - Calculate the amount of water removed by air from apple slices per hour of operation.
 - If the dryer is operated for 2 h, what will be the final moisture content of the apple slices (wet basis)?
- 9.11** Air is at a dry bulb temperature of 20°C and a wet bulb temperature of 15°C. Determine the following properties from a psychrometric chart.
- Moisture content
 - Relative humidity
 - Enthalpy
 - Dew point
 - Specific volume
- 9.12** In a humidifier, air at a dry bulb temperature of 40°C and relative humidity of 10% is humidified to a relative humidity of 40%. Determine the amount of moisture added in the humidifier per kg of dry air.
- 9.13** Air at a dry bulb temperature of 100°C and 4% relative humidity is passed over cooling coils to cool it to a dry bulb temperature of 40°C. How much heat is removed from the air in the process?
- 9.14** Air at a dry bulb temperature of 40°C and a wet bulb temperature of 20°C is first heated in a heater to a dry bulb temperature of 90°C. Then it is passed through a bed of apricot slices to dry them. The air exiting from the top of the apricot bed is at a dry bulb temperature of 60°C. It is then passed through a dehumidifier to reduce its relative humidity to 10%. Clearly show the various paths of the process on a psychrometric chart.

*Indicates an advanced level of difficulty in solving.

The air velocity through the bed and the dehumidifier is 4 m/s and the cross-sectional diameter of the bed is 0.5 m.

- a. Determine the amount of moisture removed, in grams of water/second from the apricot bed.
 - b. Determine the amount of moisture removed, in grams of water/second in the dehumidifier.
- 9.15** On a copy of a psychrometric chart, show the heating and humidification process from the following data. Initially the air is at a dry bulb temperature (dbt) of 40°C and a relative humidity of 30%. The air is heated to a dbt of 80°C. The heated air is then conveyed through a humidifier to raise its relative humidity to 25%. For this process, calculate
- a. The change in moisture content per kg of dry air.
 - b. The change in enthalpy from the initial unheated air to final humidified air.
- 9.16** Air at a dbt of 30°C and a relative humidity of 30% is conveyed through a heated dryer where it is heated to a dbt of 80°C. Then it is conveyed through a bed of granular pet food to dry it. The air exits the dryer at a dbt of 60°C. The exit air is again heated to 80°C and conveyed through another dryer containing another batch of pet food. The exit air from the second dryer leaves at saturation. Clearly show the paths of air, starting from the ambient air to the saturated air exiting the second dryer on a copy of a psychrometric chart. Determine the amount of water removed in the first and second dryer per kg of dry air.

LIST OF SYMBOLS

c_{pa}	specific heat of dry air (kJ/[kg K])
c_{pw}	specific heat of water vapor (kJ/[kg K])
c_s	humid heat of moist air (kJ/kg dry air K)
H_a	enthalpy of dry air (kJ/kg)
H_L	latent heat of vaporization (kJ/kg)
H_w	enthalpy of saturated or superheated water vapor (kJ/kg)
m_a	mass of dry air (kg)
\dot{m}	mass flow rate of moist air (kg/s)
M_w	molecular weight of water
m_w	mass of water vapor (kg)
n	number of moles
n_a	number of moles of air
n_w	number of moles of water vapor

p	partial pressure (kPa)
p_a	partial pressure of dry air (kPa)
p_B	barometric or total pressure of moist air (kPa)
p_w	partial pressure of water vapor (kPa)
p_{wb}	partial pressure of water vapor at wet bulb temperature (kPa)
p_{ws}	saturation pressure of water vapor (kPa)
ϕ	relative humidity (%)
q	rate of heat transfer (kW)
R	gas constant ($[\text{m}^3 \text{ Pa}]/[\text{kg K}]$)
R_a	gas constant dry air ($[\text{m}^3 \text{ Pa}]/[\text{kg K}]$)
R_0	universal gas constant ($8314.41 [\text{m}^3 \text{ Pa}]/[\text{kg mol K}]$)
R_w	gas constant water vapor ($[\text{m}^3 \text{ Pa}]/[\text{kg K}]$)
ρ_s	density of saturated water vapor at the dry bulb temperature (kg/m^3)
ρ_w	density of water vapor in the air (kg/m^3)
T	temperature ($^{\circ}\text{C}$)
T_A	absolute temperature (K)
T_a	dry bulb temperature ($^{\circ}\text{C}$)
T_0	reference temperature ($^{\circ}\text{C}$)
T_w	wet bulb temperature ($^{\circ}\text{C}$)
V	volume (m^3)
V'_a	specific volume of dry air ($\text{m}^3/\text{kg dry air}$)
V'_m	specific volume of moist air (m^3/kg)
V'_w	specific volume of water vapor (m^3/kg)
W	humidity ratio (kg water/kg dry air)
x_a	mole fraction for dry air
x_w	mole fraction for water vapor
x_{ws}	mole fraction for saturated air

■ BIBLIOGRAPHY

- American Society of Heating, Refrigerating and Air-Conditioning Engineers, Inc. (1997). *ASHRAE Handbook of 1997 Fundamentals*, ASHRAE, Atlanta, Georgia.
- Geankoplis, C. J. (1978). *Transport Processes and Unit Operations*, Allyn & Bacon, Boston.
- Jennings, B. H. (1970). *Environmental Engineering, Analysis and Practice*, International Textbook Company, New York.
- Martin, T. W. (1961). Improved computer oriented methods for calculation of steam properties. *J. Heat Transfer*, **83**: 515–516.
- Steltz, W. G. and Silvestri, G. J. (1958). The formulation of steam properties for digital computer application. *Trans. ASME*. **80**: 967–973.

This page intentionally left blank

Mass Transfer

In food processing, we often create conditions to encourage chemical reactions that produce desirable end-products in the most efficient manner. Frequently, in addition to desirable products, several by-products may be produced. These by-products may be undesirable from the process standpoint, but may have considerable economic value. In order to recover these secondary products, a separation step must be used to isolate the primary product of interest. In designing separation processes, an understanding of the mass transfer processes becomes important.

Mass transfer plays a key role in the creation of favorable conditions for reactants to physically come together, allowing a particular reaction to occur. Once the reactants are in proximity to a particular site, the reaction will proceed at an optimum rate. Under these circumstances, we may find that the reaction is limited by the movement of the reactants to the reaction site, or movement of end-products away from the reaction site. In other words, the reaction is mass-transfer limited, instead of being limited by the kinetics of the reaction.

To study mass transfer in food systems, it is important that we understand the term *mass transfer* as used throughout this textbook. In situations where we have a bulk flow of a fluid from one location to another, there is a movement of the fluid (of a certain mass), but the process is *not* mass transfer, according to the context being used. Our use of the term *mass transfer* is restricted to the migration of a constituent of a fluid or a component of a mixture. The migration occurs because of changes in the physical equilibrium of the system caused by the concentration differences. Such transfer may occur within one phase or may involve transfer from one phase to another.

All icons in this chapter refer to the author's web site, which is independently owned and operated. Academic Press is not responsible for the content or operation of the author's web site. Please direct your web site comments and questions to the author: Professor R. Paul Singh, Department of Biological and Agricultural Engineering, University of California, Davis, CA 95616, USA.

Email: rps@rpaulsingh.com.

Consider this example: If we carefully allow a droplet of ink to fall into a stagnant pool of water, the ink will migrate in various directions from the point where the ink made contact with the water. Initially, the concentration of ink in the droplet is very high, and the concentration of ink in the water is zero, thus establishing a concentration gradient. As the ink migration continues, the concentration gradient will decrease. When the ink becomes fully dissipated in the water, the concentration gradient becomes zero, and the mass transfer process will cease. The concentration gradient is considered the “driving force” for movement of a given component within a defined environment. For example, if you open a bottle of highly volatile material such as nail polish remover in a room, the component (acetone) will migrate to various parts of the room because of the concentration gradients of acetone. If the air is stationary, the transfer occurs as a result of random motion of the acetone molecules. If a fan or any other external means are used to cause air turbulence, the eddy currents will enhance the transfer of acetone molecules to distant regions in the room.

As we will find in this chapter, a number of similarities exist between mass transfer and heat transfer. In mass transfer, we will encounter terms that are also used in heat transfer, such as flux, gradient, resistance, transfer coefficient, and boundary layer.

According to the second law of thermodynamics discussed in Chapter 1, systems that are not in equilibrium tend to move toward equilibrium with time. For chemical reactions, any difference in the chemical potential of a species in one region of a space as compared to another region of the same space, is a departure from an equilibrium state. Over time, there will be a shift toward equilibrium, such that the chemical potential of that species is uniform throughout the region. Differences in chemical potential may occur because of the different concentration of the species from one point to another, differences in temperature and/or pressure, or differences caused by other external fields, such as gravitational force.

10.1 THE DIFFUSION PROCESS

Mass transfer involves both mass diffusion occurring at a molecular scale and bulk transport of mass due to convection flow. The diffusion process can be described mathematically using Fick’s law of

diffusion, which states that the mass flux per unit area of a component is proportional to its concentration gradient. Thus, for a component B,

$$\frac{\dot{m}_B}{A} = -D \frac{\partial c}{\partial x} \quad (10.1)$$

where \dot{m}_B is mass flux of component B (kg/s); c is the concentration of component B, mass per unit volume (kg/m³); D is the mass diffusivity (m²/s); and A is area (m²). Mass flux may also be expressed as kg-mole/s, and the concentration of component B will be kg-mole/m³.

We note that Fick's law is similar to Fourier's law of heat conduction,

$$\frac{q}{A} = -k \frac{\partial T}{\partial x}$$

and Newton's equation for shear-stress-strain relationship,

$$\sigma = -\mu \frac{\partial u}{\partial y}$$

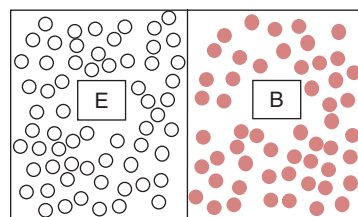
These similarities between the three transport equations suggest additional analogies among mass transfer, heat transfer, and momentum transfer. We will examine these similarities later in Section 10.1.2.

Consider two gases B and E in a chamber, initially separated by a partition (Figure 10.1a). At some instant in time, the partition is removed, and B and E diffuse in opposite directions as a result of the concentration gradients. The following derivation is developed to express the mass diffusion of gas B into gas E, and gas E into gas B. Figure 10.1b shows the gas concentrations at some time after the partition is removed. The concentrations are expressed as molecules per unit volume. In our simplistic diagram, circles represent molecules of a gas, and the molecules move in random directions. However, since the initial concentration of gas B is high on the right-hand side of the partition, there is a greater likelihood for molecules of B crossing the partition from right to left—a net transport of B from right to left. Similarly there is a net transport of E from left to right.

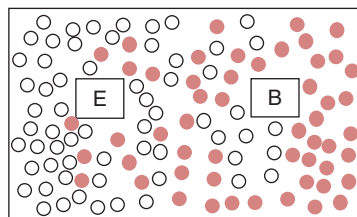
Using the ideal gas law,

$$p_B = \rho_B R_B T \quad (10.2)$$

where p_B is the partial pressure of the gas B (kPa); R_B is the gas constant for gas B; T is absolute temperature (K); and ρ_B is mass concentration of B (kg/m³).



(a)



(b)



Figure 10.1 Diffusion of gases in an enclosed chamber.

The gas constant R_B for gas B can be written in terms of the universal gas constant R_u as follows:

$$R_B = \frac{R_u}{M_B} \quad (10.3)$$

where R_u is the universal gas constant 8314.41 (m³ Pa)/(kg-mol K) or 8.314 (m³ Pa)/(g-mol K) and M_B is molecular weight of gas B.

Thus, from Equation (10.2):

$$\rho_B = \frac{p_B}{R_B T} \quad (10.4)$$

or

$$\rho_B = \frac{p_B M_B}{R_u T} \quad (10.5)$$

Since ρ_B is mass concentration, we can substitute Equation (10.5) in Equation (10.1). Thus,

$$\frac{\dot{m}_B}{A} = -D_{BE} \frac{d}{dx} \left(\frac{p_B M_B}{R_u T} \right) \quad (10.6)$$

or

$$\frac{\dot{m}_B}{A} = - \frac{D_{BE} M_B}{R_u T} \frac{dp_B}{dx} \quad (10.7)$$

The mass diffusivity D_{BE} refers to diffusivity of gas B in gas E.

Equation (10.7) expresses the diffusion of gas B in gas E. Similarly, we can obtain Equation (10.8) to express diffusion of gas E in gas B.

$$\frac{\dot{m}_E}{A} = - \frac{D_{EB} M_E}{R_u T} \frac{dp_E}{dx} \quad (10.8)$$

The magnitude of mass diffusivities for liquids or gases in solids *are* less than the mass diffusivities for gases in liquids. These differences are due to the mobility of the molecules. Mass diffusivity values are expressed as centimeters squared per second (cm²/s). In solids, the mass diffusivities range from 10⁻⁹ to 10⁻¹ cm²/s; in liquids the range of mass diffusivities is from 10⁻⁶ to 10⁻⁵ cm²/s; and for gases, the range is from 5 × 10⁻¹ to 10⁻¹ cm²/s. The mass diffusivity magnitudes are a function of temperature and concentration; in the case of gases, the mass diffusivity is substantially influenced by pressure.

Some representative values of mass diffusivities of gases in air and in water are presented in Tables 10.1a and 10.1b.

Table 10.1a Diffusion Coefficients of Selected Gases in Water at 20°C

Gas	D ($\times 10^{-9} \text{ m}^2/\text{s}$)
Ammonia	1.8
Carbon dioxide	1.8
Chlorine	1.6
Hydrogen	5.3
Nitrogen	1.9
Oxygen	2.1
For other temperatures $D_T = D_{20}[1 + 0.02(T - 20)]$	

Table 10.1b Diffusion Coefficients of Selected Gases and Vapors in Air (under Standard Conditions)

Gas	D ($\times 10^{-6} \text{ m}^2/\text{s}$)
Ammonia	17.0
Benzene	7.7
Carbon dioxide	13.8
Ethyl alcohol	10.2
Hydrogen	61.1
Methyl alcohol	13.3
Nitrogen	13.2
Oxygen	17.8
Sulfur dioxide	10.3
Sulfur trioxide	9.4
Water vapor	21.9

10.1.1 Steady-State Diffusion of Gases (and Liquids) through Solids

Assuming the mass diffusivity does not depend on concentration, from Equation (10.1) we obtain

$$\frac{\dot{m}_A}{A} = -D_{AB} \frac{dc_A}{dx} \quad (10.9)$$

where D_{AB} is mass diffusivity for gas A (or liquid A) in a solid B. Subscript A for \dot{m} and c represents a gas or liquid diffusing through a solid. In reality, D_{AB} represents an effective diffusivity through solids.

By separating variables and integrating Equation (10.9):

$$\frac{\dot{m}_A}{A} \int_{x_1}^{x_2} dx = -D_{AB} \int_{c_{A1}}^{c_{A2}} dc_A \quad (10.10)$$

$$\frac{\dot{m}_A}{A} = \frac{D_{AB}(c_{A1} - c_{A2})}{(x_2 - x_1)} \quad (10.11)$$

Equation (10.11) applies to one-dimensional diffusion when the concentration gradient is $[c_{A1} - c_{A2}]$ and constant with time at locations x_2 and x_1 . In addition, the expression applies to rectangular coordinates. For a cylindrical shape, radial coordinates would apply and the following equation is obtained:

$$\dot{m}_A = \frac{D_{AB} 2\pi L (c_{A1} - c_{A2})}{\ln \frac{r_2}{r_1}} \quad (10.12)$$

Equation (10.12) applies to a situation when diffusion is occurring in the radial direction of a cylinder; from the center to the surface or from the surface to the center. In order for the mass transfer to be steady-state the concentrations at the surface and the center must be constant with time.

The conditions of steady-state diffusion need to be emphasized. The concentrations at the boundaries must be constant with time, and diffusion is limited to molecular motion within the solid being described. In addition, the mass diffusivities, D , are not influenced by magnitude of concentration, and no temperature gradients exist within the solid. The magnitudes for mass diffusivity, D , depend on both the solid and the gas or liquid diffusing in the solid.

10.1.2 Convective Mass Transfer

When the transport of a component due to a concentration gradient is enhanced by convection, the mass flux of the component will be higher than would occur by molecular diffusion. Convective mass transfer will occur in liquids and gases, and within the structure of a porous solid. The relative contributions of molecular diffusion and convective mass transfer will depend on the magnitude of convective currents within the liquid or gas.

The convective mass transfer coefficient k_m is defined as the rate of mass transfer per unit area per unit concentration difference. Thus,

$$k_m = \frac{\dot{m}_B}{A(c_{B1} - c_{B2})} \quad (10.13)$$

where \dot{m}_B is the mass flux (kg/s); c is concentration of component B, mass per unit volume (kg/m³); A is area (m²). The units of k_m are m³/m²s or m/s. The coefficient represents the volume (m³) of component B transported across a boundary of one square meter per second.

By using the relationship presented in Equation (10.5), the mass transport due to convection becomes:

$$\dot{m}_B = \frac{k_m A M_B}{R_u T_A} (p_{B1} - p_{B2}) \quad (10.14)$$

This expression is used to estimate the mass flux based on the vapor pressure gradient in the region of mass transport.

When the specific application of mass transport is water vapor in air, Equation (9.14) can be incorporated in Equation (10.14) to obtain:

$$\dot{m}_B = \frac{k_m A M_B p}{0.622 R_u T_A} (W_1 - W_2) \quad (10.15)$$

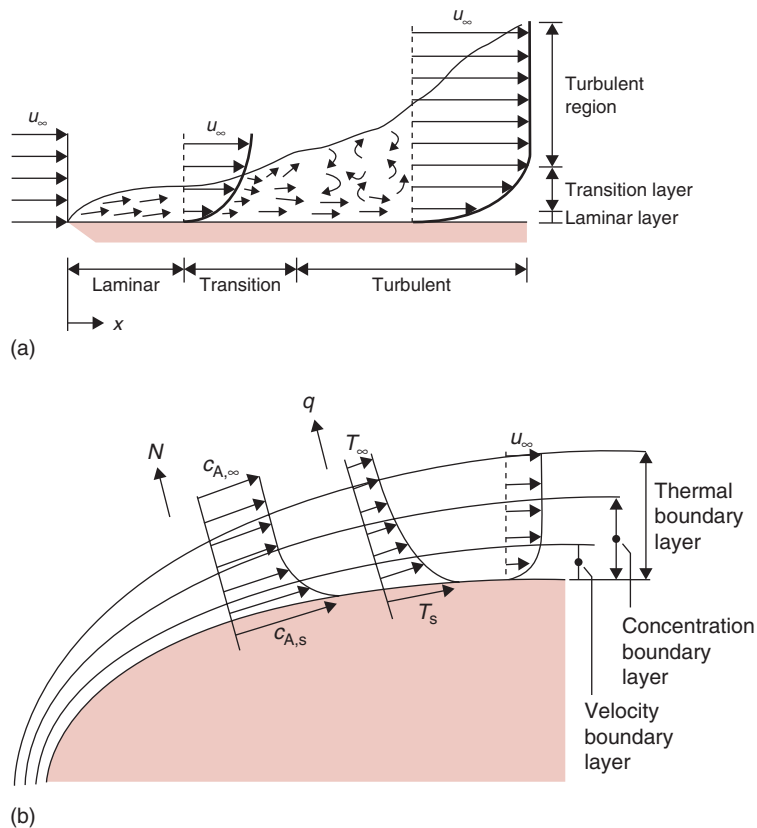
When computing the convective transport of water vapor in air, Equation (10.15) is used, and the gradient is in the form of a humidity ratio gradient in the region of convective mass transport.

Convective mass transfer coefficients can be predicted using dimensional analysis, analogous to the methods described in Chapter 4 for convective heat transfer coefficients. In this section, we will consider some of the important dimensionless numbers involved in mass transfer.

In situations that involve molecular diffusion and mass transfer due to forced convection, the following variables are important: mass diffusivity D_{AB} , for component A in fluid B; the velocity of the fluid, u ; the density of the fluid, ρ ; the viscosity of the fluid, μ ; the characteristic dimension d_c ; and the convective mass transfer coefficient k_m . In the case of natural convection, additional important variables include the acceleration due to gravity, g , and the mass density difference $\Delta\rho$. The variables are grouped in the following dimensionless numbers:

$$N_{Sh} = \frac{k_m d_c}{D_{AB}} \quad (10.16)$$

■ **Figure 10.2** (a) The development of a boundary layer on a flat plate. (b) The development of the thermal, concentration, and velocity boundary layers on a surface. (From Incropera, Dewitt, Bergman, and Lavine, 2007. Copyright © 2007 by John Wiley & Sons.)



$$N_{Sc} = \frac{\mu}{\rho D_{AB}} \quad (10.17)$$

$$N_{Re} = \frac{\rho u d_c}{\mu} \quad (10.18)$$

$$N_{Le} = \frac{k}{\rho c_p D_{AB}} \quad (10.19)$$

Consider a fluid flowing over a flat plate as shown in Figure 10.2. For the boundary layer from the leading edge of the plate, we can write the following equations for momentum, energy, and concentration, respectively.

$$u_x \frac{\partial u_x}{\partial x} + u_y \frac{\partial u_x}{\partial y} = \frac{\mu}{\rho} \frac{\partial^2 u_x}{\partial y^2} \quad (10.20)$$

$$u_x \frac{\partial T}{\partial x} + u_y \frac{\partial T}{\partial y} = \alpha \frac{\partial^2 T}{\partial y^2} \quad (10.21)$$

$$u_x \frac{\partial c_A}{\partial x} + u_y \frac{\partial c_A}{\partial y} = D_{AB} \frac{\partial^2 c_A}{\partial y^2} \quad (10.22)$$

In Equation (10.22), c_A represents concentrations of component A at locations within the boundary layer.

Note that

$$\frac{\mu}{\rho\alpha} = \frac{\mu c_p}{k} = N_{Pr} = \text{Prandtl number} \quad (10.23)$$

Thus, the Prandtl number provides the link between velocity and temperature profiles.

From Equations (10.20) and (10.22), if

$$\frac{\mu}{\rho D_{AB}} = 1 \quad (10.24)$$

then velocity and concentration profiles have the same shape. The ratio

$$\frac{\mu}{\rho D_{AB}} = N_{Sc} = \text{Schmidt number} \quad (10.25)$$

The concentration and temperature profiles will have the same shape if

$$\frac{\alpha}{D_{AB}} = 1 \quad (10.26)$$

The ratio

$$\frac{\alpha}{D_{AB}} = N_{Le} = \text{Lewis number} \quad (10.27)$$

The functional relationships that correlated these dimensional numbers for forced convection are:

$$N_{Sh} = f(N_{Re}, N_{Sc}) \quad (10.28)$$

If we compare the correlations for mass transfer with those presented for heat transfer in Chapter 4, the analogies are evident. If

the dimensionless profiles of velocity, temperature, and concentration are assumed to be similar, the Nusselt and Prandtl numbers for heat transfer can be replaced by the Sherwood and Schmidt numbers, respectively, in mass transfer. Thus, it may be deduced that

$$N_{\text{Sh}} = \frac{\text{total mass transferred}}{\text{total mass transferred by molecular diffusion}} \quad (10.29)$$

$$N_{\text{Sc}} = \frac{\text{molecular diffusion of momentum}}{\text{molecular diffusion of mass}} \quad (10.30)$$

Next, we will consider a number of dimensionless correlations used in evaluating the convective mass transfer coefficient (k_m). These correlations are based on the following assumptions:

- Constant physical properties
- No chemical reactions in the fluid
- Small bulk flow at the interface
- No viscous dissipation
- No interchange of radiant energy
- No pressure, thermal, or forced diffusion.

10.1.3 Laminar Flow Over a Flat Plate

Laminar flow over a flat plate exists when $N_{\text{Re}} < 5 \times 10^5$, and the correlation is:

$$N_{\text{Sh}_x} = \frac{k_{m,x}x}{D_{AB}} = 0.322N_{\text{Re}_L}^{1/2}N_{\text{Sc}}^{1/3} \quad N_{\text{Sc}} \geq 0.6 \quad (10.31)$$

In Equation (10.31), the convective mass transfer coefficient $k_{m,x}$ in the Sherwood number is at a fixed location; therefore, the N_{Sh_x} is termed the local Sherwood number. The characteristic dimension used in the Sherwood and Reynolds numbers is the distance from the leading edge of the plate.

When flow is laminar over the entire length of the plate, we can obtain an average Sherwood number from the following relationship:

$$N_{\text{Sh}_L} = \frac{k_{m,L}L}{D_{AB}} = 0.664N_{\text{Re}_L}^{1/2}N_{\text{Sc}}^{1/3} \quad N_{\text{Sc}} \geq 0.6 \quad (10.32)$$

In Equation (10.32), the characteristic dimension is the total length of the plate, L ; and the convective mass transfer coefficient $k_{m,L}$, obtained from the Sherwood number, is the average value for the entire plate.

Determine the rate of water evaporated from a tray full of water. Air at a velocity of 2 m/s is flowing over the tray. The temperature of water and air is 25°C. The width of the tray is 45 cm and its length along the direction of air flow is 20 cm. The diffusivity of water vapor in air is $D = 0.26 \times 10^{-4} \text{ m}^2/\text{s}$. The relative humidity of air is 50%.

Example 10.1

Given

Velocity = 2 m/s

Temperature of water and air = 25°C

Width of the tray = 45 cm

Length of the tray = 20 cm

Diffusivity = $0.26 \times 10^{-4} \text{ m}^2/\text{s}$

Kinematic viscosity of air at 25°C = $16.14 \times 10^{-6} \text{ m}^2/\text{s}$

Approach

We will first determine the Reynolds number and then use an appropriate dimensionless correlation to obtain the mass transfer coefficient and the water evaporation rate.

Solution

1. Reynolds number for the 20 cm long tray is

$$N_{Re} = \frac{2 \times 0.2}{16.14 \times 10^{-6}} = 24,783$$

Since $N_{Re} < 5 \times 10^5$, the flow is laminar.

2. We use Equation (10.32):

$$N_{Sh} = \frac{k_m L}{D_{AB}} = 0.664 (N_{Re})^{1/2} (\dot{N}_{Sc})^{1/3}$$

where

$$N_{Sc} = \frac{\nu}{D_{AB}} = \frac{16.14 \times 10^{-6}}{0.26 \times 10^{-4}} = 0.62$$

3. Thus,

$$\frac{k_m \times 0.2}{0.26 \times 10^{-4}} = 0.664 (24,783)^{1/2} (0.62)^{1/3}$$

$$k_m = 1.1587 \times 10^{-2} \text{ m/s}$$

4. The evaporation rate for the tray is

$$\dot{m}_A = k_m A (c_{A,s} - c_{A,\infty})$$

where $c_{A,s}$ is the concentration under saturated conditions,

$$c_{A,s} = \rho_{A,s} = 0.02298 \text{ kg/m}^3$$

and where $c_{A,\infty}$ is the concentration of water in the free stream; since relative humidity is 50%, then

$$\rho_{A,\infty} = (0.5)(0.02298) = 0.01149 \text{ kg/m}^3$$

5. Therefore,

$$\begin{aligned}\dot{m}_A &= (1.1587 \times 10^{-2} \text{ m/s}) \times (0.45 \text{ m} \times 0.2 \text{ m}) \\ &\quad \times (0.02298 \text{ kg/m}^3 - 0.01149 \text{ kg/m}^3) \\ \dot{m}_A &= 1.1982 \times 10^{-5} \text{ kg/s}\end{aligned}$$

6. The water evaporation rate from the tray is 0.043 kg/h.

Example 10.2

Determine the rate of water evaporated from a tray of water described in Example 10.1 by using the partial pressures of water vapor in the air and at the water surface. Relative humidity of air is 50%.

Given

Air velocity = 2 m/s

Temperature (air and water) = 25°C

Tray width = 0.45 m

Tray length = 0.2 m

Diffusivity of water vapor in air = $0.26 \times 10^{-4} \text{ m}^2/\text{s}$

Kinematic viscosity of air (25°C) = $16.14 \times 10^{-6} \text{ m}^2/\text{s}$

Relative humidity of air = 50%

Vapor pressure of water at saturation = 3.179 kPa (from Table A.4.2 at 25°C)

Molecular weight of water = 18 kg/(kg mol)

Gas constant, $R = 8.314 \text{ m}^3 \text{ kPa}/(\text{kg mol K})$

Approach

We will use the same approach as in Example 10.1 to obtain the mass transfer coefficient. The partial pressure gradient will be used to compute the water evaporation rate.

Solution

1. Based on computation from Example 10.1, the mass transfer coefficient,

$$k_m = 1.16 \times 10^{-2} \text{ m/s}$$

2. Using the definition of relative humidity, the partial pressure of 50% RH air is

$$p_{B2} = \left(\frac{\%RH}{100} \right) (p_{B1}) = \left(\frac{50}{100} \right) (3.179) = 1.5895 \text{ kPa}$$

3. Using Equation (10.14):

$$\dot{m}_B = \frac{1.16 \times 10^{-2} [\text{m/s}] \times (0.2 \times 0.45) [\text{m}^2] \times 18 [\text{kg}/(\text{kg mol})]}{8.314 [\text{m}^3 \text{ kPa}/(\text{kg mol K})] \times (25 + 273) [\text{K}] \times (3.179 - 1.5895) [\text{kPa}]}$$

4. Then

$$\dot{m}_B = 1.2 \times 10^{-5} \text{ kg/s} = 0.043 \text{ kg water/h}$$

Determine the rate of water evaporated from a tray of water described in Example 10.1 by using the humidity ratios for water vapor in the air and at the water surface.

Example 10.3

Given

Air velocity = 2 m/s

Temperature (air and water) = 25°C

Tray width = 0.45 m

Tray length = 0.2 m

Diffusivity of water vapor in air = $0.26 \times 10^{-4} \text{ m}^2/\text{s}$

Kinematic viscosity of air (25°C) = $16.14 \times 10^{-6} \text{ m}^2/\text{s}$

Relative humidity of air = 50%

Molecular weight of water = 18 kg/(kg mol)

Gas constant, $R = 8.314 \text{ m}^3 \text{ kPa}/(\text{kg mol K})$

Atmospheric pressure = 101.325 kPa

Approach

The steps used in Example 10.1 are followed to obtain the mass transfer coefficient.

The gradient of humidity ratios is used to compute the water evaporation rate.

Solution

1. From Example 10.1, the mass transfer coefficient $k_m = 1.16 \times 10^{-2} \text{ m/s}$
2. From the psychrometric chart (Fig. A.5), the humidity ratio for saturated air (25°C) at the water surface is determined.

$$W_1 = 0.0202 \text{ kg water/kg dry air}$$

3. From the psychrometric chart (Fig. A.5) the humidity ratio for 25°C air at 50% relative humidity is

$$W_2 = 0.0101 \text{ kg water/kg dry air}$$

4. Using Equation (10.15), the mass flux of water from the surface to air is determined:

$$\dot{m}_B = \frac{1.16 \times 10^{-2} [\text{m/s}] \times (0.2 \times 0.45) [\text{m}^2] \times 18 [\text{kg}/(\text{kg mol})] \times 101.325 [\text{kPa}]}{0.622 \times 8.314 [\text{m}^3 \text{kPa}/(\text{kg mol K})] \times (25 + 273) [\text{K}] \times (0.0202 - 0.0101) [\text{kg water/kg dry air}]}$$

5. Then

$$\dot{m}_B = 1.25 \times 10^{-5} \text{ kg/s} = 0.045 \text{ kg water/h}$$

10.1.4 Turbulent Flow Past a Flat Plate

The dimensionless relationship for dimensionless groups during turbulent flow ($N_{\text{Re}} > 5 \times 10^5$) past a flat plate is as follows:

$$N_{\text{Sh}_x} = \frac{k_{m,x} x}{D_{AB}} = 0.0296 N_{\text{Re}_x}^{4/5} N_{\text{Sc}}^{1/3} \quad 0.6 < N_{\text{Sc}} < 3000 \quad (10.33)$$

In Equation (10.33), the characteristic dimension is the distance from the leading edge of the plate, and the convective mass transfer coefficient is the local coefficient at the characteristic dimension, x .

The correlation to be used to determine the average convective mass transfer coefficient during turbulent flow is:

$$N_{\text{Sh}_L} = \frac{k_{mL} L}{D_{AB}} = 0.036 N_{\text{Re}}^{0.8} N_{\text{Pr}}^{0.33} \quad (10.34)$$

In Equation (10.34), the characteristic dimension is the total length of the flat plate.

10.1.5 Laminar Flow in a Pipe

For laminar flow in a pipe, the following equation is suggested:

$$\bar{N}_{\text{Sh}_d} = \frac{k_m d_c}{D_{AB}} = 1.86 \left(\frac{N_{\text{Re}_d} N_{\text{Sc}}}{L/d_c} \right)^{1/3} \quad N_{\text{Re}} < 10,000 \quad (10.35)$$

where the characteristic dimension, d_c , is the diameter of the pipe.

10.1.6 Turbulent Flow in a Pipe

For turbulent flow in a pipe,

$$\bar{N}_{\text{Sh}_d} = \frac{k_m d_c}{D_{AB}} = 0.023 N_{\text{Re}_d}^{0.8} N_{\text{Sc}}^{1/3} \quad N_{\text{Re}} > 10,000 \quad (10.36)$$

where d_c is the characteristic dimension and diameter of the pipe.

10.1.7 Mass Transfer for Flow over Spherical Objects

Mass transfer to or from a spherical object is obtained from an expression similar to the Froessling correlation presented as Equation (4.69) for heat transfer.

$$\bar{N}_{\text{Sh}_d} = 2.0 + (0.4 N_{\text{Re}_d}^{1/2} + 0.06 N_{\text{Re}_d}^{2/3}) N_{\text{Sc}}^{0.4} \quad (10.37)$$

For mass transfer from a freely falling liquid droplet, the following expression is recommended.

$$\bar{N}_{\text{Sh}_d} = 2.0 + 0.6 N_{\text{Re}_d}^{1/2} N_{\text{Sc}}^{1/3} \quad (10.38)$$

A 0.3175 cm sphere of glucose is placed in a water stream flowing at a rate of 0.15 m/s. The temperature of water is 25°C. The diffusivity of glucose in water is $0.69 \times 10^{-5} \text{ cm}^2/\text{s}$. Determine the mass transfer coefficient.

Example 10.4

Given

Diameter of sphere = 0.3175 cm = 0.003175 m

Velocity of water = 0.15 m/s

Temperature of water = 25°C

Diffusivity of glucose in water = $0.69 \times 10^{-5} \text{ cm}^2/\text{s}$

From Table A.4.1 @ 25°C

$$\text{Density} = 997.1 \text{ kg/m}^3$$

$$\text{Viscosity} = 880.637 \times 10^{-6} \text{ Pa s}$$

Approach

We will first determine the Reynolds number and Schmidt number. Since the glucose sphere is submerged in a stream of water, we will use Equation (10.38) to determine

the Sherwood number. The mass transfer coefficient will be obtained from the Sherwood number.

Solution

1. The Reynolds number is

$$N_{Re} = \frac{997.1 \text{ kg/m}^3 \times 0.15 \text{ m/s} \times 0.003175 \text{ m}}{880.637 \times 10^{-6} \text{ Pa s}} \\ = 539$$

2. The Schmidt number is

$$N_{Sc} = \frac{880.637 \times 10^{-6} \text{ Pa s} \times 10,000 \text{ cm}^2/\text{m}^2}{997.1 \text{ kg/m}^3 \times 0.69 \times 10^{-5} \text{ cm}^2/\text{s}} \\ = 1279$$

3. The Sherwood number can be obtained from Equation (10.38)

$$N_{Sh} = 2.0 + 0.6(1279)^{1/3} \times (539)^{1/2} \\ = 153$$

4. The mass transfer coefficient

$$k_m = \frac{153 \times 0.69 \times 10^{-5} \text{ cm}^2/\text{s}}{0.003175 \text{ m} \times 10,000 \text{ cm}^2/\text{m}^2} \\ = 3.32 \times 10^{-5} \text{ m/s}$$

5. The mass transfer coefficient will be $3.32 \times 10^{-5} \text{ m/s}$, assuming that by dissolving glucose in water we will not alter the physical properties of water to any significant magnitude.

10.2 UNSTEADY-STATE MASS TRANSFER

In many applications, the changes in concentration of a component within a food will occur under conditions where the rate of concentration change may increase or decrease with time. Examples would include the diffusion of salt within a solid food matrix, the diffusion of a volatile flavor within a dry food or the diffusion of an antimicrobial substance within a food. Under some conditions, the diffusion of liquid phase water may occur within a food under isothermal conditions. Finally, the uptake of moisture by a dry food during storage will occur due to the diffusion of water vapor within the dry food structure.

10.2.1 Transient-State Diffusion

The diffusion of the food component with a product mass would be described by:

$$\frac{\partial c}{\partial t} = D \left(\frac{\partial^2 c}{\partial x^2} \right) \quad (10.39)$$

where c is the concentration of the component diffusing within the solid food structure, as a function of time, t . The mass diffusivity, D , is the same property of the product and the diffusing component as described for steady-state diffusion. The analytical solutions to Equation (10.39) have been presented in many references, with Crank (1975) having the most complete array of geometries and boundary conditions. The key factors influencing the type of solution obtained are the geometry of the solid food object, and the boundary conditions needed to describe the conditions at the surface of the object. The series solutions are similar to the solutions referenced in unsteady-state heat transfer.

Unsteady-state mass transfer charts have been developed, such as Figure 10.3 from Treybal (1968). The chart presents concentration ratio versus dimensionless ratios Dt/d_c^2 for three standard geometries: infinite plate, infinite cylinder, and sphere. When using the chart in Figure 10.3, the concentration ratio contains the mass average concentration, c_{ma} , at any time, t ; the concentration of the diffusing component in the medium surrounding the food object, c_m ; and the initial concentration of the diffusing component within the food, c_i .

As introduced for unsteady-state heat transfer in Chapter 4, the characteristic dimension, d_c , changes depending on the geometry: one-half thickness for the infinite plate, radius of the infinite cylinder, and radius of the sphere. In addition, the chart in Figure 10.3 assumes that the boundary condition would represent negligible resistance to mass transfer at the surface of the object, as compared with diffusion within the food. This is a reasonable assumption in most food applications since the mass diffusivities, D , for liquids or gases within solid food structures have small magnitudes as compared with mass transfer of the gases or liquids at the boundary. Any convection at the surface will enhance mass transfer within the boundary layer at the object surface. It should be noted that the mass average concentration of the food as a function of time may not provide sufficient information, and the concentration distribution history within the food should be considered.

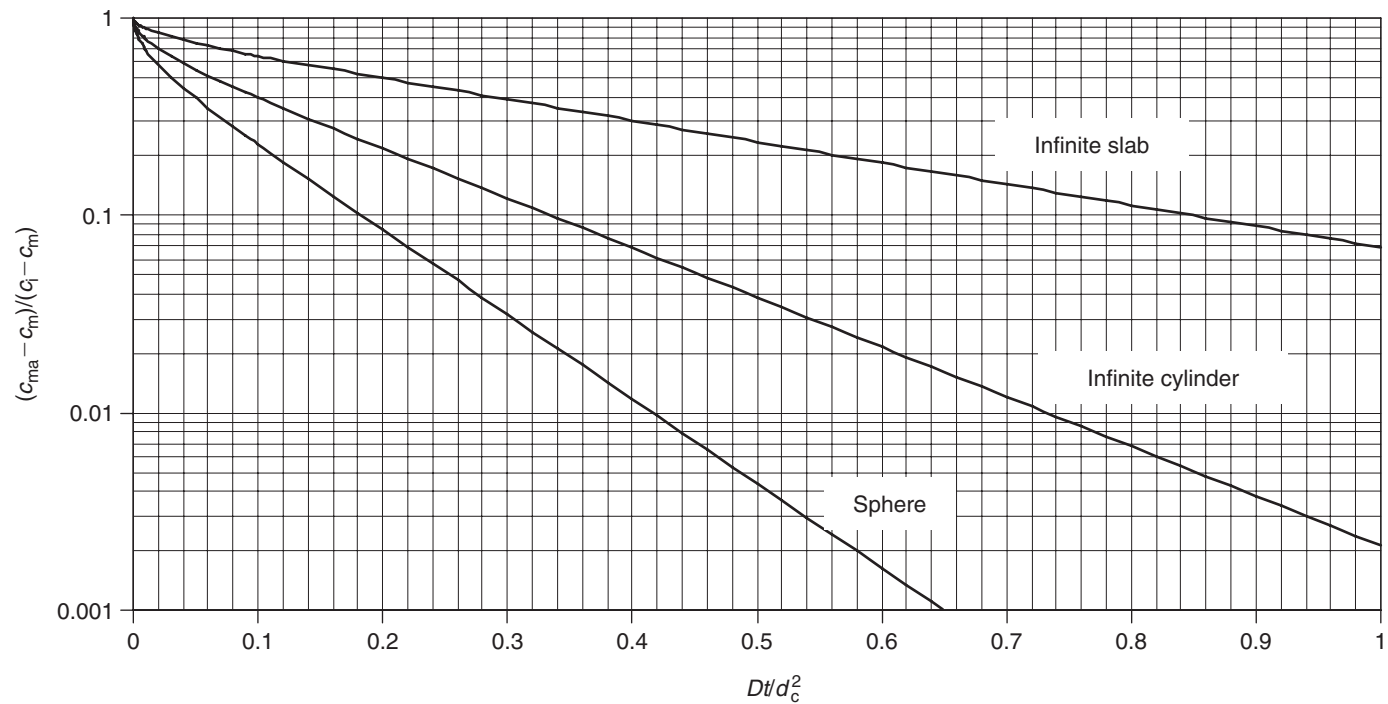


Figure 10.3 Unsteady-state mass transfer chart for mass average concentration in three standard geometries. (From Treybal, 1968)

Salt is being used to preserve a 4.8 mm slice of salmon muscle. The concentration of salt at the surface is 0.533 kg/kg salt free salmon (SFS), and the initial concentration is 0.012 kg/kg SFS. If the mass diffusivity, D , of salt in salmon muscle is $8.78 \times 10^{-11} \text{ m}^2/\text{s}$, determine the time required for the mass average concentration to reach 0.4 kg/kg SFS.

Example 10.5

Given

Characteristic dimension for an infinite slab, $d_c = 2.4 \text{ mm} = 2.4 \times 10^{-3} \text{ m}$

Salt concentration at the surface, $c_m = 0.533 \text{ kg/kg SFS}$

Initial salt concentration, $c_i = 0.012 \text{ kg/kg SFS}$

Mass average concentration, $c_{ma} = 0.4 \text{ kg/kg SFS}$

$D = 8.78 \times 10^{-11} \text{ m}^2/\text{s}$

Approach

The unsteady-state mass transfer chart (Fig. 10.3) will be used to estimate the dimensionless quantity, Dt/d_c^2 , from the concentration ratio.

Solution

1. The concentration ratio

$$\frac{c_{ma} - c_m}{c_i - c_m} = \frac{0.4 - 0.533}{0.012 - 0.533} = 0.255$$

2. From Figure 10.3,

$$\frac{Dt}{d_c^2} = 0.46$$

3. Then

$$\text{Time} = \frac{0.46 d_c^2}{D} = \frac{0.46 \times (2.4 \times 10^{-3})^2 [\text{m}^2]}{8.78 \times 10^{-11} [\text{m}^2/\text{s}]} = 3.018 \times 10^4 \text{ s}$$

$$\text{Time} = 8.38 \text{ h}$$

4. It takes 8.38 h for mass average salt concentration to reach 0.4 kg/kg SFS.

A more useful relationship for applications to unsteady-state mass transfer in foods would be:

$$\frac{c - c_m}{c_i - c_m} = f(\bar{N}_{\text{Bi}}, \bar{N}_{\text{Fo}}) \quad (10.40)$$

where

N_{Bi} = mass transfer Biot number;

\bar{N}_{Fo} = mass transfer Fourier number.

The more complete use of the solutions to Equation (10.40) would predict concentration distribution histories within a food, based on knowledge of the convective mass transfer coefficient at the boundary of the object, and the mass diffusivity of the gas or liquid within the food structure.

An alternative approach to charts, such as Figure 10.3, is based on an analogy to heat transfer, as described in Chapter 4. When applied to mass transfer, the basic expression is the **diffusion rate equation**, as follows:

$$\log(c_m - c) = -\frac{t}{\bar{f}} + \log[\bar{j}(c_m - c_i)] \quad (10.41)$$

where the diffusion rate constant, \bar{f} , represents the time required for a one log-cycle change in the concentration gradient, and the lag coefficient, \bar{j} , describes the region of nonlinearity in the relationship between the concentration gradient and time during the initial stages of diffusion.

By adapting the charts developed by Pflug et al. (1965) and presented in Chapter 4, the coefficients (\bar{f}, \bar{j}) needed for the diffusion rate equation can be determined. The diffusion rate constant, \bar{f} , is predicted by using Figure 4.40, where the dimensionless number $\bar{f}D/d_c^2$ is presented as a function of the mass transfer Biot number. Note that when using Figure 4.40 for mass transfer we use the symbols on the chart appropriately. As is evident, the influence of the mass transfer Biot number is most dramatic between magnitudes of 0.1 and 100. At values less than 0.1, the internal resistance to mass transfer is negligible, and changes in the concentration within the food would be controlled by the magnitude of the convective mass transfer coefficient at the product surface. An application of this situation might be the transport of a gas or vapor through a packaging film to a porous food during storage. At mass transfer Biot numbers greater than 100, the external resistance to mass transfer is negligible, and changes in concentration within the food as a function of time are controlled by the magnitude of the mass diffusivity, D . Since Equation (10.41) was obtained by using the first term of the series solutions, as discussed in Chapter 4, it is valid only for Fourier numbers greater than 0.2.

The magnitude of the lag coefficient, \bar{j} , is influenced by the mass transfer Biot number, as illustrated in Figures 4.41 and 4.42. In Figure 4.41, the relationships describe the influence of the mass transfer Biot number on the lag coefficient \bar{j}_c at the geometric center of the object. The lag coefficient \bar{j}_m at the location defining the mass average

concentration of the object is influenced by the mass transfer Biot number as illustrated in Figure 4.42. For both coefficients, the influence of the mass transfer Biot number is most dramatic between 0.1 and 100.

The approach presented can be used to predict the time required for the mass average concentration of a food, or for the concentration at the center of the product, to reach some defined magnitude. After the magnitude of the mass transfer Biot number is established, the appropriate values are obtained from Figures. 4.40, 4.41, and 4.42. The magnitude of the diffusion rate constant is computed, based on magnitudes of the mass diffusivity, D , and the characteristic dimension for the product. These coefficients are used to compute the time from the diffusion rate equation, when given the concentration of diffusing component in the medium surrounding the product, as well as the initial concentration in the food.

Example 10.6

The diffusion of salt in salmon muscle described in Example 10.5 can be described by the diffusion rate equation. Determine the time required to increase the mass average concentration to 0.4 kg salt per kg SFS.

Given

$$d_c = 2.4 \text{ mm} = 2.4 \times 10^{-3} \text{ m}$$

$$c_m = 0.533 \text{ kg/kg SFS}$$

$$c_i = 0.012 \text{ kg/kg SFS}$$

$$D = 8.78 \times 10^{-11} \text{ m}^2/\text{s}$$

$$c_{mc} = 0.4 \text{ kg/kg SFS}$$

Approach

The diffusion rate equation will be used to determine the time required, after estimating the diffusion rate constant (\bar{f}) and lag coefficient (\bar{J}_m) from the charts (Figs. 4.40 and 4.42).

Solution

1. Estimate the diffusion rate constant.

Since the slab concentration has been measured at the surface of the muscle, the resistance to mass transport is negligible at the surface and $\bar{N}_{Bi} \gg 40$. From Figure 4.40,

$$\frac{\bar{f} D}{d_c^2} = 0.97$$

for an infinite slab at $\bar{N}_{Bi} \gg 40$.

2. Then

$$\bar{f} = \frac{0.97 \times (2.4 \times 10^{-3})^2 [m^2]}{8.78 \times 10^{-11} [m^2/s]} = 6.36 \times 10^4 s = 17.68 h$$

3. Using Figure 4.42 at $\bar{N}_{Bi} \gg 40$,

$$\bar{j}_m = 0.82$$

4. Using the diffusion rate equation:

$$\log(0.533 - 0.4) = -\frac{t}{17.68} + \log[0.82(0.533 - 0.012)]$$

$$-0.876 = -\frac{t}{17.68} + (-0.369)$$

$$t = 17.68(0.876 - 0.369)$$

$$t = 8.96 h$$

10.2.2 Diffusion of Gases

The specific application of the diffusion rate equation to unsteady-state mass transfer of a gas can be accomplished by recognizing that the concentration is directly related to the partial pressure, as indicated in Equation (10.5). Given this relationship, the diffusion rate equation can be expressed as follows:

$$\log(p_m - p) = -\frac{t}{\bar{f}} + \log[\bar{j}(p_m - p_i)] \quad (10.42)$$

and the changes in partial pressure of a diffusing gas within a food product structure can be predicted in terms of partial pressures of that gas. This form of the diffusion rate equation would have specific application to diffusion of oxygen and similar gases within food products.

By considering the definition of water activity in terms of partial pressures of water vapor, the diffusion rate equation can be presented as:

$$\log(a_{wm} - a_w) = -\frac{t}{\bar{f}} + \log[\bar{j}(a_{wm} - a_{wi})] \quad (10.43)$$

and the changes in water activity of a dry food can be predicted, based on exposure to an environment with a water activity (relative humidity) different for the product. This form of the equation can be used to predict water activity within a food after a defined storage period in a defined environment, or to predict the time required for the product

to reach a water activity limit during storage. These applications are closely associated with shelf-life predictions for dry and intermediate moisture content foods.

Example 10.7

Individual pieces of dry pasta are exposed to an environment at 15°C and 50% relative humidity. The mass diffusivity for water vapor within the pasta is $12 \times 10^{-12} \text{ m}^2/\text{s}$, and the mass transfer coefficient in the environment around the pasta has been estimated to be $1.2 \times 10^{-4} \text{ m/s}$. The pieces of pasta have a diameter of 1 cm. If the initial water activity is 0.05, estimate the water activity of the pasta after one week.

Given

Characteristic dimension, infinite cylinder, $d_c = 0.005 \text{ m}$

$$k_m = 1.2 \times 10^{-4} \text{ m/s}$$

$$D = 12 \times 10^{-12} \text{ m}^2/\text{s}$$

$$a_{wm} = 0.5 \text{ (from relative humidity = 50\%)}$$

$$a_{wi} = 0.05$$

Approach

The first step in the solution is computation of the mass transfer Biot number, followed by determination of the appropriate coefficients to be used in the diffusion rate equation.

Solution

1. The mass transfer Biot number for the individual pieces of pasta is

$$\bar{N}_{Bi} = 5 \times 10^4$$

2. Using Figure 4.40,

$$\frac{\bar{f}D}{d_c^2} = 0.4$$

$$\bar{f} = \frac{0.4 \times (0.005)^2 [\text{m}^2]}{12 \times 10^{-12} [\text{m}^2/\text{s}]} = 8.3 \times 10^5 \text{ s} = 231.5 \text{ h}$$

3. Using Figure 4.42,

$$\bar{j}_m = 0.7$$

4. Using the diffusion rate equation,

$$\log(0.5 - a_w) = -\frac{168}{231.5} + \log[0.7(0.5 - 0.05)]$$

$$\text{and } a_w = 0.44$$

5. Based on the steps used, the mass average water activity of the pasta after one week is 0.44.

The application of the diffusion rate equation to finite geometries is accomplished in the same manner as previously described for heat transfer. The key expressions for a finite cylinder and a finite slab, respectively, are:

$$\frac{1}{\bar{f}} = \frac{1}{\bar{f}_{IS}} + \frac{1}{\bar{f}_{IC}} \quad (10.44)$$

$$\frac{1}{\bar{f}} = \frac{1}{\bar{f}_{IS1}} + \frac{1}{\bar{f}_{IS2}} + \frac{1}{\bar{f}_{IS3}} \quad (10.45)$$

Similarly, coefficient \bar{j} for finite cylinder and finite slab are, respectively:

$$\bar{j} = \bar{j}_{IS} \times \bar{j}_{IC} \quad (10.46)$$

$$\bar{j} = \bar{j}_{IS1} \times \bar{j}_{IS2} \times \bar{j}_{IS3} \quad (10.47)$$

By using the appropriate expressions, the coefficients (\bar{f} , \bar{j}) are obtained and the diffusion rate equation is used to predict concentrations, partial pressures, or water activities, as a function of time.

Example 10.8

Determine the time required for the center of pieces of the pasta in Example 10.7 to reach a water activity of 0.3. The pieces have a length of 2 cm and diameter of 1 cm.

Given

Characteristic dimension, infinite cylinder, $d_c = 0.005$ m

Characteristic dimension, infinite slab, $d_c = 0.01$ m

$k_m = 1.2 \times 10^{-4}$ m/s

$D = 12 \times 10^{-12}$ m²/s

$a_{wm} = 0.5$ (from relative humidity = 50%)

$a_{wi} = 0.05$

$a_w = 0.3$

Approach

After determination of the mass transfer Biot number, the charts (Figs. 4.40 and 4.41) are used to determine the coefficients for the diffusion rate equation.

Solution

1. Both mass transfer Biot numbers (based on infinite slab and infinite cylinder) exceed 5×10^4 .

2. Using computations from Example 10.7,

$$\bar{f}_{lc} = 231.5 h$$

3. Using Figure 4.40 (for infinite slab),

$$\frac{\bar{f}D}{d_c^2} = 0.97$$

4. Then

$$\bar{f}_s = \frac{0.97 \times (0.01)^2}{12 \times 10^{-12}} = 8.08 \times 10^6 s = 2245.4 h$$

5. From Figure 4.41,

$$\bar{j}_{cs} = 1.27 \text{ (for infinite slab)}$$

$$\bar{j}_{ci} = 1.60 \text{ (for infinite cylinder)}$$

6. Using Equation (10.44),

$$\frac{1}{\bar{f}} = \frac{1}{2245.4} + \frac{1}{231.5}$$

$$\bar{f} = 209.86 h$$

7. Using Equation (10.46),

$$\bar{j}_c = 1.27 \times 1.60 = 2.04$$

8. Based on the diffusion rate equation,

$$\log(0.5 - 0.3) = -\frac{t}{209.86} + \log[2.04(0.5 - 0.05)]$$

$$t = 138.89 h$$

9. Time for water activity to reach 0.3 at the center of the pasta pieces is 138.89 h or 5.8 days.

PROBLEMS

- 10.1** A droplet of water is falling through 20°C air at the terminal velocity. The relative humidity of the air is 10% and the droplet is at the wet bulb temperature. The diffusivity of water vapor in air is $0.2 \times 10^{-4} \text{ m}^2/\text{s}$. Estimate the convective mass transfer coefficient for a 100 μm diameter droplet.
- 10.2** The Sherwood Number for vapor transport from the surface of a high moisture food product to the surrounding air is 2.78.

Compute the convective mass transfer coefficient, when the dimension of the product in the direction of air movement is 15 cm, and the mass diffusivity for water vapor in air is $1.8 \times 10^{-5} \text{ m}^2/\text{s}$.

- 10.3** A flavor compound is held within a 5 mm diameter time-release sphere. The sphere is placed in a liquid food and will release the flavor compound after one month of storage at 20°C . The concentration of flavor within the sphere is 100% and the mass diffusivity for the flavor compound within the liquid food is $7.8 \times 10^{-9} \text{ m}^2/\text{s}$. Estimate the steady-state mass flux of flavor into the liquid food from the surface of the time-release sphere. The convective mass transfer coefficient is 50 m/s.
- 10.4** A desiccant is being used to remove water vapor from a stream of air with 90% RH at 50°C . The desiccant is a flat plate with 25 cm length and 10 cm width, and maintains a water activity of 0.04 at the surface exposed to the air stream. The stream of air has velocity of 5 m/s moving over the surface in the direction of the 25 cm length. The mass diffusivity for water vapor in air is $0.18 \times 10^{-3} \text{ m}^2/\text{s}$. Compute the mass flux of water vapor from the air to the desiccant surface.
- *10.5** Cucumbers are preserved by storage in a salt brine with a concentration of 20% NaCl. The initial NaCl concentration in the cucumber is 0.6% and the moisture content is 96.1% (wb). The convective mass transfer coefficient at the surface of the cucumbers is sufficiently high to cause the mass transfer Biot number to be greater than 100. The mass diffusivity for NaCl in water is $1.5 \times 10^{-9} \text{ m}^2/\text{s}$. Estimate the time required for the center of a 2 cm cucumber to reach 15%. Note that the concentration percentages in the cucumber are kg NaCl per kg of cucumber, whereas the brine concentration is kg NaCl per kg water.
- 10.6** An apple slice with 1 cm thickness is exposed to 80% RH for one week. After one week, the water activity of the apple has increased to 0.6, from an initial value of 0.1. The convective mass transfer coefficient at the product surface is $8 \times 10^{-3} \text{ m/s}$. Estimate the mass diffusivity for water vapor in the apple.

*Indicates an advanced level in solving.

LIST OF SYMBOLS

\dot{m}	mass flow rate (kg/s)
\bar{j}	lag coefficient for mass transfer (dimensionless)
\bar{N}_{Bi}	mass transfer Biot number (dimensionless)
\bar{N}_{Fo}	mass transfer Fourier number (dimensionless)
\bar{f}	time required for a one log-cycle change in concentration
	gradient (s)
A	area (m ²)
a_w	water activity
c	concentration (kg/m ³ or kg mol/m ³)
c_p	specific heat (kJ/[kg °C])
D	mass diffusivity (m ² /s)
d_c	characteristic dimension (m)
E_p	activation energy for permeability (kcal/mol)
k	thermal conductivity (W/[m °C])
k_m	mass transfer coefficient (m/s)
L	length (m)
\dot{m}	mass flow rate (kg/s)
M	molecular weight
N_{Le}	Lewis number (dimensionless)
N_{Re}	Reynolds number (dimensionless)
N_{Sc}	Schmidt number (dimensionless)
N_{Sh}	Sherwood number (dimensionless)
p	partial pressure of gas (kPa)
P	permeability coefficient
q	rate of heat transfer (W)
R	gas constant (m ³ Pa/[kg K])
r	radial coordinate (m)
R_u	universal gas constant (m ³ Pa/[kg mol K])
σ	shear stress (Pa)
S	solubility (mol/[cm ³ atm])
T	temperature (K)
t	time (s)
ν	kinematic viscosity (m ² /s)
u	fluid velocity (m/s)
W	humidity ratio (kg water/kg dry air)
x	distance coordinate (m)
α	thermal diffusivity (m ² /s)
μ	viscosity (Pa s)
ρ	mass concentration (kg/m ³)

Subscripts: A, component A; B, component B; E, component E; i, initial; IC, infinite cylinder; IS, infinite slab; m, medium; ma, mass average; S, surface location; x, variable distance; 1, location 1; 2, location 2.

■ BIBLIOGRAPHY

- Crank, J. (1975). *The Mathematics of Diffusion*, 2nd ed. Oxford University Press, London.
- Incropera, F. P., Dewitt, D. P., Bergman, T., and Lavine, A. (2007). *Fundamentals of Heat and Mass Transfer*, 6th ed. John Wiley & Sons Inc., New York.
- McCabe, W. L., Smith, J. C., and Harriott, P. (1985). *Unit Operations of Chemical Engineering*. McGraw-Hill, New York.
- Pflug, I. J., Blaisdell, J. L., and Kopelman, J. (1965). Developing temperature–time curves for objects that can be approximated by a sphere, infinite plate, or infinite cylinder. *ASHRAE Trans.* **71**(1): 238–248.
- Rotstein, E., Singh, R. P., and Valentas, K. (1997). *Handbook of Food Engineering Practice*. CRC Press, Boca Raton, Florida.
- Treybal, R. E. (1968). *Mass Transfer Operations*, 2nd ed. McGraw-Hill, New York.

Membrane Separation

Membrane separation systems have been used extensively in the chemical process industry. Their use in the food industry is now becoming more common. Some of the typical food-related applications include purification of water, and the concentration and clarification of fruit juices, milk products, alcoholic beverages, and wastewater.

The most popular method for concentration of a liquid food is the evaporation process. During evaporation, a sufficient amount of thermal energy, equivalent to the latent heat of vaporization, must be added to the product to initiate phase change for water within the product (see Chapter 8). In an evaporator, the latent heat of vaporization represents a substantial part of the energy requirements or operating costs. In membrane separation systems, water is removed from the liquid product without phase change.

In a membrane separation system, a fluid containing two or more components is in contact with a membrane that permits selected components (for example, water in the fluid) to permeate more readily than other components. The physical and chemical nature of the membrane—for example, pore size and pore-size distribution—affect the separation of liquid streams. As shown in Figure 11.1, the membrane in a reverse-osmosis system allows water to permeate whereas salts and sugars are rejected. Ultrafiltration membranes are useful in fractionating components by rejecting macromolecules. In microfiltration, the membranes separate suspended particulates. The application of each of the membranes for separating different materials is shown in Figure 11.2.

Permeation of the selected component(s) is the result of a “driving force.” For dialysis, the concentration difference across the membrane

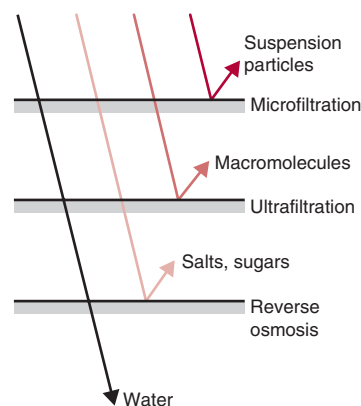
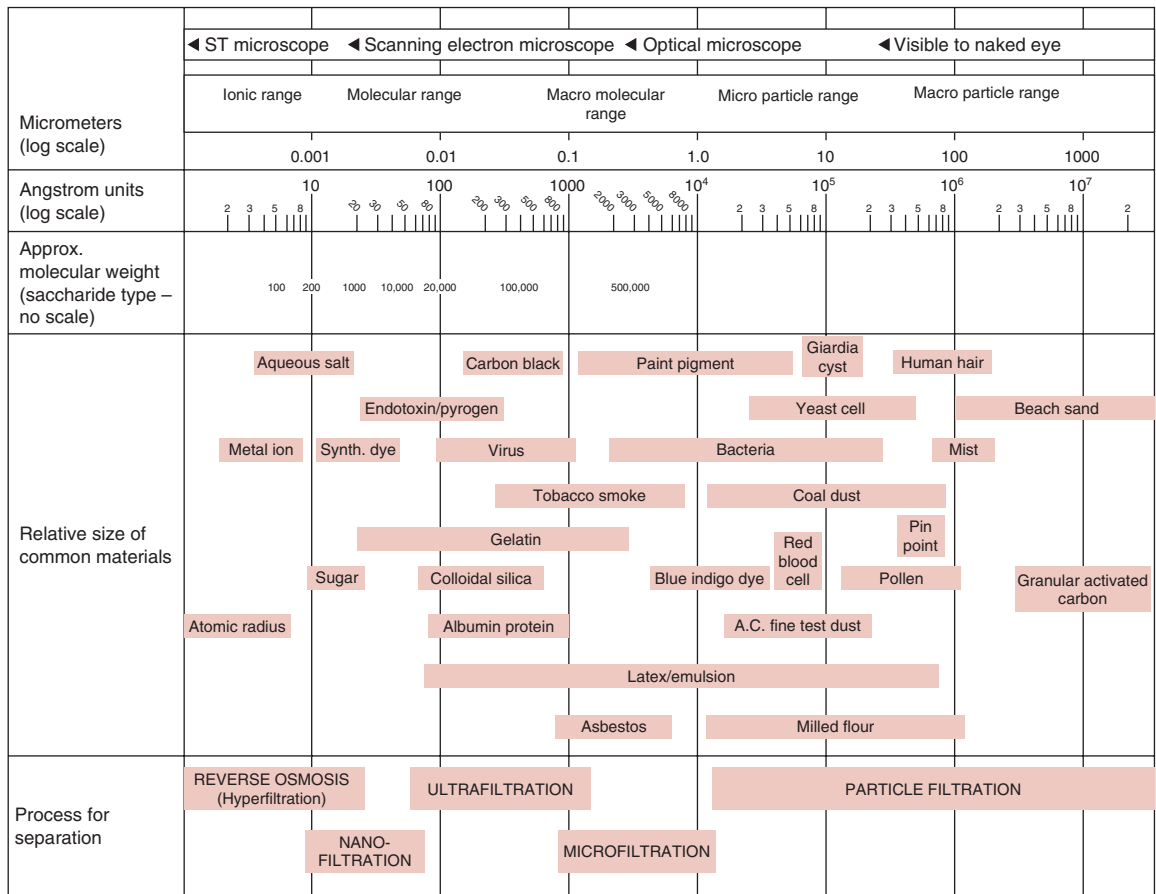


Figure 11.1 Use of membrane systems to separate substances of different-sized molecules. (From Cheryan, 1989)

All icons in this chapter refer to the author's web site, which is independently owned and operated. Academic Press is not responsible for the content or operation of the author's web site. Please direct your web site comments and questions to the author: Professor R. Paul Singh, Department of Biological and Agricultural Engineering, University of California, Davis, CA 95616, USA. Email: rps@rpaulsingh.com. **623**



■ **Figure 11.2** A separation spectrum. (Courtesy of Osmonics)

is the driving force, whereas in the case of reverse osmosis, ultrafiltration, and microfiltration systems, hydrostatic pressure is the key driving force. Microfiltration membrane systems require the lowest amount of hydraulic pressure; about 1 to 2 bar (or 15 to 30 psig). Ultrafiltration membrane systems operate at higher pressures; on the order of 1 to 7 bar (or 15 to 100 psig). These pressure levels are required to overcome the hydraulic resistance caused by a macromolecular layer at the membrane surface, as discussed in Section 11.5. In a reverse-osmosis system, considerably higher hydraulic pressures, in the range of 20 to 50 bar (300 to 750 psig), are necessary to overcome the osmotic pressures.

We can best understand the process of selective permeation by examining the structure of a membrane. Figure 11.3 is a visualization of a



■ **Figure 11.3** The structure of an ultrafiltration membrane. (From Lacey, 1972)

membrane represented as a composite material consisting of polymeric chain interconnected by cross-linking. Any material being transported through a membrane must move through the interstitial spaces. When the interstitial openings are small, the transporting material makes its way through a membrane by pushing aside the neighboring polymeric chains. The resistance to the movement of a given material through a membrane depends on how “tight” or “loose” a membrane is. A polymeric membrane with a considerable degree of cross-linkages and crystallinity is considered tight, and it will offer considerable resistance to the permeation of a transporting material.

We will now consider three types of membrane systems: electrodialysis, reverse osmosis, and ultrafiltration.

11.1 ELECTRODIALYSIS SYSTEMS

The separation process in an electrodialysis system is based on the selective movement of ions in solution. The membranes in these systems derive their selectivity from the ions (anions or cations) that are allowed to permeate through them. Selected ions are removed from water as they pass through the semipermeable membranes. These membranes do not permit permeation of water.

If a polymeric chain in a membrane has a fixed negative charge, it will repulse any anion that tries to enter the membrane. This is shown schematically in Figure 11.4. For example, a negatively charged chain attracts cations and allows them to move through. In this type of membrane,



Figure 11.4 The movement of ions in ion-selective membranes. (From Applegate, 1984)

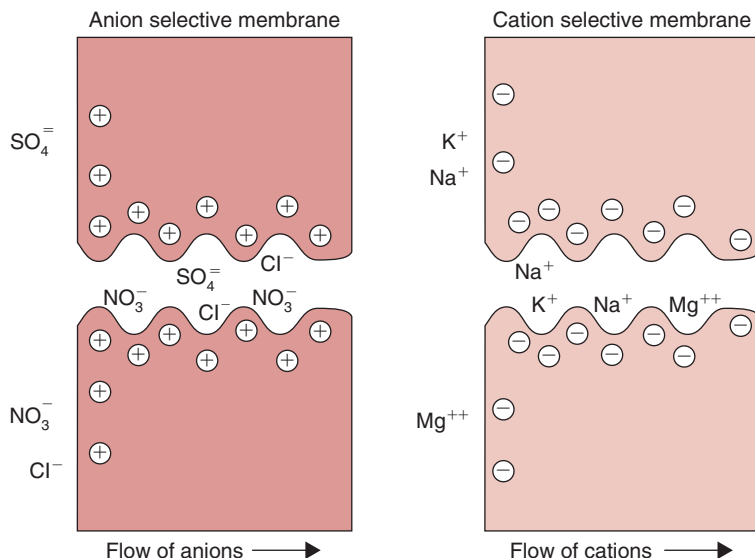
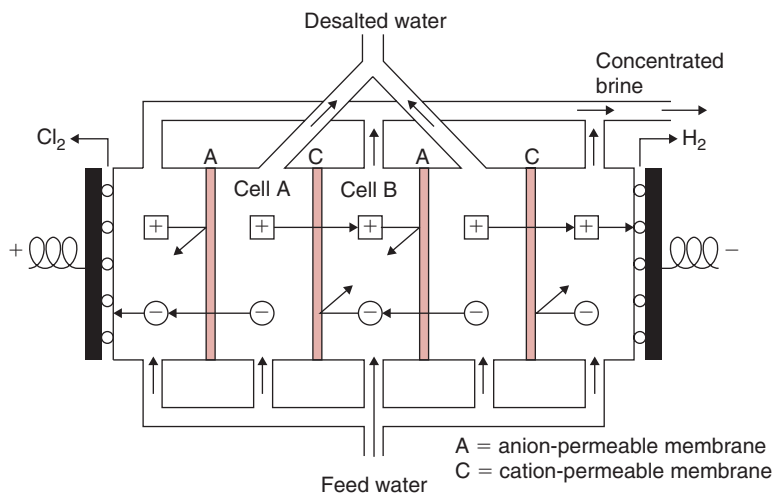


Figure 11.5 Desalting of water with an electrodialysis system. (From Lacey, 1972)



the distance between the cross-linkages of the polymeric chain should be large enough to minimize the resistance offered to the transporting ion. At the same time, the distance between the cross-linkages must not be too large, or the repulsive forces will be insufficient to provide the desired selectivity. This functional property of an ion membrane system is used in the electrodialysis system, as shown in Figure 11.5.

The electrodialysis system uses an electric current to transfer ions through a membrane. The membranes have fixed ionic groups that are chemically bound to the structure of the membrane. As shown in Figure 11.5, the electrodialysis system involves an array of membranes, alternating between anion-exchange and cation-exchange membranes. In between the membranes are small compartments (0.5 to 1.0 mm thick) that contain the solution. Electrodes are used to apply an electric charge to both sides of the membrane assembly. Depending on the fixed charge of the polymer chain in the membrane, only the compatible ions are able to move through a given membrane. Thus, cations will readily move through cation-exchange membranes but will be repulsed by anion-exchange membranes.

Let us follow the path of cations (such as Na^+ in a salt solution) shown in Figure 11.5. The cations in cell A are attracted toward the anode, and they readily move through the cation-exchange membrane. However, the anions are repulsed back into the solution. After the cations move to cell B, they cannot move farther to the right because they are repulsed toward the left by the anion-exchange membrane. Thus, either ion-concentrated or ion-depleted solution streams are obtained from alternating chambers.

Electrodialysis has been used extensively in desalting processes employing membranes that are permeable to ions, but impervious to water. Water leaving from the ion-depleted cells is the desalted product, and brine is obtained from the ion-concentrated cells. For the desalting applications, anion-selective membranes are made from cross-linked polystyrene with quaternary ammonia groups; cation-selective membranes are made from cross-linked polystyrene that is sulfonated, such that sulfonate groups are attached to the polymer. The sulfonate (SO_4) and ammonium (NH_4) groups provide the electronegative and electropositive charges, respectively. Ions attach with opposite electric charges on the membrane and easily migrate from one charge to another. This migration of ions causes the flow of electric current. The pores in these membranes are too small to allow water to transport through them. The electrodialysis process does not remove colloidal material, bacteria, or un-ionized matter.

The energy consumption for the electrodialysis process is given by

$$E = I^2 n R_c t \quad (11.1)$$

where E is energy consumption (J), I is electric current through the stack (A), n is the number of cells in the stack, R_c is the resistance of the cell (Ω), and t is time (s).

The electric current I can be calculated from the following equation:

$$I = \frac{zF\dot{m}\Delta c}{U} \quad (11.2)$$

where z is electrochemical valence; F is Faraday's constant, 96,500 A/s equivalent; \dot{m} is feed solution flow rate (L/s); Δc is concentration difference between feed and product; U is current utilization factor; and I is direct current (A).

From Equations (11.1) and (11.2),

$$E = (nR_c) \left(\frac{zF\dot{m}\Delta c}{U} \right)^2 \quad (11.3)$$

For applications involving desalination of water, it is evident from Equation (11.3) that the energy required to desalt water is directly proportional to the concentration of salt in the feed. When the salt concentration is very high, the energy consumption will be correspondingly high. Application of electrodialysis to feedwater of less than 10,000 ppm total dissolved solids is usually limited by economics. Typically, for commercial applications, the most favorable economic application of electrodialysis requires a feed with a total dissolved solids content (TDS) of 1000 to 5000 mg/L to obtain a product with a TDS content of 500 mg/L. The U.S. Public Health Service Drinking Water Standards require that potable water should not contain more than 500 ppm TDS (although up to 1000 ppm may be considered acceptable). Table 11.1 presents the terms used to express the solids content of different levels of saline water.

Table 11.1 Total Dissolved Solids Content of Saline Water

Term	Total dissolved solids (ppm)
Fresh	<1000
Brackish	
Mildly brackish	1000–5000
Moderately brackish	5000–15,000
Heavily brackish	15,000–35,000
Sea water	35,000 (approximately)

In Japan, the electrodialysis process has been used extensively to obtain table salt from sea water. Other food applications of the electrodialysis process include removing salts from whey and orange juice.

11.2 REVERSE OSMOSIS MEMBRANE SYSTEMS

It is well known that when a plant or an animal membrane is used to separate two solutions of different solute concentrations, pure water passes through the membrane. The movement of water occurs from a solution with high concentration of water to a solution with low concentration of water, thus tending to equalize the water concentration on the two sides of the membrane. This movement of water is generally referred to as *osmosis*. Plant root hairs absorb water from the soil according to this phenomenon. The water is usually present in high concentration in soil surrounding the root hairs, whereas the water concentration inside the root cell is low due to dissolved sugars, salts, and other substances. Osmotic diffusion moves water from the soil into the root hairs.

Consider a solution of water containing a solute. In Figure 11.6a, a semipermeable membrane separates the solutions of the same solute concentration contained in chambers A and B. Since the chemical potential of the solvent (water) is the same on both sides of the membrane, no net flow of water occurs through the membrane. In Figure 11.6b, chamber A contains a solution with a higher solute concentration than chamber B; that is, chamber A has lower water concentration than chamber B. This also means that the chemical potential of the solvent (water) in chamber A will be lower compared with that of chamber B. As a result, water will flow from chamber B to chamber A. As seen in Figure 11.6c, this movement of water will cause an increase in the volume of water in chamber A. Once equilibrium is reached, the increased volume represents a change in head, or pressure, which will be equal to the osmotic pressure. If an external pressure greater than the *osmotic pressure* is then applied to chamber A, as shown in Figure 11.6d, the chemical potential of water in chamber A will increase, resulting in water flow from chamber A to chamber B. The reversal in the direction of water flow, obtained by application of an external pressure that exceeds the osmotic pressure, is termed *reverse osmosis*.

A reverse-osmosis membrane system is used to remove water from a water-solute mixture by application of external pressure. In contrast

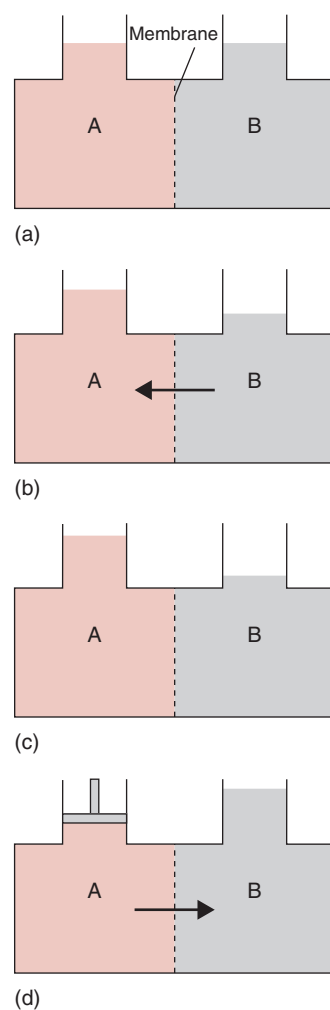
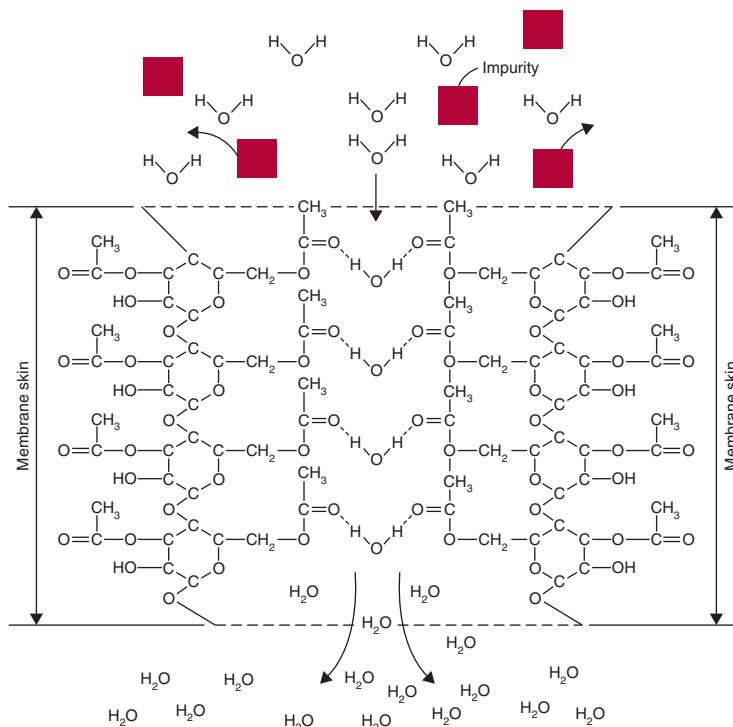


Figure 11.6 The reverse-osmosis process: (a) solute concentration same in cells A and B; (b) water movement from cell B to cell A; (c) osmosis equilibrium; (d) reverse osmosis—water movement from cell A to cell B.

■ **Figure 11.7** The movement of water through a cellulose acetate membrane. (From Lacey, 1972)



to electrodialysis, the membrane used in the reverse-osmosis system must be permeable to water.

In the 1950s, it was discovered that cellulose acetate, a highly organized polymer, has groups that can hydrogen-bond with water as well as with other solvents such as ammonia or alcohol. Figure 11.7 shows the chemical structure of cellulose acetate polymer. The hydrogen in the water molecule bonds to the carbonyl group of cellulose acetate. The water molecules hydrogen-bond on one side of the membrane, then move through the membrane by bonding to neighboring carbonyl groups. This process continues as water permeates the membrane to the other side. As illustrated in Figure 11.7, the polymer must be highly organized with carbonyl groups occurring at fixed locations, or water molecules will be unable to permeate the membrane. The driving force for the water molecules to move from one set of hydrogen-bonding sites to the next is the pressure difference across the membrane.

Structurally, a polymeric membrane can be viewed as strands of the polymer and interstitial spaces. Since the polymer used in a reverse-osmosis

membrane is highly organized, its structure must be tight, such that the interstitial spaces are small.

To obtain high flux rates throughout the membrane, the thickness of the membrane must be small. In the late 1950s, Loeb and Sourirajan invented a method to fabricate extremely thin films of anisotropic cellulose acetate attached to a supporting matrix with an open structure. Since their initial discovery, many developments have taken place in the selection of membrane materials.

In a reverse-osmosis system, water is the permeating material referred to as "permeate," and the remaining solution concentrated with the solutes is called "retentate."

The osmotic pressure Π of a dilute solution can be obtained by Van't Hoff's equation, which uses colligative properties of dilute solutions.

$$\Pi = \frac{cRT}{M} \quad (11.4)$$

where Π is osmotic pressure (Pa), c is solute concentration (kg/m^3) of solution, T is absolute temperature (K), R is gas constant, and M is molecular weight.

Estimate the osmotic pressure of orange juice with 11% total solids at 20°C.

Example 11.1

Given

Concentration of solids = 11% = 0.11 kg solids/kg product

Temperature = 20°C = 293 K

Approach

The Van't Hoff equation (Eq. (11.4)) will be used for computation, while assuming that glucose is the predominant component influencing the osmotic pressure.

Solution

1. The density of orange juice is estimated based on density of carbohydrates at $1593 \text{ kg}/\text{m}^3$.

$$\begin{aligned} \rho &= 0.11(1593) + 0.89(998.2) \\ &= 1063.6 \text{ kg}/\text{m}^3 \end{aligned}$$

2. The concentration, c , for Equation (11.4) becomes

$$\begin{aligned} c &= 0.11 [\text{kg solids/kg product}] \times 1063.6 [\text{kg product/m}^3 \text{ product}] \\ &= 117 \text{ kg solids/m}^3 \text{ product} \end{aligned}$$

3. Using Equation (11.4),

$$\Pi = \frac{117 [\text{kg solids / m}^3 \text{ product}] \times 8.314 [\text{m}^3 \text{ kPa / (kg mol K)}] \times 293 [\text{K}]}{180 [\text{kg / (kg mol)}]}$$

4. $\Pi = 1583.5 \text{ kPa}$

From Equation (11.4), we observe that the presence of small molecules in a solution results in a high osmotic pressure. Another equation found to be more accurate over a wider range of solute concentrations uses Gibb's relationship, given as

$$\Pi = - \frac{RT \ln X_A}{V_m} \quad (11.5)$$

where V_m is the molar volume of pure liquid, and X_A is mole fraction of pure liquid.

Osmotic pressures of some food materials are given in Table 11.2. Foods with smaller molecular-weight constituents have higher

Table 11.2 Osmotic Pressure of Foods and Food Constituents at Room Temperature

Food	Concentration	Osmotic pressure (kPa)
Milk	9% solids-not-fat	690
Whey	6% total solids	690
Orange juice	11% total solids	1587
Apple juice	15% total solids	2070
Grape juice	16% total solids	2070
Coffee extract	28% total solids	3450
Lactose	5% w/v	380
Sodium chloride	1% w/v	862
Lactic acid	1% w/v	552
Source: Cheryan (1998)		

osmotic pressure. Data on osmotic pressures of foods or food components is very limited. These data are important in membrane processing. For example, in order to achieve separation in a reverse-osmosis membrane, the pressure applied to the feed solution must exceed the osmotic pressure.

Estimate the osmotic pressure of orange juice with 11% total solids at 20°C, using the Gibb's relationship.

Example 11.2

Given

Concentration of solids = 11%

Temperature = 20°C

Approach

The Gibb's relationship is Equation (11.5) and requires computation of the mole fraction and the molar volume of pure liquid.

Solution

1. Based on the total solids of 0.11 kg solids/kg product, the mole fraction is:

$$X_A = \frac{\frac{0.89}{18}}{\frac{0.89}{18} + \frac{0.11}{180}} = 0.9878$$

2. The molar volume for water:

$$\frac{1}{V_m} = \frac{0.89[\text{kg water/kg product}] \times 1063.6[\text{kg product/m}^3 \text{ product}]}{18[\text{kg/kg mol}]}$$

$$V_m = 0.019 \text{ m}^3/\text{kg mol}$$

where product density is obtained from Example 11.1.

3. Using Equation (11.5),

$$\Pi = -\frac{8.314[\text{m}^3 \text{ kPa}/(\text{kg mol K})] \times 293[\text{K}]}{0.019[\text{m}^3/\text{kg mol}]} \ln(0.9878)$$

$$\Pi = 1573.8 \text{ kPa}$$

The Hagen–Poiseuille law is useful in developing a relationship between the flux through a membrane and the pressure differential across it. Thus,

$$N = K_p(\Delta P - \Delta \Pi) \quad (11.6)$$

where N is flux of solvent permeation, K_p is the permeability coefficient of the membrane, ΔP is the difference in transmembrane hydrostatic pressure, and $\Delta \Pi$ is the difference in the osmotic pressure between the feed solution and the permeate.

The more specific expression for water flux through a reverse osmosis membrane has been proposed by Matsuura et al. (1973), as follows:

$$N = K_p[\Delta P - \pi(X_{c2}) + \pi(X_{c3})] \quad (11.7)$$

where X_c is the weight fraction of carbon in the solution being separated. The weight fraction (X_{c2}) is the carbon content in the concentrated boundary solution at the membrane surface, and the X_{c3} is the carbon weight fraction in the water passing through the membrane. The magnitude of X_{c2} will exceed the magnitude in the feed stream and the concentrated product leaving the system. Matsuura et al. (1973) have proposed the following expression for the permeability coefficient:

$$K_p = \frac{N_w}{3600A_e\Delta P} \quad (11.8)$$

where N_w is a pure water permeation rate for an effective area of membrane surface, and A_e is the effective membrane area. The magnitude of K_p is a function of membrane properties such as porosity, pore-size distribution, and membrane thickness. In addition, the viscosity of the solvent will influence the permeability coefficient. For membranes that provide high rejection—that is, they do not allow most of the impurities in water to pass through—the osmotic pressure of the permeate is negligible. Matsuura et al. (1973) have measured the permeability coefficient for the cellulose acetate membrane and found a value of 3.379×10^{-6} kg water/(m² s kPa).

Matsuura et al. (1973) have proposed alternative expressions for water flux in a reverse-osmosis membrane, as follows:

$$N = S_p \left[\frac{1 - X_{c3}}{X_{c3}} \right] [c_2 X_{c2} - c_3 X_{c3}] \quad (11.9)$$

$$N = k_m c_1 (1 - X_{c3}) \ln \left[\frac{X_{c2} - X_{c3}}{X_{c1} - X_{c3}} \right] \quad (11.10)$$

where S_p is a solute transport parameter, which is a function of the solute and the membrane characteristics. Typical magnitudes for the parameter have been measured, as presented in Table 11.3. The concentrations (c_1 , c_2 , c_3) in Equations (11.9) and (11.10) are the weight concentrations (kg water/m³) in the feed stream, at the membrane boundary, and in the water passing through the membrane pore, respectively. The magnitude of the mass transfer coefficient (k_m) is a

Table 11.3 Effect of Feed Concentration on $D/K\delta$ for Fruit Juice Solutes at 4137 kPa (600 psig)^a

Film number	Feed solution	Carbon content in feed solution (ppm)	Soluble transport parameter S_p ($\times 10^5$ cm/s)
J7	Apple juice	29,900	0.81
		43,800	0.84
		61,900	0.66
		84,800	0.36
J8	Pineapple juice	29,800	0.64
		47,300	0.43
		62,200	0.24
		80,400	0.35
J9	Orange juice	30,800	1.32
		45,000	0.97
		80,200	1.18
J10	Grapefruit juice	31,700	0.66
		45,900	0.35
		58,500	0.77
		86,900	0.43
J11	Grape juice	33,300	1.12
		48,100	0.63
		62,700	0.39
		81,500	0.69

Source: Matsuura et al. (1973)

^aExperiments carried out in nonflow-type cell.

function of product flow over the membrane surface, and can be evaluated by the dimensionless expressions presented in Chapter 10.

The osmotic pressure of a liquid feed is useful in selecting membranes, since the membrane must be able to physically withstand transmembrane pressure higher than the osmotic pressure.

11.3 MEMBRANE PERFORMANCE

The flow of water through a membrane is described by

$$\dot{m}_w = \frac{K_w A (\Delta P - \Delta \Pi)}{t} \quad (11.11)$$

where \dot{m}_w is water flow rate (kg/s), ΔP is the hydraulic pressure differential across the membrane (kPa), $\Delta \Pi$ is the osmotic pressure difference across the membrane (kPa), t is time (s), A is area (m²), and K_w is the coefficient of water permeability through the membrane (kg/[m²kPa]).

The flow of a solute through a membrane is given by

$$\dot{m}_s = \frac{K_s A \Delta c}{t} \quad (11.12)$$

where \dot{m}_s is the solute flow rate, Δc is the differential of solute concentration across the membrane (kg/m³), and K_s is the coefficient of solute permeability through the membrane (L/m).

From Equations (11.11) and (11.12), it is evident that water flow rate through the membrane is increased by increasing the hydraulic pressure gradient across the membrane. The hydraulic pressure gradient has no effect on the solute flow rate. The solute flow is influenced by the concentration gradient across the membrane.

The performance of a membrane system is often described by the "retention factor," R_f .

$$R_f = \frac{(c_f - c_p)}{c_f} \quad (11.13)$$

where c_f is the concentration of a solute in the feed stream (kg/m³) and c_p is the concentration of a solute in the permeate stream (kg/m³).

Another factor used to describe the performance of a membrane system is the “rejection factor,” R_j .

$$R_j = \frac{(c_f - c_p)}{c_p} \quad (11.14)$$

Membrane performance may be expressed as “molecular weight cut-off,” or the maximum molecular weight for the solute to pass through the membrane.

Another term used to denote membrane performance is conversion percentage, Z .

$$Z = \frac{\dot{m}_p \times 100}{\dot{m}_f} \quad (11.15)$$

where \dot{m}_p is product flow rate and \dot{m}_f is the feed flow rate. Thus, operating a membrane at a conversion percentage of 70% means that a feed of 100 kg/h will yield 70 kg/h of product (permeate) and 30 kg/h of retentate.

11.4 ULTRAFILTRATION MEMBRANE SYSTEMS

Ultrafiltration membranes have pore sizes much larger than the reverse-osmosis membrane. Ultrafiltration membranes are used primarily for fractionating purposes: that is, to separate high-molecular-weight solutes from those with low molecular weight. Since the ultrafiltration membranes have larger pore sizes, the hydraulic pressures required as a driving force are much smaller when compared with the reverse osmosis membrane systems. Typically, pressures in the range of 70 to 700 kPa are needed for ultrafiltration membrane systems. As shown in Figure 11.2, the pore size of ultrafiltration membrane ranges from 0.001 to 0.02 m, with molecular weight cutoffs from 1000 to 80,000.

The flux rate through an ultrafiltration membrane can be obtained from the following equation:

$$N = KA\Delta P \quad (11.16)$$

where ΔP is pressure difference across the membrane, K is membrane permeability constant ($\text{kg}/[\text{m}^2 \text{kPa s}]$), and A is membrane surface area (m^2).

Example 11.3

The concentration of whey is being accomplished by using an ultrafiltration membrane to separate water. The 10 kg/min feed stream has 6% total solids and is being increased to 20% total solids. The membrane tube has a 5 cm inside diameter, and the pressure difference applied is 2000 kPa. Estimate the flux of water through the membrane and the length of the membrane tube when the permeability constant is 4×10^{-5} kg water/(m² kPa s).

Given

Feed concentration = 6% total solids = 0.06 kg solids/kg product

Final concentration = 20% total solids = 0.2 kg solids/kg product

Tube diameter = 5 cm = 0.05 m

Operating pressure = 2000 kPa

Membrane permeability constant = 4×10^{-5} kg water/(m² kPa s)

Approach

Use Equation (11.16) and a mass balance to determine the mass flux and the membrane tube length.

Solution

- Using a mass balance on the membrane system, feed stream = water flux + concentrated product

$$10 = N + N_p$$

and

$$10(0.06) = N_p(0.2)$$

$$N_p = 3 \text{ kg/min of concentrated product}$$

Then

$$N = 7 \text{ kg/min of water through membrane}$$

- Using Equation (11.16)

$$A = \frac{7 [\text{kg water/min}]}{4 \times 10^{-5} \text{ kg water}/(\text{m}^2 \text{ kPa s}) \times 2000 [\text{kPa}] \times 60 [\text{s/min}]}$$

$$A = 1.46 \text{ m}^2$$

- Since $d = 0.05 \text{ m}$

$$L = \frac{1.46 [\text{m}^2]}{\pi \times 0.05 [\text{m}]} = 9.28 \text{ m}$$

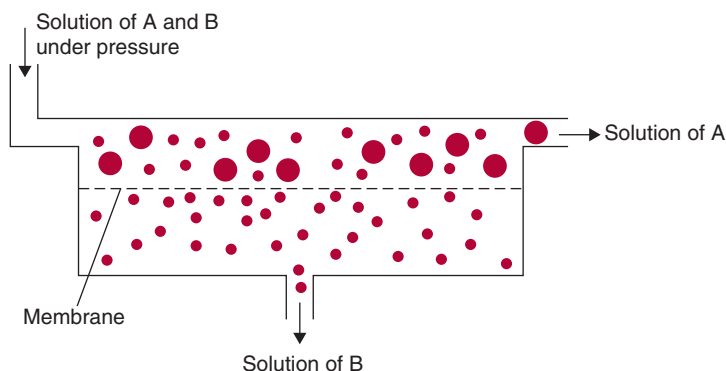


Figure 11.8 Separation process in a pressure-driven membrane system. (From Lacey, 1972)

11.5 CONCENTRATION POLARIZATION

In membrane separation processes, when a liquid solution containing salts and particulates is brought next to a semipermeable membrane, some of the molecules accumulate in the boundary layer next to the membrane surface (Fig. 11.8). Thus, the concentration of a retained species will be higher in the boundary layer adjacent to the membrane than in bulk. This phenomenon is called concentration polarization, and it has a major effect on the performance of a membrane system.

Concentration polarization occurs in both reverse-osmosis and ultrafiltration systems. In addition, the causes of concentration polarization are the same, but the consequences are different. During reverse-osmosis, the low-molecular-weight material is retained on the membrane surface and increases the solute concentration and the osmotic pressure (Eq. (11.4)). For a given transmembrane pressure, increasing the osmotic pressure will decrease the flux through the membrane (Eq. (11.6)). In ultrafiltration membranes, the influence of larger molecules on osmotic pressure is small since the molecules are retained on the membrane surface. However, the retained molecules can lead to precipitation and formation of a solid layer at the membrane surface. This phenomenon of gel formation will be explained later in this section.

The concentration profiles of a solute adjacent to the membrane surface can be described using Figure 11.9. As permeation of a solute proceeds through the membrane, the solute concentration at the membrane surface, c_w , increases compared with the solute concentration in the bulk fluid, c_b . This is attributed to convective transport of

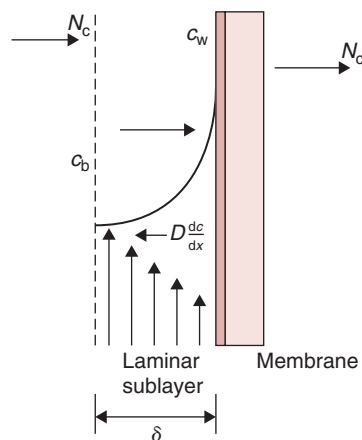


Figure 11.9 A profile of solute concentration during ultrafiltration, showing concentration polarization. (From Schweitzer, 1979)

the solute toward the membrane. Due to the increased concentration of the solute at the membrane surface, there will be a concentration gradient set up between the concentration at the wall and the concentration in the bulk, resulting in back diffusion of the solute. At steady state, the back diffusion must equal the convective flux. The rate of convective transport of the solute can be written as

$$\text{convective transport of a solute} = N_c c \quad (11.17)$$

where N_c is the permeate flux rate, $\text{m}^3/(\text{m}^2 \text{s})$; and c is the concentration of a solute (kg/m^3).

The solute rejected at the wall moves back into the bulk liquid. The back-transport flux rate of the solute is expressed as

$$\text{flux rate of a solute due to back transport} = D \frac{dc}{dx} \quad (11.18)$$

where D is the diffusion coefficient of the solute (m^2/s).

Under steady-state conditions, the convective transport of a solute equals the back transport due to concentration gradient; thus,

$$D \frac{dc}{dx} = N_c c \quad (11.19)$$

Separating the variables and integrating with boundary conditions, $c = c_w$ at $x = 0$ and $c = c_b$ at $x = \delta$, we obtain

$$\frac{N_c \delta}{D} = \ln \frac{c_w}{c_b} \quad (11.20)$$

$$N_c = \frac{D}{\delta} \ln \frac{c_w}{c_b} \quad (11.21)$$

The preceding equation may be rearranged as

$$\frac{c_w}{c_b} = \exp \left(\frac{N_c \delta}{D} \right) \quad (11.22)$$

According to Equation (11.22), c_w/c_b , also referred to as concentration modulus, increases exponentially with transmembrane flux and with the thickness of the boundary layer, and it decreases exponentially with increasing value of solute diffusivity. Thus, the influence of concentration polarization is particularly severe with membranes that

have high permeability, such as ultrafiltration membranes, and solutes that have high molecular weights. The thickness of the boundary layer is the result of the flow conditions next to the membrane surface.

This derivation is valid for both reverse osmosis and ultrafiltration membranes. In the case of ultrafiltration membranes, as observed in the preceding paragraph, the solute concentration will increase rapidly and the solute may precipitate, forming a gel layer (Fig. 11.10). The resistance to permeation by this gel layer may become more prominent than the membrane resistance. Under these conditions, the solute concentration at the surface of the gel layer, referred to as c_g , becomes a constant and it is no longer influenced by the solute concentration in the bulk, the membrane characteristics, operating pressures, or the fluid flow conditions.

For situations when the pressure has no more influence on the flux, we can rewrite Equation (11.22) as

$$N_c = k_m \ln \left(\frac{c_w}{c_b} \right) \quad (11.23)$$

where k_m is the mass transfer coefficient ($L/[m^2 h]$).

Equation (11.23) indicates that the ultrafiltration rate N_c is influenced mainly by the solute concentration in the bulk, c_b , and the mass transfer coefficient, k_m .

The mass transfer coefficient can be evaluated using dimensional analysis.

$$N_{sh} = (N_{Re})^a (N_{Sc})^b \quad (11.24)$$

where

$$\text{Sherwood number, } N_{Sh} = \frac{k_m d_c}{D}$$

$$\text{Reynolds number, } N_{Re} = \frac{\rho \bar{u} d_c}{\mu}$$

$$\text{Schmidt number, } N_{Sc} = \frac{\mu}{\rho D}$$

$$d_c = 4 \left(\frac{\text{cross section available for flow}}{\text{wetted perimeter}} \right)$$

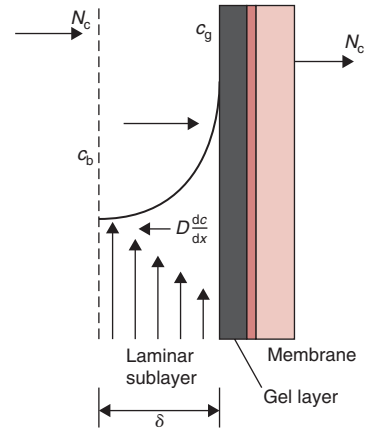


Figure 11.10 A concentration profile showing the formation of a gel layer on an ultrafiltration membrane. (From Schweitzer, 1979)

For turbulent flow,

$$N_{Sh} = 0.023(N_{Re})^{0.8}(N_{Sc})^{0.33} \quad (11.25)$$

Examples 11.4 and 11.5 illustrate the use of dimensional analysis to determine the mass-transfer coefficient (Cheryan, 1998).

Typical materials used in ultrafiltration membranes include cellulose acetate, polyvinyl chloride, polysulfones, polycarbonates, and polyacrylonitriles.

Example 11.4

A reverse osmosis (RO) system is being used to concentrate apple juice at 20°C with an initial total solids content of 10.75%. The system contains 10 tubes with 1.5 cm diameter and the feed rate is 150 kg/min. The density of the feed stream is 1050 kg/m³ and the viscosity is 1 × 10⁻³ Pa s. Estimate the flux of water through the RO membrane, when the solute diffusivity is 8 × 10⁻⁸ m²/s, and operating pressure is 6895 kPa.

Given

Feed concentration = 0.1075 kg solids/kg product

Feed rate = 150 kg/min or 15 kg/min per tube

Product density = 1050 kg/m³

Product viscosity = 1 × 10⁻³ Pa s

Approach

The molar concentration at the membrane boundary will be estimated using Equations (11.7) and (11.10). After the concentration at the boundary is determined, the flux of water will be estimated from Equation (11.7).

Solution

1. Since Equation (11.10) requires the convective mass transfer coefficient k_m as input, the dimensionless relationship (Eq. (11.24)) will be used.
2. Based on the mass flow rate of 15 kg/min:

$$\begin{aligned} \bar{u} &= \frac{15[\text{kg/min}]}{\left(\pi \frac{(1.5/100)^2}{4} \right) [\text{m}]^2 \times 60[\text{s/min}] \times 1050[\text{kg/m}^3]} \\ &= 1.35 \text{ m/s} \end{aligned}$$

3. Then the Reynolds number is:

$$N_{Re} = \frac{1050[\text{kg/m}^3] \times 1.35[\text{m/s}] \times 0.015[\text{m}]}{1.0 \times 10^{-3}[\text{Pa s}]} = 21,263$$

4. Then the Schmidt number is:

$$N_{Sc} = \frac{1 \times 10^{-3} [\text{Pa s}]}{1050 [\text{kg/m}^3] \times (8 \times 10^{-8}) [\text{m}^2/\text{s}]} = 11.9$$

5. Using Equation (11.25),

$$N_{Sh} = 0.023(21,263)^{0.8}(11.9)^{0.33} = 150.9$$

and

$$k_m = \frac{150.9 \times (8 \times 10^{-8})}{0.015} = 8.05 \times 10^{-4} \text{ m}^2/\text{s}$$

6. Using Equation (11.7), with $K_p = 3.379 \times 10^{-6} \text{ kg water}/(\text{m}^2 \text{ s kPa})$ (for cellulose acetate membrane) and using Equation (11.4),

$$\begin{aligned} \Pi &= \frac{0.1075 \times 1050 [\text{kg/m}^3] \times 8.314 [\text{m}^3 \text{ kPa}/(\text{kg mol K})] \times 293 [\text{K}]}{180 [\text{kg/kg mol}]} \\ &= 1528 \text{ kPa} \end{aligned}$$

$$X_{c2} = \text{unknown}$$

$$X_{c3} = \text{assumed to be zero}$$

$$\Delta P = 6895 \text{ kPa}$$

7. Using Equation (11.10), where $c_1 = (0.1075 \text{ kg solids/kg product}) (1050 \text{ kg product}/\text{m}^3 \text{ product})$

$$c_1 = 112.875 \text{ kg solids}/\text{m}^3 \text{ product}$$

$$k_m = 8.05 \times 10^{-4} \text{ m}^2/\text{s}$$

$$X_{c3} = \text{assumed to be zero}$$

$$X_{c1} = 0.0438 \text{ (carbon weight fraction from Table 11.3)}$$

then

$$\begin{aligned} N &= 112.875 [\text{kg solids}/\text{m}^3 \text{ product}] \times (8.05 \times 10^{-4}) [\text{m}^2/\text{s}] \\ &\times \ln \left[\frac{X_{c2}}{0.0438} \right] \end{aligned}$$

8. Using Equations (11.7) and (11.10):

$$X_{c2} = 0.0565$$

becomes the weight fraction of carbon at the membrane boundary

9. Using the magnitude of X_{c2}

$$\begin{aligned} N &= 23.1 \times 10^{-3} \text{ kg water}/(\text{m}^2 \text{ s}) \\ &= 1.388 \text{ kg water}/(\text{m}^2 \text{ min}) \\ &= 83.3 \text{ kg water}/(\text{m}^2 \text{ h}) \end{aligned}$$

Example 11.5

Determine the flux rate expected in a tubular ultrafiltration system being used to concentrate milk. The following conditions apply: density of milk = 1.03 g/cm^3 , viscosity = 0.8 cP , diffusivity = $7 \times 10^{-7} \text{ cm}^2/\text{s}$, $c_B = 3.1\%$ weight per unit volume. Diameter of tube = 1.1 cm , length = 220 cm , number of tubes = 15 , and fluid velocity = 1.5 m/s .

Given

Density of milk = $1.03 \text{ g/cm}^3 = 1030 \text{ kg/m}^3$

Viscosity of milk = $0.8 \text{ cP} = 0.8 \times 10^{-3} \text{ Pa s}$

Mass diffusivity = $7 \times 10^{-7} \text{ cm}^2/\text{s} = 7 \times 10^{-11} \text{ m}^2/\text{s}$

Bulk concentration = 0.031 kg/m^3

Gel concentration = 0.22 kg/m^3

Tube diameter = 0.011 m

Length of tube = $220 \text{ cm} = 2.2 \text{ m}$

Number of tubes = 15

Fluid velocity = 1.5 m/s

Approach

The convective mass transfer coefficient will be estimated by the dimensionless equation, and the flux of water will be determined by Equation (11.23).

Solution

1. Computation of the Reynolds number:

$$N_{Re} = \frac{1030[\text{kg/m}^3] \times 1.5[\text{m/s}] \times 0.011[\text{m}]}{0.8 \times 10^{-3}[\text{Pa s}]} = 21,244$$

2. Computation of Schmidt number:

$$N_{Sc} = \frac{0.8 \times 10^{-3}[\text{Pa s}]}{1030[\text{kg/m}^3] \times (7 \times 10^{-11})[\text{m}^2/\text{s}]} = 11.1 \times 10^3$$

3. Since flow is turbulent

$$N_{Sh} = 0.023(21,244)^{0.8}(11.1 \times 10^3)^{0.33}$$

$$N_{Sh} = 1440$$

4. Then

$$k_m = \frac{1440 \times (7 \times 10^{-11})[\text{m}^2/\text{s}]}{0.011[\text{m}]} = 9.16 \times 10^{-6} \text{ m/s}$$

5. Using Equation (11.23),

$$\begin{aligned} N &= (9.16 \times 10^{-6})[\text{m/s}] \times 998.2[\text{kg/m}^3] \times \ln\left(\frac{0.22}{0.031}\right) \\ &= 0.018 \text{ kg}/(\text{m}^2 \text{ s}) \end{aligned}$$

where density of water at 20°C is used

$$N = 64.8 \text{ kg water}/(\text{m}^2 \text{ h})$$

6. By using the membrane surface area

$$A = \pi (0.011)(2.2) = 0.076 \text{ m}^2/\text{tube}$$

$$\text{Total area} = 0.076 (15 \text{ tubes}) = 1.14 \text{ m}^2$$

7. Total flux of water through membrane:

$$\begin{aligned} \text{flux} &= (64.8 \text{ kg water}/[\text{m}^2 \text{ h}]) (1.14 \text{ m}^2) \\ &= 73.87 \text{ kg water/h} \end{aligned}$$

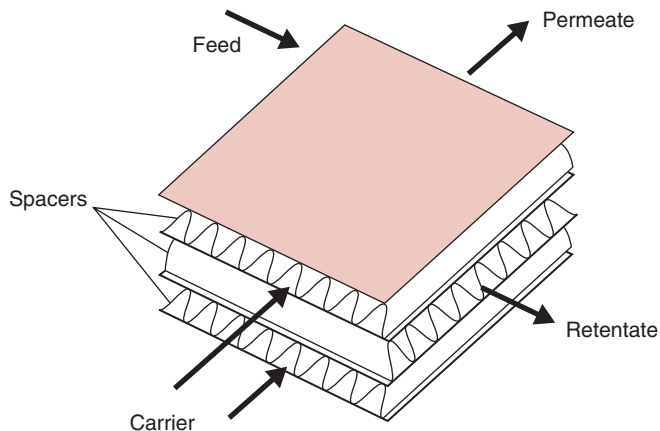
11.6 TYPES OF REVERSE-OSMOSIS AND ULTRAFILTRATION SYSTEMS

Four major types of membrane devices are used for reverse-osmosis and ultrafiltration systems: plate-and-frame, tubular, spiral-wound, and hollow-fiber. Table 11.4 provides a general comparison among

Table 11.4 Comparison of Process-Related Characteristics for Membrane Module Configurations

Characteristic	Module type			
	Plate-and-frame	Spiral-wound	Tube-in-shell	Hollow-fiber
Packing density (m^2/m^3)	200–400	300–900	150–300	9000–30,000
Permeate flux ($\text{m}^3/[\text{m}^2 \text{ day}]$)	0.3–1.0	0.3–1.0	0.3–1.0	0.004–0.08
Flux density ($\text{m}^3/[\text{m}^3 \text{ day}]$)	60–400	90–900	45–300	36–2400
Feed channel diameter (mm)	5	1.3	13	0.1
Method of replacement	As sheets	As module assembly	As tubes	As entire module
Replacement labor	High	Medium	High	Medium
Pressure drop				
Product side	Medium	Medium	Low	High
Feed side	Medium	Medium	High	Low
Concentration polarization	High	Medium	High	Low
Suspended solids buildup	Low/medium	Medium/high	Low	High

■ **Figure 11.11** A module used in a plate-and-frame membrane system.



these four types. A brief description of each type of membrane is given in the following.

11.6.1 Plate-and-Frame

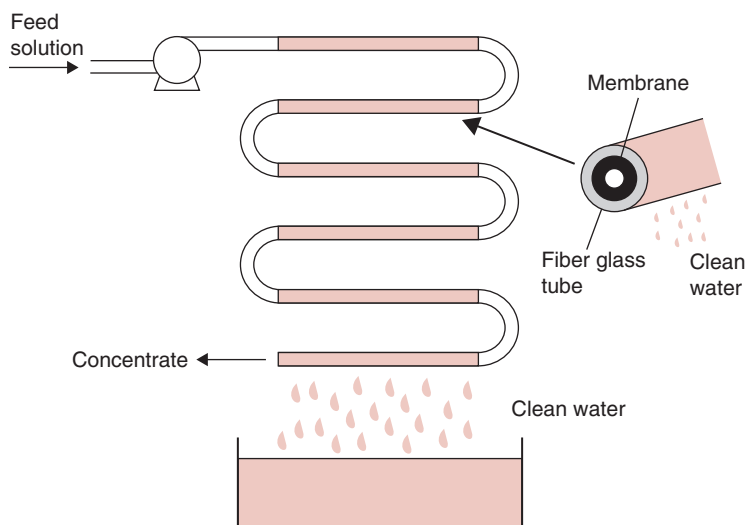
The plate-and-frame membrane systems involve a large number of flat membranes that are sandwiched together with the use of spacers. As shown in Figure 11.11, the spacers provide the channels for flow. The membranes (usually 50 to 500 μm thick) are bonded on a porous, inert matrix that offers little resistance to the fluid flow. The flow of feed and retentate occur in alternate channels. This arrangement of membranes is very similar to the plate heat-exchanger described in Chapter 4.

11.6.2 Tubular

The tubular design was the first commercial design of a reverse-osmosis system. It consists of a porous tube coated with the membrane material such as cellulose acetate. Typically, feed solution is pumped into the tube through one end and forced in the radial direction through the porous pipe and the membrane (Fig. 11.12). Water drips from the outer surface of the membrane while the concentrated stream “retentate” leaves through the outer end of the tube. This type of reverse-osmosis device is expensive to use for high volumetric flow rates, since the membrane area is relatively small.

11.6.3 Spiral-Wound

To increase the membrane surface area per unit volume, a spiral-wound configuration was a key commercial development following



W

Figure 11.12 A tubular membrane system. (From Applegate, 1984)

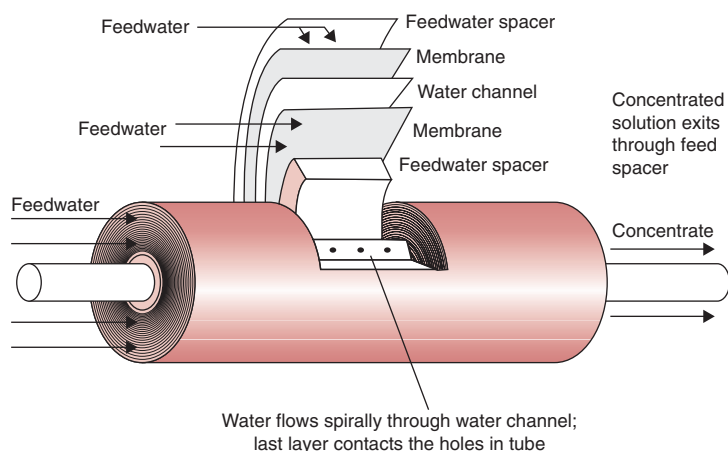
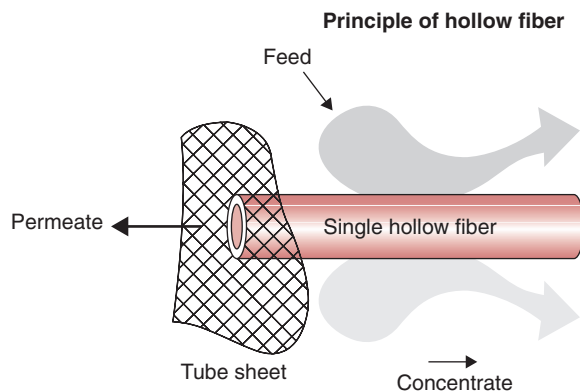
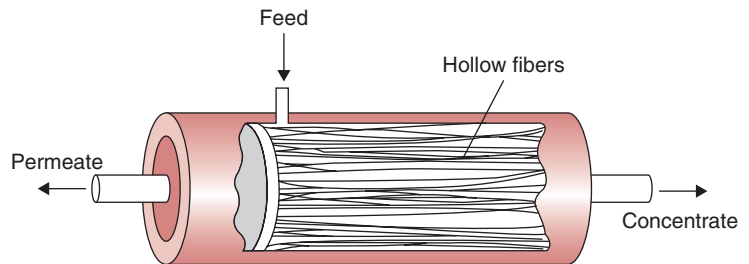


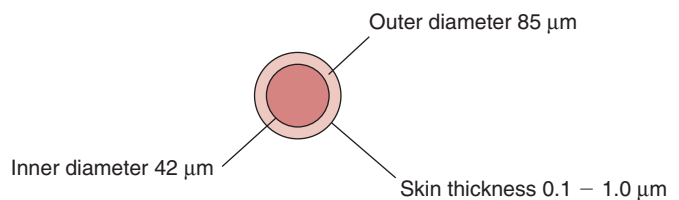
Figure 11.13 A spiral-wound membrane system with a cross-sectional view showing the water flow patterns.

the tubular design. This design, shown in Figure 11.13, can be visualized as a composite of multilayers. The two layers of membrane are separated by a plastic mesh, and on either side of the membrane is a porous sheet. These five layers are then spirally wound around a perforated tube. The ends of the rolled layers are sealed to prevent mixing of feed and product streams. The whole spiral assembly is housed in a tubular metal jacket that can withstand applied pressures. Feed is pumped through the perforated tube on one side of the spiral-wound roll. Feed enters inside the plastic mesh, which aids in creating

■ **Figure 11.14** A hollow-fiber membrane system.



Typical hollow fiber cross section



turbulence and minimizing fouling. The feed then permeates the membrane in a radial direction and exits the membrane into porous layers. The permeate (water) transports through the porous sheet in a spiral manner and leaves the assembly through the exit tube, whereas the retentate leaves through the other end of the spiral-wound roll. Typical dimensions of spiral cartridges are 11 cm in diameter, 84 cm in length, with 0.7 mm membrane spacing, and 5 m² area. The spiral-wound systems are similar for both reverse-osmosis and ultrafiltration applications.

11.6.4 Hollow-Fiber

A hollow-fiber, made out of aramid, was first introduced by DuPont in 1970. Hollow-fibers, finer than human hair, have an internal diameter of about $40\text{ }\mu\text{m}$, and an external diameter of about $85\text{ }\mu\text{m}$. A large number of hollow-fibers (several millions) are arranged in a bundle around a perforated distributor tube (Fig. 11.14). In the reverse-osmosis system, the fibers are glued with epoxy to either end. These fibers provide extremely large surface areas; thus, hollow fiber membrane systems can be made very compact. Feed water is introduced through the distributor pipe; the permeate flows through the annular space of the fibers into the hollow bore of the fibers and moves to the tube sheet end, discharging from the exit port. The retentate or brine stays on the outside of the fibers and leaves the device from the brine port. Hollow fibers are used mainly to purify water. Liquid foods are difficult to handle in hollow fiber systems because of problems associated with fouling of the fibers.

The hollow-fibers used for ultrafiltration membranes are quite different from those used for reverse-osmosis systems. For ultrafiltration applications, hollow fibers are made from acrylic copolymers.

Most membrane systems in the food industry have been in dairy and fruit juice applications. Other commercial applications include processing of coffee, tea, alcohol, gelatins, eggs, and blood, and corn refining and soybean processing.

PROBLEMS

- 11.1 An ultrafiltration system is being used to concentrate gelatin. The following data were obtained: A flux rate was 1630 L/m^2 per day at 5% solids by weight concentration, and a flux rate was 700 L/m^2 per day at 10% solids by weight. Determine the concentration of the gel layer and the flux rate at 7% solids.
- 11.2 Estimate the osmotic pressure of a 20% sucrose solution at a temperature of 10°C .
- 11.3 Determine the transmembrane pressure required to maintain a flux of $220\text{ kg}/(\text{m}^2\text{ h})$ in a reverse-osmosis system when the feed solution is 6% total solids whey. The permeability coefficient of the membrane is $0.02\text{ kg}/(\text{m}^2\text{ h kPa})$.
- 11.4 An ultrafiltration system is being used to concentrate orange juice at 30°C from an initial solids content of 10%

to 35% total solids. The ultrafiltration system contains six tubes with 1.5 cm diameter. The product properties include density of 1100 kg/m^3 , viscosity of $1.3 \times 10^{-3} \text{ Pa s}$, and solute diffusivity of $2 \times 10^{-8} \text{ m}^2/\text{s}$. The concentration of solute at the membrane surface is 25%. Estimate the length of ultrafiltration tubes required to achieve the desired concentration increase.

- *11.5** A reverse osmosis (RO) system, with 100 tubes of 10 m length and 1.0 cm diameter, is used to concentrate orange juice from 11% to 40% total solids. The permeability coefficient for the RO membrane is $0.2 \text{ kg water/m}^2 \text{ hr kPa}$ and the product feed rate is 200 kg/min .
- Determine the flux of water (kg water/hr) through the membrane needed to accomplish the magnitude of concentration indicated.
 - Estimate the difference in transmembrane hydrostatic pressure (ΔP) needed for the system to operate.

LIST OF SYMBOLS

A	area (m^2)
A_e	effective membrane area (m^2)
c	concentration of a solute (kg/m^3)
c_b	concentration in bulk stream (kg/m^3)
c_f	concentration of a solute in the feed stream (kg/m^3)
c_g	concentration at gel layer surface (kg/m^3)
c_p	concentration of a solute in permeate stream (kg/m^3)
c_w	concentration of water (kg/m^3)
d_c	characteristic dimension (m)
D	diffusion coefficient of the solute (m^2/s)
Δc	differential of solute concentration (kg/m^3)
δ	laminar sublayer
E	energy consumption (J)
F	Faraday's constant (96,500 A/s equivalent)
I	electric current through the stack (A)
K	membrane permeability constant ($\text{kg}/[\text{m}^2 \text{ kPa s}]$)
k_m	mass transfer coefficient ($\text{L}/[\text{m}^2 \text{ h}]$)
K_p	permeability coefficient of the membrane

*Indicates an advanced level in solving.

K_s	coefficient of solute permeability through the membrane (L/m)
K_w	coefficient of water permeability through the membrane (kg/[m ² kPa])
\dot{m}	feed solution flow rate (L/s)
\dot{m}_p	product flow rate (kg/s)
\dot{m}_s	solute flow rate (kg/s)
\dot{m}_w	water flow rate (kg/s)
M	molecular weight
μ	viscosity (Pa s)
n	number of cells in the stack
N	permeate flux rate (m ³ /[m ² s])
N_c	convective permeate flux rate (m ³ /[m ² s])
N_{Re}	Reynolds Number, dimensionless
N_{Sc}	Schmidt Number, dimensionless
N_{Sh}	Sherwood Number, dimensionless
N_w	pure water permeation rate for an effective area of membrane surface (m ³ /[m ² s])
Π	osmotic pressure (Pa)
$\Delta\Pi$	difference in the osmotic pressure between the feed solution and the permeate
ΔP	difference in transmembrane hydrostatic pressure (Pa)
ρ	density (kg/m ³)
R	universal gas constant (m ³ Pa/[kg mol K])
R_c	resistance of the cell (Ω)
R_f	retention factor
R_j	rejection factor
S_p	solute transport parameter
T	temperature (absolute)
t	time (s)
U	current utilization factor
\bar{u}	mean velocity (m/s)
V_m	molar volume of pure liquid
X_A	mole fraction of pure liquid
X_c	weight fraction of carbon in the solution being separated
Z	membrane performance conversion percentage
z	electrochemical valence

■ BIBLIOGRAPHY

Applegate, L. (1984). Membrane separation processes. *Chem. Eng.* (June 11), 64–89.

- Cheryan, M. (1998). *Ultrafiltration Handbook*. Technomic Publishing Co., Lancaster, Pennsylvania.
- Cheryan, M. (1989). Membrane separations: Mechanisms and models. In *Food Properties and Computer-Aided Engineering of Food Processing Systems*, R. P. Singh and A. Medina, eds. Kluwer Academic Publishers, Amsterdam.
- Lacey, R. E. (1972). Membrane separation processes. *Chem. Eng.* (Sept. 4), 56–74.
- Matsuura, T., Baxter, A. G., and Sourirajan, S. (1973). Concentration of juices by reverse osmosis using porous cellulose acetate membranes. *Acta Aliment.* 2: 109–150.
- McCabe, W. L., Smith, J. C., and Harriott, P. (1985). *Unit Operations of Chemical Engineering*. McGraw-Hill, New York.
- Schweitzer, P. A. (1979). *Handbook of Separation Processes*. McGraw-Hill, New York.

Dehydration

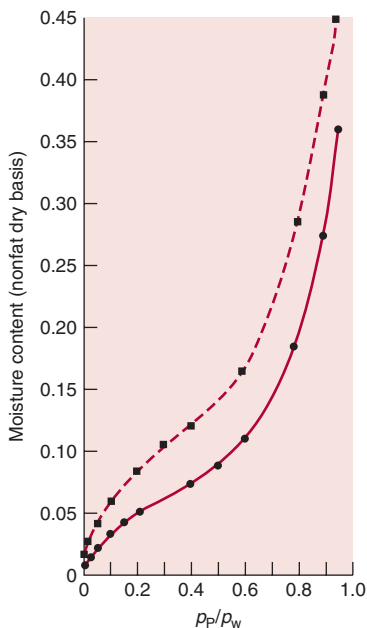
The removal of moisture from a food product is one of the oldest preservation methods. By reducing the water content of a food product to very low levels, the opportunity for microbial deterioration is eliminated and the rates of other deteriorative reactions are reduced significantly. In addition to preservation, dehydration reduces product mass and volume by significant amounts and improves the efficiency of product transportation and storage. Often, the dehydration of a food product results in a product that is more convenient for consumer use.

The preservation of fruits, vegetables, and similar food products by dehydration offers a unique challenge. Due to the structural configuration of these types of products, the removal of moisture must be accomplished in a manner that will be the least detrimental to product quality. This requires that the process produce a dry product that can be returned to approximately the original quality after rehydration. To achieve the desired results for dehydrated foods, with a defined physical structure, the process must provide the optimum heat and mass transfer within the product. The design of these processes requires careful analysis of the heat and mass transfer occurring within the product structure. Only through analysis and understanding of the transfer processes can the maximum efficiency and optimum quality be achieved.

12.1 BASIC DRYING PROCESSES

To achieve moisture removal from a food product in the most efficient manner, the design of the dehydration system must account for the various processes and mechanisms occurring within the product.

All icons in this chapter refer to the author's website which is independently owned and operated. Academic Press is not responsible for the content or operation of the author's website. Please direct your website comments and questions to the author: Professor R. Paul Singh, Department of Biological and Agricultural Engineering, University of California, Davis, CA 95616, USA.
Email: rps@rpaulsingh.com



■ **Figure 12.1** Equilibrium moisture content isotherm for a freeze-dried food product, illustrating hysteresis. ■, Desorption; ●, adsorption. (Adapted from Heldman and Singh, 1981)

These processes and mechanisms are of particular importance for foods with a defined physical structure, due to the influence of product structure on the movement of moisture from the product.

12.1.1 Water Activity

One of the important parameters in food dehydration is the equilibrium condition that establishes a limit to the process. Although the parameter represents an important portion of the gradient for moisture movement, water activity is important in analysis of storage stability for dry foods.

By definition, water activity is the equilibrium relative humidity of the product divided by 100. For most food products, the relationship between moisture content and water activity is as illustrated in Figure 12.1. The sigmoid isotherm is typical for dry foods, as is the difference between the adsorption and desorption isotherms for the same product. In addition to the water activity values establishing the storage stability of the product against various deterioration reactions (Fig. 12.2), the equilibrium moisture contents are the lower limit of the gradient for moisture removal from the product. As might be expected, higher temperatures result in lower equilibrium moisture content and a large moisture gradient for moisture movement.

One of the most widely used models for description of equilibrium moisture isotherms is the GAB model (named after Guggenheim-Anderson-DeBoer). This model is used to fit and draw the sorption data obtained for a given food. The GAB model is expressed as follows:

$$\frac{w}{w_m} = \frac{Cka_w}{(1 - ka_w)(1 - ka_w + Cka_w)} \quad (12.1)$$

where:

- w = the equilibrium moisture content, fraction dry basis
- w_m = the monolayer moisture content, fraction dry basis
- C = the Guggenheim constant = $C' \exp(H_1 - H_m)/RT$
- H_1 = heat of condensation of pure water vapor
- H_m = total heat of sorption of the first layer on primary sites
- k = a factor correcting properties of multiplayer with respect to the bulk liquid,
 $= k' \exp(H_1 - H_q)/RT$
- H_q = total heat of sorption of the multilayers.

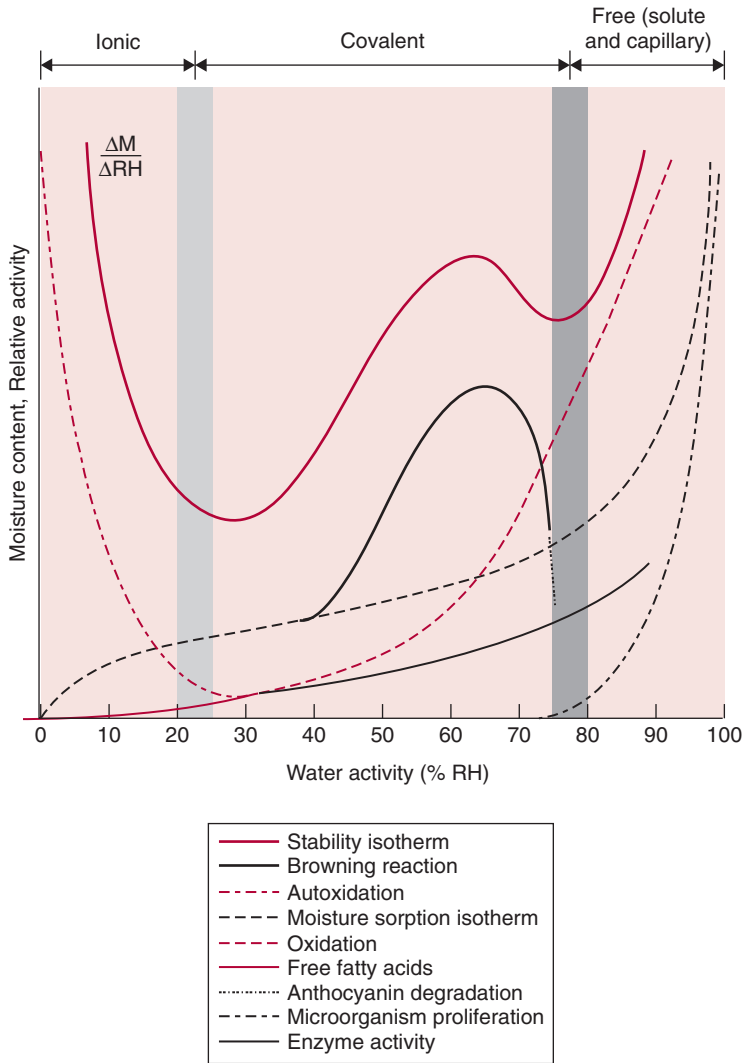


Figure 12.2 Influence of water activity on rates of various deterioration reactions in foods. (From Rockland and Nishi, 1980. Copyright © by Institute of Food Technologists. Reprinted with permission of *Food Technology*.)

The GAB model can be used to a maximum water activity of 0.9. The following procedure is suggested by Bizot (1983) to fit data on water activities and equilibrium moisture content.

Equation (12.1) can be transformed as follows:

$$\frac{a_w}{w} = \alpha a_w^2 + \beta a_w + \gamma \quad (12.2)$$

where

$$\alpha = \frac{k}{w_m} \left[\frac{1}{C} - 1 \right]$$

$$\beta = \frac{1}{w_m} \left[1 - \frac{2}{C} \right]$$

$$\gamma = \frac{1}{w_m C k}$$

Equation (12.2) indicates that the GAB equation is a three-parameter model. The water activity and equilibrium moisture content data are regressed using Equation (12.2), and values of the three coefficients α , β , and γ are obtained. From these coefficients, the values of k , w_m , and C can be obtained.

Example 12.1

A dry food product has been exposed to a 30% relative-humidity environment at 15°C for 5 h without a weight change. The moisture content has been measured and is at 7.5% (wet basis). The product is moved to a 50% relative-humidity environment, and a weight increase of 0.1 kg/kg product occurs before equilibrium is achieved.

- Determine the water activity of the product in the first and second environments.
- Compute the moisture contents of the product on a dry basis in both environments.

Given

Equilibrium relative humidity = 30% in first environment

Product moisture content = 7.5% wet basis in first environment

For 30% relative-humidity environment, moisture content will be 0.075 kg H₂O/kg product.

Approach

Water activities of product are determined by dividing equilibrium relative humidity by 100. Dry-basis moisture contents for product are computed by expressing mass of water in product on a per unit dry solids basis.

Solution

- The water activity of the food product is equilibrium relative humidity divided by 100; the water activities are 0.3 in the first environment and 0.5 in the second.

2. The dry basis moisture of the product at equilibrium in 30% RH is

$$7.5\% = \frac{7.5 \text{ kg H}_2\text{O}}{100 \text{ kg product}} = 0.075 \text{ kg H}_2\text{O/kg product}$$

$$\begin{aligned} \frac{0.075 \text{ kg H}_2\text{O/product}}{0.925 \text{ kg solids/kg product}} &= 0.08108 \text{ kg H}_2\text{O/kg solids} \\ &= 8.11\% \text{ MC (dry basis)} \end{aligned}$$

3. Based on weight gain at 50% RH,

$$\begin{aligned} 0.075 \text{ kg H}_2\text{O/kg product} + 0.1 \text{ kg H}_2\text{O/kg product} \\ = 0.175 \text{ kg H}_2\text{O/kg product} = 17.5\% \text{ MC (wet basis)} \end{aligned}$$

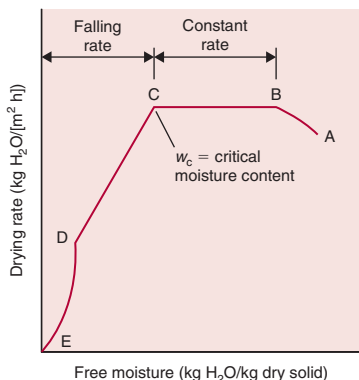
or

$$\begin{aligned} 0.175 \text{ kg H}_2\text{O/kg product} &= 0.212 \frac{\text{kg H}_2\text{O}}{\text{kg solids}} \\ &= 21.2\% \text{ MC (dry basis)} \end{aligned}$$

12.1.2 Moisture Diffusion

Significant amounts of moisture removal from a food product will occur due to diffusion of liquid water and/or water vapor through the product structure. This phase of moisture movement will follow the evaporation of water at some location within the product. The rate of moisture diffusion can be estimated by the expressions for molecular diffusion, as introduced in Chapter 10. The mass flux for moisture movement is a function of the vapor pressure gradient, as well as the mass diffusivity for water vapor in air, the distance for water vapor movement within the product structure, and temperature. Since thermal energy is required for moisture evaporation, the process becomes simultaneous heat and mass transfer.

The moisture removal from the product will depend, in part, on convective mass transfer at the product surface. Although this transport process may not be rate-limiting, the importance of maintaining the optimum boundary conditions for moisture transport cannot be overlooked.



■ **Figure 12.3** Illustration of constant-rate and falling-rate drying periods. (Adapted from Heldman and Singh, 1981)

12.1.3 Drying-Rate Curves

The removal of moisture from a typical food product will follow a series of drying rates, as illustrated in Figure 12.3. The initial removal of moisture (AB) occurs as the product and the water within the product experience a slight temperature increase. Following the initial stages of drying, significant reductions in moisture content will occur at a constant rate (BC) and at a constant product temperature. The constant-rate drying period occurs with the product at the wet bulb temperature of the air. In most situations, the constant-rate drying period will continue until the moisture content is reduced to the critical moisture content. At moisture contents below the critical moisture content, the rate of moisture removal decreases with time. One or more falling-rate drying periods (CE) will follow. The critical moisture content is well defined due to the abrupt change in the rate of moisture removal.

12.1.4 Heat and Mass Transfer

As indicated previously, the removal of moisture from a food product involves simultaneous heat and mass transfer. Heat transfer occurs within the product structure and is related to the temperature gradient between the product surface and the water surface at some location within the product. As sufficient thermal energy is added to the water to cause evaporation, the vapors are transported from the water surface within the product to the product surface. The gradient causing moisture-vapor diffusion is vapor pressure at the liquid water surface, as compared with the vapor pressure of air at the product surface. The heat and the mass transfer within the product structure occurs at the molecular level, with heat transfer being limited by thermal conductivity of the product structure, whereas mass transfer is proportional to the molecular diffusion of water vapor in air.

At the product surface, simultaneous heat and mass transfer occurs but is controlled by convective processes. The transport of vapor from the product surface to the air and the transfer of heat from the air to the product surface is a function of the existing vapor pressure and temperature gradients, respectively, and the magnitude of the convective coefficients at the product surface.

Since the drying rate is directly proportional to the slowest of the four processes, it is important to account for all processes. In most products, the heat and mass transfer within the product structure will be rate-limiting processes.

The initial moisture content of a food product is 77% (wet basis), and the critical moisture content is 30% (wet basis). If the constant drying rate is $0.1 \text{ kg H}_2\text{O}/(\text{m}^2 \text{ s})$, compute the time required for the product to begin the falling-rate drying period. The product has a cube shape with 5-cm sides, and the initial product density is $950 \text{ kg}/\text{m}^3$.

Example 12.2

Given

Initial moisture content = 77% wet basis

Critical moisture content = 30% wet basis

Drying rate for constant rate period = $0.1 \text{ kg H}_2\text{O}/(\text{m}^2 \text{ s})$

Product size = cube with 5-cm sides

Initial product density = $950 \text{ kg}/\text{m}^3$

Approach

The time for constant-rate drying will depend on mass of water removed and the rate of water removal. Mass of water removed must be expressed on dry basis, and rate of water removal must account for product surface area.

Solution

1. The initial moisture content is

$$0.77 \text{ kg H}_2\text{O}/\text{kg product} = 3.35 \text{ kg H}_2\text{O}/\text{kg solids}$$

2. The critical moisture content is

$$0.3 \text{ kg H}_2\text{O}/\text{kg product} = 0.43 \text{ kg H}_2\text{O}/\text{kg solids}$$

3. The amount of moisture to be removed from product during constant-rate drying will be

$$3.35 - 0.43 = 2.92 \text{ kg H}_2\text{O}/\text{kg solids}$$

4. The surface area of the product during drying will be

$$0.05 \text{ m} \times 0.05 \text{ m} = 2.5 \times 10^{-3} \text{ m}^2/\text{side}$$

$$2.5 \times 10^{-3} \times 6 \text{ sides} = 0.015 \text{ m}^2$$

5. The drying rate becomes

$$0.1 \text{ kg H}_2\text{O}/(\text{m}^2 \text{ s}) \times 0.015 \text{ m}^2 = 1.5 \times 10^{-3} \text{ kg H}_2\text{O}/\text{s}$$

6. Using the product density, the initial product mass can be established.

$$950 \text{ kg}/\text{m}^3 \times (0.05)^3 \text{ m}^3 = 0.11875 \text{ kg product}$$

$$0.11875 \text{ kg product} \times 0.23 \text{ kg solid}/\text{kg product} = 0.0273 \text{ kg solid}$$

7. The total amount of water to be removed becomes

$$2.92 \text{ kg H}_2\text{O/kg solids} \times 0.0273 \text{ kg solids} = 0.07975 \text{ kg H}_2\text{O}$$

8. Using the drying rate, the time for constant-rate drying becomes

$$\frac{0.07975 \text{ kg H}_2\text{O}}{1.5 \times 10^{-3} \text{ kg H}_2\text{O/s}} = 53.2 \text{ s}$$

12.2 DEHYDRATION SYSTEMS

Based on the analysis of heat and mass transfer, the most efficient dehydration systems will maintain the maximum vapor-pressure gradient and maximum temperature gradient between the air and the interior parts of the product. These conditions, along with high convective coefficients at the product surface, can be maintained in several different designs of dehydration systems. The systems we will describe are representative of the systems used for dehydration of foods.

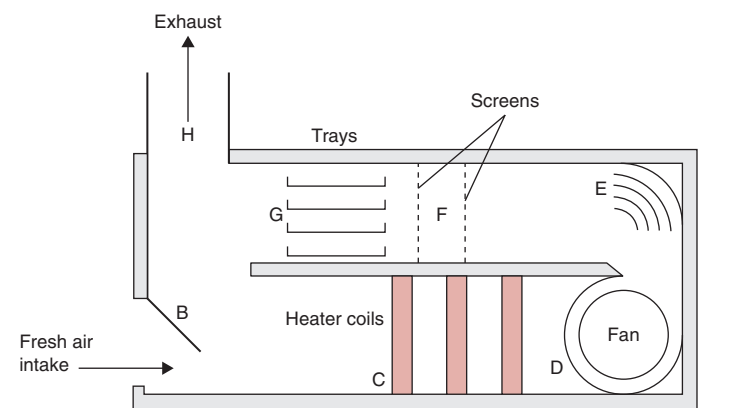
12.2.1 Tray or Cabinet Dryers

These types of drying systems use trays or similar product holders to expose the product to heated air in an enclosed space. The trays holding the product inside a cabinet or similar enclosure (Fig. 12.4) are exposed to heated air so that dehydration will proceed. Air movement over the product surface is at relatively high velocities to ensure that heat and mass transfer will proceed in an efficient manner.

A slight variation of the cabinet dryer incorporates a vacuum within the chamber (Fig. 12.5). This type of dehydration system uses a



Figure 12.4 Schematic illustration of a cabinet-type tray drier. (From Van Arsdel et al., 1973)



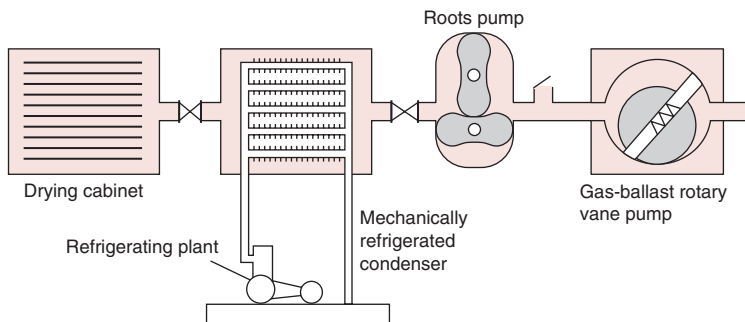


Figure 12.5 Cabinet dryer with vacuum. (From Potter, 1978)

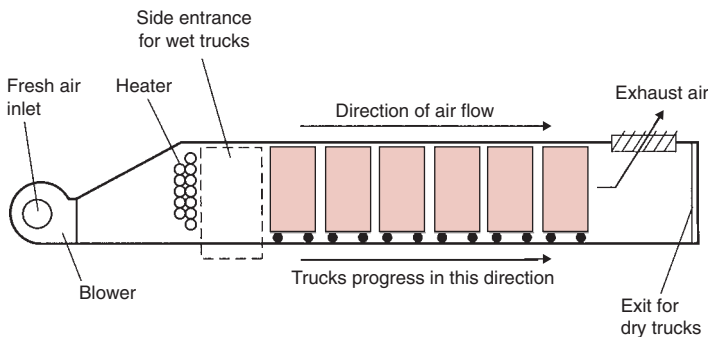


Figure 12.6 Schematic illustration of a concurrent-flow tunnel dryer. (From Van Arsdel, 1951)

vacuum to maintain the lowest possible vapor pressure in the space around the product. The reduction in pressure also reduces the temperature at which product moisture evaporates, resulting in improvements in product quality.

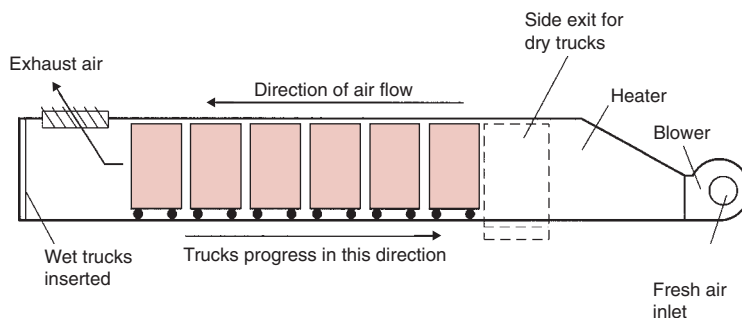
In most cases, cabinet dryers are operated as batch systems and have the disadvantage of nonuniform drying of a product at different locations within the system. Normally, the product trays must be rotated to improve uniformity of drying.

12.2.2 Tunnel Dryers

Figures 12.6 and 12.7 show examples of tunnel dryers. As illustrated, the heated drying air is introduced at one end of the tunnel and moves at an established velocity through trays of products being carried on trucks. The product trucks are moved through the tunnel at a rate required to maintain the residence time needed for dehydration. The product can be moved in the same direction as the air flow to provide concurrent dehydration (Fig. 12.6), or the tunnel can



■ **Figure 12.7** Schematic illustration of a countercurrent-flow tunnel dryer. (From Van Arsdel, 1951)



be operated in countercurrent manner (Fig. 12.7), with the product moving in the direction opposite to air flow. The arrangement used will depend on the product and the sensitivity of quality characteristics to temperature.

With concurrent systems, a high-moisture product is exposed to high-temperature air, and evaporation assists in maintaining lower product temperature. At locations near the tunnel exit, the lower-moisture product is exposed to lower-temperature air. In countercurrent systems, a lower-moisture product is exposed to high-temperature air, and a smaller temperature gradient exists near the product entrance to the tunnel. Although the overall efficiency of the countercurrent system may be higher than the concurrent, product quality considerations may not allow its use. The concept of air recirculation is used whenever possible to conserve energy.

12.2.3 Puff-Drying

A relatively new process that has been applied successfully to several different fruits and vegetables is explosion puff-drying. This process is accomplished by exposing a relatively small piece of product to high pressure and high temperature for a short time, after which the product is moved to atmospheric pressure. This results in flash evaporation of water and allows vapors from the interior parts of the product to escape. Products produced by puff-drying have very high porosity with rapid rehydration characteristics. Puff-drying is particularly effective for products with significant falling-rate drying periods. The rapid moisture evaporation and resulting product porosity contribute to rapid moisture removal during the final stages of drying.

The puff-drying process is accomplished most efficiently by using 2-cm cube shapes. These pieces will dry rapidly and uniformly and

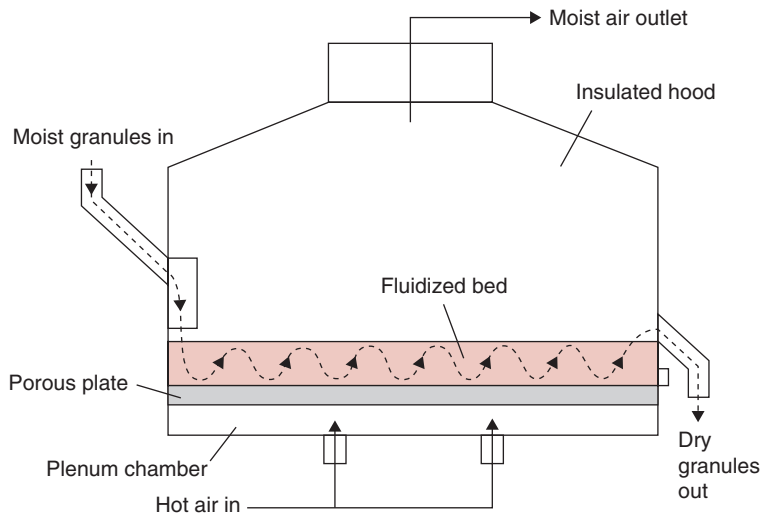


Figure 12.8 Schematic illustration of a fluidized-bed dryer. (From Joslyn, 1963)

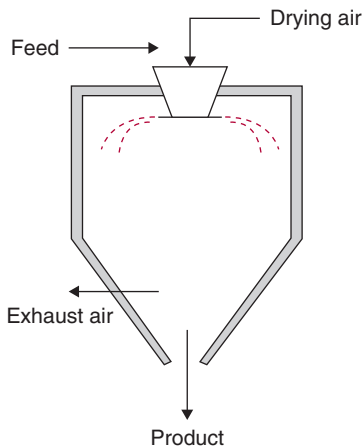
will rehydrate within 15 minutes. Although the process may not have applications for all foods, the superior quality encourages additional investigation of the process.

12.2.4 Fluidized-Bed Drying

A second relatively new design for drying solid-particle foods incorporates the concept of the fluidized bed. In this system, the product pieces are suspended in the heated air throughout the time required for drying. As illustrated in Figure 12.8, the movement of product through the system is enhanced by the change in mass of individual particles as moisture is evaporated. The movement of the product created by fluidized particles results in equal drying from all product surfaces. The primary limitation to the fluidized-bed process is the size of particles that will allow efficient drying. As would be expected, smaller particles can be maintained in suspension with lower air velocities and will dry more rapidly. Although these are desirable characteristics, not all products can be adapted to the process.

12.2.5 Spray Drying

The drying of liquid food products is often accomplished in a spray dryer. Moisture removal from a liquid food occurs after the liquid is atomized or sprayed into heated air within a drying chamber. Although various configurations of the chamber are used, the arrangement

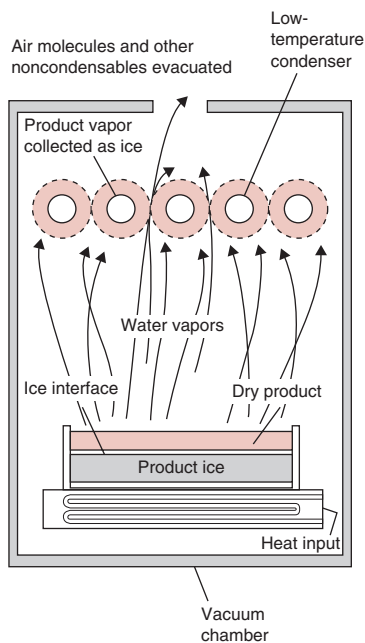


W
Figure 12.9 Schematic illustration of a spray-drying system.

shown in Figure 12.9 illustrates the introduction of liquid droplets into a heated air stream.

While liquid food droplets are moving with the heated air, the water evaporates and is carried away by the air. Much of the drying occurs during a constant-rate period and is limited by mass transfer at the droplet surface. After reaching the critical moisture content, the dry food particle structure influences the falling-rate drying period. During this portion of the process, moisture diffusion within the particle becomes the rate-limiting parameter.

After the dry food particles leave the drying chamber, the product is separated from air in a cyclone separator. The dried product is then placed in a sealed container at moisture contents that are usually below 5%. Product quality is considered excellent due to the protection of product solids by evaporative cooling in the spray dryer. The small particle size of dried solids promotes easy reconstitution when mixed with water.



W
Figure 12.10 Schematic illustration of a freeze-drying system. (Courtesy of the Vitris Company, Inc.)

12.2.6 Freeze-Drying

Freeze-drying is accomplished by reducing the product temperature so that most of the product moisture is in a solid state, and by decreasing the pressure around the product, sublimation of ice can be achieved. When product quality is an important factor for consumer acceptance, freeze-drying provides an alternative approach for moisture removal.

The heat- and mass-transfer processes during freeze-drying are unique. Depending on the configuration of the drying system (Fig. 12.10), heat transfer can occur through a frozen product layer or through a dry product layer. Obviously, heat transfer through the frozen layer will be rapid and not rate-limiting. Heat transfer through the dry product layer will be at a slow rate due to the low thermal conductivity of the highly porous structure in a vacuum. In both situations, the mass transfer will occur in the dry product layer. The diffusion of water vapor would be expected to be the rate-limiting process because of the low rates of molecular diffusion in a vacuum.

The advantages of the freeze-drying process are superior product quality resulting from low temperature during sublimation and the maintenance of product structure. These advantages are balanced against the energy-intensive aspects of the product freezing and vacuum requirements.



■ **Figure 12.11** Mass and energy balance for a dehydration process.

12.3 DEHYDRATION SYSTEM DESIGN

The design of a dehydration system involves several considerations. The factors that have a direct influence on the capacity of a drying system include the quantity and characteristics of air available for drying, along with the drying time required for individual components of the product being dried. These factors require somewhat different approaches to analysis.

12.3.1 Mass and Energy Balance

By application of a mass and energy balance to the entire dehydration system, as illustrated in Figure 12.11, several parameters influencing design of the system are considered. Although the analysis being illustrated is for a countercurrent system, a similar approach could be applied to a concurrent system or a batch system.

An overall balance on water entering and leaving the system gives

$$\dot{m}_a W_2 + \dot{m}_p w_1 = \dot{m}_a W_1 + \dot{m}_p w_2 \quad (12.3)$$

where

\dot{m}_a = air flow rate (kg dry air/h)

\dot{m}_p = product flow rate (kg dry solids/h)

W = absolute humidity (kg water/kg dry air)

w = product moisture content, dry basis (kg water/kg dry solids)

It is important to note that the balance presented in Equation (12.3) is conducted on the basis of dry air and moisture-free product solids.

A cabinet dryer is being used to dry a food product from 68% moisture content (wet basis) to 5.5% moisture content (wet basis). The drying air enters the system at 54°C and 10% RH and leaves at 30°C and 70% RH. The product temperature is 25°C throughout drying. Compute the quantity of air required for drying on the basis of 1 kg of product solids.

Example 12.3

Given

Initial product moisture content $w_1 = 0.68/0.32 = 2.125 \text{ kg H}_2\text{O/kg solids}$

Final product moisture content $w_2 = 0.055/0.945 = 0.0582 \text{ kg H}_2\text{O/kg solids}$

Air entering dryer = 54°C and 10% RH

Air leaving dryer = 30°C and 70% RH

Product temperature = 25°C

Computations based on 1 kg product solids

Approach

The air requirements for drying can be determined by using Equation (12.3) with the following modifications:

$$(\dot{m}_a/\dot{m}_p)W_2 + w_1 = (\dot{m}_a/\dot{m}_p)W_1 + w_2$$

Solution

1. Using the psychrometric chart from Appendix A.5:

$W_1 = 0.0186 \text{ kg H}_2\text{O/kg dry air}$ (using 30°C and 70% RH)

$W_2 = 0.0094 \text{ kg H}_2\text{O/kg dry air}$ (using 54°C and 10% RH)

2. Using the modification of Equation (12.3):

$$\begin{aligned} & \dot{m}_a/\dot{m}_p(0.0094 \text{ kg H}_2\text{O/kg dry air}) \\ & \quad + 2.125 \text{ kg H}_2\text{O/kg solids} \\ & = \dot{m}_a/\dot{m}_p(0.0186 \text{ kg H}_2\text{O/kg dry air}) \\ & \quad + 0.0582 \text{ kg H}_2\text{O/kg solids} \\ & 0.0092\dot{m}_a/\dot{m}_p = 2.067 \\ & \dot{m}_a/\dot{m}_p = 224.65 \text{ kg dry air/kg solids} \end{aligned}$$

An energy balance on the dehydration system is described by the following relationship:

$$\dot{m}_a H_{a2} + \dot{m}_p H_{p1} = \dot{m}_a H_{a1} + \dot{m}_p H_{p2} + q \quad (12.4)$$

where

q = thermal energy loss from the dehydration system

H_a = the thermal energy content of air (kJ/kg dry air)

H_p = the thermal energy content of product (kJ/kg dry solids)

The expressions for thermal energy content of air and product include:

$$H_a = c_s(T_a - T_0) + WH_L \quad (12.5)$$

where

c_s = humid heat of air (kJ/[kg dry air K]) = $1.005 + 1.88 W$ (see Eq. (9.17))

T_a = air temperature ($^{\circ}\text{C}$)

T_0 = reference temperature = 0°C

H_L = latent heat of vaporization for water (kJ/kg water).

In addition:

$$H_p = c_{pp}(T_p - T_0) + wc_{pw}(T_p - T_0) \quad (12.6)$$

where

c_{pp} = specific heat of product solids (kJ/[kg solids K])

T_p = product temperature ($^{\circ}\text{C}$)

c_{pw} = specific heat of water (kJ/[kg water K])

Using these equations, we can determine the quantity of air required for drying a defined amount of product for a known quantity of air at the inlet and establish the moisture characteristics of air at the system outlet.

Example 12.4

A fluidized-bed dryer is being used to dry diced carrots. The product enters the dryer with 60% moisture content (wet basis) at 25°C . The air used for drying enters the dryer at 120°C after being heated from ambient air with 60% RH at 20°C . Estimate the production rate when air is entering the dryer at 700 kg dry air/h and product leaving the dryer is at 10% moisture content (wet basis). Assume product leaves the dryer at the wet bulb temperature of air and the specific heat of product solid is $2.0 \text{ kJ}/(\text{kg } ^{\circ}\text{C})$. Air leaves the dryer 10°C above the product temperature.

Given

Initial product moisture content $w_1 = 0.6/0.4 = 1.5 \text{ kg H}_2\text{O}/\text{kg solids}$

Initial air condition = 20°C and 60% RH ($W_2 = 0.009 \text{ kg H}_2\text{O}/\text{kg dry air}$)

Air temperature entering dryer = 120°C

Air flow rate $\dot{m}_a = 700 \text{ kg dry air}/\text{h}$

Final product moisture content (w_2) = $0.1/0.9 = 0.111 \text{ kg H}_2\text{O}/\text{kg solids}$

Specific heat of product solids (c_{pp}) = $2.0 \text{ kJ}/(\text{kg K})$

Final product temperature = wet bulb temperature of air

Final air temperature (T_{a1}) = $T_{p2} + 10^{\circ}\text{C}$

Approach

The product production rate will be determined using the material balance, Eq. (12.3), and the energy balance, Eq. (12.4), along with parameters obtained from the psychrometric chart (Appendix A.5).

Solution

1. Using Equation (12.3):

$$\begin{aligned} & (700 \text{ kg dry air/h})(0.009 \text{ kg water/kg dry air}) \\ & + \dot{m}_p (1.5 \text{ kg water/kg solids}) \\ & = (700 \text{ kg dry air/h})W_1 + \dot{m}_p (0.111 \text{ kg water/kg solids}) \end{aligned}$$

2. To use Equation (12.4), the following computations are required from Equations (12.5) and (12.6):

For the air:

$$H_{a2} = c_{s2}(120 - 0) + 0.009H_{L2}$$

where

$$c_{s2} = 1.005 + 1.88(0.009) = 1.0219 \text{ kJ/(kg dry air K)}$$

$$H_{L2} = 2202.59 \text{ kJ/kg water at } 120^\circ\text{C (from Table A.4.2)}$$

Therefore,

$$\begin{aligned} H_{a2} &= (1.0219 \text{ kJ/[kg dry air K]})(120^\circ\text{C}) \\ &+ (0.009 \text{ kg water/kg dry air})(2202.59 \text{ kJ/kg water}) \\ H_{a2} &= 142.45 \text{ kJ/kg dry air} \end{aligned}$$

since $T_{p2} = 38^\circ\text{C}$ [wet bulb temperature of air (Appendix A.5)]

$$T_{a1} = 38 + 10 = 48^\circ\text{C}$$

Then,

$$H_{a1} = c_{s1}(T_{a1} - 0) + W_1(H_{L1})$$

where

$$c_{s1} = 1.005 + 1.88W_1$$

and

$$H_{L1} = 2387.56 \text{ kJ/kg water at } 48^\circ\text{C (from Table A.4.2)}$$

Therefore,

$$H_{a1} = (1.005 + 1.88W_1)(48^\circ\text{C}) + W_1(2387.56 \text{ kJ/kg water})$$

For the product:

$$H_{p1} = (2.0 \text{ kJ/[kg solids K]})(25^\circ\text{C} - 0) \\ + (1.5 \text{ kg water/kg solids})(4.178 \text{ kJ/[kg water K]}) \times (25^\circ\text{C} - 0)$$

$$\text{Then } H_{p1} = 206.75 \text{ kJ/kg solids}$$

$$H_{p2} = (2.0 \text{ kJ/[kg solids K]})(T_{p2}^\circ\text{C} - 0) \\ + (0.111 \text{ kg water/kg solids})(4.175 \text{ kJ/[kg water K]}) \times (T_{p2}^\circ\text{C} - 0)$$

Then from Equation (12.4),

$$(700 \text{ kg dry air/h})(142.45 \text{ kJ/kg dry air}) + \dot{m}_p(206.75 \text{ kJ/kg solids}) \\ = (700 \text{ kg dry air/h})[(1.005 + 1.88W_1)(48^\circ\text{C}) \\ + W_1(2387.56/\text{kg water})] \\ + \dot{m}_p\{(2.0 \text{ kJ/[kg solids K]})(38^\circ\text{C}) \\ + (0.111 \text{ kg water/kg solids})(4.175 \text{ kJ/[kg water K]})(38^\circ\text{C})\} \\ + 0$$

where $q = 0$, indicating negligible heat loss from surface of dryer.

3. The material-balance (step 1) and energy-balance (step 2) equations can be solved simultaneously:

$$\text{a. } 700(0.009) + 1.5 \dot{m}_p = 700W_1 + 0.111 \dot{m}_p$$

$$\text{b. } 700(142.45) + \dot{m}_p(206.75) = 700\{(1.005 + 1.88W_1)(48) \\ + 2387.56W_1\} + \dot{m}_p\{(2.0)(38) + (0.111)(4.175)(38)\}$$

$$\text{a. } 6.3 + 1.5\dot{m}_p = 700W_1 + 0.111\dot{m}_p$$

$$\text{b. } 99,715 + 206.75\dot{m}_p = 700(48.24 + 2477.8W_1) + 93.61\dot{m}_p$$

$$\text{a. } W_1 = (1.389\dot{m}_p + 6.3)/700$$

$$\text{b. } 65,947 + 113.14\dot{m}_p = 1,734,460W_1$$

Then

$$65,947 + 113.14\dot{m}_p = 1,734,460(1.389\dot{m}_p + 6.3)/700 \\ \dot{m}_p = 15.12 \text{ kg solids/h}$$

4. The absolute humidity of air leaving the dryer is

$$W_1 = (1.389 \times 15.12 + 6.3)/700 \\ = 0.039 \text{ kg water/kg dry air}$$

indicating that air leaving the dryer will be 48°C and 55% RH.

12.3.2 Drying-Time Prediction

To determine the time required to achieve the desired reduction in product moisture content, the rate of moisture removal from the product must be predicted. For the constant-rate drying period, the moisture removal rate would be described by:

$$\dot{m}_c = \frac{w_o - w_c}{t_c} \quad (12.7)$$

where:

\dot{m}_c = moisture removal rate during constant rate drying (s^{-1})

w_c = critical moisture content (kg water/kg dry solids)

w_o = initial moisture content (kg water/kg dry solids)

t_c = time for constant-rate drying (s)

During the constant-rate drying period, thermal energy is being transferred from the hot air to the product surface, while water vapor is transferred from the product surface to the heated air. The magnitude of thermal energy transfer is described by:

$$q = hA(T_a - T_s) \quad (12.8)$$

where:

q = rate of heat transfer (W)

h = convective heat transfer coefficient (W/[m^2 K])

A = surface area of product exposed to heated air (m^2)

T_a = heated air temperature ($^{\circ}C$)

T_s = product surface temperature ($^{\circ}C$)

It should be noted that during constant-rate drying, the product surface temperature will remain at the wet bulb temperature of the heated air.

The magnitude of water vapor transfer during constant-rate drying is described by the following mass transfer expression:

$$\dot{m}_c = \frac{k_m A M_w P}{0.622 R T_A} (W_s - W_a) \quad (12.9)$$

where:

k_m = convective mass transfer coefficient (m/s)

A = product surface area (m^2)

M_w = molecular weight of water

P = atmospheric pressure (kPa)

R = universal gas constant (8314.41 m³Pa/[kg mol K])

T_A = absolute temperature (K)

W_a = humidity ratio for air (kg water/kg dry air)

W_s = humidity ratio at product surface (kg water/kg dry air).

When using Equation (12.9), the magnitude of the humidity ratio at the product surface is the value at saturation for air moving over the surface, and would be determined by using a psychrometric chart.

If the rate of constant-rate drying is based on thermal energy transfer, where the thermal energy is used to cause phase change of water at the product surface, the following expression will apply:

$$q = \dot{m}_c H_L \quad (12.10)$$

where H_L is the latent heat of vaporization for water at the wet bulb temperature of heated air (kJ/kg water).

By combining Equations (12.10) and (12.8), the following expression for rate of water vapor transfer is obtained:

$$\dot{m}_c = \frac{w_o - w_c}{t_c} = \frac{hA}{H_L} (T_a - T_s) \quad (12.11)$$

Then, by solving for time, the following equation for prediction of the constant-rate drying time is obtained:

$$t_c = \frac{H_L(w_o - w_c)}{hA(T_a - T_s)} \quad (12.12)$$

As indicated by Equation (12.12), the time for constant-rate drying is directly proportional to the difference between the initial moisture content and the critical moisture content, and is inversely proportional to the temperature gradient between the product surface and the heated air.

The time for constant-rate drying can be based on mass transfer by using Equations (12.7) and (12.9), and solving for drying time, as follows:

$$t_c = \frac{0.622RT_A(w_o - w_c)}{k_m AM_w P(W_s - W_a)} \quad (12.13)$$

This expression indicates that the constant-rate drying time is inversely proportional to the gradient of humidity ratios at the product surface and in the heated air.

Example 12.5

Air at 90°C is being used to dry a solid food in a tunnel dryer. The product, with 1 cm thickness and a 5 cm by 10 cm surface, is exposed to the heated air with convective mass transfer coefficient of 0.1 m/s. Estimate the constant-rate drying time, when the initial moisture content is 85% and the critical moisture content is 42%. The air has been heated from 25°C and 50% RH. The product density is 875 kg/m³.

Given

Initial moisture content, $w_0 = 0.85/0.15 = 5.67$ kg water/kg solids

Critical moisture content, $w_c = 0.42/0.58 = 0.724$ kg water/kg solids

Air temperature, $T_a = 90^\circ\text{C}$

Convective mass transfer coefficient, $k_m = 0.1$ m/s

Product surface area, $A = 0.05 \times 0.1 = 0.005$ m²

Molecular weight of water, $M_w = 18$ kg/mol

Atmospheric pressure, $P = 101.325$ kPa

Approach

During the constant-rate period of drying, the rate of water removal from the product surface will be described by mass transfer from the product surface to the air flowing over the surface.

Solution

1. In order to use Equation (12.13), the humidity ratio for the heated air and at the product surface must be evaluated.
2. Since the heated air was heated from 25°C and 50% RH, the humidity ratio (W_a) is 0.01 kg water/kg dry air, as determined from the psychrometric chart (Fig. A.5).
3. The humidity ratio (W_s) at the product surface is evaluated at the saturation condition for the heated air. From the psychrometric chart, W_s is 0.034 kg water/kg dry air at a wet bulb temperature of 33.7°C.
4. The temperature in Equation (12.13) is the mean of heated air temperature (90°C) and the product surface (33.7°C), so:

$$T_A = 62.85 + 273 = 335.85 \text{ K}$$

5. Then Equation (12.13) becomes

$$t_c = \frac{0.622[\text{kg water/kg dry air}] \times 8.314 [\text{m}^3\text{kPa}/(\text{kg mol K})] \times 335.85 [\text{K}] \times (5.67 - 0.724)[\text{kg water/kg solids}]}{0.1 [\text{m/s}] \times 0.005[\text{m}^2] \times 18 [\text{kg water/mol}] \times 101.325 [\text{kPa}] \times (0.034 - 0.01)[\text{kg water/kg dry air}]}$$

$$t_c = 3.925 \times 10^5 \text{ s/kg solids}$$

6. Since each piece of product has

$$0.05 \times 0.1 \times 0.01 = 5 \times 10^{-5} \text{ m}^3$$

and

$$5 \times 10^{-5} [\text{m}^3] \times 875 [\text{kg/m}^3] = 0.04375 \text{ kg}$$

or

$$\begin{aligned} 0.04375 [\text{kg}] \times 0.15 [\text{kg solids/kg product}] \\ = 6.5625 \times 10^{-3} \text{ kg solids} \end{aligned}$$

7. Based on the solids content of each product piece

$$\begin{aligned} t_c &= 3.925 \times 10^5 [\text{s/kg solids}] \times 6.5625 \times 10^{-3} [\text{kg solids}] \\ t_c &= 2575.85 \text{ s} = 42.9 \text{ min} \end{aligned}$$

8. The result indicates that the constant rate drying time is 42.9 min for each product piece.

As indicated in Section 12.1.3, a portion of the moisture removal from a food occurs during a falling-rate drying period. This period of drying begins at the critical moisture content, w_c , and continues until the moisture content decreases to the equilibrium moisture content, w_e . During this period of drying, the product temperature begins to increase to magnitudes above the wet bulb temperature, and the diffusion of moisture from the internal product structure becomes a rate-controlling factor. In addition, the expressions used to describe the moisture diffusion process are dependent on product shape. For an infinite-plate geometry, the falling-rate drying period is described as follows:

$$\frac{w - w_e}{w_c - w_e} = \frac{8}{\pi^2} \exp \left[-\frac{\pi^2 D t}{4d_c^2} \right] \quad (12.14)$$

where:

d_c = characteristic dimension, half-thickness of the slab (m)

D = effective mass diffusivity (m^2/s)

t = drying time (s)

The expression for drying time will be:

$$t_F = \frac{4d_c^2}{\pi^2 D} \ln \left[\frac{8}{\pi^2} \left(\frac{w_c - w_e}{w - w_e} \right) \right] \quad (12.15)$$

An expression for the drying time of a product with an infinite cylinder geometry will be:

$$t_F = \frac{d_c^2}{\beta^2 D} \ln \left[\frac{4}{\beta^2} \left(\frac{w_c - w_e}{w - w_e} \right) \right] \quad (12.16)$$

where d_c is the characteristic dimension, the radius of the cylinder (m), and β is the first root of the zero-order Bessel function equation, with a magnitude of 2.4048. Finally, the falling-rate drying time for a spherical product will be predicted by the following expression:

$$t_F = \frac{d_c^2}{\pi^2 D} \ln \left[\frac{6}{\pi^2} \left(\frac{w_c - w_e}{w - w_e} \right) \right] \quad (12.17)$$

where d_c is the characteristic dimension, the radius of the sphere (m).

The key parameter in all three of the prediction equations for the falling-rate drying period is the effective mass diffusivity for moisture movement within the product structure. The magnitude of this property will approach a value for diffusion of water vapor in air, but will be influenced by the structure of the food product.

Example 12.6

The drying of a noodle occurs during the falling-rate period between the critical moisture content of 0.58 kg water/kg solids and a final moisture content of 0.22 kg water/kg solids. The mass diffusivity for water vapor within the noodle is $2 \times 10^{-7} \text{ cm}^2/\text{s}$ and the noodle thickness is 3 mm. The equilibrium moisture content is 0.2 kg water/kg solids. Estimate the falling-rate drying time.

Given

Characteristic dimension (half-thickness), $d_c = 0.0015 \text{ m}$

Mass diffusivity, $D = 2 \times 10^{-7} \text{ cm}^2/\text{s} = 2 \times 10^{-11} \text{ m}^2/\text{s}$

Critical moisture content, $w_c = 0.58 \text{ kg water/kg solids}$

Equilibrium moisture content, $w_e = 0.22 \text{ kg water/kg solids}$

Final moisture content, $w = 0.2 \text{ kg water/kg solids}$

Approach

The falling-rate drying time can be estimated by assuming the noodle geometry is described as an infinite slab.

Solution

Using Equation (12.15),

$$\begin{aligned}
 t_F &= \frac{4 \times 0.0015^2 [m^2]}{\pi^2 \times 2 \times 10^{-11} [m^2/s]} \ln \left(\frac{8}{\pi^2} \frac{(0.58 - 0.20)}{(0.22 - 0.20)} \right) \\
 &= 1.24675 \times 10^5 \text{ s} \\
 t_F &= 34.6 \text{ h}
 \end{aligned}$$

An example of a drying process where constant-rate drying is limited by evaporation from a free water surface is spray drying. Within the drying chamber, the droplets of liquid food are moving through heated air, while water at the droplet surface changes to a vapor phase. The water vapor is removed from the droplet surface by heated air. During the constant-rate drying period, the rate is limited by heat and mass transfer at the droplet surface.

During the constant-rate period of drying, a spray drying process may be described by heat transfer from the heated air to the droplet surface or by mass transfer from the droplet surface to the heated air. When the process is described in terms of heat transfer, the convective heat transfer coefficient may be estimated by Equation (4.69). For descriptions in terms of mass transfer, the mass transfer coefficient is estimated by Equation (10.38). The similarity between the expressions used to estimate the surface coefficients is obvious.

During the falling-rate drying periods, the rate of spray drying is controlled by heat and mass transfer within the product particle structure. For a heat transfer limited process, the heat transfer is described by conduction through the product structure and will be proportional to the thermal conductivity of the product solids and parameters describing the porous structure of the product. Mass transfer occurs as a result of diffusion of water vapor through the gas phase in the porous structure of the product particle.

A specific expression for drying time during spray drying is based on Equations (12.12) and (12.17). By recognizing that the surface area of a sphere is $4\pi R_d^2$, Equation (12.12) is modified to become:

$$t_c = \frac{H_L(w_o - w_c)}{4\pi R_d^2 h (T_a - T_s)} \quad (12.18)$$

where R_d is the radius of the liquid food droplet.

Ranz and Marshall (1952) have demonstrated that the convective heat transfer coefficient at the surface of a droplet during spray drying can be estimated by the ratio of the thermal conductivity of air to the droplet radius. Using this relationship, the time for constant-rate drying of a liquid droplet during spray drying is

$$t_c = \frac{H_L(w_0 - w_c)}{4\pi R_d k_a (T_a - T_s)} \quad (12.19)$$

A similar relationship for constant-rate drying time, based on mass transfer, can be developed.

Using these developments, the prediction expression for total drying time during spray drying of a liquid food droplet will be

$$t = \frac{H_L(w_0 - w_c)}{4\pi R_d k_a (T_a - T_s)} + \frac{R_p^2}{\pi^2 D} \ln \left[\frac{6}{\pi^2} \left(\frac{w_c - w_e}{w - w_e} \right) \right] \quad (12.20)$$

where R_p is the radius of the product particle at the critical moisture content. In Equation (12.20), the first term on the right side of the equation is the time for the constant-rate drying period. The second term represents the time for falling-rate drying. One of the critical parameters in Equation (12.20) is the droplet/particle radius (R_p) at the critical moisture content (w_c). Although these two parameters are most often established through experimental measurements, most other inputs required for Equation (12.20) can be obtained from handbooks or tables of properties.

Example 12.7

Skim milk with 5% total solids is being spray dried to a final moisture content of 4% using 120°C air with 7% RH. The density of the skim milk product is 1000 kg/m³, and the largest droplet diameter is 120 μm. The critical moisture content is 45%, and the diameter of the particle at the critical moisture content is 25.5 μm. The equilibrium moisture content is 3.85%, and the mass diffusivity for water vapor within the particle is 5×10^{-11} m²/s. Estimate the drying time for product within the spray drier.

Given

Initial moisture content, $w_0 = 0.95$ kg water/kg product = 19 kg water/kg solids

Critical moisture content, $w_c = 0.45$ kg water/kg product = 0.818 kg water/kg solids

Final moisture content, $w = 0.04$ kg water/kg product = 0.042 kg water/kg solids

Equilibrium moisture content, $w_e = 0.0385$ kg water/kg product = 0.04 kg water/kg solids

Heated air temperature = $T_a = 120^\circ\text{C}$

Heated air relative humidity = $RH = 7\%$

Droplet radius, $R_d = 60 \times 10^{-6}$ m

Particle radius, $R_p = 12.75 \times 10^{-6} \text{ m}$

Mass diffusivity, $D = 5 \times 10^{-11} \text{ m}^2/\text{s}$

Liquid product density, $\rho = 1000 \text{ kg/m}^3$

Approach

The total time for drying the droplets of skim milk will include time for constant-rate drying and time for the falling-rate period.

Solution

1. In order to use Equation (12.19) to predict the constant-rate drying time, the temperature at the droplet surface must be estimated, and the latent heat of the vaporization must be determined.
2. Using the psychrometric chart (Fig. A.5), the wet bulb temperature for the heated air (120°C, 7% RH) is 57.1°C. Since the droplet temperature will not be above the wet bulb temperature of air during the constant-rate period of drying, the droplet surface temperature can be estimated at 57.1°C.
3. Using the properties of saturated steam (Table A.4.2) at 57.1°C, the latent heat of vaporization is determined as 2354 kJ/kg.
4. The thermal conductivity of the heated air at 120°C is $k_a = 0.032 \text{ W/(m } ^\circ\text{C)}$ from Table A.4.4.
5. Using Equation (12.19),

$$t_c = \frac{2354[\text{kJ/kg water}] \times (19 - 0.818)[\text{kg water/kg solids}] \times 1000[\text{J/kJ}]}{4\pi \times 60 \times 10^{-6}[\text{m}] \times 0.032[\text{W/(m } ^\circ\text{C})] \times (120 - 57.1)[^\circ\text{C}]}$$

$$= 2.82 \times 10^{10} \text{ s per kg solids}$$

6. Since Equation (12.19) presents the results per unit of product solids, the mass of solids per droplet must be estimated.

Using the volume, density, and fraction of solids in each droplet,

$$\text{mass [kg solids/droplet]} = \rho V(0.05)[\text{kg solids/kg product}]$$

$$\text{mass} = 1000[\text{kg product/m}^3] \times \left\{ \frac{4}{3} (60 \times 10^{-6})^3 \pi [\text{m}^3] \right\}$$

$$\times 0.05 [\text{kg solids/kg product}]$$

$$\text{mass} = 4.52 \times 10^{-11} \text{ kg solids/droplet}$$

7. Constant rate drying time = 1.276 s.
8. In order to estimate the falling-rate drying time, the particle is assumed to be spherical, and Equation (12.17) will be used as follows:

$$t_F = \frac{(12.75 \times 10^{-6})^2 [\text{m}^2]}{\pi^2 \times 5 \times 10^{-11} [\text{m}^2/\text{s}]} \ln \left\{ \frac{6}{\pi^2} \left[\frac{(0.818 - 0.04)}{(0.042 - 0.04)} \right] \right\}$$

$$t_F = 1.801 \text{ s}$$

9. Total drying time:

$$t = 1.276 + 1.801 = 3.077 \text{ s}$$

A drying process that illustrates the type of drying that occurs when the drying rate is limited by internal mass transfer is freeze-drying. An analysis of the heat and mass transfer for the system in Figure 12.10 is simplified, since heat transfer occurs from the hot plate to the drying front through the frozen product layer of dry product, and moisture diffusion becomes the rate-limiting process.

The heat and mass transfer during freeze-drying as illustrated in Figure 12.10 has been analyzed by King (1970, 1973). His analysis provided an equation for estimating the drying time, as follows:

$$t = \frac{RT_A L^2}{8DMV_w(P_i - P_a)} \left(1 + \frac{4D}{k_m L} \right) \quad (12.21)$$

where L is the thickness of product layer (m), T_A is the absolute temperature (K), M is the molecular weight (kg/kg mol), V_w is the specific volume of water (m^3/kg water), P_i is the vapor pressure of ice (Pa), P_a is the vapor pressure of air at the condenser surface (Pa), k_m is the mass transfer coefficient ($\text{kg mol}/[\text{s m}^2 \text{ Pa}]$), R is universal gas constant ($8314.41 \text{ m}^3 \text{ Pa}/[\text{kg mol K}]$), and D is the diffusion coefficient (m^2/s).

Equation (12.21) is limited to situations where the drying time is based on a process where rate is limited by moisture diffusion within the structure of the dry product layer. The calculation of drying time requires knowledge of the moisture diffusivity, D , and mass transfer coefficient, k_m , and the magnitude of both is likely to be product-dependent. Often, these property values must be measured for individual situations.

Example 12.8

A concentrated liquid coffee is being freeze-dried by placing a 2 cm thick frozen layer of the product over a heated platen. The product is frozen to -75°C initially and before placing over the 30°C platen. The freeze-drying is accomplished in a chamber at a pressure of 38.11 Pa with a condenser temperature of -65°C . Properties needed to describe the process have been measured in an experimental system; mass diffusivity $= 2 \times 10^{-3} \text{ m}^2/\text{s}$ and mass transfer coefficient $= 1.5 \text{ kg mole}/\text{s m}^2 \text{ Pa}$. The initial moisture content of the concentrate is 40% and the density of dry product solids is $1400 \text{ kg}/\text{m}^3$. Compute the drying time for the product.

Given

Thickness of product layer $= 2 \text{ cm} = 0.02 \text{ m}$

Mass diffusivity $= 2 \times 10^{-3} \text{ m}^2/\text{s}$

Mass transfer coefficient $= 1.5 \text{ kg mole}/\text{s m}^2 \text{ Pa}$

Approach

We will compute the drying time for the coffee concentrate by using Equation (12.21).

Solution

1. To use Equation (12.21), several parameters must be determined from the thermodynamic tables.

Universal gas constant = $8314.41 \text{ m}^3 \text{ Pa/kg mol K}$

Absolute temperature (T_A) = 243 K (based on ice temperature at pressure 38.11 Pa)

Vapor pressure of ice (P_i) = 38.11 Pa

Vapor pressure of condenser surface (P_a) = 0.5 Pa

Molecular weight of water (M_w) = 18

2. The specific volume of water is computed from initial moisture content of product and density of product solids.

Moisture content (dry basis) = $0.4/0.6 = 0.667 \text{ kg water/kg solids}$

Then

$$V_w = \frac{1}{(0.667)(1400)} = 0.00107 \frac{\text{m}^3 \text{ solid}}{\text{kg water}}$$

3. Using Equation (12.21),

$$t = \frac{(8314.41)(243)(0.02)^2}{8(2 \times 10^{-3})(18)(0.00107)(38.11 - 0.5)} \left(1 + \frac{4(2 \times 10^{-3})}{(1.5)(0.02)} \right)$$

$$t = 88324 \text{ s} = 1472 \text{ min} = 24.5 \text{ hr}$$

The dehydration process for foods results in products with reduced mass and possible reductions in volume. These reductions provide for increased efficiency in transportation and storage, in addition to effective preservation. The selection of the most appropriate process for a given food product will depend on two primary considerations: cost of drying and product quality.

Of the processes discussed in this chapter, air drying by cabinet or tunnel will have the lowest cost when expressed as cost per unit of water removed. The use of vacuum increases the cost of water removal somewhat, and the value will be comparable to fluidized-bed drying. The explosion puff-drying process will be more costly than previously mentioned processes, but it appears to be more efficient than freeze-drying.

The product quality resulting from the various processes will be opposite to the cost comparisons. The freeze-drying process produces the highest-quality product and can be used for products where the quality characteristics allow product pricing to recover the extra drying cost. Based on available literature, the puff-drying process produces quality that is comparable to that of freeze-drying, with somewhat lower cost. The product quality resulting from fluidized-bed drying and vacuum drying should be somewhat similar to, but lower than, that for puff-drying and freeze-drying processes. The lowest-quality dehydrated products are produced by the lowest-cost processes—tunnel and cabinet drying using heated air. Although these comparisons suggest a direct trade-off between dehydration cost and dry product quality, we need to recognize that the selection of the process will depend on the adaptability of the product to a given process. The physical characteristics of the product before and/or after drying may dictate which process is used for dehydration.

PROBLEMS

- 12.1** The following equilibrium moisture-content data have been collected for a dry food:

Water activity	Equilibrium moisture content (g H ₂ O/g product)
0.1	0.060
0.2	0.085
0.3	0.110
0.4	0.122
0.5	0.125
0.6	0.148
0.7	0.173
0.8	0.232

Develop a plot of the equilibrium moisture isotherm for moisture content on a dry weight basis.

- 12.2** A product enters a tunnel dryer with 56% moisture content (wet basis) at a rate of 10 kg/h. The tunnel is supplied with 1500 kg dry air/h at 50°C and 10% RH, and the air leaves at 25°C in equilibrium with the product at 50% RH. Determine the moisture content of product leaving the dryer and the final water activity.

- *12.3** A countercurrent tunnel dryer is being used to dry apple slices from an initial moisture content (wet basis) of 70% to 5%. The heated air enters at 100°C with 1% RH and leaves at 50°C. If the product temperature is 20°C throughout the dryer and the specific heat of product solids is 2.2 kJ/(kg °C), determine the quantity of heated air required for drying the product at a rate of 100 kg/h. Determine the relative humidity of outlet air.
- 12.4** A cabinet dryer is to be used for drying of a new food product. The product has an initial moisture content of 75% (wet basis) and requires 10 minutes to reduce the moisture content to a critical level of 30% (wet basis). Determine the final moisture of the product if a total drying time of 15 minutes is used.
- 12.5** The following data were obtained by Labuza et al. (1985) on fish flour at 25°C. Determine the GAB model for these data and the values of k , w_m , and C .

a_w	g water/ 100 g solids
0.115	2.12
0.234	3.83
0.329	5.53
0.443	6.82
0.536	7.65
0.654	10.29
0.765	13.40
0.848	17.50

- 12.6** Pistachios are to be dried using a countercurrent dryer operating at steady state. The nuts are dried from 80% (wet basis) to 12% (wet basis) at 25°C. Air enters the heater at 25°C (dry bulb temperature) and 80% relative humidity. The heater supplies 84 kJ/kg dry air. The air exits the dryer at 90% relative humidity. For this given information solve the following parts:
- What is the relative humidity of the air leaving the heater section of the dryer?
 - What is the temperature (dry bulb temperature) of air leaving the dryer?
 - What is the flow rate (m^3/s) of air required to dry 50 kg/h of pistachio nuts?

*Indicates an advanced level of difficulty in solving.

- 12.7** A sample of a food material weighing 20 kg is initially at 450% moisture content dry basis. It is dried to 25% moisture content wet basis. How much water is removed from the sample per kg of dry solids?
- 12.8** Air enters a counterflow drier at 60°C dry bulb temperature and 25°C dew point temperature. Air leaves the drier at 40°C and 60% relative humidity. The initial moisture content of the product is 72% (wet basis). The amount of air moving through the drier is 200 kg of dry air/h. The mass flow rate of the product is 1000 kg dry solid per hour. What is the final moisture content of the dried product (in wet basis)?
- 12.9** The constant rate portion of drying for a new food product must be accomplished within 5 min; a reduction from an initial moisture content of 75% to the critical moisture content of 40%. Heated air at 95°C and 10% RH is used for drying. The surface of product exposed to the air is 10 cm wide and 20 cm in the direction of air movement over the surface. The mass diffusivity for water vapor in air is $1.3 \times 10^{-3} \text{ m}^2/\text{s}$. The product thickness is 5 cm and density is 900 kg/m^3 .
- Estimate the mass transfer coefficient needed at the product surface.
 - Compute the air velocity required.
- 12.10** A spray drier with a 5 m diameter and 10 m height is used to dry skim milk to a final moisture content of 5%. The air entering the drier is 120°C, is heated from ambient air at 25°C and 75% RH, and flows concurrently with the product droplets (and particles) through the system. The skim milk is atomized into the hot air at 45°C with a maximum droplet size of 120 micron diameter. The critical moisture content for the product is 30%, and the particle diameter is 25 micron at the critical moisture content. The equilibrium moisture content of the dry skim milk is 3.5% at the exit temperature of 55°C from the drier. The mass diffusivity for water vapor within the product particles is $7.4 \times 10^{-7} \text{ m}^2/\text{s}$ and the specific heat of product solids is 2.0 kJ/kgK . The heated air leaves the system at 5°C above the product temperature. The initial moisture content of skim milk is 90.5% wet basis. Determine the production rate for the spray drier; kg of 5% moisture content product per unit time.
- 12.11** A spray drier with a 5 m diameter and 10 m height is used to dry skim milk to a final moisture content of 5%. The air

entering the drier is 120°C, is heated from ambient air at 25°C and 75% RH, and flows concurrently with the product droplets (and particles) through the system. The air flow rate is 1000 m³/min. The skim milk enters the dryer at 45°C with 90.5% moisture content and the exit temperature is 55°C. The specific heat of product solids is 2.0 kJ/kgK. The heated air leaves the system at 5°C above the product temperature. Determine

- a. The production rate for the system; kg of 5% moisture content product per unit time.
- b. The temperature and % RH of air leaving the dryer.
- c. The thermal energy for heating the air entering the dryer.

12.12 A tunnel dryer is used to reduce the moisture content of a food from an initial magnitude of 85%. The produce is conveyed through the dryer on a 1 m wide conveyor with a 10 m length. The volumetric flow rate of heated air is 240 m³/min at 100°C, heated from 25°C and 40% RH. The cross-sectional area for air flow through the dryer is 4 m², and the thickness of product on the conveyor is 1.5 cm.

- a. Estimate the temperature and % RH of air leaving the dryer, when all moisture removal from the product occurs during a constant-rate drying period.
- b. Determine the moisture content of product leaving the dryer.

12.13 The falling rate portion of the drying time for a particle of skim milk begins at the critical moisture content of 25%, and the final moisture content is 4%. The air used for drying is 120°C and was heated from ambient air of 20°C and 40% RH. The particle size at the critical moisture content is 20 microns, and the specific heat of the product solids is 2.0 kJ/kgK. The mass diffusivity for water within the product particle is 3.7×10^{-12} m²/s, and the density of the product particle is 1150 kg/m³.

- a. If the equilibrium moisture content for the product is 3.5%, estimate the time for the falling rate portion of drying.
- b. If 5000 m³/min of heated air is needed for product drying, determine the thermal energy needed to heat the air to 120°C.

12.14 A concurrent tunnel dryer is used to dry a new food product carried in 10 cm by 10 cm by 1 cm trays. Moisture removal from the product occurs from the upper surface only. The heated air is 100°C, and has been heated from ambient conditions at 25°C and 40% RH at a rate of 1000 m³/min.

The product leaves the system at a temperature 5°C above the wet bulb temperature, and the air leaves 10°C above the product temperature. The initial moisture content of the product is 85%, the density of the product entering the dryer is 800 kg/m³, and the initial temperature is 20°C. The critical moisture content of the product is 30% and the equilibrium moisture content is 3.0%. The product volume does not change during drying. The convective heat transfer coefficient at the product surface in the dryer is 500 W/m²K and the mass diffusivity for vapor within the product is 1.7×10^{-7} m²/s. The specific heat of product solids (c_{psolids}) is 2.0 kJ/kgK. Estimate the following:

- The amount of final product leaving the dryer at 4.0% moisture.
- The temperature and RH of air leaving the dryer.
- The thermal energy for heating the air entering the dryer.
- The length of the dryer tunnel, if the conveyor carrying the product moves at a rate of 1 m/min.

- 12.15** Use MATLAB® to evaluate and plot equilibrium desorption and adsorption moistures over the range of humidities ($0.01 < a_w < 0.95$) for rough rice at 25°C predicted by the empirical equations given as follows.

Desorption (Basunia and Abe, 2001):

$$M = C_1 - C_3 \ln[-(T + C_2) \ln(a_w)]; \quad C_1 = 31.652, C_2 = 19.498, \\ C_3 = 5.274$$

Adsorption (Basunia and Abe, 1999):

$$M = \frac{-1}{b_3} \ln \left[- \left(\frac{T + b_2}{b_1} \right) \ln(a_w) \right]; \quad b_1 = 594.85, b_2 = 49.71, \\ b_3 = 0.2045$$

M = Moisture content (% dry basis)

T = temperature (°C)

a_w = water activity (decimal)

- 12.16** Use the MATLAB® nonlinear regression function, *nlinfit*, to find the Guggenheim-Anderson-DeBoer (GAB) parameters (m_0 , A , B) for rough rice (desorption) given in the following table.

$$m = \frac{m_0 A B a_w}{(1 - B a_w)(1 - B a_w + A B a_w)}$$

Water activity Sample 1(%db) Sample 2 (%db) Sample 3 (%db)

0.05	6.5	6.2	6.3
0.1	7.5	7.3	7.7
0.2	8.2	8.5	8.4
0.3	10.5	10.5	10.7
0.4	12.2	12.0	12.0
0.5	13.5	13.4	13.7
0.6	15.0	15.1	15.3
0.7	17.0	17.2	17.0
0.8	19.8	19.7	19.4
0.9	23.5	23.3	23.8
0.95	27.4	27.6	27.9

LIST OF SYMBOLS

a_w	water activity (dimensionless)
A	surface area of product exposed to heated air (m^2)
β	first root of the zero-order Bessel function equation
C	the Guggenheim constant = $C' \exp(H_1 - H_m)/RT$
c_{pp}	specific heat of product solids (kJ/[kg solids K])
c_{pw}	specific heat of water (kJ/[kg water K])
c_s	humid heat of air (kJ/[kg dry air K]) = $1.005 + 1.88 W$ (Eq. 9.17)
D	diffusion coefficient (m^2/s)
d_c	characteristic dimension (m)
h	convective heat transfer coefficient ($W/[m^2K]$)
H_1	heat of condensation of pure water vapor
H_a	thermal energy content of air (kJ/[kg dry air])
H_L	latent heat of vaporization for water (kJ/kg water)
H_m	total heat of sorption of the first layer on primary sites
H_p	thermal energy content of product (kJ/kg dry solids)
H_q	total heat of sorption of the multilayers
K	factor correcting properties of multilayer with respect to the bulk liquid, = $k' \exp(H_1 - H_q)/RT$
k_m	convective mass transfer coefficient (m/s) or (kg mol/[s m^2 Pa])
L	thickness of product layer (m)
M	molecular weight (kg/[kg mol])
\dot{m}_a	air flow rate (kg dry air/h)
\dot{m}_c	moisture removal rate during constant-rate drying (s^{-1})
\dot{m}_p	product flow rate (kg dry solids/h)
P	atmospheric pressure (kPa)
P_a	vapor pressure of air at the condenser surface (Pa)

P_i	vapor pressure of ice (Pa)
q	rate of heat transfer (W)
R	universal gas constant (8314.41 m ³ Pa/[kg mol K])
R_d	radius of the liquid food droplet
R_p	radius of the product particle at the critical moisture content
t	drying time
T_0	reference temperature at 0 °C
T_a	air temperature (°C)
T_A	absolute temperature (K)
t_c	time for constant-rate drying (s)
T_p	product temperature (°C)
T_s	product surface temperature (°C)
V_w	specific volume of water (m ³ /kg water)
w	product moisture content, dry basis (kg water/kg dry solids)
w_c	critical moisture content (kg water/kg dry solids)
w_e	equilibrium moisture content, fraction dry basis
w_m	monolayer moisture content, fraction dry basis
w_0	initial moisture content (kg water/kg dry solids)
W	absolute humidity (kg water/kg dry air)
W_a	humidity ratio for air (kg water/kg dry air)
W_s	humidity ratio at product surface (kg water/kg dry air)

Subscript: w, water

■ BIBLIOGRAPHY

- Basunia, M. A. and Abe, T. (1999). Moisture adsorption isotherms of rough rice. *J. Food Engr.* 42: 235–242.
- Basunia, M. A. and Abe, T. (2001). Moisture desorption isotherms of medium grain rough rice. *J. Stored Prod. Res.* 37: 205–219.
- Bizot, H. (1983). Using the GAB model to construct sorption isotherms. In *Physical Properties of Foods*, R. Jowitt, F. Escher, B. Hallstrom, H. Th. Meffert, W. E. L. Spiess, and G. Vos, eds., 43–54. Applied Science Publishers, London.
- Charm, S. E. (1978). *The Fundamentals of Food Engineering*, 3rd ed. AVI Publ. Co., Westport, Connecticut.
- Eisenhardt, N. H., Cording, J., Jr., Eskew, R. K., and Sullivan, J. F. (1962). Quick-cooking dehydrated vegetable pieces. *Food Technol.* 16(5): 143–146.
- Fish, B. P. (1958). Diffusion and thermodynamics of water in potato starch gel. *Fundamental Aspects of Dehydration of Foodstuffs*, 143–157. Macmillan, New York.

- Flink, J. M. (1977). Energy analysis in dehydration processes. *Food Technol.* 31(3): 77.
- Forrest, J. C. (1968). Drying processes. In *Biochemical and Biological Engineering Science*, N. Blakebrough, ed., 97–135. Academic Press, New York.
- Gorling, P. (1958). Physical phenomena during the drying of foodstuffs. In *Fundamental Aspects of the Dehydration of Foodstuffs*, 42–53. Macmillan, New York.
- Heldman, D. R. and Hohner, G. A. (1974). Atmospheric freeze-drying processes of food. *J. Food Sci.* 39: 147.
- Jason, A. C. (1958). A study of evaporation and diffusion processes in the drying of fish muscle. In *Fundamental Aspects of the Dehydration of Foodstuffs*, 103–135. Macmillan, New York.
- Joslyn, M. A. (1963). Food processing by drying and dehydration. In *Food Processing Operations*, M. A. Joslyn and J. L. Heid, eds., Vol. 2, 545–584. AVI Publ. Co., Westport, Connecticut.
- King, C. J. (1970). Freeze-drying of foodstuffs. *CRC Crit. Rev. Food Technol.* 1: 379.
- King, C. J. (1973). Freeze-drying. In *Food Dehydration*, W. B. Van Arsdel, M. J. Copley, and A. I. Morgan, Jr, eds., 2nd ed., Vol. 1, 161–200. AVI Publ. Co, Westport, Connecticut.
- Labuza, T. P. (1968). Sorption phenomena in foods. *CRC Crit. Rev. Food Technol.* 2: 355.
- Labuza, T. P., Kaanane, A., and Chen, J. Y. (1985). Effect of temperature on the moisture sorption isotherms and water activity shift of two dehydrated foods. *J. Food. Sci.* 50: 385.
- Potter, N. N. (1978). *Food Science*, 3rd ed. AVI Publ. Co., Westport, Connecticut.
- Ranz, W. E. and Marshall, W. R., Jr (1952). Evaporation from drops. *Chem. Eng. Prog.* 48: 141–180.
- Rockland, L. B. and Nishi, S. K. (1980). Influence of water activity on food product quality and stability. *Food Technol.* 34(4): 42–51.
- Sherwood, T. K. (1929). Drying of solids. *Ind. Eng. Chem.* 21: 12.
- Sherwood, T. K. (1931). Application of theoretical diffusion equations to the drying of solids. *Trans. Am. Inst. Chem. Eng.* 27: 190.
- Van Arsdel, W. B. (1951). Tunnel-and-truck dehydrators, as used for dehydrating vegetables. *USDA Agric. Res. Admin. Pub. AIC-308.*, Washington, D.C.
- Van Arsdel, W. B., Copley, M. J., and Morgan, A. I., Jr, (eds.) (1973). *Food Dehydration*, 2nd ed., Vol. 1. AVI Publ. Co., Westport, Connecticut.

This page intentionally left blank

Supplemental Processes

In this chapter, various supplemental processes used in the food industry are presented. Some of these processes are ubiquitous in food processing such as mixing. Others such as filtration, sedimentation, and centrifugation are more uniquely applied to specific applications. For each process, we will consider mathematical relationships that are useful in their design and operation.

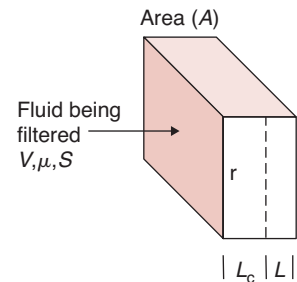
13.1 FILTRATION

Solid particles are removed from liquids by somewhat different mechanisms than used for removing solid particles from air. The removal process can be described by standard equations. In this section, we will examine some of these equations and discuss specific applications of filtration techniques.

13.1.1 Operating Equations

In general, the filtration process is described by the manner in which the fluid being filtered flows through the filter medium where the solids are deposited (Fig 13.1). As the solids are removed from the fluid, they accumulate in the filter medium, resulting in an increased resistance to flow as the filtration process continues. All these factors result in a description of filtration rate. In addition, this filtration rate depends on several other factors, including

- The pressure drop across the filter medium
- The area of the filtering surface
- The viscosity of the filtrate
- The resistance of the filter cake as determined by the solids removed from the fluid
- The resistance of the filter medium.



■ **Figure 13.1** Schematic illustration of filtration process.

All icons in this chapter refer to the author's web site, which is independently owned and operated. Academic Press is not responsible for the content or operation of the author's web site. Please direct your web site comments and questions to the author: Professor R. Paul Singh, Department of Biological and Agricultural Engineering, University of California, Davis, CA 95616, USA
Email: rps@rpaulsingh.com.

The rate of filtration can be written as follows:

$$\text{Rate of filtration} = \frac{\text{Driving force}}{\text{Resistance}} \quad (13.1)$$

where the driving force is the pressure required to move the fluid through the filter medium and the resistance is dependent on several factors. The overall resistance can be described by the following expression:

$$R = \mu r' (L_c + L) \quad (13.2)$$

where L_c represents the thickness of accumulated solids in the filter cake, μ is the fluid viscosity, and L is a fictitious thickness of the filter material or medium. The parameter r' in Equation (13.2) represents the specific resistance of the filter cake and it is a property of the particles forming the filter cake. Earle (1983) describes L_c by the following expression:

$$L_c = \frac{SV}{A} \quad (13.3)$$

where S is the solids content of the fluid being filtered, and V is the volume that has passed through the filter with cross-sectional area (A).

The thickness of the filter cake represents a fictitious value to describe the total thickness of all solids accumulated. In some filtration processes, this may approach the real situation. Utilizing Equations (13.2) and (13.3), the total resistance can be written in the following manner:

$$R = \mu r' \left(\frac{SV}{A} + L \right) \quad (13.4)$$

Combining Equations (13.1) and (13.4), an expression for the rate of filtration is obtained as follows:

$$\frac{dV}{dt} = \frac{A\Delta P}{\mu r' \left(\frac{SV}{A} + L \right)} \quad (13.5)$$

Equation (13.5) is an expression used to describe the filtration process and can be used for scale-up if converted to appropriate forms.

The filtration process may occur in two phases: (1) constant-rate filtration, normally occurring during the early stages of the process, and (2) constant-pressure filtration, occurring during the final stages of the process.

13.1.1.1 Constant-Rate Filtration

Constant-rate filtration is described by the following integrated forms of Equation (13.5), which can be used to determine the required pressure drop as a function of the filtration rate:

$$\frac{V}{t} = \frac{A\Delta P}{\mu r' \left(\frac{SV}{A} + L \right)} \quad (13.6)$$

or

$$\Delta P = \frac{\mu r'}{A^2 t} [SV^2 + LAV] \quad (13.7)$$

Equation (13.6) can be expressed in a different form if the thickness (L) of the filter medium is considered negligible. The following equation for pressure drop as a function of time is obtained

$$\Delta P = \frac{\mu r' SV^2}{A^2 t} \quad (13.8)$$

In many situations, Equation (13.8) can be used to predict pressure drop requirements for a filter during the early stages of the process.

An air filter is used to remove small particles from an air supply to a quality control laboratory. The air is supplied at a rate of $0.5 \text{ m}^3/\text{s}$ through an air filter with a 0.5 m^2 cross-section. If the pressure drop across the filter is 0.25 cm water after one hour of use, determine the life of the filter if a filter change is required when the pressure drop is 2.5 cm of water.

Example 13.1

Given

Volumetric flow rate of air = $0.5 \text{ m}^3/\text{s}$

Area of filter = 0.5 m^2

Pressure drop = 0.25 cm water

Time of use = 1 hr

Pressure drop before filter change = 2.5 cm of water

Approach

We will use Equation (13.8) to determine the product of specific resistance and particle content of air. Using this calculated value and Equation (13.8) with a pressure drop of 2.5 cm of water we will obtain the time when the filter should be changed.

Solution

1. Due to the nature of air filtration, constant-rate filtration can be assumed and the filter medium thickness is negligible.
2. Based on the information given and Equation (13.8), the product of the specific resistance (r') and the particle content of air (S) can be established

$$r'S = \frac{\Delta P A^2 t}{\mu V^2}$$

3. The pressure drop of 0.25 cm of water can be expressed in consistent units (Pa) by

$$0.25 \text{ cm of water} = 24.52 \text{ Pa}$$

4. Using Equation (13.8) (for 1 hr of filtration)

$$r'S = \frac{(24.52 \text{ Pa})(0.5 \text{ m}^2)^2 (3600 \text{ s})}{(1.7 \times 10^{-5} \text{ kg/ms})(0.5 \times 3600)^2}$$

where $\mu = 1.7 \times 10^{-5}$ (viscosity of air at 0°C from Table A.4.4)

$$r'S = 396/\text{m}^2$$

5. Using $r'S = 396$ and Equation (13.8), the time required for ΔP to increase to 2.5 cm water can be computed.
6. Converting ΔP to consistent units

$$2.5 \text{ cm of water} = 245.16 \text{ Pa}$$

then

$$\frac{t}{V^2} = \frac{(1.7 \times 10^{-5})(396)}{(0.5)^2 (245.16)} = 1.11 \times 10^{-4} \text{ s/m}^6$$

7. Since the volumetric flow rate through the filter is 0.5 m³/s

$$\frac{V}{t} = 0.5 \text{ m}^3/\text{s}$$

Therefore

$$V^2 = 0.25t^2$$

or

$$t = 1.11 \times 10^{-4} \times 0.25t^2 = 2.778 \times 10^{-5}t^2$$

and

$$t = \frac{1}{2.775 \times 10^{-5}} = 35,997s$$

$$t = 10 \text{ hr}$$

8. Thus the filter should be changed after 10 hours of operation.

13.1.1.2 Constant-Pressure Filtration

An expression for describing constant-pressure filtration can be obtained from the following form of Equation (13.5):

$$\frac{\mu r' S}{A} \int_0^V V dV + \mu r' L \int_0^V dV = A \Delta P \int_0^t dt \quad (13.9)$$

Integration leads to the following design equation:

$$\frac{tA}{V} = \frac{\mu r' SV}{2\Delta PA} + \frac{\mu r' L}{\Delta P} \quad (13.10)$$

or the following equation if filter medium thickness (L) can be assumed to be negligible:

$$t = \frac{\mu r' SV^2}{2A^2 \Delta P} \quad (13.11)$$

Essentially, Equation (13.11) indicates the time required to filter a given volume of fluid when a constant pressure is maintained. Various procedures are followed in using this equation to obtain information that is not readily available. For example, the specific resistance of the filter cake (r') may not be known for some types of solids and must be determined experimentally. Earle (1983) presented procedures for determining these parameters, and Charm (1978) discussed determination of filtration constants that are more complex than those proposed in the previous presentation.

Example 13.2

A liquid is filtered at a pressure of 200 kPa through a 0.2-m² filter. Initial results indicate that 5 min is required to filter 0.3 m³ of liquid. Determine the time that will elapse until the rate of filtration drops to 5×10^{-5} m³/s.

Given

Pressure drop = 200 kPa

Filter area = 0.2 m²

Time = 5 min

Volume of liquid = 0.3 m³

Rate of filtration = 5×10^{-5} m³/s

Approach

We will use Equation (13.11) to determine $\mu r' S$. Next we will use Equation (13.5) to obtain the volume followed by calculation of time using Equation (13.11).

Solution

1. Since the filtration is assumed to be in the constant-pressure regime, based on data obtained at 5 min, Equation (13.11) will apply as follows

$$\mu r' S = \frac{2A^2 \Delta P t}{V^2} = \frac{2(0.2)^2 (200,000)(5 \times 60)}{0.3^2}$$

$$\mu r' S = 53.33 \times 10^6 \text{ kg/m}^3 \text{ s}$$

2. Using Equation (13.5) (where L is assumed to be negligible)

$$5 \times 10^{-5} = \frac{(0.2)^2 (200,000)}{(53.33 \times 10^6) V}$$

$$V = 3 \text{ m}^3$$

3. Using Equation (13.11):

$$t = \frac{(53.33 \times 10^6)(3)^2}{2(0.2)^2 (200,000)} = 29,998 \text{ s}$$

$t = 499.9 \text{ min}$; indicates that 500 min of filtration at a constant pressure would occur before the rate dropped to 5×10^{-5} m³/s.

Reference to Equation (13.5) reveals that the filtration process is directly dependent on two factors: the filter medium and the fluid being filtered. In Equation (13.5) a filter medium is described in terms of area (A) and the specific resistance (r'). The filter medium

will depend considerably on the type of fluid being filtered. In the case of liquid filtration, the filter medium, to a large extent, will contain the solids removed from the liquid. This filter cake must be supported by some type of structure that plays only a limited role in the filtration process. In some cases, these supporting materials may be woven (wool, cotton, linen) or they may be granular materials for particular types of liquids. In any case, the primary role of the material is to support the collected solids so that the solids can act as a filter medium for the liquid.

The design of filters for the removal of particles from air is significantly different. In this application, the entire filter medium is designed into the filter and the collected solids play a very minor role in the filtration process. The filter medium is a porous collection of filter fibers of the same magnitude in size as the particles to be removed from the air. This results in filtration processes that are nearly constant-flow rate in all situations.

The second factor of Equation (13.5) that influences filtration rate is the fluid being filtered as described by the fluid viscosity (μ). The rate of filtration and the viscosity of the fluid being filtered are inversely related; as the viscosity of the fluid increases, the rate of filtration must decrease. Fluid viscosity plays a very important role in the filtration process and must be accounted for in all design computations.

13.1.2 Mechanisms of Filtration

The mechanisms involved in removing small particles from air are relatively well-defined. Whitby and Lundgren (1965) have listed four mechanisms as follows: (1) Brownian diffusion, (2) interception, (3) inertial impaction, and (4) electrical attraction. Decker et al. (1962) indicated that deposition according to Stoke's law could be considered as an additional mechanism. The mechanism of Brownian diffusion will have very little influence on removal of particles larger than 0.5 micron. This particular mechanism contributes to the particle collection by causing particles to deviate from the streamline of air flow around the filter fibers and bringing them into contact with the fiber. Somewhat larger particles may be removed by interception even when the particles do not deviate from the air streamline.

When these particles follow the air streamline and the streamline brings them sufficiently close to the fiber, the particles will be

removed by direct interception. The larger particles will not follow the air streamline and will be removed by inertial impaction. Particles larger than 1 micron will normally be removed by this mechanism. When the particles and fiber have different or opposite electrical charges, the particles will deviate from the air streamline and deposit on the fiber as a result of this mechanism. Very large particles may be influenced by gravity and deviate from the air streamline due to gravitational force, resulting in deposition on the filter fiber. The contribution of this mechanism to small-particle removal is probably very small.

In the case of removing solids from liquids, the mechanisms of removal are not well-defined and may be considerably different, depending on the mode of filtration considered. During the initial stages when the liquid is moving through the filter medium at a rapid rate, the mechanisms are most likely to be direct interception or inertial impaction. After the filter cake is established and constant-pressure filtration occurs, the liquid will flow through the filter cake in a streamline fashion.

13.1.3 Design of a Filtration System

Although the expressions presented for describing filtration rate by a given system are relatively straightforward, use of these equations requires knowledge of several system parameters. In most cases, the viscosity and specific resistance values may not be known. To obtain some indication of the relationships involved, the approach normally followed is to make a small-scale filtration experiment followed by a scale-up of the entire process. Expressions of the type presented as Equations (13.7) and (13.11) are ideal for this purpose. A small or pilot-scale operation usually results in determination of the filtrate volume after given periods of time at a constant pressure on the small-scale filter.

Earle (1983) showed that this information can be used to determine a plot of the type given in Figure E13.1. To obtain the filtration graph, we use Equation (13.10), in which L is not assumed to be negligible. By using pilot-scale data to obtain a relationship for Figure E13.1, we can evaluate appropriate constants for use in the scale-up of the filtration process. In some situations, it is desirable to collect pilot-scale data at different pressures and/or different filter areas.

A filtration system is designed to filter 4 m^3 of a slurry in 2 hr using a constant pressure of 400 kPa. The necessary design conditions were established on a laboratory scale using a filter with 0.1 m^2 surface area and 140 kPa constant pressure. The following results were obtained on a laboratory scale:

Example 13.3

Time (min)	Filtration Volume ($\times 10^{-2} \text{ m}^3$)
10	2.3
20	3.7
30	4.9
40	6.1
50	6.8

Determine the filter area required to provide the desired conditions for the design situation.

Given

Volume = 4 m^3

Time = 2 hour

Pressure = 400 kPa

Laboratory filter area = 1 m^2

Pressure in laboratory scale experiment = 140 kPa

Approach

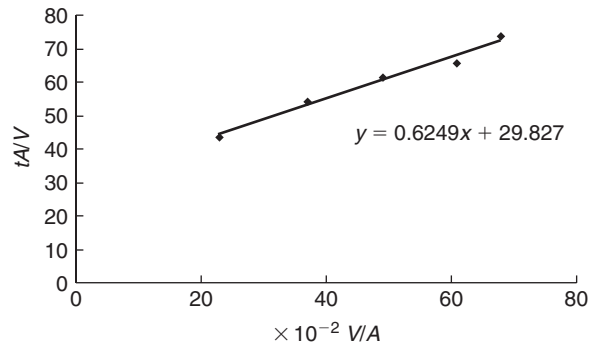
We will first plot tA/V vs. V/A and obtain slope and intercept. This will provide us with a design equation that we will use to determine the required area.

Solution

- Using Equation (13.10), a plot of tA/V versus V/A should provide a linear relationship with the slope equal to $\mu r' S / \Delta P$ and a vertical axis intercept of $\mu r' L / \Delta P$.
- From the experimental data provided

$V/A \times 10^{-2}$	tA/V
23	43.48
37	54.05
49	61.22
61	65.57
68	73.53

■ **Figure E13.1** A graph of data obtained from operating pilot-scale filtration equipment.



3. From the results presented in Figure E13.1, a slope of 62.5 and a vertical intercept of 29.83 provide the design equation

$$\frac{tA}{V} = 62.5 \frac{V}{A} + 29.83$$

4. Since pressure and area are the two variables existing between the laboratory and design situation, appropriate changes must be incorporated

$$\text{Slope} = 62.5 = \frac{\mu' S}{2(140,000)}; \quad \mu' S = 1.75 \times 10^7$$

$$\text{Intercept} = 29.83 = \frac{\mu' L}{140,000}; \quad \mu' L = 4,176,200$$

Thus the design equation becomes

$$\frac{tA}{V} = \frac{1.75 \times 10^7}{\Delta P} \left(\frac{V}{A} \right) + \frac{4,176,200}{\Delta P}$$

5. For the filtration system being designed: $t = 2 \text{ hr} = 120 \text{ min.}$; $V = 4 \text{ m}^3$; $\Delta P = 400 \text{ kPa}$.

Then

$$\frac{120A}{4} = \frac{1.75 \times 10^7}{400,000} \left(\frac{4}{A} \right) + \frac{4,176,200}{400,000}$$

$$30A = \frac{175}{A} + 10.44$$

$$A = 2.6 \text{ m}^2$$

6. An area of 2.6 m^2 is obtained when the positive solution of the quadratic equation is selected.

13.2 SEDIMENTATION

Sedimentation is the separation of solids from fluid streams by gravitational or centrifugal force. In the food industry, most processes involving sedimentation are used to remove particle solids from either liquid or gas. As will become obvious, the use of gravity in particular for removing solids from fluids has considerable application.

13.2.1 Sedimentation Velocities for Low-Concentration Suspensions

Particles in a low-concentration suspension will settle at a rate representing the terminal velocity of the particle in the suspension fluid.

The terminal velocity of each particle is established as though each individual particle is the only particle in the suspension. This type of sedimentation is usually referred to as free settling, since there is no interaction between particles and the suspension. The terminal velocity of the particle can be predicted and established by examining the forces acting on the particle. The force that resists the gravitational force is referred to as the drag force and can be described by the following expression:

$$F_D = 3\pi\mu du \quad (13.12)$$

where u represents the relative velocity between the particle and the fluid, d is particle diameter, and μ is fluid viscosity. Equation (13.12) applies as long as the particle Reynolds number is less than 0.2, which will be the case for most applications in food processing. Expressions to use when the particle Reynolds number is greater than 0.2 have been developed and are presented by Coulson and Richardson (1978). The gravitational force (F_G) is a function of particle volume and density difference along with gravitational acceleration, as illustrated by the following equation:

$$F_G = \frac{1}{6} \pi d^3 (\rho_p - \rho_f) g \quad (13.13)$$

where d is the particle diameter, assuming a spherical shape. By setting Equation (13.12) equal to Equation (13.13) (the conditions that must exist at the terminal velocity of the particle), we can solve and obtain an equation representing the terminal velocity as follows:

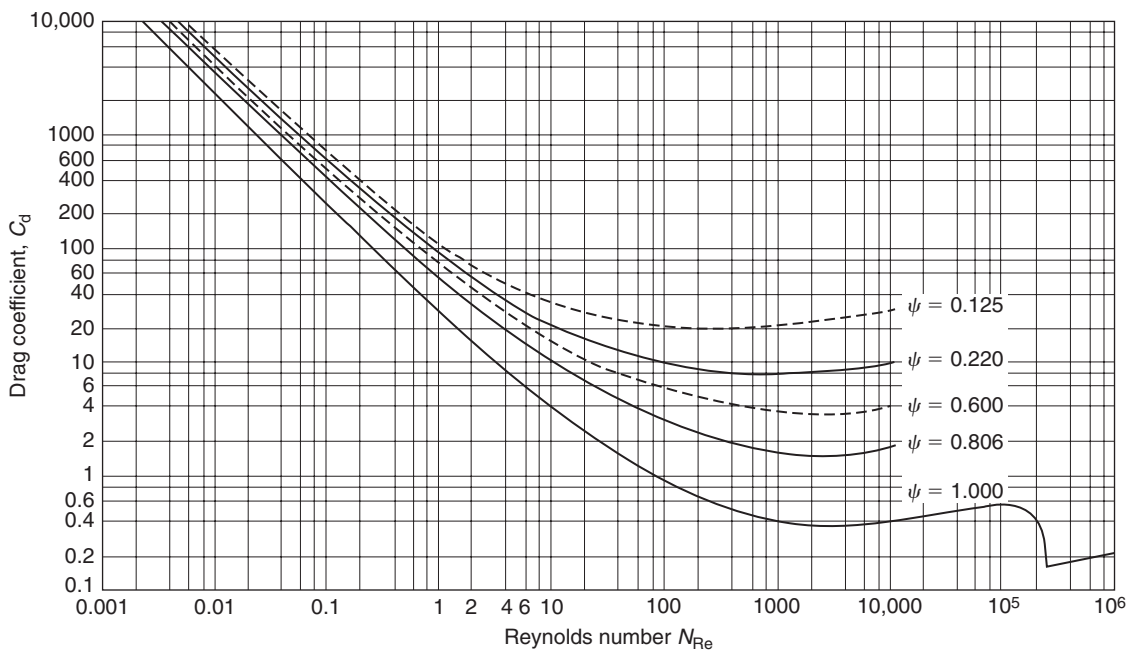
$$u_t = \frac{d^2 g}{18\mu} (\rho_p - \rho_f) \quad (13.14)$$

From Equation (13.14), we can see that the terminal velocity is related directly to the square of the particle diameter. In addition, the terminal velocity is dependent on the density of the particle and properties of the fluid. Equation (13.14) is the most common form of Stoke's law and should be applied only for streamline flow and spherical particles. When the particles are not spherical, the usual approach is to introduce a shape factor to account for the irregular shape of the particle and the corresponding influence of this factor on terminal velocity.

When streamline or laminar flow does not exist at Reynolds numbers above 1000, the conditions must be modified to account for the drag forces. For these conditions, the equation for terminal velocity becomes:

$$u_t = \sqrt{\left(\frac{4dg(\rho_p - \rho_g)}{3C_d\rho_f} \right)} \quad (13.15)$$

where the drag coefficient C_d is a function of the Reynolds Number, as illustrated in Figure 13.2.



■ **Figure 13.2** Influence of the Reynolds number on drag coefficient for spheres. ψ represents sphericity. (Adapted from Foust et al., 1960)

The damage to blueberries and other fruits during handling immediately after harvest is closely related to the terminal velocity in air. Compute the terminal velocity of a blueberry with a diameter of 0.60 cm and density of 1120 kg/m³ in air at 21°C and atmospheric pressure.

Example 13.4

Given

Diameter of blueberries = 0.6 cm

Density = 1120 kg/m³

Air temperature = 21°C

Approach

We will use Equation (13.14) to determine the terminal velocity. Next, we will check the validity of the equation by calculating the Reynolds number. If the equation is not valid then we will use Figure 13.2 and Equation (13.15) to obtain drag coefficient and recalculate terminal velocity.

Solution

1. Equation (13.14) can be used with the following parameter values:

$$d = 0.60 \text{ cm}, \quad g = 9.806 \text{ m/s}^2, \quad \mu = 1.828 \times 10^{-5} \text{ kg/ms}, \quad \rho_p = 1120 \text{ kg/m}^3, \quad \rho_f = 1.2 \text{ kg/m}^3.$$

2. Using Equation (13.14)

$$u_t = \frac{(0.006)^2(9.806)}{(18)(1.828 \times 10^{-5})} [1120 - 1.2] = 1200 \text{ m/s}$$

3. A check of the particle Reynolds number

$$N_{Re} = \frac{(1.2)(0.006)(1200)}{1.828 \times 10^{-5}} = 4.73 \times 10^5$$

indicates that streamline flow does not exist and conditions for using Equation (13.14) do not apply.

4. By using Equation (13.15), and the $C_d = 0.2$ from Figure 13.2, obtained at $N_{Re} = 4.73 \times 10^5$

$$u_t = \left[\frac{4}{3} \frac{(0.006)(9.806)}{(0.2)(1.2)} (1120 - 1.2) \right]^{1/2} = 19.1 \text{ m/s}$$

5. A check of the Reynolds number

$$N_{Re} = \frac{(1.2)(0.006)(19.1)}{1.828 \times 10^{-5}} = 7523$$

indicates that $C_d = 0.4$ and

$$u_t = \left[\frac{4}{3} \frac{(0.006)(9.806)}{(0.4)(1.2)} (1120 - 1.20) \right]^{1/2} = 13.5 \text{ m/s}$$

6. A final check of the Reynolds number

$$N_{Re} = \frac{(1.2)(0.006)(13.5)}{1.828 \times 10^{-5}} = 5317$$

indicates that $C_d = 0.4$ is appropriate and the terminal velocity is 13.5 m/s when the spherical geometry is assumed.

13.2.2 Sedimentation in High-Concentration Suspensions

When the concentration of solids in the suspension becomes sufficiently high, Stoke's law no longer describes the velocity of settling. In situations where the range of particle sizes is between 6 and 10 microns, the particles making up the solid suspension will fall at the same rate. This rate will correspond to the velocity predicted by Stoke's law, using a particle size that is the mean of the smallest and the largest particle size in the suspension. Physically it is apparent that the rate at which the larger particles settle is reduced by the influence of the smaller particles on the properties of the fluid. The rate at which the smaller particles fall is accelerated by the movement of the larger particles.

The settling of particles results in very well-defined zones of solids concentrations. The movement of the solids at a constant rate results in a clear liquid at the top of the column suspension. Directly below the clear liquid is the concentration of solids, which is moving at a constant rate. Below the solids that are settling is a zone of variable concentration within which the solids are collecting. At the bottom of the suspension column is the collected sediment, which contains the largest particles in the suspension. The definition of these zones will be influenced by the size of particles involved and the range of these sizes.

The rates at which solids settle in high-concentration suspensions have been investigated on an empirical basis and have been reviewed by Coulson and Richardson (1978). One approach is to modify Stoke's law by introducing the density and viscosity of the suspension

in place of the density and viscosity of the fluid. This may result in an equation for the settling rate of the suspension as follows:

$$u_s = \frac{KD^2(\rho_p - \rho_s)g}{\mu_s} \quad (13.16)$$

where K is a constant to be evaluated experimentally. In most cases, attempts are made to predict the density and viscosity of the suspension on the basis of the composition. Another approach is to account for the void between suspension particles, which allows movement of fluid to the upper part of the suspension column. The expression for the particle settling velocity was obtained as follows:

$$u_p = \frac{D^2(\rho_p - \rho_s)g}{18\mu} f(e) \quad (13.17)$$

where $f(e)$ is a function of the void in a suspension. Equation (13.17) is still a modification of Stoke's law, where the density of the suspension and the viscosity of the fluid are used. The function of the void space in the suspension must be determined experimentally for each situation in which the expression is utilized. Although there are definite limitations to Equations (13.16) and (13.17), they will provide practical results for high-concentration suspensions of large particles. Description of settling rates for small-particle suspensions is subject to considerable error and acceptable approaches need to be developed.

A sedimentation tank is used to remove larger-particle solids from wastewater leaving a food-processing plant. The ratio of liquid mass to solids in the inlet to the tank is 9 kg liquid/kg solids; the inlet flow rate is 0.1 kg/s. The sediment leaving the tank bottom should have 1 kg liquid/kg solids. Density of water is 993 kg/m³. If the sedimentation rate for the solids in water is 0.0001 m/s, determine the area of sedimentation necessary.

Example 13.5

Given

Ratio of liquid mass to solids in the inlet = 9 kg liquid/kg solids

Inlet flow rate = 0.1 kg/s

Sediment composition = 1 kg liquid/kg solids

Sedimentation rate of solids in water = 0.0001 m/s

Approach

We will first obtain an upward velocity of the liquid in the tank. Then using the given information we will obtain the area when the upward liquid velocity is equal to the sedimentation velocity for solids.

Solution

1. Using the mass flow equation and the difference between inlet and outlet conditions on the wastewater, the following equation for upward velocity of liquid in the tank is obtained

$$u_f = \frac{(c_i - c_o)w}{A\rho}$$

where c_i and c_o are mass ratios for liquid to solids in waste water.

2. Based on information given

$$\begin{array}{ll} c_i = 9 & w = 0.1 \\ c_o = 1 & \rho = 993 \end{array}$$

3. Since the upward liquid velocity should equal sedimentation velocity for the solids, the area becomes

$$A = \frac{(9-1)(0.1)}{(0.0001)(993)} = 8 \text{ m}^2$$

In addition to the properties of the solid and fluid in the suspension, other factors influence the sedimentation process. The height of the suspension generally will not affect the rate of sedimentation or the consistency of the sediment produced. By experimentally determining the height of the liquid or fluid-sediment interface as a function of time for a given initial height, the results for any other initial height can be predicted. The diameter of the sedimentation column may influence the rate of sedimentation if the ratio of the column diameter to the particle diameter is less than 100. In this particular situation, the walls may have a retarding influence on sedimentation rate. In general, the concentration of the suspension will influence the rate of sedimentation, with higher concentrations tending to reduce the rate at which the sediment settles.

It is possible to use sedimentation to remove solid particles from air, such as after spray-drying processes. By introducing the particle suspension into a static air column, the solid particles tend to settle to the floor surface. Relatively simple, straightforward computations using expressions presented previously in this chapter will illustrate that such sedimentation processes are quite slow for particles of the type normally encountered. Because of this, the sedimentation is not used often in this regard. Procedures using other forces on the particle to accelerate removal are preferred and will be discussed more thoroughly in the next section.

13.3 CENTRIFUGATION

In many processes, the use of sedimentation to separate two liquids or a liquid and a solid does not progress rapidly enough to accomplish separation efficiently. In these types of applications the separation can be accelerated through the use of centrifugal force.

13.3.1 Basic Equations

The first basic equation describes the force acting on a particle moving in a circular path as follows:

$$F_c = \frac{mr\omega^2}{g_c} \quad (13.18)$$

where ω represents the angular velocity of the particle. Since ω can be expressed as the tangential velocity of the particle and its radial distance to the center of rotation (r), Equation (13.18) can be presented as:

$$F_c = \left(\frac{m}{g_c} \right) \frac{u^2}{r} \quad (13.19)$$

Earle (1983) illustrated that if the rotational speed is expressed in revolutions per minute, Equation (13.19) can be written as:

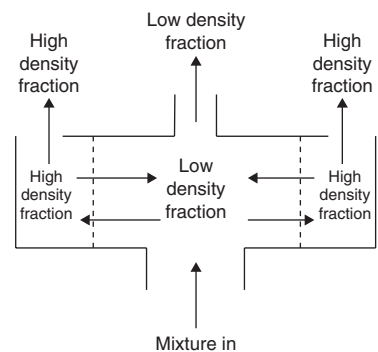
$$F_c = 0.011 \frac{mrN^2}{g_c} \quad (13.20)$$

where N represents the rotational speed in revolutions per minute.

Equation (13.20) indicates that the centrifugal force acting on a particle is directly related to and dependent on the distance of the particle from the center of rotation r , the centrifugal speed of rotation N , and the mass of the particle considered m . For example, if a fluid containing particles of different densities is placed in a rotating bowl, the higher-density particles will move to the outside of the bowl as a result of the greater centrifugal force acting upon them. This will result in a movement of the lower-density particles toward the interior portion of the bowl, as illustrated in Figure 13.3. This principle is used in the separation of liquid food products that contain components of different densities.

13.3.2 Rate of Separation

The rate at which the separation of materials of different densities can occur is usually expressed in terms of the relative velocity between the two phases. An expression for this velocity is the same as the equation



■ **Figure 13.3** Separation of fluids with different densities using centrifugal force.

for terminal velocity given as Equation (13.14), in which the gravitational acceleration (g) is replaced by an acceleration parameter describing the influence of centrifugal force. This acceleration can be expressed in the following way:

$$a = r \left(\frac{2\pi N}{60} \right)^2 \quad (13.21)$$

where N is the rotational speed of the centrifuge in revolutions per minute. Substitution of Equation (13.21) into Equation (13.14) results in the following expression to describe the velocity of spherical particles in a centrifugal force field:

$$u_c = \frac{D^2 N^2 r (\rho_p - \rho_s)}{1640 \mu} \quad (13.22)$$

Equation (13.22) can be applied to any situation in which there are two phases with different densities. The expression clearly illustrates that the rate of separation as expressed by velocity (u_c) is directly related to the density between phases, the distance from the center of rotation, the speed of rotation, and the diameter of the particles in the higher density phase.

Example 13.6

The solid particles in a liquid-solid suspension are to be separated by centrifugal force. The particles are 100 microns in diameter with a density of 800 kg/m^3 . The liquid is water with a density of 993 kg/m^3 , and the effective radius for separation is 7.5 cm. If the required velocity for separation is 0.03 m/s , determine the required rotation speed for the centrifuge.

Given

Particle diameter = 100 microns

Density = 800 kg/m^3

Density of water = 993 kg/m^3

Effective radius for separation = 7.5 cm

Required velocity for separation = 0.03 m/s

Approach

We will use Equation (13.22) to obtain the rotational speed of the cartridge.

Solution

1. Using Equation (13.22) with the viscosity of water at 5.95×10^{-4} kg/ms

$$N^2 = \frac{1640\mu u_c}{D^2 r(\rho_p - \rho_s)} = \frac{1640(5.95 \times 10^{-4})}{(0.075)(100 \times 10^{-6})^2(993 - 800)}(0.03)$$

$$N^2 = 2.02 \times 10^5 \text{ (1/s}^2\text{)}$$

$$N = 26,940 \text{ rpm}$$

13.3.3 Liquid-Liquid Separation

In the case of separation involving two liquid phases, it is usually easier to describe the process in terms of the surface that separates the two phases during separation. The differential centrifugal force acting on an annulus of the liquid in the separation cylinder can be written as:

$$dF_c = \frac{dm}{g_c} r \omega^2 \quad (13.23)$$

where (dm) represents the mass in the annulus of liquid. Equation (13.23) can be rewritten as:

$$\frac{dF_c}{2\pi r b} = dP = \frac{\rho \omega^2 r dr}{g_c} a \quad (13.24)$$

where (dP) represents the differential pressure across the annulus of liquid and b represents the height of the separation bowl. By integration of Equation (13.24) between two different radii in the separation cylinder, the difference in pressure between these two locations can be computed from the following expression:

$$P_2 - P_1 = \frac{\rho \omega^2 (r_2^2 - r_1^2)}{2g_c} \quad (13.25)$$

At some point in the cylinder, the pressure of one phase must equal that of the other phase so that expressions of the type given by Equation (13.25) can be written for each phase and represent the radius of equal pressure in the following manner:

$$\frac{\rho_A \omega^2 (r_n^2 - r_1^2)}{2g_c} = \frac{\rho_B \omega^2 (r_n^2 - r_2^2)}{2g_c} \quad (13.26)$$

By solving for the radius of equal pressures for the two phases, the following expression is obtained:

$$r_n^2 = \left[\frac{(\rho_A r_1^2 - \rho_B r_2^2)}{\rho_A - \rho_B} \right] \quad (13.27)$$

where ρ_A equals the density of the heavy liquid phase and ρ_B is the low-density liquid phase. Equation (13.27) is a basic expression for use in the design of the separation cylinder. The radius of equal pressure, which represents the radius at which the two phases may be or are separated is dependent on two radii (r_1 and r_2). These two values can be varied independently to provide optimum separation of the two phases involved and will account for the density of each phase as illustrated.

Example 13.7

Design the inlet and discharge for a centrifugal separation of cream from whole milk. The density of the skim milk is 1025 kg/m^3 . Illustrate the discharge conditions necessary if the cream outlet has a 2.5-cm radius and the skim milk outlet has a 5-cm radius. Suggest a desirable radius for the inlet. Cream density is 865 kg/m^3 .

Given

Density of milk = 1025 kg/m^3

Cream outlet radius = 2.5 cm

Skim milk outlet radius = 5 cm

Cream density = 865 kg/m^3

Approach

We will use Equation (13.27) to obtain the radius of the neutral zone and then we will use this information to develop a diagram to illustrate the design.

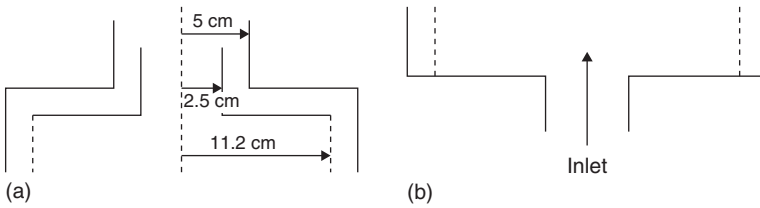
Solution

1. Using Equation (13.27), the radius of the neutral zone can be computed:

$$r_n^2 = \frac{1025(0.05)^2 - 865(0.025)^2}{1025 - 865}$$

$$r_n^2 = 0.0126$$

$$r_n = 0.112 \text{ m} = 11.2 \text{ cm}$$



■ **Figure E13.2** Schematic representation of a centrifugal separator.

2. Based on information given and the computation of neutral zone radius, the separator discharge should be designed as shown in Figure E13.2a.
3. Similarly the inlet should be designed to allow the product to enter with least disturbance possible to the neutral zone (Fig. E13.2b).

13.3.4 Particle-Gas Separation

The separation of solids from a gas phase is a common operation in many food-processing operations. Probably the most common is the separation of a spray-dried product from the air stream after the drying operation is completed. This is usually accomplished in what is known as a cyclone separator. The basic equations presented earlier in this section will apply, and Equation (13.22) will provide some indication of the rate at which separation of solid particles from an air stream can be accomplished.

It is obvious from this expression that the diameter of the particles must be known, along with the density of the solid and the density of the air stream.

13.4 MIXING

Mixing is a common operation in the food industry. A mixing device is required whenever an ingredient is added to a food. The type of device used is usually based on the properties of the food undergoing mixing. Because the quality of a mixed product is judged by the even distribution of its ingredients, the design of the mixing device and its operation must be chosen carefully to accomplish the desired results.

In industrial applications, agitation is used for mixing. Agitation is defined as the application of mechanical force to move a material in a circulatory or similar manner in a vessel. Mixing may involve

two or more materials of the same or different phases. Mechanical force is used in mixing to cause one material to randomly distribute in another. Examples of mixing include mixing a solid in a fluid, a solid in a solid, or a fluid in a fluid, where a fluid may be a liquid or a gas.

The difference between the terms “mixing” and “agitation” can be understood from the following. Mixing always requires two or more materials or two or more phases of the same material. For example, we can *agitate* a vessel full of cold water, but in *mixing* we would add hot water to cold water to raise the temperature of the mixture, or we would add a material of a different phase such as sugar into water.

When two or more materials are mixed, the goal of mixing is to obtain a homogenous final mixture. However, “homogeneity” depends on the sample size taken from a mixture. Mixing two liquids such as corn syrup and water may yield a greater homogeneity than mixing two solids of different particulate size, such as raisins mixed in flour. Obviously, the sample size taken from a mixture containing raisins and flour must be larger than the size of a single raisin or the mixture will be devoid of raisins.

In food processing, we agitate liquid foods for a variety of reasons such as to blend one liquid into another miscible liquid (corn syrup and water), disperse gas in a liquid such as in carbonation, or create emulsions such as mayonnaise where one liquid is immiscible in another. Many fragile foods require mixing when ingredients are added to them while taking care to prevent any physical damage to the product (e.g., potato salad, macaroni salad).

Mixing operations in the food industry vary in their complexity. Simple systems involve mixing two miscible liquids of low viscosity, whereas mixing gum into a liquid can become complicated as the viscosity of the mix changes during mixing. When small quantities of one material are mixed into a bulk, such as spices into flour, the mixer must ensure that the entire bulk contents are well mixed. In mixing of many free-flowing particulate materials such as breakfast cereals, there is a tendency of the materials being mixed to actually segregate, counteracting the desired objective.

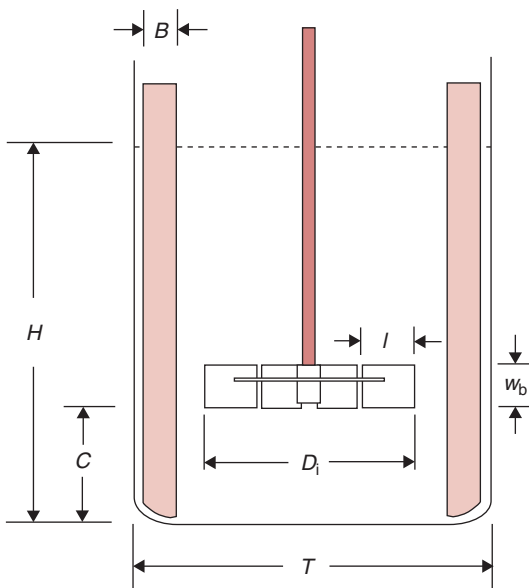
Mixing processes in the industry are carried out either in bulk or continuous mode. Although continuous systems are smaller in size and desirable for minimizing variations between runs, they require materials that have appropriate flow characteristics. In batch systems, there

is more variation between runs during mixing. Furthermore, batch units require more labor but they are easy to modify simply by changing impellers.

13.4.1 Agitation Equipment

A typical vessel used for agitation is shown in Figure 13.4. The vessel may be open or closed and at times may be operated under vacuum. Inside the vessel, a shaft along the middle axis of the vessel is connected at the top to a motor. When heating or cooling is desired during agitation, the vessel is surrounded with a jacket containing a circulating heat transfer medium. An impeller is installed at the bottom of the shaft. In some applications, the shaft may be located off the central axis. In other applications, more than one impeller may be installed in the same vessel. The tank bottom is rounded because sharp corners restrict fluid movement. Typical geometric ratios of the impeller size and location with respect to the tank size are shown in Table 13.1.

There are three types of commonly used impellers: propellers, paddles, and turbines.

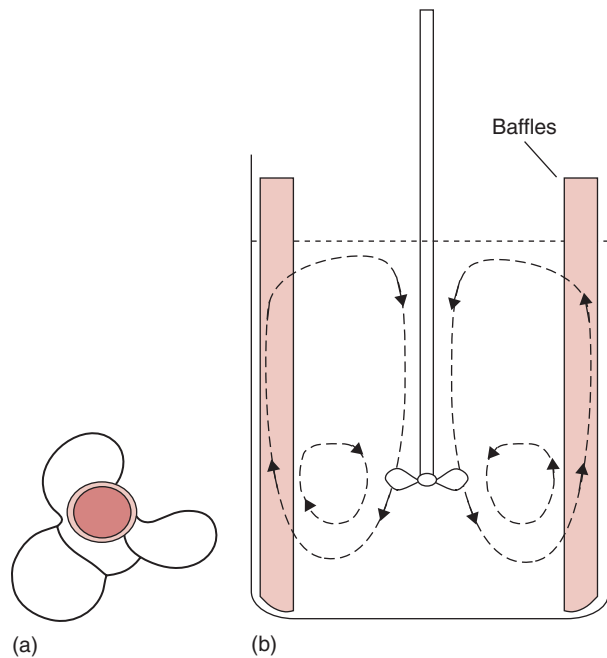


■ **Figure 13.4** Schematic illustration of an agitation vessel with an impeller and baffles.

Table 13.1 Typical Geometric Ratios of Commonly Used Impellers

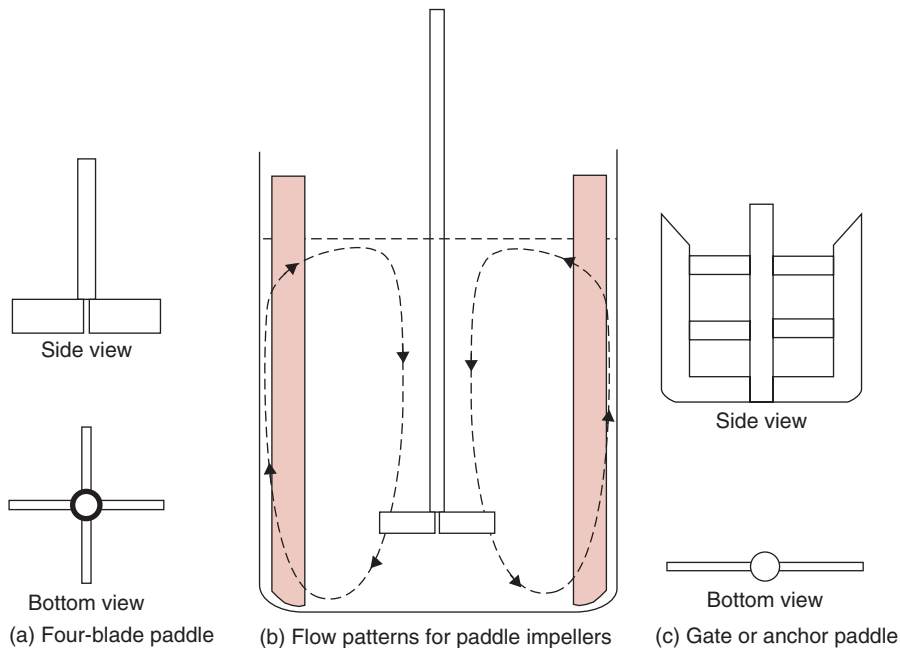
Ratio	Typical Range	Ratios for a “standard” agitating system
H/T	1–3	1
D_i/T	$1/4$ – $2/3$	$1/3$
C/T	$1/4$ – $1/2$	$1/3$
C/D_i	~ 1	1
B/T	$1/12$ – $1/10$	$1/10$
w_b/D_i	$1/8$ – $1/5$	$1/5$

■ **Figure 13.5** Amarine type propeller and flow behavior inside an agitation vessel.



13.4.1.1 Marine-type Propeller Impellers

As shown in Figure 13.5, a propeller-type impeller typically has three blades, similar to propellers used in boats for propulsion in water. Propeller-type impellers are used largely for low-viscosity fluids and

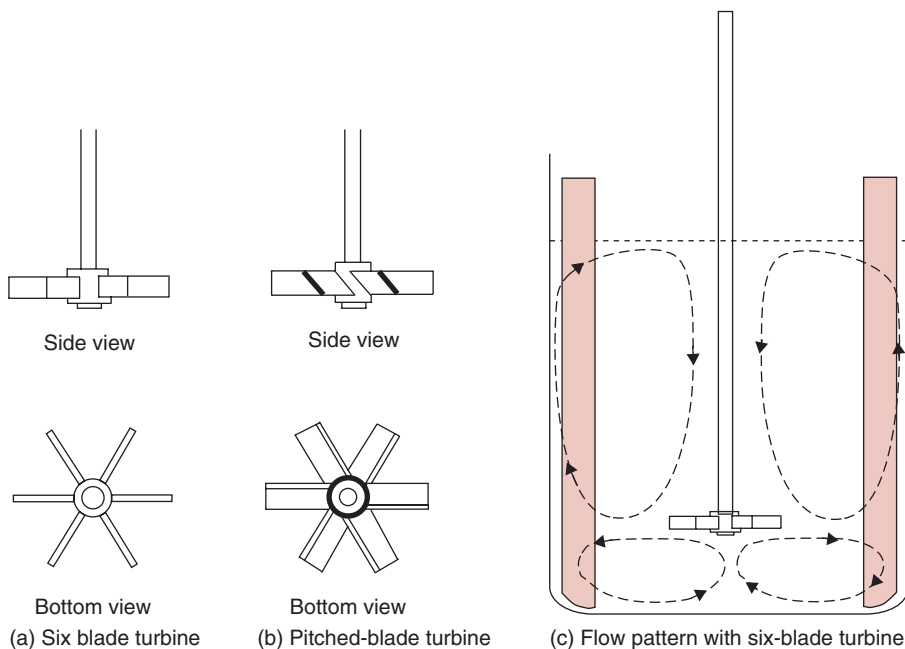


■ **Figure 13.6** Paddle impellers and flow behavior inside an agitation vessel.

are operated at high speeds. The discharge flow in a propeller is parallel to the axis. This type of flow pattern is called axial flow. As shown in Figure 13.5, the fluid moves up along the sides and down along the central axis.

13.4.1.2 Paddle Impellers

Paddle impellers usually have either two or four blades (Fig. 13.6). The blades may be flat or pitched at an angle. As the paddles turn, the liquid is pushed in the radial and tangential direction. There is no motion in the vertical direction. These impellers are effective for agitating fluid at low speeds (20 to 150 rpm). When paddle impellers are operated at high speeds, the mixing vessel must be equipped with a baffle to prevent the material from moving in a plug-flow pattern. The ratio of impeller-to-tank diameter is in the range of 0.5 to 0.9. In situations requiring scraping of the inside surface of the vessel to minimize fouling when the product is heated, an anchor-type design for the impeller is used, as shown in Figure 13.6.



■ **Figure 13.7** Turbine agitator and flow behavior inside a vessel.

13.4.1.3 Turbine Agitators

Turbine agitators are similar to paddle impellers equipped with short multiple blades. The diameter of the turbine is usually less than half of the diameter of the vessel. Axial flow is induced when pitched blades are used, as shown in Figure 13.7. Flat-bladed turbines discharge in the radial direction. In curved-bladed turbines, the blade curves away from the direction of rotation. This modification causes less mechanical shear of the product and is more suitable for products with friable solids.

Table 13.2 shows various types of agitators and the recommended range of product viscosities.

13.4.2 Power Requirements of Impellers

In designing agitation systems, the power needed to drive an impeller must be known. The power requirement of an impeller is influenced by several product and equipment variables. Because the large number of variables does not permit development of an analytical

Table 13.2 Suitability of Agitators for Different Ranges of Viscosity

Agitator type	Viscosity range of product (Pas)
Propellor	<3
Turbine	<100
Anchor	50–500
Helical and ribbon type	500–1000

relationship useful for design purposes, we must use empirical computations to estimate the required power for driving the impeller.

In the empirical approach, we use dimensional analysis to develop relationships between various measurable quantities. The power required by the impeller is a function of the size and shape of the impeller and tank, the rotational speed of the impeller, gravitational forces, and properties of the fluid such as viscosity and density. Using Buckingham π theorem (Appendix A.9), the following functional equation is obtained for various quantities important in an agitation system:

$$f\left(\frac{\rho ND_i^2}{\mu}, \frac{N^2 D_i}{g}, \frac{P_r}{\rho N^3 D_i^5}, \frac{D_i}{T}, \frac{D_i}{H}, \frac{D_i}{C}, \frac{D_i}{p}, \frac{D_i}{w_b}, \frac{D_i}{l}, \frac{n_2}{n_1}\right) = 0 \quad (13.28)$$

where ρ is the fluid density, kg/m^3 ; D_i is the diameter of the impeller, m ; and μ is the viscosity of the fluid, kg/ms ; N is the rotational speed of the impeller, revolutions/s ; g is the acceleration due to gravity, m/s^2 ; P_r is the power consumption by the impeller, J/s ; H is the liquid depth in the tank, m ; C is clearance of the impeller off the vessel bottom, m ; l is the blade length, m ; w_b is the blade width, m ; p is the pitch of blades; n is the number of blades.

In Equation (13.28), the last seven terms on the left side are related to the geometry of the impeller and the vessel. The last term is the ratio of number of blades.

The first three dimensionless numbers in Equation (13.28) are as follows. The first term is the Reynolds number,

$$N_{\text{Re}} = \frac{\rho ND_i^2}{\mu} \quad (13.29)$$

The second number is the Froude number that is a ratio of the inertial to gravitational forces.

$$N_{\text{Fr}} = \frac{N^2 D_i}{g} \quad (13.30)$$

The Froude number plays an important role in many situations involving agitation. Consider a vessel open to the atmosphere and with a free liquid surface. If the tank does not contain baffles, then upon the action of the impeller, a vortex is formed and the role of gravitational forces becomes important in defining the shape of the vortex. When vessels contain baffles, the role of Froude number becomes negligible.

The third number is called the Power number, N_p . It is defined as follows:

$$N_p = \frac{P_r}{\rho N^3 D_i^5} \quad (13.31)$$

N_p is a dimensionless number. The dimensions cancel when the units of power are written in base units as kgm^2/s^3 .

Relationships between the Power number and the Reynolds number have been reported for a variety of impeller designs and geometrical considerations by several investigators (Rushton et al., 1950; Bates et al., 1966). For agitated tanks, a Reynolds number less than 10 indicates laminar flow, greater than 100,000 is turbulent flow, and between 10 and 100,000 the flow field is considered to be transitional.

Experimental data obtained from trials with different type of agitation systems are plotted on a log-log graph, with the Power number as the y-ordinate and the Reynolds number as the abscissa as shown in Figure 13.8. We can use Figure 13.8 for calculating power requirements of an agitation system, but it is important to note that this figure is applicable only for the impeller design and geometrical considerations for which this figure was developed. Therefore, we must first ensure that the conditions of a given problem are similar to the ones shown in the figure. Similar graphical relationships are available in the literature for other types of impeller designs and geometrical considerations.

From Figure 13.8, we observe that for paddle and turbine impellers operating in the laminar region, there is a linear decrease in the Power number with Reynolds number. In the turbulent region, the Power number remains fairly constant.

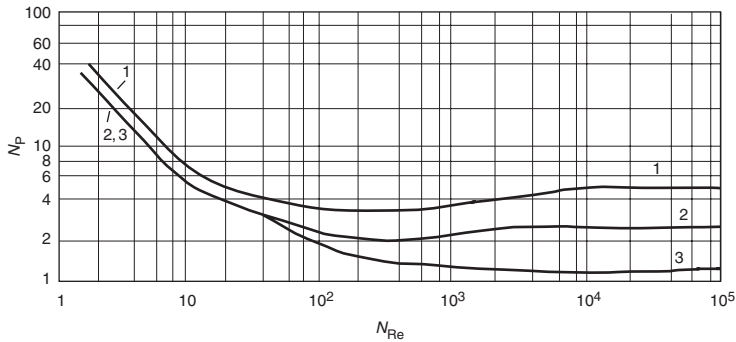


Figure 13.8 Correlation between the Power number and the Reynolds number for various impellers. (Curve 1 is for a flat six-blade turbine with disk and four baffles; $w_b/D_i = 1/5$, $B/T = 1/12$; Curve 2 is for a flat six-blade open turbine with four baffles, $w_b/D_i = 1/8$, $B/T = 1/12$; Curve 3 is for a six blade open turbine with blades pitched at 45° and four baffles, $w_b/D_i = 1/8$, $B/T = 1/12$). (Adapted from Bates et al., 1963)

A concentrated fruit juice with a viscosity of $0.03 \text{ Pa}\cdot\text{s}$ and a density of 1100 kg/m^3 is being agitated in an agitation system containing a turbine impeller. The impeller has a disk with six blades. The tank diameter is 1.8 m . The height of the liquid in the tank is the same as the tank diameter. The impeller diameter is 0.5 m . The width of the blade is 0.1 m . The tank is equipped with four baffles, each with a width of 0.15 m . If the turbine is operated at 100 rpm , determine the required power.

Example 13.8

Given

Diameter of the impeller, $D_i = 0.5 \text{ m}$

Diameter of the tank, $T = 1.8 \text{ m}$

Width of the blade, $w_b = 0.1 \text{ m}$

Width of the baffle, $B = 0.15 \text{ m}$

Impeller speed, $N = 100 \text{ rpm}$

Density of fluid, $\rho = 1100 \text{ kg/m}^3$

Viscosity of fluid, $\mu = 0.03 \text{ Pa}\cdot\text{s}$

Approach

We will first calculate the Reynolds number. We observe that the turbine type, size and number of blades, and size and number of baffles in this example are the same as shown for curve 1 in Figure 13.8. Therefore, we will use Figure 13.8 to determine the Power number using the calculated Reynolds number. Power requirements will be obtained from the Power number.

Solution

1. From Equation (13.29),

$$N_{Re} = \frac{D_i^2 N \rho}{\mu} = \frac{(0.5\text{ m})^2 (1.667\text{ rev/s}) (1100\text{ kg/m}^3)}{0.03(\text{ kg/ms})}$$

$$N_{Re} = 15,280$$

2. In Figure 13.8, curve 1 is for a flat six-blade turbine with disk, for $D_i/w_b = 5$ and the tank containing four baffles with $B/T = 1/12$. These conditions match the given dimensions therefore we will use curve 1 to obtain the Power number. From Figure 13.8, for a Reynolds number of 1.5×10^4 , the power number

$$N_p = 5$$

3. From Equation (13.31)

$$P_r = N_p \rho N^3 D_i^5 = 5.0 (1100\text{ kg/m}^3) (1.667\text{ rev/s})^3 (0.5\text{ m})^5$$

$$P_r = 796.2\text{ J/s} = 0.796\text{ kW}$$

4. The impeller requires power input of 0.796 kW. Therefore the motor selected for the mixer must be larger than 0.8 kW.

PROBLEMS

- 13.1** An air filter normally requires change after 100 hours of use when the pressure drop is 5 cm. The filter is $1\text{ m} \times 3\text{ m}$ and is designed for an air flow rate of $1.5\text{ m}^3/\text{s}$. Compute the influence of increasing the air flow rate to $2.5\text{ m}^3/\text{s}$ on the life of the filter.
- 13.2** The effective diameter of strawberry fruit is being estimated from terminal velocity measurements. Compute the effective diameter from a terminal velocity of 15 m/s and fruit density of 1150 kg/m^3 .
- 13.3** The 50-micron particles in a water suspension are to be removed using a centrifugal separator operating at 70,000 rpm. Compute the effective radius for separation when the velocity of separation is 0.05 m/s and the particle density is 850 kg/m^3 .
- *13.4** A 0.5-m^2 filter is used to filter a liquid at a pressure of 100 kPa. A 1-cm^2 laboratory-scale version of the filter media was used to filter 0.01 m^3 of the liquid in 1 minute at the same pressure. Compute the rate of filtration after 2 hours through the commercial filter.

* Indicates an advanced level in solving.

- 13.5** Cream is separated from skim milk using a centrifugal separator. The separator inlet has a 25-cm radius, and the skim milk outlet is 10 cm radius. Estimate the cream outlet radius when the cream density is 865 kg/m^3 and skim milk density is 1025 kg/m^3 .

LIST OF SYMBOLS

A	area, m^2
a	acceleration, m/s^2
b	height of centrifugal separation bowl, m
B	width of baffles, m
c	solids concentration in solution expressed as mass of liquid per unit mass solids, kg liquid/kg solid
C	clearance of the impeller off the vessel bottom, m
d	particle diameter, micron, 10^{-6} m
D_i	Diameter of impeller, m
F	force, N
$f(e)$	function used in Equation (13.17)
g	acceleration due to gravity, m/s^2
g_c	constant in Equations (13.18) and (13.19)
H	Liquid height in the tank, m
K	experimental constant
L	thickness of filter material in liquid filtration system, m
L_c	thickness of filter cake in liquid filtration system, m
l	blade length, m
m	particle mass in centrifugal force field, kg
n	number of blades
N	rotational speed, revolutions/min
N_p	Power number
N_{Re}	Reynolds number
N_{Fr}	Froude number
p	pitch of blades, degrees
P	total pressure at some location in the separation, Pa
P_r	Power, $\text{kg m}^2/\text{s}^3$
R	resistance in filtration separation system
N_{Re}	Reynolds number
r	radius, m
r'	specific resistance of filter cake
S	solids content of liquid being filtered, $\text{kg solid/m}^3 \text{ liquid}$
t	time, s
u	velocity, m/s

V	volume of liquid being filtered, m^3
w	mass flow rate, kg/s
w_b	blade width, m
μ	viscosity, kg/ms
ω	angular velocity
ρ	density, kg/m^3
ψ	sphericity

Subscripts: A, high-density fraction in Equation (13.26); B, low-density fraction in Equation (13.26); c, centrifugal separation system reference; D, drag in particle; f, fluid fraction reference; G, gravitation reference in separation system; i, input condition reference; n, location of equal pressure in centrifugal separation system; o, outlet condition reference; p, solid or particle fraction reference; s, suspension during separation; t, terminal condition; 1,2, general location or time references

■ BIBLIOGRAPHY

- Bates, R. L., Fondy, P. L., and Corpstein, R. R. (1963). An examination of some geometric parameters of impeller power. *Ind. Eng. Chem. Proc. Des. Dev.* 2: 310.
- Charm, S. E. (1978). *The Fundamentals of Food Engineering*, 3rd ed. AVI Publishing Co, Westport, Conn.
- Coulson, J. M. and Richardson, J. F. (1978). *Chemical Engineering*, 3rd ed., Volume 11. Pergamon Press, Elmsford, N.Y.
- Decker, H. M., Buchanan, L. M., Hall, L. B., and Goddard, K. R. (1962). *Air Filtration of Microbial Particles*. Public Health Service, Publ. 593, U.S. Govt. Printing Office, Washington, D.C.
- Earle, R. L. (1983). *Unit Operations in Food Processing*, 2nd ed. Pergamon Press, Elmsford, N.Y.
- Foust, A. S., Wenzel, L. A., Clump, C. W., Maus, L., and Anderson, L. B. (1960). *Principles of Unit Operations*. John Wiley & Sons, New York.
- Geankoplis, C. J. (2003). *Transport Processes and Separation Principles*, 4th ed., Pearson Education Inc, New Jersey.
- Rushton, J. H., Costich, E. W., and Everett, H. J. (1950). Power characteristics of mixing impellers. *Chem. Eng. Progr.* 46: 395, 467.
- Whitby, K. T. and Lundgren, D. A. (1965). The mechanics of air cleaning. *Trans. Am. Soc. Chem. Engrs.* 8(3): 342.

Extrusion Processes for Foods

Extrusion is a process that converts raw material into a product with desired shape and form by forcing the material through a small opening using pressure. The process involves a series of unit operations such as mixing, kneading, shearing, heating, cooling, shaping and forming. Many food products are manufactured by extrusion cooking—a process that uses both thermal energy and pressure to convert raw food ingredients into popular products such as breakfast cereals, pastas, pet foods, snacks and meat products.

14.1 INTRODUCTION AND BACKGROUND

The origins of the extrusion process are closely associated with polymer science and technology. In the mid-1850s, extrusion was used to produce the first seamless lead pipe. The first man-made thermoplastic, celluloid, was manufactured in the 1860s based on a reaction between cellulose and nitric acid. The manufacturing of Bakelite in 1907, and the protective coating resin, glyptal, in 1912, was dependent on extrusion processing. Formal applications of extrusion processes to foods began in the 1930s and evolved over the following 50 years, as equipment for extrusion processing increased in capabilities and complexity.

In general, all extrusion systems contain five key components. These components are:

- Primary feed system consisting of a container and delivery system for the primary ingredients involved in the process
- Pump to move all ingredients through the steps associated with the extrusion process
- Reaction vessel where key actions such as mixing, kneading, shearing, heating, and cooling occur

All icons in this chapter refer to the author's web site, which is independently owned and operated. Academic Press is not responsible for the content or operation of the author's web site. Please direct your web site comments and questions to the author: Professor R. Paul Singh, Department of Biological and Agricultural Engineering, University of California, Davis, CA 95616, USA.
Email: rps@rpaulsingh.com.

- Secondary feed system for adding secondary ingredients or energy as needed to achieve the desired product characteristics
- Exit assembly designed to restrict flow and contribute to the shaping and forming of the final product (usually referred to as the die)

These components appear in different ways and may be identified differently in various extrusion systems, depending on the specific equipment used and the product being manufactured.

Early examples of extrusion processing include pasta products (macaroni, spaghetti, etc.) and pellets for conversion into ready-to-eat cereals. Current applications include commercial production of cereal-based products (cornflakes, puffed rice, crispbreads, snacks), fruit-based products (fruit gums, licorices, hard candies), protein-based products (textured vegetable proteins), animal feeds (pet foods), and spice-based products (flavors).

The application of the extrusion process to food manufacturing is very complex and cannot be described and discussed in detail in this text. Numerous references provide in-depth information on the design of the process, the equipment used, and the products created by the process. Some key references include Harper (1981); Mercier, Linko, and Harper (1989); Kokini, Ho and Karwe (1992); and Levine and Miller (2006). The goal of the information presented here is to provide undergraduate food science students with an introduction to the quantitative and qualitative aspects of the extrusion process.

14.2 BASIC PRINCIPLES OF EXTRUSION

Extrusion involves a combination of transport processes, including flow of materials within the system, thermal energy transfer to and within the material, and mass transfer to and within the material during extrusion. The flow of materials within the channels of the system occurs in all types of extrusion. Food ingredients of various types may be processed by extrusion and are referred to as *extrudates*. All ingredients involved in the extrusion process flow through a channel with a defined geometry. The power requirements for the process are directly dependent on the flow characteristics through the channel. As indicated in Chapter 2, these requirements are also dependent on properties of the fluid used. In general, these properties are part of extrudate rheology.

The relationships used in extrudate rheology include many of the basic expressions presented in Chapter 2, beginning with basic relationships

presented to define viscosity. The relationship between shear stress (σ) and rate of shear ($\dot{\gamma}$) was presented as Equation (2.10):

$$\sigma = \mu \left[\frac{du}{dy} \right]$$

The primary property of the extrudate in this relationship is viscosity (μ). Since most food extrudates are highly non-Newtonian, the apparent viscosity decreases with increasing rate of shear. As illustrated in Chapter 2, these materials are described by the Herschel-Bulkley model or Equation (2.161):

$$\sigma = K \left[\frac{du}{dy} \right]^n + \sigma_o$$

When applied to extrudates, this three-parameter model is usually reduced to the following two-parameter model:

$$\sigma = K \left[\frac{du}{dy} \right]^n \quad (14.1)$$

where the consistency coefficient (K) and the flow behavior index (n) are parameters describing the rheological properties of the extrudate. Based on investigations of the flow behavior of food extrudates, the flow behavior index is normally less than 1.0.

Two additional parameters with significant influence on flow of food extrudates are moisture content and temperature. In order to account for the additional factors, the following relationship has been proposed:

$$\sigma = K_o e^{\left(\frac{A}{T}\right)} e^{(BM)} \left[\frac{du}{dy} \right]^n \quad (14.2)$$

This relationship contains two additional parameters: an activation energy constant (A) to account for the influence of temperature (T), and a similar exponential constant (B) to account for the influence of dry basis moisture content (M). Typical rheological properties and constants for food extrudates are presented in Table 14.1. These properties and constants are likely to change during the extrusion process, but the magnitudes presented are acceptable for preliminary estimates of extruder performance.

Although the flow of an extrudate within the extrusion system may occur in a tube or pipe geometry, the channels include several flow

Table 14.1 Reported Power Law Models (Eq. 14.2) for Food Extrudates

Material	K_o	n	Temperature range (°C)	Moisture range (%)	A (K)	B (1/%M _{DB})	Reference
Cooked cereal dough (80% corn grits, 20% oat flour)	78.5	0.51	67–100	25–30	2500	–7.9 ^a	Harper et al., 1971
Pregelatinized corn flour	36.0	0.36	90–150	22–35	4390	–14	Cervone and Harper, 1978
Soy grits	0.79	0.34	35–60	32	3670	–	Remsen and Clark, 1978
Hard wheat dough	1885	0.41	35–52	27.5–32.5	1800	–6.8	Levine, 1982
Corn grits	28,000	~0.5	177	13	–	–	van Zuilichem et al., 1974
	17,000	~0.5	193	13	–	–	
	7600	~0.5	207	13	–	–	
Full-fat soybeans	3440	0.3	120	15–30	–	–	Fricke et al., 1977
Moist food products	223	0.78	95	35	–	–	Tsao et al., 1978
Pregelatinized corn flour	17,200	0.34	88	32	–	–	Hermann and Harper, 1974
Sausage emulsion	430	0.21	15	63	–	–	Toledo et al., 1977
Semolina flour	20,000	0.5	45	30	–	–	Nazarov et al., 1971
Defatted soy	110,600	0.05	100	25	–	–	Jao et al., 1978
	15,900	0.40	130	25	–	–	
	671	0.75	160	25	–	–	
	78,400	0.13	100	28	–	–	
	23,100	0.34	130	28	–	–	
	299	0.65	160	28	–	–	
	28,800	0.19	100	35	–	–	
	28,600	0.18	130	35	–	–	
	17,800	0.16	160	35	–	–	
Wheat flour	4450	0.35	33	43	–	–	Launay and Bure, 1973
Defatted soy flour	1210	0.49	54	25	–	–	Luxenburg et al., 1985
	868	0.045	54	50	–	–	
	700	0.43	54	75	–	–	
	1580	0.37	54	85	–	–	
	2360	0.31	54	100	–	–	
	2270	0.31	54	110	–	–	

^aWet basis moisture content

geometries. In many situations, the flow geometry may be described as a rectangular cross-section within the barrel of the extruder (Harper, 1981). To model the flow behavior within the extruder, it is assumed that the flow is incompressible, steady, laminar and fully developed. In addition, the rectangular cross-section channel formed between the screw flights and the barrel surface is assumed as an infinite plate sliding across the channel (Harper, 1981). Based on these assumptions, for an axial flow in rectangular Cartesian coordinates, the differential equation for the momentum flux is

$$\frac{d\sigma}{dy} = \frac{\Delta P}{L} \quad (14.3)$$

where L represents the length of the channel (distance in the downstream direction), and y is the element distance from the barrel surface to the surface of the screw (distance in the vertical direction). Upon integration, we obtain an expression for the shear stress (σ) for a laminar flow in the channel, as:

$$\sigma = \frac{\Delta P}{L}y + C \quad (14.4)$$

where C is a constant of integration. It must be noted that the preceding equation holds for both Newtonian and non-Newtonian fluids. In the case of a Newtonian fluid this expression is combined with Equation (2.28) to obtain the following expression.

$$\mu \frac{du}{dy} = \frac{\Delta P}{L}y + C \quad (14.5)$$

The fluid velocity distribution within the channel can be obtained by integration of the previous expression in the following manner,

$$\int du = \int \left[\left(\frac{\Delta P}{\mu L} \right) y + C_1 \right] dy \quad (14.6)$$

Following integration, the velocity profile is described as:

$$u = \frac{\Delta P}{2\mu L} y^2 + C_1 y + C_2 \quad (14.7)$$

where the constants of integration (C_1 and C_2) are determined by considering that the fluid velocity distribution ranges from zero (at the barrel surface, $y = 0$) to u_{wall} at the surface of the screw ($y = H$)

$$u = \frac{\Delta P H^2}{2\mu L} \left[\frac{y}{H} - \frac{y^2}{H^2} \right] + \frac{u_{\text{wall}}}{H} y \quad (14.8)$$

where ΔP is the absolute value of the pressure drop across the channel length (L).

In order to evaluate the volumetric flow rate for this fluid, the following general expression applies

$$dV = u(y)Wdy \quad (14.9)$$

By integration of Equation (14.9) over the rectangular cross-section we obtain

$$\int_0^V dV = \int_0^H \left(\frac{\Delta PH^2}{2\mu L} \left[\frac{y}{H} - \frac{y^2}{H^2} \right] + \frac{u_{\text{wall}}}{H} y \right) W dy \quad (14.10)$$

Upon evaluating the integrals, the following expression for volumetric flow rate of the Newtonian fluid in the channel cross-section is obtained.

$$V = \frac{\Delta PWH^3}{12\mu L} + \frac{u_{\text{wall}}HW}{2} \quad (14.11)$$

The mean velocity through the channel may be calculated from the following equation

$$u_{\text{mean}} = \frac{V}{WH} = \frac{\Delta PH^2}{12\mu L} + \frac{u_{\text{wall}}}{2} \quad (14.12)$$

Example 14.1

Corn meal with a moisture content of 18% (wb) is being extruded through a metering zone of an extruder with the following dimensions of the channel: width 5 cm, height 2 cm, length 50 cm. The wall velocity is estimated to be 0.3 m/s. The rheological properties of the extrudate can be estimated by a viscosity of 66,700 Pa s and a density of 1200 kg/m³. If the pressure drop is maintained at 3000 kPa, estimate the mass flow rate of extrudate through the die.

Given

Moisture content	18% wet basis
Channel cross-section	5 cm × 2 cm
Channel length	50 cm
Viscosity	66,700 Pa.s
Density	1200 kg/m ³
Pressure	3000 kPa

Approach

We will use Equation (14.11) to obtain the volumetric flow rate and convert it into mass flow rate using the given density.

Solution

Using Equation (14.11),

$$V = \frac{(3 \times 10^6)(0.05)(0.02)^3}{(12)(66,700)(0.5)} + \frac{(0.3)(0.02)(0.05)}{2}$$

$$V = 1.53 \times 10^{-4} \text{ m}^3/\text{s}$$

Using the density of the extrudate of 1200 kg/m^3 , the mass flow rate may be computed as follows:

$$\dot{m} = (1.53 \times 10^{-4})(1200) = 0.1835 \text{ kg/s} = 660 \text{ kg/hr}$$

As indicated earlier, most food materials involved in extrusion are non-Newtonian and require appropriate relationships to describe the flow characteristics. The flow characteristics of these types of fluids in cylindrical pipes were described in Section 2.9. In an extrusion system, the flow would most likely occur in a rectangular cross-section channel (generally assumed to be a plane narrow slit) and the expression for shear stress is given by Equation (14.4).

In the case of a power-law fluid the shear stress is given by

$$\sigma = K \left(\frac{du}{dy} \right)^n \quad (14.13)$$

where the consistency coefficient (K) and the flow behavior index (n) are properties of the power-law fluid.

By combining Equations (14.4) and (14.13), the following relationship is obtained.

$$K \left(\frac{du}{dy} \right)^n = \frac{\Delta P}{L} y + C \quad (14.14)$$

By assuming that du/dy is positive inside the channel (where the velocity increases from zero at $y = 0$ to u_{wall} at $y = H$), the previous equation can be arranged as,

$$\frac{du}{dy} = \left(\frac{\Delta P}{KL} y + C_1 \right)^{\frac{1}{n}} \quad (14.15)$$

The previous equation is integrated in the following manner

$$\int du = \int \left(\frac{\Delta P}{KL} y + C_1 \right)^{\frac{1}{n}} dy \quad (14.16)$$

Following integration the following expression is obtained.

$$u(y) = \frac{nKL}{(n+1)\Delta P} \left(\frac{\Delta P}{KL} y + C_1 \right)^{\frac{n+1}{n}} + C_2 \quad (14.17)$$

The integration constants (C_1 and C_2) are determined by considering the boundary conditions for the velocity field within the channel (i.e., $u = 0$ at $y = 0$ and $u = u_{\text{wall}}$ at $y = H$). However, unlike the case of a Newtonian fluid, the explicit expressions for C_1 and C_2 can not be obtained. Instead, the following relationships are obtained.

$$\left[\left(\frac{\Delta P}{KL} H + C_1 \right)^{\frac{n+1}{n}} - C_1^{\frac{n+1}{n}} \right] = \frac{u_{\text{wall}}(n+1)\Delta P}{nKL} \quad (14.18)$$

$$C_2 = - \frac{nKL}{(n+1)\Delta P} C_1^{\frac{n+1}{n}} \quad (14.19)$$

In order to obtain the velocity profile of a power-law fluid, Equation (14.17) must be combined with Equation (14.18) and (14.19). Note that in Equation (14.17), (14.18) and (14.19) ΔP corresponds to the actual pressure drop across a channel of length " L " (i.e., ΔP is a negative value).

The analytical solutions of this system of equations are usually not possible and numerical or approximate solutions are generally pursued.

Rauwendaal (1986) approximated the volumetric flow rate at the extruder outlet for non-Newtonian fluids by using the following equation.

$$V = \frac{(4+n)}{10} WHu_{\text{wall}} - \frac{1}{(1+2n)} \frac{WH^3}{4K} \left(\frac{u_{\text{wall}}}{H} \right)^{1-n} \frac{\Delta P}{L} \quad (14.20)$$

This approximation is valid for screw pitch angles between 15 and 25 degrees and flow indices between 0.2 and 1.0.

A non-Newtonian (power-law) soy flour extrudate with 25% moisture content (wb) is being pumped through an extruder. The channel in the metering section has the following dimensions: width 5 cm, height 2 cm, length 50 cm. The properties of the extrudate are described by a consistency coefficient of 1210 Pa·sⁿ, flow behavior index of 0.49, and density of 1100 kg/m³. Estimate the pressure drop if the mass flow rate of 600 kg/hr is to be maintained.

Example 14.2

Given

Moisture content	25% wet basis
Channel cross-section	5 cm × 2 cm
Channel length	50 cm
Consistency coefficient	1210 Pa·s ⁿ
Flow behavior index	0.49
Density	1100 kg/m ³
Mass flow rate	600 kg/hr

Approach

We will first obtain volumetric flow rate and then use Equation (14.20) to calculate pressure drop.

Solution

For a mass flow rate of 600 kg/hr, the volumetric flow rate is

$$V = \frac{600}{1100} = 0.545 \frac{\text{m}^3}{\text{hr}} = 1.39 \times 10^{-4} \text{ m}^3/\text{s}$$

Using Equation (14.20):

$$\begin{aligned} \Delta P &= \left[1.39 \times 10^{-4} - \frac{(4 + 0.49)0.05 \times 0.02 \times 0.3}{10} \right] \\ &\quad \times \frac{(1 + 2 \times 0.49) \times 4 \times 1210 \times 0.5}{0.05 \times 0.02^3} \left[\frac{0.02}{0.3} \right]^{(0.49-1)} \\ \Delta P &= 204,972 \text{ Pa} = 205 \text{ kPa} \end{aligned}$$

14.3 EXTRUSION SYSTEMS

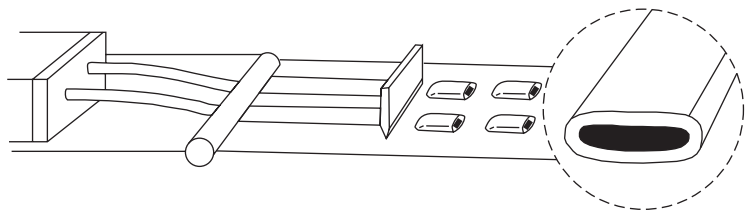
Extrusion systems can be divided into four different categories. These four categories include two different methods of operations—cold extrusion or extrusion cooking—and two different barrel configurations—single or twin screw. Both barrel configurations may be used for either method of operation.

14.3.1 Cold Extrusion

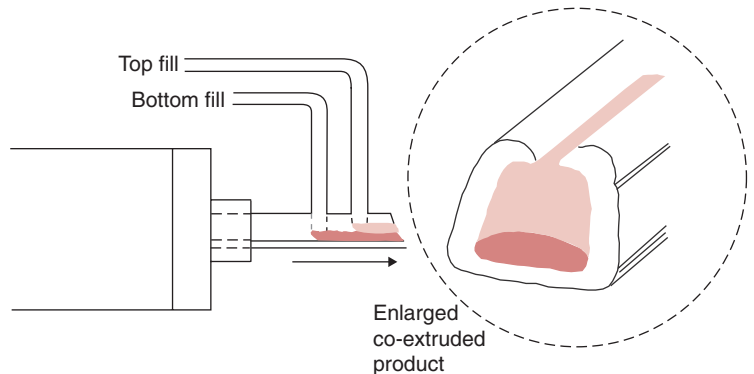
Cold extrusion is used most often to form specific shapes of extrudate at locations downstream from the die. In this process, the extrudate is pumped through a die without the addition of external thermal energy. Systems as simple as kneading steps in the preparation of dough before baking could be referred to as cold extrusion. Alternatively, more complex systems used to create coextruded products (Fig. 14.1) can also be cold extrusion. As illustrated, one component of the final product is pumped through an opening of defined shape to create a continuous tube of the first component. At the same time, the second component of the final product is introduced just before the die and becomes a filler for the interior space within the outer tube, as illustrated in Figure 14.2. During a final step in the process, the tubular product is cut into appropriate lengths.

In general, cold extrusion is used to mix, knead, disperse, texturize, dissolve, and form a food product or product ingredient. Typical food products include pastry dough, individual pieces of candy or confections, pasta pieces, hot dogs, and selected pet foods. These types of extruders would be considered low-shear systems and would create relatively low pressures upstream from the die.

■ **Figure 14.1** A cold extrusion operation.
(Adapted from Moore, 1994)



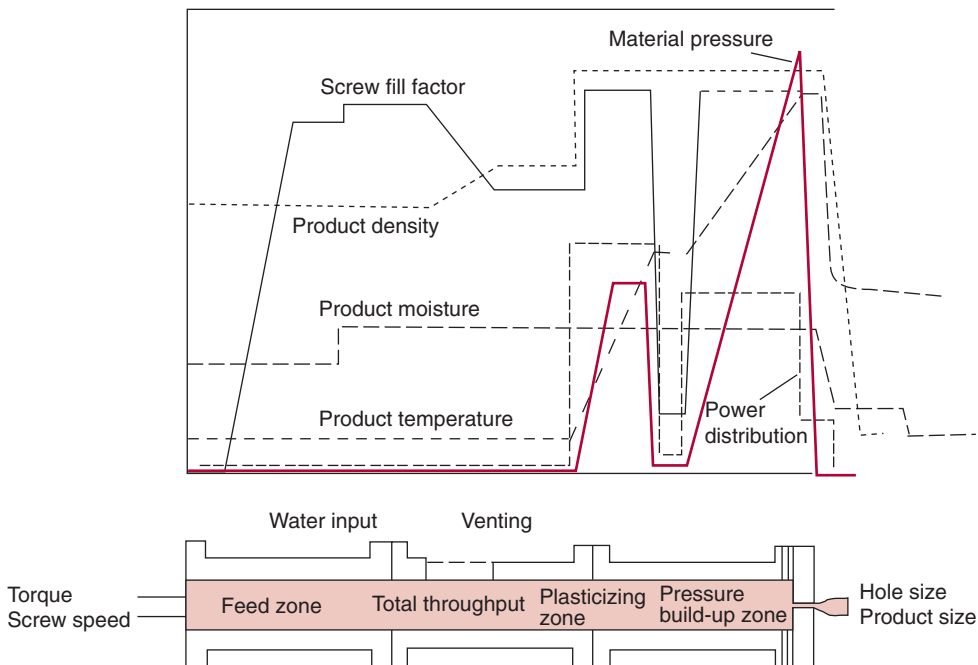
■ **Figure 14.2** Filled products using co-extrusion. (Adapted from Moore, 1994)



14.3.2 Extrusion Cooking

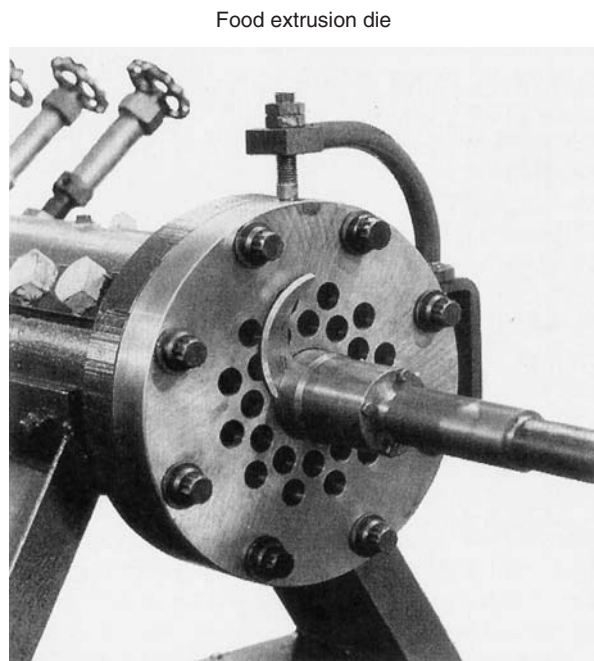
When thermal energy becomes a part of the extrusion process, the process is referred to as extrusion cooking. Thermal energy may be added to the extrudate during the process from an external source or may be generated by friction at internal surfaces of the extruder in contact with the extrudate. As illustrated in Figure 14.3, the addition of thermal energy occurs at the surface of the barrel of the extrusion system. Thermal energy may be transferred through the walls and surfaces of the barrel to ingredients used to create the extrudate. In addition, mechanical energy created by friction between surfaces and ingredients within the barrel is dissipated as thermal energy in the extrudate.

The “cooking” process during extrusion is unique from most other thermal processes. As the ingredients are introduced to form the extrudate, they are exposed to elevated pressures as well as temperatures. The geometry of the extrusion barrel is designed to increase the pressure on the ingredients as movement from entrance to exit proceeds. The exit from the barrel is the “die”—an opening with much smaller cross-sectional area than that of the barrel. A portion of the cooking process occurs



■ **Figure 14.3** Single-screw extruder components. (Adapted from Werner and Pfleiderer, Ltd.)

■ **Figure 14.4** Process variables during extrusion cooking. (From Miller and Mulvaney, 2000)



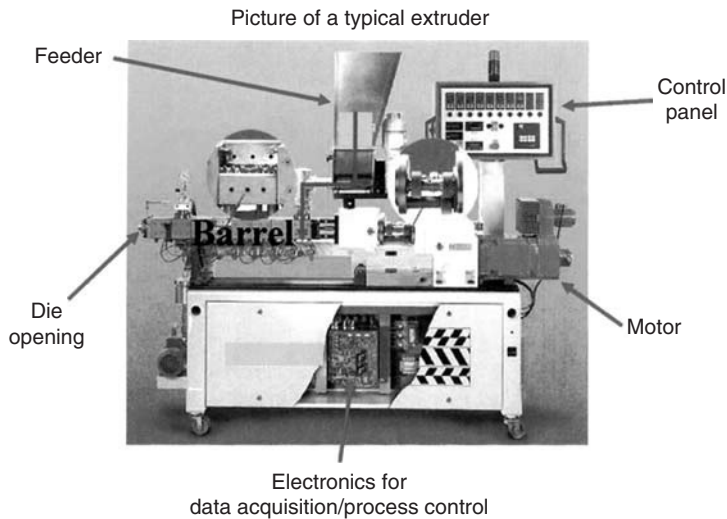
downstream from the die due to the rapid change in pressure. The pressure change results in a rapid reduction in temperature and a release of moisture from the extrudate. These changes are illustrated in Figure 14.4. The combinations of temperatures, pressures, and moisture contents may be used to create an unlimited range of product characteristics. For example, the density of individual pieces of extrudate will be a function of the pressure difference across the die.

14.3.3 Single Screw Extruders

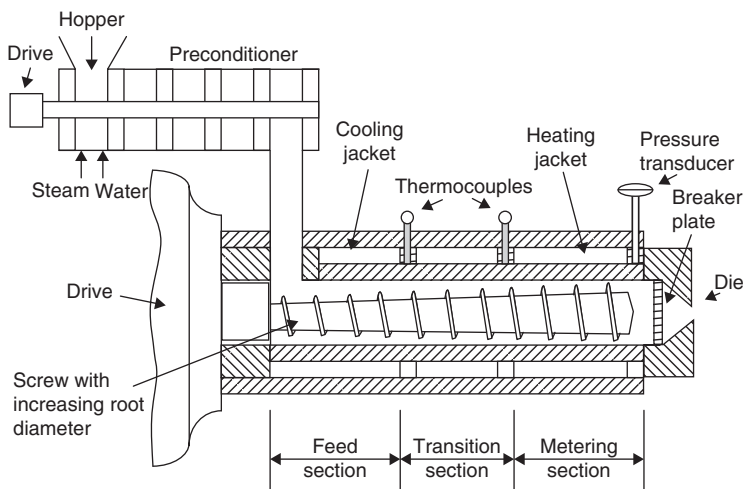
In a single-screw extrusion system, the barrel of the extruder contains a single screw or auger that moves the extrudate through the barrel. As shown in the photograph in Figure 14.5, the extrudate is carried through the barrel in the space between the core of the screw and the barrel. The flow rate of the extrudate through the system will be proportional to the rotation speed (rpm) of the screw.

A single-screw extrusion system has three components or sections (Fig. 14.6):

- Feed section, where the various ingredients are introduced and initial mixing occurs. The rotating action of the screw moves the ingredients to the transition or compression section.



■ **Figure 14.5** Photograph of single-screw extruder. (Courtesy of Leistritz Company)



■ **Figure 14.6** Sections within the barrel of a single screw extruder. (Adapted from Harper, 1989)

- Compression or transition section, where the ingredients begin the transition to the extrudate as pressure and temperature begin to increase. As the dimensions of the flow channel decrease, the material is compressed and mechanical energy is dissipated as temperature increases. This section may be referred to as a kneading section, with significant changes in the physical and chemical characteristics of the ingredients occurring.
- Metering (or cooking) section, where additional compression of the extrudate occurs as a result of additional reductions in

the dimensions of the flow channel and increased shearing action. In some designs, the overall dimensions of the barrel are reduced as well.

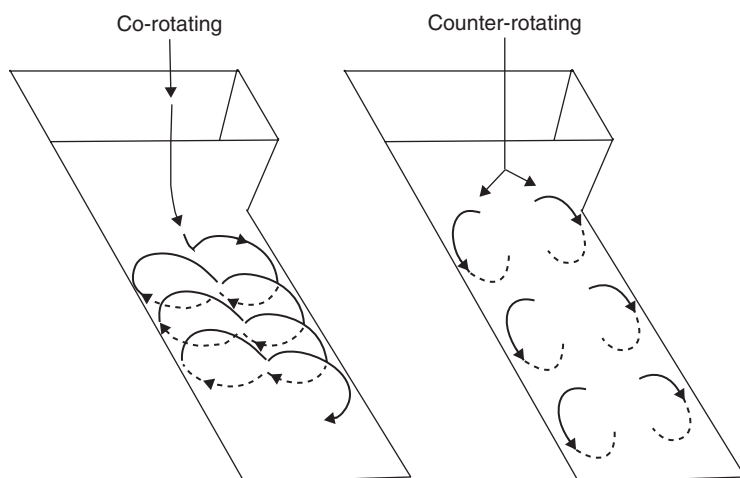
Single-screw extruders may be classified according to shearing action as well. Generally, low shear extruders will include smooth barrel surfaces, relatively large flow channels, and low screw speeds (3–4 rpm). Characteristics of moderate shear extruders include grooved barrel surfaces, reduced flow channel cross-sections and moderate screw speeds (10–25 rpm). High shear extrusion systems operate at high screw speeds (30–45 rpm), variable pitch and flight depth screws, and grooved barrel surfaces. Each of these types of extrusion systems will create extruded products with different properties and characteristics.

An additional dimension of operation within the single-screw extrusion system is associated with flow characteristics within the barrel and around the flights of the screw. Although the forward flow is caused by action of the screw, backward flow occurs between the flights and the barrel surface. The backward flow is the result of increased pressure as the extrudate moves from one section of the extruder to the next. The second component of backward flow is the leakage between the flights and the barrel; this type of flow may be reduced by grooves in the barrel surface.

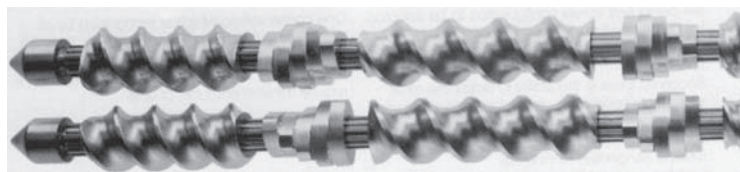
14.3.4 Twin-Screw Extruders

Twin-screw extrusion systems incorporate two parallel screws into the extruder barrel. The screws may be co-rotating or counter-rotating, as illustrated in Figure 14.7. Various configurations of the screw or auger have been developed, including the fully intermeshing, self-wiping, co-rotating twin-screw system in Figure 14.8. This particular system has been used in many food applications due to the self-cleaning, better mixing, moderate shear force and higher capacity characteristics.

Twin-screw extrusion systems have numerous advantages. The throughput of these systems can be independent of feed rate and screw speed. Process variables include degree of fill, temperature-shear history, and heat transfer, all of which may influence the properties of the extruded product. Twin-screw systems provide increased flexibility in terms of higher moisture content extrudates, as well as higher concentrations of ingredients (lipids, carbohydrates, etc.). These systems usually have less wear due to shorter sections of the barrel being exposed to the high pressures required for product extrusion. Finally, twin-screw extruders will accommodate a wider range of particle sizes in the ingredients.



■ **Figure 14.7** Screw rotation in a twin-screw extruder. (Adapted from Weidman, 1992)



■ **Figure 14.8** Configuration of screws in a twin-screw extruder.

Other configurations of twin-screw extrusion systems include counter-rotating with non-intermeshing systems, counter-rotating with intermeshing systems, and co-rotating with non-intermeshing systems. Each of these configurations may be used in specific applications and require unique and complex analysis for design and scale-up.

14.4 EXTRUSION SYSTEM DESIGN

The power requirement for operating an extrusion system is a key design factor. Power consumption is a complex function of properties of the material being extruded, extruder design, extruder motor type and extrusion conditions. Although there are unique aspects associated with estimating power consumption for single- versus twin-screw systems, a general approach for estimating total power consumption (p_t) is:

$$p_t = p_s + V_d \Delta P \quad (14.21)$$

where p_s is the portion of the power consumption for viscous dissipation associated with shear of the feed ingredients, and the second

term of the expression is the power needed to maintain flow through the barrel and die of the extrusion system.

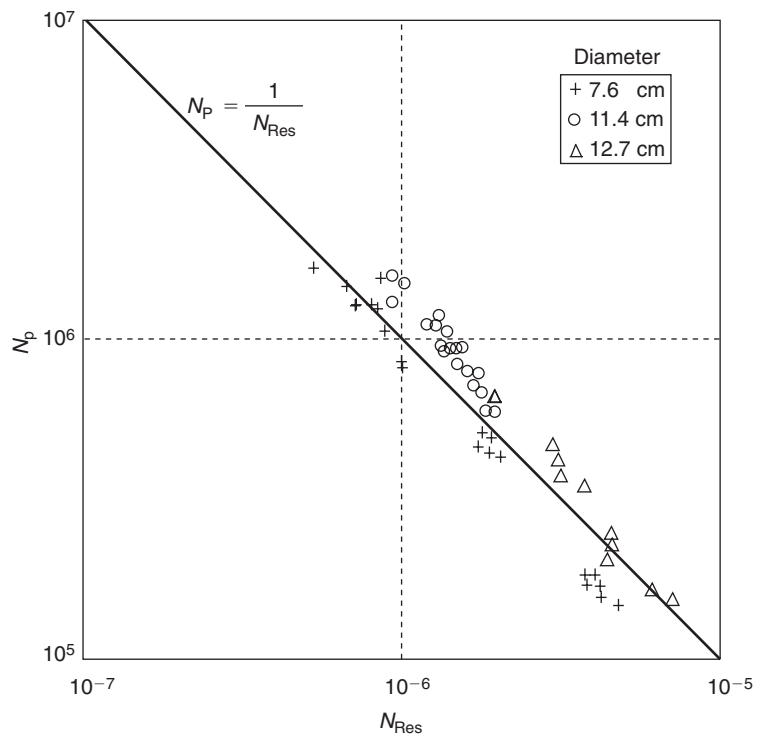
The power needed for viscous dissipation has been expressed in terms of the Screw Power number (N_p), as follows:

$$N_p = \frac{p_s}{\rho N^3 D^4 L} \quad (14.22)$$

where the screw speed (N), screw diameter (D), screw length (L), as well as density of extrudate (ρ) are considered. The magnitude of the Screw Power number is dependent on the Screw Rotational Reynolds number (N_{Res}), as illustrated by Figure 14.9. For extrudate with rheological properties described by the power-law model, the Screw Rotational Reynolds number is defined as follows:

$$N_{Res} = \frac{[\rho(DN)^{2-n} H^n]}{K \pi^{2+n}} \quad (14.23)$$

■ **Figure 14.9** Dimensionless correlation for extruder power consumption. (Adapted from Levine, 1982)



The drag flow rate (V_d) for the extruder screw can be estimated as follows:

$$V_d = \frac{(\pi NDWH)}{2} \quad (14.24)$$

and is a key expression in approximating the overall power requirements for the extrusion system.

Estimate the mechanical power requirements for a single-screw extrusion system during extrusion of 30% moisture content (wb) corn meal. The apparent viscosity of the extrudate is 1765 Pa.s at 135°C, and the density is 1200 kg/m³. The diameter of the screw is 7.5 cm, the length of the screw is 50 cm. The channel depth within the barrel is 2 cm and width is 2.5 cm. The system is operating at a flow rate of 300 kg/hr with a screw speed of 75 rpm. The estimated wall velocity is 0.3 m/s.

Example 14.3

Given

Moisture content	30% wet basis
Apparent viscosity	1765 Pa.s
Temperature	135°C
Density	1200 kg/m ³
Diameter of screw	7.5 cm
Length of screw	50 cm
Channel depth	2 cm
Channel width	2.5 cm
Mass flow rate	300 kg/hr
Screw speed	75 rpm

Approach

We will use Equation (14.23) to calculate the Screw Rotational Reynolds Number, and Figure 14.9 to obtain the Screw Power number. This result will be used to calculate power consumption due to viscous dissipation. We will calculate the total power requirement from the pressure drop determined from volumetric flow rate and the power consumption due to viscous dissipation.

Solution

1. The total mechanical power for the extrusion system is estimated by using Equation (14.21). The power for viscous dissipation is obtained by computing

the Screw Rotational Reynolds Number (Eq. (14.23)). Note that $n = 1$

$$N_{Res} = \frac{(1200)(0.075)\left(\frac{75}{60}\right)(0.02)}{(1765)(\pi)^3}$$

$$N_{Res} = 4.11 \times 10^{-5}$$

2. Using Figure 14.9, the Screw Power Number is determined as follows

$$N_p = 2.4323 \times 10^4$$

3. Based on Equation (14.22), the power consumption for viscous dissipation is computed as follows

$$p_s = (1200)\left(\frac{75}{60}\right)^3 (0.075)^4 (0.5)(2.4323 \times 10^4) = 901.8 \text{ W}$$

4. The pressure change across the die is estimated using Equation (14.11), after converting the mass flow rate to volumetric flow rate

$$V = \frac{(300 \text{ kg/hr})}{(3600 \text{ s/hr})(1200 \text{ kg/m}^3)} = 6.944 \times 10^{-5} \text{ m}^3/\text{s}$$

Then

$$\Delta P = \left(6.944 \times 10^{-5} - \frac{0.3 \times 0.02 \times 0.025}{2} \right) \frac{(12)(1765)(0.5)}{(0.025)(0.02)^3}$$

$$\Delta P = -2.94 \times 10^5 \text{ Pa}$$

Note that we will use the absolute value of ΔP in the following calculations.

5. The power requirement using Equation (14.21), becomes

$$p_t = 901.8 + (2.94 \times 10^5)(6.944 \times 10^{-5})$$

$$p_t = 922 \text{ W} = 0.92 \text{ kW}$$

Example 14.4

A wheat flour dough is being extruded in a single-screw extruder. The screw length is 50 cm and its diameter is 6 cm. The channel dimensions are as follows, width 2 cm and height 1 cm. The properties of the dough include a consistency coefficient of 4450 Pa s^n , flow behavior index of 0.35 and density of 1200 kg/m^3 . Estimate the power requirements for the system when the flow rate is 270 kg/hr and the screw rotation speed is 200 rpm with an estimated wall velocity of 0.6 m/s .

Given

Screw diameter	6 cm
Screw length	50 cm
Channel depth	1 cm
Channel width	2 cm
Consistency coefficient	4450 Pa s ⁿ
Flow behavior index	0.35
Density	1200 kg/m ³
Flow rate	270 kg/hr
Screw rotation speed	200 rpm
Wall velocity	0.6 m/s

Approach

We will first calculate the Screw Rotation Reynolds Number and use Figure 14.9 to obtain the Screw Power Number. Then using Equation (14.22), we will obtain the power requirement due to viscous dissipation. Next, we will determine pressure change across the die using Equation (14.20). Then Equation (14.21) will be used to calculate total power requirement.

Solution

1. The first step in estimating the power for viscous dissipation within the shear within the barrel is obtained by using Equation (14.23). The Screw Rotation Reynolds Number is computed as follows

$$N_{Res} = \frac{(1200) \left[\left(\frac{6}{100} \right) \left(\frac{200}{60} \right) \right]^{(2-0.35)} \left(\frac{1}{100} \right)^{0.35}}{(4450)(\pi)^{2.35}}$$

$$= 2.566 \times 10^{-4}$$

2. Then, using Figure 14.9

$$N_p = \frac{1}{N_{Res}} = \frac{1}{2.566 \times 10^{-4}}$$

$$N_p = 3.897 \times 10^3$$

3. Based on Equation (14.22), the power for viscous dissipation is

$$p_s = (1200) \left(\frac{200}{60} \right)^3 \left(\frac{6}{100} \right)^4 \left(\frac{50}{100} \right) (3.897 \times 10^3)$$

$$p_s = 1122 \text{ W} = 1.12 \text{ kW}$$

4. The second step in estimating mechanical power is for maintaining flow through the die. The pressure change across the die is obtained by using Equation (14.20) with its terms rearranged to solve for ΔP

$$\Delta P = \left(6.25 \times 10^{-5} - \frac{4.35 \times 0.02 \times 0.01 \times 0.6}{10} \right) \times \left(\frac{(1+0.7) \times 4 \times 4450}{0.02 \times (0.01)^3} \right) (0.5) \left(\frac{0.6}{0.01} \right)^{(0.35-1)}$$

with

$$V = \left(\frac{270}{1200 \times 3600} \right) = 6.25 \times 10^{-5} \text{ m}^3/\text{s}$$

then

$$\Delta P = 5.443 \times 10^5 \text{ Pa}$$

5. Using Equation (14.21)

$$p_t = 1122 + (5.443 \times 10^5)(6.25 \times 10^{-5})$$

$$p_t = 1122 + 34.02$$

$$p_t = 1156 \text{ W} = 1.16 \text{ kW}$$

14.5 DESIGN OF MORE COMPLEX SYSTEMS

The concepts presented in this chapter provide the basic steps involved in the design of an extrusion system. However, numerous additional factors should be considered when designing a typical extrusion system for a food product. The analysis and examples presented have distinguished between materials with Newtonian flow characteristics as compared with materials with non-Newtonian flow characteristics.

Many of the complex design considerations are associated with the extrusion system barrel and screw configuration. Adjustments in the basic design expressions are needed in order to account for the influence of barrel configuration, including channel depth and width, screw diameter, downstream flow geometry, and so forth. These adjustments are a function of flow characteristics such as the flow behavior index. Additional adjustments are required for leakage flow within the extruder barrel, usually backward flow through gaps between the screw and barrel. The die configuration also has a significant impact on the operating characteristics of the extrusion system. The dimensions and shape of the die as well as the relationship to barrel dimensions and

shape can influence many operating parameters. Temperature is not normally considered in detail.

The properties and characteristics of the material being extruded will change dramatically as the material moves from the feed zone to the exit from the die. Typical design expressions require specific input properties and do not account for changes in properties imposed by the process. The configuration of the screw will impact the operating characteristics of the system. The diameter and channel dimensions often change with distance along the barrel length. When considering twin-screw systems, the configuration of the two screws within the barrel requires special consideration. Adjustment factors for the expressions presented have been developed and are available in appropriate references.

Since control of temperature during the extrusion process is important, heat transfer to and from the material being extruded must be considered. Although limited information is available, a few key expressions are available for use in estimating the impacts. An additional factor impacting the characteristics of the extruded material is residence time distribution. All reactions and changes occurring within the system are a function of time, and the characteristics of the extruded material will be influenced by residence time.

PROBLEMS

- 14.1** A cereal dough is being extruded in a single-screw extruder with the following dimensions, screw length 25 cm, channel height 0.5 cm, and channel width 3 cm. The apparent viscosity of the dough is 1700 Pa s. The density is 1200 kg/m³. The wall velocity is estimated to be 0.3 m/s. If a mass flow rate of 108 kg/hr is desired, calculate the pressure drop.
- 14.2** A single screw extruder is being used to process pregelatinized starch. The screw dimensions are as follows: channel width 3 cm, channel height 0.5 cm and screw length 50 cm. The wall velocity is estimated to be 0.31 m/s. The consistency coefficient is 3300 Pa sⁿ and the flow behavior index is 0.5. A mass flow rate of 91 kg/hr is desired. The density is 1200 kg/m³. Calculate the pressure drop.
- *14.3** A cereal dough is being processed in a single-screw extruder. Estimate the power requirements if the following information is known. The screw length is 50 cm and its diameter is 10 cm.

*Indicates an advanced level in solving.

The channel width is 3 cm, and the channel height is 1 cm. The estimated wall velocity is 0.4 m/s. The density of the dough is 1200 kg/m³ and the apparent viscosity is 1765 Pa s. The mass flow rate is 254 kg/hr. The rotational speed is 75 rpm.

LIST OF SYMBOLS

A	activation energy constant (J/kg)
B	constant to account for moisture content (% db)
C_1	integration constant (see Eq. (14.16))
D	screw diameter (m)
γ	rate of shear (1/s)
H	height; channel (m)
K	consistency coefficient (Pa s ^{<i>n</i>})
K_o	consistency coefficient (see Eq. (14.2))
L	length; channel or screw (m)
μ	viscosity (Pa s)
\dot{m}	mass flow rate (kg/s)
M	moisture content (% db)
n	flow behavior index
N	screw speed (rpm)
N_p	Screw Power number
N_{Res}	Screw Rotation Reynolds number
ΔP	Pressure drop (Pa)
p_t	extruder power consumption (W)
p_s	power consumption for viscous dissipation (W)
ρ	density (kg/m ³)
σ	shear stress (Pa)
T	temperature (C) or (K)
u	velocity (m/s)
u_{max}	maximum velocity (m/s)
u_{mean}	mean velocity (m/s)
V	volumetric flow rate (m ³ /s)
V_d	drag flow rate (m ³ /s)
W	width of channel (m)
z	vertical dimension
ΔP	pressure difference or change (Pa)

■ BIBLIOGRAPHY

Cervone, N. W. and Harper, J. M. (1978). Viscosity of an intermediate moisture dough. *J. Food Process Eng.* 2: 83–95.

- Fang, Q., Hanna, M. A., and Lan, Y. (2003). Extrusion system components. *Encyclopedia of Agricultural, Food and Biological Engineering*, 301–305. Marcel Dekker, Inc, New York.
- Fang, Q., Hanna, M. A., and Lan, Y. (2003). Extrusion system design. *Encyclopedia of Agricultural, Food and Biological Engineering*, 306–309. Marcel Dekker, Inc., New York.
- Fellows, P. J. (1988). Chapter 13: Extrusion. In *Food Processing Technology*. Ellis Horwood, Ltd., London.
- Fricke, A. L., Clark, J. P., and Mason, T. F. (1977). Cooking and drying of fortified cereal foods: extruder design. *AIChE Symp. Ser.* 73: 134–141.
- Harper, J. M. (1981). *Extrusion of Foods*, Vol. 1, Vol. 2. CRC Press, Inc., Boca Raton, Florida.
- Harper, J. M. (1989). Food extruders and their applications. In *Extrusion Cooking*, C. Mercier, P. Linko, and J. M. Harper, eds. American Association of Cereal Chemists, St. Paul, Minnesota.
- Harper, J. M., Rhodes, T. P., and Wanninger, L. A. (1971). Viscosity model for cooked cereal dough. *AIChE Symp. Ser.* 67: 40–43.
- Hermann, D. V. and Harper, J. M. (1974). Modeling a forming foods extruder. *J. Food Sci.* 39: 1039–1044.
- Hsieh, Fu-hung. (2003). Extrusion power requirements. *Encyclopedia of Agricultural, Food and Biological Engineering*, 298–300. Marcel Dekker, Inc., New York.
- Jao, Y. C., Chen, A. H., Leandowski, D., and Irwin, W. E. (1978). Engineering analysis of soy dough. *J. Food Process Eng.* 2: 97–112.
- Kokini, J. L., Ho, C-T., and Karwe, M. V. (eds.) (1992). *Food Extrusion Science and Technology*. Marcel Dekker, Inc., New York.
- Launay, B. and Bure, J. (1973). Application of a viscometric method to the study of wheat flour doughs. *J. Texture Stud.* 4: 82–101.
- Levine, L. and Miller, R. C. (2006). Chapter 12: Extrusion Processes. *Handbook of Food Engineering*. Marcel Dekker, Inc., New York.
- Levine, L. (1982). Estimating output and power of food extruders. *J. Food Process Eng.* 6: 1–13.
- Luxenburg, L. A., Baird, D. O., and Joseph, E. O. (1985). Background studies in the modeling of extrusion cooking processes for soy flour doughs. *Biotechnol. Prog.* 1: 33–38.
- Mercier, C., Linko, P., and Harper, J. M. (eds.). *Cooking Extrusion*. American Association of Cereal Chemists, St. Paul, Minnesota.
- Miller, R. C. and Mulvaney, S. J. (2000). Unit operations and equipment IV. Extrusion and Extruders, Chapter 6. In *Breakfast Cereals and How They Are Made*, R. B. Fast and E. F. Caldwell, eds. American Association of Cereal Chemists, St. Paul, Minnesota.

- Moore, G. (1994). Snack food extrusion, Chapter 4. In *The Technology of Extrusion Cooking*, N. D. Frame, ed. Blackie Academic & Professional, London.
- Nazarov, N. I., Azarov, B. M., and Chaplin, M. A. (1971). Capillary viscometry of macaroni dough. *Izv. Vyssh. Uchebn. Zaved. Pishch. Teknol.* **1971**: 149.
- Rauwendaal, C. (1986). *Polymer Extrusion*. Carl Hanser, New York.
- Remson, C. H. and Clark, P. J. (1978). Viscosity model for a cooking dough. *J. Food Process Eng.* **2**: 39–64.
- Toledo, R., Cabot, J., and Brown, D. (1977). Relationship between composition, stability and rheological properties of rat comminuted meat batters. *J. Food Sci.* **42**: 726.
- Tsao, T. F., Harper, J. M., and Repholz, K. M. (1978). The effects of screw geometry on the extruder operational characteristics. *AIChE Symp. Ser.* **74**: 142–147.
- van Zuilichem, D. J., Buisman, G., and Stolp, W. (1974). Shear behavior of extruded maize. Paper presented at the 4th Int. Cong. Food Sci. Technol., International Union of Food Science and Technology, Madrid.
- Wiedmann, W. (1992). Improved product quality through twin-screw extrusion and closed-loop quality control, Chapter 35. In *Food Extrusion Science and Technology*, J. L. Kokini, C. T. Ho, and M. V. Karwe, eds. Marcel Dekker, Inc, New York.

Packaging Concepts

Developments in food packaging have evolved in response to the need for protection of the food product from both external and internal environments and in response to consumer expectations for convenience and product safety. A recent survey indicated that 72% of consumers in the United States are willing to pay extra for guaranteed product freshness delivered by the type of packaging. Many new packaging developments have focused on extending the shelf life of the product and on delivering a higher quality product to the consumer. These developments would not be possible without significant advances in the materials used in packaging and the incorporation of various types of sensors into food packaging.

15.1 INTRODUCTION

Historically, the packaging of foods has evolved in response to a variety of expectations. The functions of packaging for food have been documented by Yam et al. (1992), March (2001), Robertson (2006), and Krochta (2007). The four basic functions of a food package are:

- Containment
- Protection
- Communication
- Convenience

Containment is defined by the food product, with different types of packages required for liquids as compared with solids or dry powders. Product protection is a key function for most packages in order to maintain the quality and safety of the food. The communication function is most obvious in the various types of information presented on the outside surface of packages, including simple product

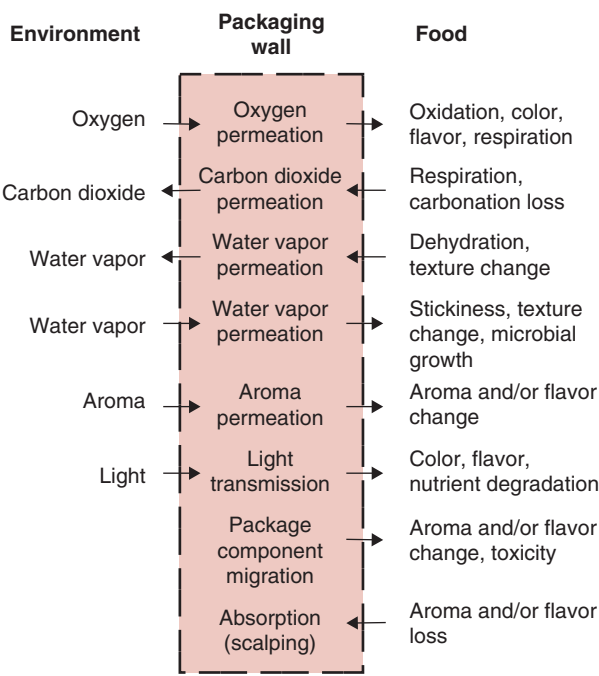
All icons in this chapter refer to the author's web site which is independently owned and operated. Academic Press is not responsible for the content or operation of the author's web site. Please direct your web site comments and questions to the author: Professor R. Paul Singh, Department of Biological and Agricultural Engineering, University of California, Davis, CA 95616, USA.
Email: rps@rpaulsingh.com

descriptions and details of product composition. The convenience of many foods is highly dependent on package design. These four basic functions of food packages take on different levels of importance with different food products. Additional factors that can impact packaging include efficiency in package manufacturing, the impact of the package on the environment, and level of food safety provided by the package.

15.2 FOOD PROTECTION

The degree of protection required by a food product is a key factor in selecting the packaging material and design. Figure 15.1 summarizes the role of the food package in this regard. In general, protection is defined in terms of a variety of factors that can impact the quality attributes of the food product from the time the product is placed in the container to the time of consumption. Environmental parameters such as oxygen, nitrogen, carbon dioxide, water vapor or aromas, in direct or indirect contact with the product, are influenced by the package properties. Many foods are sensitive to the oxygen concentration

■ **Figure 15.1** Interactions among the food, the package, and the environment. (Adapted from Linssen and Roozen, 1994)



in the immediate environment due to the deterioration associated with oxidation. The shelf life of fresh food commodities is impacted by concentrations of carbon dioxide in direct contact with the product. In a similar manner, the water vapor concentration in the environment in direct contact with a dry and/or intermediate moisture food must be controlled. In all situations, the properties of the packaging material have a significant role in establishing the shelf life and quality of the product reaching the consumer.

15.3 PRODUCT CONTAINMENT

The function of the package in containing the food product is directly related to the packaging material. A variety of materials are used for food packages including glass, metals, plastics, and paper. Each material has unique properties and applications for food packaging.

Glass containers for foods provide an absolute barrier for gases, water vapors, and aromas but do not protect products with sensitivities to light in the environment surrounding the product package. A major disadvantage of glass is weight compared with other packaging materials.

Metal containers are used for a significant number of shelf-stable food products such as fruits and vegetables, and offer an excellent alternative to glass containers. The metals used include steel, tin, and aluminum, with each representing a unique application for foods or beverages. Due to structural integrity, metal containers have been used for thermally processed foods, with many applications for foods processed in retorts at high temperatures and pressures. Metal containers are relatively heavy, and the container manufacturing process is complex.

Plastic packaging materials are used for an increasing number and variety of food products. Most plastic packaging materials are either thermoplastic or thermoset polymers. Thermoplastic polymers are the basic material used for a large number of food products, and provide significant flexibility in package design based on the specific needs of the food. Plastic films are lightweight and provide an unobscured view of the product within the package. The permeability of polymers to oxygen, carbon dioxide, nitrogen, water vapor, and aromas provides both challenges and opportunities in the design of packaging materials for specific food requirements.

Due to its broad use in all levels of packaging, paper is used for food packaging more than any other material. It is the most versatile and flexible type of material. Its key disadvantage is the lack of a barrier to oxygen, water vapor, and similar agents that cause deterioration of product quality.

15.4 PRODUCT COMMUNICATION

The package of a food product is used to communicate information about the product to consumers. This information is presented on the label and includes both legally required information about the ingredients and information needed to market the product.

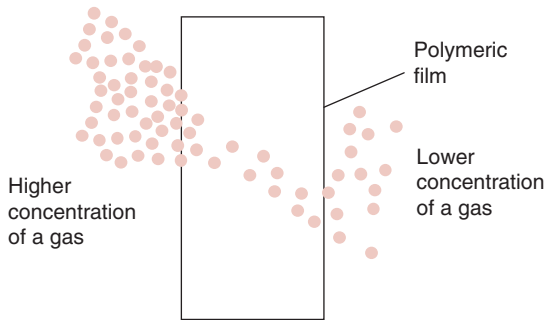
15.5 PRODUCT CONVENIENCE

A variety of designs have been incorporated into food packages in an effort to increase convenience. These designs include innovation in opening the packages, dispensing the product, resealing the package, and the ultimate preparation of the product before consumption. Convenience will continue to provide innovation in the future.

15.6 MASS TRANSFER IN PACKAGING MATERIALS

An important requirement in selecting packaging systems for foods is the barrier property of the packaging material. To keep a food product crisp and fresh, the package must provide a barrier to moisture. Rancidity can be minimized by keeping a food protected from light. To reduce oxidation of food constituents, the packaging material must provide a good barrier to oxygen. The original aroma and flavor of a food can be maintained by using a packaging material that offers a barrier to a particular aroma. Thus, properly selected packaging materials are beneficial in extending the shelf life of foods. The barrier properties of a packaging material can be expressed in terms of permeability.

The permeability of a packaging material provides a measure of how well a certain gas or vapor can penetrate the packaging material. In quantitative terms, permeability is the mass of gas or vapor transferred per unit of time, area, and a "driving force." In the case of diffusional mass transfer, the driving force is a difference in concentration or in partial pressures. If the driving force is a difference in total pressure, the mass transfer occurs due to bulk flow of a gas or vapor. A polymeric membrane may be thought of as an aggregate of wriggling



■ **Figure 15.2** Mass transfer of a gas through a polymeric material.

worms, with worms representing the long chains of polymers. The space between the worms is like the interstitial space through which a species passes. The wriggling of worms is representative of the thermal motion of polymeric chains.

Mass transport through polymeric materials can be described as a step process. Referring to Figure 15.2, in step 1, the gas vapor or liquid molecules dissolve in the polymeric material on the side of the film exposed to the higher concentration. In step 2, the gas or vapor molecules diffuse through the polymeric material moving toward the side of the film exposed to the lower concentration. The movement of molecules depends on the availability of “holes” in the polymeric material. The “holes” are formed as large chain segments of the polymer slide over each other due to thermal agitation. Finally, step 3 involves the desorption of the gas or vapor molecules and evaporation from the surface of the film.

We can again use Fick’s law of diffusion to develop an expression for the transport process of a gas through a polymeric material. From Equation (10.11):

$$\frac{\dot{m}_B}{A} = \frac{D_B(c_{B1} - c_{B2})}{(x_2 - x_1)} \quad (15.1)$$

This equation would be sufficient to determine the rate of flux, \dot{m}_B/A , but the concentrations of a gas at the film surfaces are more difficult to measure than partial pressures. The concentrations can be converted to partial pressures by using Henry’s law,

$$c = Sp \quad (15.2)$$

where S is solubility (moles/[cm³ atm]) and p is partial pressure of gas (atm). Thus, we have

$$\dot{m}_B = \frac{D_B S A (p_{B1} - p_{B2})}{(x_2 - x_1)} \quad (15.3)$$

The quantity $D_B S$ is known as the permeability coefficient, P_B .

$$P_B = \frac{(\text{amount of gas vapor})(\text{thickness of film})}{(\text{area})(\text{time})(\text{pressure difference across the film})} \quad (15.4)$$

A wide variety of units are used to report the permeability coefficient (Table 15.1).

Another parameter used by some authors is *permeance*, which is not corrected to a unit thickness. Sometimes permeance to water vapor is

Table 15.1 Conversion Factors for Various Units of Permeability Coefficient

	$\frac{\text{cm}^3 \text{ cm}}{\text{s cm}^2 (\text{cmHg})}$	$\frac{\text{cm}^3 \text{ cm}}{\text{s cm}^2 (\text{Pa})}$	$\frac{\text{cm}^3 \text{ cm}}{\text{day m}^2 (\text{atm})}$
$\frac{\text{cm}^3 \text{ cm}}{\text{s cm}^2 (\text{cmHg})}$	1	7.5×10^{-4}	6.57×10^{10}
$\frac{\text{cm}^3 \text{ mm}}{\text{s cm}^2 (\text{cmHg})}$	10^{-1}	7.5×10^{-5}	6.57×10^9
$\frac{\text{cm}^3 \text{ mm}}{\text{s cm}^2 (\text{atm})}$	1.32×10^{-2}	9.9×10^{-6}	8.64×10^8
$\frac{\text{cm}^3 \text{ mil}}{\text{day m}^2 (\text{atm})}$	3.87×10^{-14}	2.9×10^{-17}	2.54×10^{-3}
$\frac{\text{in}^3 \text{ mil}}{\text{day } 100 \text{ in}^2 (\text{atm})}$	9.82×10^{-12}	7.37×10^{-15}	6.46×10^{-1}
$\frac{\text{cm}^3 \text{ cm}}{\text{day m}^2 (\text{atm})}$	1.52×10^{-11}	1.14×10^{-14}	1

Source: Yasuda and Stannett (1989)

reported in units that are neither corrected to unit thickness nor to unit pressure, but this value must always be reported with specified thickness, humidity, and temperature. For example, water vapor permeability is defined as grams of water per day per 100 cm² of package surface for a specified thickness and temperature and/or a relative humidity on one side of approximately 0% and on the other side of 95%.

15.6.1 Permeability of Packaging Material to "Fixed" Gases

Gases such as oxygen, nitrogen, hydrogen, and carbon dioxide, which have low boiling points, are known as "fixed" gases. They show similar ideal behavior with respect to permeability through packaging materials. The permeability of O₂, CO₂, and N₂ for several polymeric materials is shown in Table 15.2. It is evident that for any given gas

Table 15.2 Permeability Coefficients, Diffusion Constants, and Solubility Coefficients of Polymers^a

Polymer	Permeant	T[°C]	$P \times 10^{10}$	$D \times 10^6$	$S \times 10^2$
Poly(ethylene) (density 0.914)	O ₂	25	2.88	0.46	4.78
	CO ₂	25	12.6	0.37	25.8
	N ₂	25	0.969	0.32	2.31
	H ₂ O	25	90		
Poly(ethylene) (density 0.964)	O ₂	25	0.403	0.170	1.81
	CO ₂	25	1.69	0.116	11.1
	CO	25	0.193	0.096	1.53
	N ₂	25	0.143	0.093	1.17
	H ₂ O	25	12.0		
Poly(propylene)	H ₂	20	41	2.12	
	N ₂	30	0.44		
	O ₂	30	2.3		
	CO ₂	30	9.2		
	H ₂ O	25	51		
Poly(oxyethyleneoxyterephthaloyl) (Poly(ethylene terephthalate)) crystalline	O ₂	25	0.035	0.0035	7.5
	N ₂	25	0.0065	0.0014	5.0
	CO ₂	25	0.17	0.0006	200
	H ₂ O	25	130		
Cellulose acetate	N ₂	30	0.28		
	O ₂	30	0.78		
	CO ₂	30	22.7		
	H ₂ O	25	5500		

(Continued)

Table 15.2 (Continued)

Polymer	Permeant	$T [^{\circ}\text{C}]$	$P \times 10^{10}$	$D \times 10^6$	$S \times 10^2$
Cellulose (Cellophane)	N ₂	25	0.0032		
	O ₂	25	0.0021		
	CO ₂	25	0.0047		
	H ₂ O	25	1900		
Poly(vinyl acetate)	O ₂	30	0.50	0.055	6.3
Poly(vinyl alcohol)	H ₂	25	0.009		
	N ₂	14 ^b	<0.001		
		14 ^c	0.33	0.045	5.32
	O ₂	25	0.0089		
	CO ₂	25	0.012		
		23 ^b	0.001		190
		23 ^d	11.9	0.0476	
	ethylene oxide	0	0.002		
Poly(vinyl chloride)	H ₂	25	1.70	0.500	2.58
	N ₂	25	0.0118	0.00378	2.37
	O ₂	25	0.0453	0.0118	2.92
	CO ₂	25	0.157	0.00250	47.7
	H ₂ O	25	275	0.0238	8780.0
Poly(vinylidene chloride) (Saran)	N ₂	30	0.00094		
	O ₂	30	0.0053		
	CO ₂	30	0.03		
	H ₂ O	25	0.5		
Poly[imino (1-oxohexamethylene)] (Nylon 6)	N ₂	30	0.0095		
	O ₂	30	0.038		
	CO ₂	20	0.088		
		30 ^b	0.10		
		30 ^e	0.29		
	H ₂ O	25	177		
Poly[imino (1-oxoundecamethylene)] (Nylon 11)	CO ₂	40	1.00	0.019	40

Notes: See overleaf.

Source: Yasuda and Stannett (1989)

^a Units used are as follows: P in $[\text{cm}^3 \text{ (STP) cm cm}^{-2} \text{ s}^{-1} (\text{cm Hg})^{-1}]$, D in $[\text{cm}^2 \text{ s}^{-1}]$, and S in $[\text{cm}^3 \text{ (STP) cm}^{-3} \text{ atm}^{-1}]$. To obtain corresponding coefficients in SI units, the following factors should be used: $P \times 7.5 \times 10^{-4} = [\text{cm}^3 \text{ (STP) cm cm}^{-2} \text{ s}^{-1} \text{ Pa}^{-1}]$; $S \times 0.987 \times 10^{-5} = [\text{cm}^3 \text{ (STP) cm}^{-3} \text{ Pa}^{-1}]$

^b Relative humidity 0%.^c Relative humidity 90%.^d Relative humidity 94%.^e Relative humidity 95%.

there exist materials with widely differing permeabilities. For example, Saran is 100,000 times less permeable to oxygen than silicone rubber. Moreover, there are certain regularities in the transmission of different gases through the same material. For example, carbon dioxide permeates four to six times faster than oxygen, and oxygen four to six times faster than nitrogen. Since carbon dioxide is the largest of the three gas molecules, we would expect its diffusion coefficient to be low, and it is. Its permeability coefficient is high because its solubility S in polymers is much greater than that for other gases.

Fixed gases also show ideal behaviors:

1. Permeabilities can be considered independent of concentration.
2. The permeabilities change with temperature in accordance with the following relation:

$$P = P_0 e^{-E_p/RT} \quad (15.5)$$

where E_p is the activation energy for permeability (kcal/mol).

For some materials there is a break in the permeability temperature curve, and above a critical temperature the material is much more permeable. For polyvinyl acetate, that temperature is around 30°C and for polystyrene it is around 80°C. Breaks are due to a glass transition temperature T_g' , below which the material is glassy, and above which it is rubbery.

The permeability coefficient for a 0.1-mm polyethylene film is being measured by maintaining a moisture vapor gradient across the film in a sealed test apparatus. The high moisture vapor side of the film is maintained at 90% RH and a salt ($\text{ZnCl} \cdot \frac{1}{2} \text{H}_2\text{O}$) maintains the opposite side at 10% RH. The area of film exposed to vapor transfer is 10 cm by 10 cm. When the test is conducted at 30°C, a weight gain of 50 g in the desiccant salt is recorded after 24 h. From these given data, calculate the permeability coefficient of the film.

Example 15.1

Given

Film thickness = 0.1 mm = 1×10^{-4} m

High relative humidity = 90%

Low relative humidity = 10%

Temperature = 30°C

Film area = 10 cm × 10 cm = 100 cm² = 0.01 m²

Moisture rate of flow = 50 g/24 h = 5.787×10^{-4} g water/s

Approach

We will use Equation (15.4) to calculate the permeability coefficient (P_B) after vapor pressures are expressed in terms of moisture contents of air.

Solution

1. By using Equation (9.16) modified with vapor pressures,

$$\phi = \frac{p_w}{p_{ws}} \times 100$$

2. From Table A.4.2,

$$p_{ws} = 4.246 \text{ kPa at } 30^\circ\text{C}$$

3. From steps 1 and 2, at 10% relative humidity,

$$\begin{aligned} p_w &= 4.246 \times 10/100 \\ &= 0.4246 \text{ kPa} \end{aligned}$$

At 90% relative humidity,

$$\begin{aligned} p_w &= 4.246 \times 90/100 \\ &= 3.821 \text{ kPa} \end{aligned}$$

Using Equation (15.4) and solving for permeability coefficient,

$$\begin{aligned} P_B &= \frac{(5.787 \times 10^{-4} \text{ g water/s})(1 \times 10^{-4} \text{ m})}{(0.01 \text{ m}^2)(3.821 \text{ kPa} - 0.4246 \text{ kPa})(1000 \text{ Pa/kPa})} \\ P_B &= 1.7 \times 10^{-9} [(\text{g water m})/(\text{m}^2 \text{ Pa s})] \end{aligned}$$

4. The permeability coefficient of the film is calculated to be $1.7 \times 10^{-9} [(\text{g water m})/(\text{m}^2 \text{ Pa s})]$; the units may be converted to any other form desired using Table 15.1.

15.7 INNOVATIONS IN FOOD PACKAGING

Innovations in food packaging have created an array of new terms associated with the role of packaging in the improvement of safety, shelf life, and convenience of the food product. There are three broad categories of packaging for foods: passive, active, and intelligent. The two types of active packaging systems include simple and advanced. Intelligent packaging systems are simple and interactive.

15.7.1 Passive Packaging

A passive packaging system is a system that serves as a physical barrier between the product and the environment surrounding the package.

Most conventional packaging used for food products would be described as passive packaging systems. Metal cans, glass bottles, and many of the flexible packaging materials provide a physical barrier between the product and the environment. These packaging systems ensure that most properties of the environment and the agents contained in the environment are prevented from making contact with the food. In general, these packages are expected to provide maximum protection of the product but are not responsive to any of the changes that might occur within the container.

Innovations in passive packaging systems continue with the development of new barrier coatings for polymer containers and films. These new materials reduce or control permeability of agents that could impact the safety or shelf-life of the food product within the container.

15.7.2 Active Packaging

An active packaging system is a system that detects or senses changes within the package environment, followed by modification of package properties in response to the detected change.

15.7.2.1 Simple Active

A packaging system that does not incorporate an active ingredient and/or actively functional polymer is referred to as a simple active system. An active packaging system responds in some manner to changes occurring within the package. One of the earliest active packaging systems was Modified Atmosphere Packaging (MAP). The package materials for MAP have properties that attempt to control the atmosphere within the package in contact with the food product. A simple example is packaging films that help maintain desired concentration of oxygen and carbon dioxide in a package containing respiring fruits and vegetables.

15.7.2.2 Advanced Active

A packaging system that contains an active ingredient and/or an actively functional polymer is an advanced active system. Advanced active packaging systems can be divided into two categories. The incorporation of an oxygen scavenger into the package is an example of a system that absorbs an unwanted agent within the environment

of the package and in contact with the product. Usually, scavengers are included as small sachets inserted into the package to reduce the level of oxygen within the package. An alternative to the sachets is the integration of an active scavenging system into packaging materials, such as films or closures.

A second example of the “absorbing” type of system is an ethylene scavenger. Ethylene triggers ripening, accelerates senescence, and reduces the shelf life of climacteric fruits and vegetables. By incorporating an ethylene-absorbing material into the packaging system, the shelf life of the product can be extended.

Moisture content or water activity becomes a shelf life limiting factor for many foods. For these products, the incorporation of water-absorbing material into the package can be beneficial. More sophisticated control may be required within packages for products requiring regulation of humidity levels.

Another example of an advanced active packaging system would be MAP with barrier properties in combination with gas flushing to achieve a desirable steady-state atmosphere composition around the product. Other active absorbing packaging systems are available to control concentrations of undesirable flavor constituents or carbon dioxide.

Advanced active packaging systems are continuing to evolve with the development of systems designed to release agents in response to undesirable activity within the package. For example, in response to microbial growth, the release of antimicrobial agents can be used to extend the shelf-life of refrigerated foods. Similarly, antioxidants can be incorporated into packaging films to protect the film and the product within the package from degradation. The potential for incorporation of flavor compounds into a package represents a significant opportunity. The release of these compounds during the shelf life of a food product could mask off-odors or improve the sensory attributes of the product.

15.7.3 Intelligent Packaging

A packaging system that senses changes in the environment and responds with corrective action is defined as an intelligent packaging system. Four objectives for intelligent packaging systems have been identified:

1. Improved product quality and product value
2. Increased convenience

3. Changes in gas permeability properties
4. Protection against theft, counterfeiting, and tampering

15.7.3.1 Simple Intelligent

A packaging system that incorporates a sensor, an environmental reactive component, and/or a computer-communicable device is a simple intelligent system. Quality or freshness indicators are examples of simple intelligent packaging systems and are used to communicate changes in a product quality attribute. These internal or external indicators/sensors may indicate elapsed time, temperature, humidity, time-temperature, shock abuse, or gas concentration. The primary function of the sensor is to indicate quality losses during storage and distribution. Other sensors are available for changes in color, physical condition (damage), and microbial growth.

A second type of simple intelligent package system is the time-temperature indicator (Taoukis et al., 1991). Temperature-indicating labels are attached to the external surface of the package and report the maximum temperature to which the surface has been exposed. Time-temperature integrators provide more refined information by integrating the impact of time and temperature at the package surface (Wells and Singh, 1988a, 1988b; Taoukis and Labuza, 1989). The disadvantage of both types of indicators is that the output may not reveal the actual impact on the product.

Internal gas-level indicator sensors are components of a simple intelligent packaging system. These sensors are placed in the package to monitor gas concentrations and provide rapid visual monitoring based on color changes. In addition to monitoring food product quality, the sensor can detect package damage. Indicators are available for monitoring oxygen (O₂) and carbon dioxide (CO₂). A variation on these types of indicators may be used for detecting microbial growth by monitoring for increased CO₂ levels.

Simple intelligent package systems for supply chain management and traceability use automatic data capture during distribution and with connection to the Internet. Examples include systems to trace containers of fruits from the fields to the point of delivery to the customer. Currently, Radio Frequency Identification (RFID) tags are attached to bulk containers to provide information on content, weight, location, and times throughout the distribution channels. It is possible that in the future RFID labels will be placed on individual food packages.

Another convenience-type of simple intelligent packaging system may be incorporated into intelligent cooking appliance systems. These systems carry essential information about the food product and the package on a bar code and assist appliances by providing preparation instructions, maintaining food product inventories, and identifying expiration dates.

15.7.3.2 Interactive Intelligent

Interactive intelligent packaging systems incorporate mechanisms to respond to a signal (sensor, indicator, or integrator). For example, an interactive intelligent packaging system can change permeability properties to accommodate changes in freshness and quality of the packaged food product during storage and distribution. New and improved intelligent breathable films change permeability in response to different fresh produce or changes in temperature of the produce. These packaging films have been developed based on knowledge of respiration rates as a function of temperature. The systems are ideal for high-respiratory-rate fresh and fresh-cut produce.

An evolving expectation for interactive intelligent packaging systems includes detection of theft, counterfeiting, and tampering. To accomplish this, simple intelligent packaging systems could include labels or tapes that are invisible before tampering but change color permanently if tampering occurs. More complex devices would respond to counterfeiting and theft by using holograms, special inks and dyes, laser labels, bar codes, and electronic data tags.

15.8 FOOD PACKAGING AND PRODUCT SHELF-LIFE

The packaging provided for a food product may have a significant impact on its shelf-life. These impacts are closely related to the types of protection provided by the package, as mentioned earlier. The impact of the package can be quantified using information on the deterioration of the product in combination with the type of protection provided by the package. We will first develop mathematical relationships that are useful in describing the deterioration of food products during storage.

15.8.1 Scientific Basis for Evaluating Shelf Life

The scientific basis for evaluating shelf life of a food product relies on principles of chemical kinetics (Labuza, 1982; Singh, 2000). In this

section, we will examine changes in a quality attribute, Q , measured over time. The general rate expression for the quality attribute may be written as

$$\pm \frac{d[Q]}{dt} = k[Q]^n \quad (15.6)$$

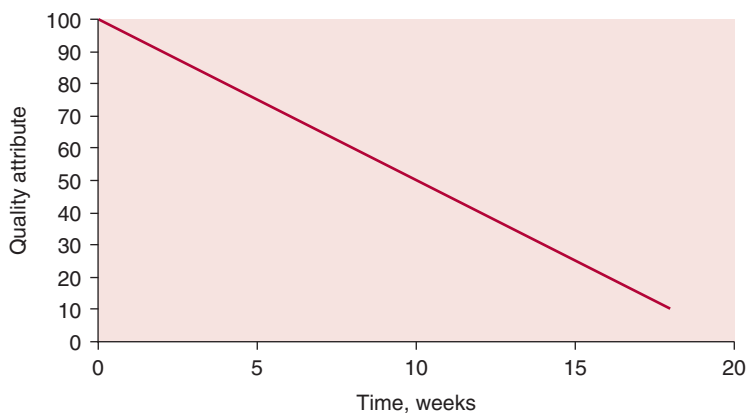
where \pm indicates that the quality attribute may increase or decrease during storage, k is the pseudo forward rate constant, and n is the order of reaction. We will first assume that the environmental factors that influence shelf life such as storage temperature, moisture, and light are kept constant.

If the quality attribute decreases with time, then we may write Equation (15.6) as

$$-\frac{d[Q]}{dt} = k[Q]^n \quad (15.7)$$

15.8.1.1 Zero-Order Reaction

In Figure 15.3, the measured amount of a quality attribute remaining at different storage times is plotted. The plot is linear, suggesting that the rate of loss of quality attribute remains constant over the entire period. This type of behavior is observed in many shelf-life studies, including quality changes due to enzymatic degradation and non-enzymatic browning. Similar behavior is observed for lipid oxidation, which often causes the development of rancid flavors.



■ **Figure 15.3** A linear decrease in the remaining quality attribute plotted against time.

The linear plot in Figure 15.3 represents a zero-order reaction. Therefore, if we substitute $n = 0$ in Equation (15.7), then we get

$$-\frac{dQ}{dt} = k \quad (15.8)$$

We can solve this equation using the procedure of separation of variables to obtain an algebraic solution. We will consider that initially the amount of quality attribute is represented by Q_i and after some storage time, t , it is Q .

Then,

$$-\int_{[Q_i]}^{[Q]} d[Q] = k \int_0^t dt \quad (15.9)$$

Integrating, we get,

$$-[Q]_{[Q_i]}^{[Q]} = kt \quad (15.10)$$

or

$$[Q_i] - [Q] = kt \quad (15.11)$$

In Equation (15.11), the left-hand side denotes the extent of reaction, ξ , for a reaction that follows a zero-order kinetics. Thus,

$$\xi = kt \quad (15.12)$$

if we specify that the end of shelf life of a food product, t_s , is reached when the quality attribute, Q , reaches Q_f . Then, from Equation (15.11),

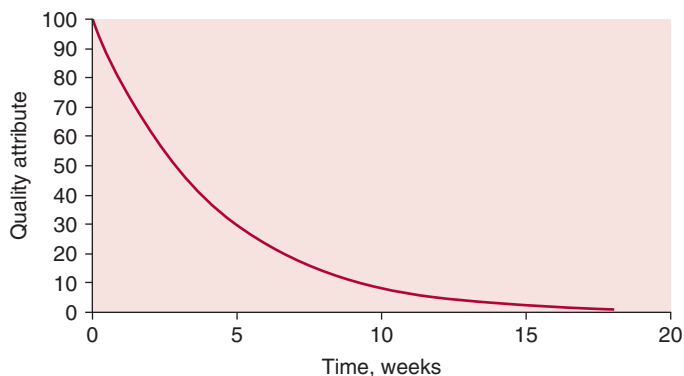
$$[Q_f] = [Q_i] - kt_s \quad (15.13)$$

or, the shelf life of a food product based on a quality attribute that follows zero-order kinetics is

$$t_s = \frac{[Q_i] - [Q_f]}{k} \quad (15.14)$$

15.8.1.2 First-Order Reaction

Let us consider another shelf life study where the measured quality attribute follows a profile as shown in Figure 15.4. This plot shows an



■ **Figure 15.4** An exponential decrease in the remaining quality attribute plotted against time.

exponential decrease of the quality attribute. In this study, the rate of loss of quality attribute depends upon the amount of remaining quality attribute. Food deterioration reactions that show an exponential decrease include loss of vitamins and protein, and microbial growth as we learned in Chapter 5. The exponential decrease in a quality attribute is described by the first-order kinetics, where the rate of reaction, $n = 1$. Thus we may rewrite Equation (15.7) as

$$-\frac{d[Q]}{dt} = k[Q] \quad (15.15)$$

We again use the method of separation of variables to integrate this equation as

$$-\frac{d[Q]}{[Q]} = kdt \quad (15.16)$$

Again, we assume that initially the quality attribute is $[Q_i]$ and after time t it decreases to $[Q]$, then

$$-\int_{[Q_i]}^{[Q]} \frac{d[Q]}{[Q]} = k \int_0^t dt \quad (15.17)$$

Integrating, we get,

$$-|\ln[Q]|_{[Q_i]}^{[Q]} = k|t|_0^t \quad (15.18)$$

or

$$\ln[Q_i] - \ln[Q] = kt \quad (15.19)$$

Thus for a first-order reaction, the extent of reaction is determined as

$$\xi = \ln[Q_i] - \ln[Q] \quad (15.20)$$

We may also rewrite Equation (15.19) as

$$\ln \frac{[Q]}{[Q_i]} = -kt \quad (15.21)$$

To determine the fraction of quality change after a certain storage period, Equation (15.21) may be rewritten as

$$\frac{[Q]}{[Q_i]} = e^{-kt} \quad (15.22)$$

In Equation (15.21), $[Q]$ is the amount of quality attribute remaining after a storage time t .

If $[Q_f]$ represents the amount of quality attribute at the end of shelf life, then from Equation (15.21) we obtain

$$t_s = \frac{\ln \frac{[Q_i]}{[Q_f]}}{k} \quad (15.23)$$

Equation (15.23) can easily be modified if we want to know time for half-life of a quality attribute. We substitute $Q_f = 0.5Q_i$ to obtain

$$t_{1/2} = \frac{\ln 2}{k} = \frac{0.693}{k} \quad (15.24)$$

Equations (15.14) and (15.24) have been used to predict shelf life of a food product, or the time that would elapse from when the product is placed in storage until the quality attribute deteriorates to an unacceptable level $[Q_f]$. The rate constant (k) has been established for key deterioration reactions in foods, or it can be determined during shelf life evaluations.

The impact of environmental conditions during product storage is expressed through the magnitude of the rate constant (k). The most evident environmental variable is temperature, and the influence of temperature on the rate constant is expressed by the Arrhenius equation (Eq. (5.9)):

$$k = Be^{\left(-\frac{E_A}{RT_A}\right)} \quad (15.25)$$

where the activation energy constant (E_A) quantifies the influence of temperature on the rate of product quality deterioration during storage. This expression is used primarily during accelerated shelf life testing, when elevated temperatures are used under experimental conditions to accelerate the deterioration of the product. These approaches allow us to quantify shelf life in a relatively short period of time (days or weeks) at elevated temperatures, whereas the actual shelf life may be much longer (1 to 2 years).

In most situations, the impact of the package on product shelf life is a function of environmental parameters other than temperature. As indicated earlier, the concentrations of oxygen, water vapor, nitrogen, carbon dioxide, and other environmental parameters may influence the deterioration reactions in foods. In order to incorporate the impact of these parameters into the prediction of shelf life, we will need to know the influence of these variables on rate constants. These additional relationships are then used in combination with expressions describing the transport of the agent across the package barrier. These expressions, as based on Equation (15.1) and appropriate permeability coefficients, were presented earlier in this chapter.

A dry breakfast cereal has been fortified with ascorbic acid (Vitamin C). The degradation of ascorbic acid during storage of the cereal is a function of water activity of the product. The package used for the cereal must ensure that the water activity is maintained at a sufficiently low level to preserve the desired level of Vitamin C.

Example 15.2

The initial water activity of the cereal is 0.1, and the moisture content is 3.0% (d.b.). The relationship between product moisture content and water activity was established as

$$w = 0.175a_w + 0.0075$$

The rate constant (k) for degradation of ascorbic acid is $1.701 \times 10^{-5}/\text{min}$ at a water activity of 0.1, and the rate constant increases with increasing water activity according to the following relationship:

$$k = 2.733 \times 10^{-5} a_w + 1.428 \times 10^{-5}$$

The package dimensions are $20\text{ cm} \times 30\text{ cm} \times 5\text{ cm}$, and there is 0.5 kg of product in the package. Select the package film permeability, with 1 mm thickness, to ensure that 60% of the original ascorbic acid is retained in the product after 14 days of storage in an environment with a relative humidity of 60% and 30°C .

Given

Product initial moisture content (w) = 3.0% (d.b.)

Product initial water activity (a_w) = 0.1

Storage environment relative humidity = 60%

Ascorbic acid degradation rate constant (k) = $1.701 \times 10^{-5}/\text{min}$

Shelf-life expectation = 14 days

Package surface area = 0.17 m^2

Approach

The key expression used in the solution is Equation (15.3), with the permeability (P_B) = $D_B S$. The degradation rate of ascorbic acid is used to establish the maximum product water activity allowed to prevent degradation beyond 60% within the 14-day shelf life. Given the maximum allowable water activity, we can determine the total amount of water that can be added to the product over the 14 days of storage, and the permeability of the package film with a given thickness.

Solution

1. Use Equation (15.22) to determine the average rate constant for the time period of product shelf life:

$$0.6 = \exp[-(k_{\text{ave}})(14\text{ days})(24\text{ hr/day})(60\text{ min/hr})]$$

$$k_{\text{ave}} = 2.53 \times 10^{-5}/\text{min}$$

2. Given the relationship between water activity and the rate constant:

$$2.53 \times 10^{-5} = 2.733 \times 10^{-5} a_w + 1.428 \times 10^{-5}$$

$$a_w = 0.4$$

3. In order to determine the amount of moisture change needed to increase the water activity to 0.4, the water activity must be converted to moisture content. The typical relationship is given by Equation (12.1), but the relationship for this product for the range of water activities between 0.1 and 0.4 is

$$w = 0.175a_w + 0.0075$$

Given this relationship, the product moisture content at a water activity of 0.4 is

$$w = 0.175(0.4) + 0.0075 = 0.0775 \quad \text{or} \quad 7.75\% \text{ (d.b.)}$$

4. During the 14 days of storage, the moisture content can increase from 3% to 7.75% or

$$0.0775 - 0.03 = 0.0475 \text{ kg water/kg product solids}$$

and 0.02375 kg water per package

is the amount of moisture transfer through the package film over a period of 14 days. Then the transfer rate becomes

$$= \frac{0.02375 \text{ kg water}}{(14 \text{ days})(24 \text{ hr/day})(60 \text{ min/hr})}$$

$$= 1.178 \times 10^{-6} \text{ kg water/min}$$

5. Using Equation (15.3):

$$P_B = \frac{(1.178 \times 10^{-6} \text{ kg water/min})(1 \times 10^{-3} \text{ m})}{(60 \text{ s/min})(0.17 \text{ m}^2)(2.5476 - 0.4246 \text{ kPa})(1000 \text{ Pa/kPa})}$$

$$\text{where: } p_{ws} = 4.246(0.6) = 2.5476$$

$$p_w = 4.246(0.1) = 0.4246$$

$$P_B = 5.44 \times 10^{-14} \text{ kg m}/(\text{m}^2 \text{ Pa s})$$

6. By converting to units consistent with Table 15.1:

$$P_B = 6.44 \times 10^{-10} \text{ cm}^3 \text{ cm}/(\text{cm}^2 \text{ s cm Hg})$$

7. Based on information presented in Table 15.2, polyvinylidene chloride would be the appropriate package film to ensure the desired shelf life.

15.9 SUMMARY

Recent innovations in packaging for foods and food products have resulted in an array of developments that improve the safety, convenience, shelf life, and overall quality of the products. New packaging provides opportunities for detection of changes in the product during storage and distribution and the potential for corrective action based on package design. Future developments will provide more sophisticated packaging to extend shelf life and improve quality attributes of the food product.

The evolution of “nano-scale science” has potential impacts for future packaging innovations. The outcomes from nano-scale research will lead to nano-materials with unique properties for protection of foods from all types of harmful agents. These materials will provide such opportunities as antimicrobial surfaces and sensing of microbiological and biochemical activities for all packaging systems. The application of nano-scale science will lead to packaging materials that will adjust to changes in pH, pressure, temperature, and light as well as to other byproducts of reactions occurring within the package.

PROBLEMS

- 15.1** A dry food product is contained in a $1\text{ cm} \times 4\text{ cm} \times 3\text{ cm}$ box using a polymer film to protect the oxygen sensitivity of the product. The concentration gradient across the film is defined by the oxygen concentration in air and 1% within the package. The oxygen diffusivity for the polymer film is $3 \times 10^{-16}\text{ m}^2/\text{s}$. Estimate the film thickness needed to ensure a product shelf life of 10 months. The shelf life of the product is established as the time when oxidation reactions within the product have used 0.5 mol of oxygen.
- *15.2** A dry food product is being stored in a package with a 0.75 mm polypropylene film. The dimensions of the package are $15\text{ cm} \times 15\text{ cm} \times 5\text{ cm}$, and the amount of product in the package is 0.75 kg. The initial water activity of the product is 0.05, and the initial moisture content is 2% (d.b.). A key component of the product is sensitive to water activity, and the rate constant for degradation of the component is described by

$$k = 5 \times 10^{-5} a_w + 1.5$$

* Indicates an advanced level in solving.

The relationship of the product water activity to moisture content is described by the following GAB constants

$$K = 1.05$$

$$C = 5.0$$

$$w_o = 1.1\%$$

The product is stored in a 25°C environment with 50% relative humidity. Predict the shelf life of the product when the shelf life is established by the time period for the intensity of the key component to decrease to 50% of the original amount.

LIST OF SYMBOLS

A	area (m ²)
a_w	water activity
B	Arrhenius constant
C	GAB constant
c	concentration (kg/m ³ or kg mole/m ³)
D	mass diffusivity (m ² /s)
E_A	activation energy for temperature (kJ/kg)
E_p	activation energy for permeability (kcal/mole)
K	GAB constant
k	rate constant for quality change (1/s)
m	mass flux (kg/s)
n	order of reaction
p	partial pressure of gas (kPa)
P	package film permeability
Q	amount of quality attribute
R	gas constant (m ³ Pa/kg mol K)
S	solubility (moles/cm ³ atm)
ξ	extent of reaction
T	temperature (C)
T_A	absolute temperature (K)
t	time (s)
t_s	shelf life (s)
$t_{1/2}$	half life (s)
w	moisture content (% , d.b.)
w_o	monolayer moisture content (% , d.b.)
x	distance coordinate (m)

Subscripts: B, component B; i, initial condition; f, final condition; o, standard condition; w, water vapor; ws, water vapor at saturation; 1, location 1; 2, location 2.

■ BIBLIOGRAPHY

- Brody, A. L. (2003). Modified atmosphere packaging. In *Encyclopedia of Agricultural, Food and Biological Engineering*, D. R. Heldman, ed., 666–670. Marcel Dekker Inc, New York.
- De Kruijf, N. and van Beest, M. D. (2003). Active Packaging. In *Encyclopedia of Agricultural, Food and Biological Engineering*, D. R. Heldman, ed., 5–9. Marcel Dekker Inc., New York.
- Krochta, J. M. (2003). Package Permeability. In *Encyclopedia of Agricultural, Food and Biological Engineering*, D. R. Heldman, ed., 720–726. Marcel Dekker Inc., New York.
- Krochta, J. M. (2007). Food Packaging. In *Handbook of Food Engineering*, D. R. Heldman and D. B. Lund, eds. CRC Press, Taylor & Francis Group, Boca Raton, Florida.
- Labuza, T. P. (1982). *Shelf-Life Dating of Foods*. Food and Nutrition Press, Westport, Connecticut.
- Linssen, J. P. H. and Roozen, J. P. (1994). Food flavour and packaging interactions. In *Food Packaging and Preservation*, M. Mathlouthi, ed., 48–61. Blackie Academic and Professional, New York.
- March, K. S. (2001). Looking at packaging in a new way to reduce food losses. *Food Technology* 55: 48–52.
- Robertson, G. L. (2006). *Food Packaging—Principles and Practice*. CRC Press, Taylor & Francis Group, Boca Raton, Florida.
- Rodrigues, E. T. and Han, J. H. (2003). Intelligent Packaging. In *Encyclopedia of Agricultural, Food and Biological Engineering*, D. R. Heldman, ed., 528–535. Marcel Dekker Inc., New York.
- Shellhammer, T. H. (2003). Flexible Packaging. In *Encyclopedia of Agricultural, Food and Biological Engineering*, D. R. Heldman, ed., 333–336. Marcel Dekker Inc, New York.
- Singh, R. P. (2000). Scientific Principles of Shelf-Life Evaluation. In *Shelf-Life Evaluation of Foods*, C. M. D. Man and A. A. Jones, eds., 3–22. Aspen Publication, Maryland.
- Steven, M. D. and Hotchkiss, J. H. (2003). Package Functions. In *Encyclopedia of Agricultural, Food and Biological Engineering*, D. R. Heldman, ed., 716–719. Marcel Dekker Inc., New York.
- Taoukis, P. S. and Labuza, T. P. (1989). Applicability of time-temperature indicators as food quality monitors under non-isothermal conditions. *J. Food Sci.* 54: 783.
- Taoukis, P. S., Fu, B., and Labuza, T. P. (1991). Time temperature indicators. *Food Tech.* 45(10): 70–82.
- Wells, J. H. and Singh, R. P. (1988a). A kinetic approach to food quality prediction using full-history time-temperature indicators. *J. Food Sci.* 53(6): 1866–1871, 1893.

- Wells, J. H. and Singh, R. P. (1988b). Application of time-temperature indicators in monitoring changes in quality attributes of perishable and semiperishable foods. *J. Food Sci.* 53(1): 148–156.
- Yam, K. L., Paik, J. S., and Lai, C. C. (1992). Food Packaging, Part 1. General Considerations. In *Encyclopedia of Food Science & Technology*, Y. H. Hui, ed. John Wiley & Sons, Inc., New York.
- Yasuda, H. and Stannett, V. (1989). Permeability coefficients. In *Polymer Handbook*, 3rd, J. Brandrup and E. H. Immergut, eds. Wiley, New York.

This page intentionally left blank

Appendices

A.1 SI SYSTEM OF UNITS AND CONVERSION FACTORS

A.1.1 Rules for Using SI Units

The following rules for SI usage are based on recommendations from several international conferences, the International Organization for Standardization, and the American Society of Agricultural Engineers.

A.1.1.1 SI Prefixes

The prefixes along with the SI symbols are given in Table A.1.1. The prefix symbols are printed in roman (upright) type without spacing between the prefix symbol and the unit symbol. The prefixes provide an order of magnitude, thus eliminating insignificant digits and decimals. For example,

19,200 m or 19.2×10^3 m becomes 19.2 km

Table A.1.1 SI Prefixes

Factor	Prefix	Symbol	Factor	Prefix	Symbol
10^{18}	exa	E	10^{-1}	deci	d
10^{15}	peta	P	10^{-2}	centi	c
10^{12}	tera	T	10^{-3}	milli	m
10^9	giga	G	10^{-6}	micro	μ
10^6	mega	M	10^{-9}	nano	n
10^3	kilo	k	10^{-12}	pico	p
10^2	hecto	h	10^{-15}	femto	f
10^1	deka	da	10^{-18}	atto	a

An exponent attached to a symbol containing a prefix indicates that the multiple or submultiple of the unit is raised to the power expressed by the exponent. For example,

$$1 \text{ mm}^3 = (10^{-3} \text{ m})^3 = 10^{-9} \text{ m}^3$$

$$1 \text{ cm}^{-1} = (10^{-2} \text{ m})^{-1} = 10^2 \text{ m}^{-1}$$

Compound prefixes, formed by the juxtaposition of two or more SI prefixes, are not to be used. For example,

$$1 \text{ nm} \quad \text{but not} \quad 1 \text{ m}\mu\text{m}$$

Among the base units, the unit of mass is the only one whose name, for historical reasons, contains a prefix. To obtain names of decimal multiples and submultiples of the unit mass, attach prefixes to the word "gram."

Attach prefixes to the numerator of compound units, except when using "kilogram" in the denominator. For example, use

$$2.5 \text{ kJ/s} \quad \text{not} \quad 2.5 \text{ J/ms}$$

but

$$550 \text{ J/kg} \quad \text{not} \quad 5.5 \text{ dJ/g}$$

In selecting prefixes, a prefix should be chosen so that the numerical value preferably lies between 0.1 and 1000. However, double prefixes and hyphenated prefixes should not be used. For example, use

$$\text{GJ} \quad \text{not} \quad \text{kMJ}$$

A.1.1.2 Capitalization

The general principle governing the writing of unit symbols is as follows: roman (upright) type, in general lowercase, is used for symbols of units; however, if the symbols are derived from proper names, capital roman type is used (for the first letter), for example, K, N. These symbols are not followed by a full stop (period).

If the units are written in an unabbreviated form, the first letter is not capitalized (even for those derived from proper nouns): for example, kelvin, newton. The numerical prefixes are not capitalized except for symbols E (exa), P (peta), T (tera), G (giga), and M (mega).

A.1.1.3 Plurals

The unit symbols remain the same in the plural form. In unabbreviated form the plural units are written in the usual manner. For example:

45 newtons or 45 N
22 centimeters or 25 cm

A.1.1.4 Punctuation

For a numerical value less than one, a zero should precede the decimal point. The SI symbols should not be followed by a period, except at the end of a sentence. English-speaking countries use a centered dot for a decimal point; others use a comma. Large numbers should be grouped into threes (thousands) by using spaces instead of commas. For example,

3 456 789.291 22

not

3,456,789.291,22

A.1.1.5 Derived Units

The product of two or more units may be written in either of the following ways:

$\text{N} \cdot \text{m}$ Nm

A solidus (oblique stroke, /), a horizontal line, or negative powers may be used to express a derived unit formed from two others by division. For example:

m/s $\frac{\text{m}}{\text{s}}$ m s^{-1}

A solidus must not be repeated on the same line. In complicated cases, parentheses or negative powers should be used. For example:

m/s^2 or m s^{-2} but not m/s/s
 $\text{J}/(\text{s m K})$ or $\text{J s}^{-1} \text{m}^{-1} \text{K}^{-1}$ but not J/s/m/K

Table A.1.2 Useful Conversion Factors

Acceleration of gravity

$$g = 9.80665 \text{ m/s}^2$$

$$g = 980.665 \text{ cm/s}^2$$

$$g = 32.174 \text{ ft/s}^2$$

$$1 \text{ ft/s}^2 = 0.304799 \text{ m/s}^2$$

Area

$$1 \text{ acre} = 4.046856 \times 10^3 \text{ m}^2$$

$$1 \text{ ft}^2 = 0.0929 \text{ m}^2$$

$$1 \text{ in}^2 = 6.4516 \times 10^{-4} \text{ m}^2$$

Density

$$1 \text{ lb}_m/\text{ft}^3 = 16.0185 \text{ kg/m}^3$$

$$1 \text{ lb}_m/\text{gal} = 1.198264 \times 10^2 \text{ kg/m}^3$$

$$\text{Density of dry air at } 0^\circ\text{C, } 760 \text{ mm Hg} = 1.2929 \text{ g/L}$$

$$1 \text{ kg mol ideal gas at } 0^\circ\text{C, } 760 \text{ mm Hg} = 22.414 \text{ m}^3$$

Diffusivity

$$1 \text{ ft}^2/\text{h} = 2.581 \times 10^{-5} \text{ m}^2/\text{s}$$

Energy

$$1 \text{ Btu} = 1055 \text{ J} = 1.055 \text{ kJ}$$

$$1 \text{ Btu} = 252.16 \text{ cal}$$

$$1 \text{ kcal} = 4.184 \text{ kJ}$$

$$1 \text{ J} = 1 \text{ N m} = 1 \text{ kg m}^2/\text{s}^2$$

$$1 \text{ kW h} = 3.6 \times 10^3 \text{ kJ}$$

Enthalpy

$$1 \text{ Btu/lb}_m = 2.3258 \text{ kJ/kg}$$

Force

$$1 \text{ lb}_f = 4.4482 \text{ N}$$

$$1 \text{ N} = 1 \text{ kg m/s}^2$$

$$1 \text{ dyne} = 1 \text{ g cm/s}^2 = 10^{-5} \text{ kg m/s}^2$$

Heat flow

$$1 \text{ Btu/h} = 0.29307 \text{ W}$$

$$1 \text{ Btu/min} = 17.58 \text{ W}$$

$$1 \text{ kJ/h} = 2.778 \times 10^{-4} \text{ kW}$$

$$1 \text{ J/s} = 1 \text{ W}$$

Heat flux

$$1 \text{ Btu}/(\text{h ft}^2) = 3.1546 \text{ W/m}^2$$

Heat transfer coefficient

$$1 \text{ Btu}/(\text{h ft}^2 ^\circ\text{F}) = 5.6783 \text{ W}/(\text{m}^2 \text{ K})$$

$$1 \text{ Btu}/(\text{h ft}^2 ^\circ\text{F}) = 1.3571 \times 10^{-4} \text{ cal}/(\text{s cm}^2 ^\circ\text{C})$$

Length

$$1 \text{ ft} = 0.3048 \text{ m}$$

$$1 \text{ micron} = 10^{-6} \text{ m} = 1 \mu\text{m}$$

$$1 \text{ \AA} = 10^{-10} \text{ m}$$

$$1 \text{ in} = 2.54 \times 10^{-2} \text{ m}$$

$$1 \text{ mile} = 1.609344 \times 10^3 \text{ m}$$

Mass

$$1 \text{ carat} = 2 \times 10^{-4} \text{ kg}$$

$$1 \text{ lb}_m = 0.45359 \text{ kg}$$

$$1 \text{ lb}_m = 16 \text{ oz} = 7000 \text{ grains}$$

$$1 \text{ ton (metric)} = 1000 \text{ kg}$$

Mass transfer coefficient

$$1 \text{ lb mol}/(\text{h ft}^2 \text{ mol fraction}) = 1.3562 \times 10^{-3} \text{ kg mol}/(\text{s m}^2 \text{ mol fraction})$$

(Continued)

Table A.1.2 (Continued)**Power**

$$\begin{aligned}
 1 \text{ hp} &= 0.7457 \text{ kW} \\
 1 \text{ W} &= 14.34 \text{ cal/min} \\
 1 \text{ hp} &= 550 \text{ ft lb}_f/\text{s} \\
 1 \text{ Btu/h} &= 0.29307 \text{ W} \\
 1 \text{ hp} &= 0.7068 \text{ Btu/s} \\
 1 \text{ J/s} &= 1 \text{ W}
 \end{aligned}$$

Pressure

$$\begin{aligned}
 1 \text{ psia} &= 6.895 \text{ kPa} \\
 1 \text{ psia} &= 6.895 \times 10^3 \text{ N/m}^2 \\
 1 \text{ bar} &= 1 \times 10^5 \text{ Pa} = 1 \times 10^5 \text{ N/m}^2 \\
 1 \text{ Pa} &= 1 \text{ N/m}^2 \\
 1 \text{ mm Hg (0}^\circ\text{C)} &= 1.333224 \times 10^2 \text{ N/m}^2 \\
 1 \text{ atm} &= 29.921 \text{ in. Hg at } 0^\circ\text{C} \\
 1 \text{ atm} &= 33.90 \text{ ft H}_2\text{O at } 4^\circ\text{C} \\
 1 \text{ atm} &= 14.696 \text{ psia} = 1.01325 \times 10^5 \text{ N/m}^2 \\
 1 \text{ atm} &= 1.01325 \text{ bar} \\
 1 \text{ atm} &= 760 \text{ mm Hg at } 0^\circ\text{C} = 1.01325 \times 10^5 \text{ Pa} \\
 1 \text{ lb}_f/\text{ft}^2 &= 4.788 \times 10^2 \text{ dyne/cm}^2 = 47.88 \text{ N/m}^2
 \end{aligned}$$

Specific heat

$$\begin{aligned}
 1 \text{ Btu}/(\text{lb}_m \text{ } ^\circ\text{F}) &= 4.1865 \text{ J}/(\text{g K}) \\
 1 \text{ Btu}/(\text{lb}_m \text{ } ^\circ\text{F}) &= 1 \text{ cal}/(\text{g } ^\circ\text{C})
 \end{aligned}$$

Temperature

$$\begin{aligned}
 T_{^\circ\text{F}} &= T_{^\circ\text{C}} \times 1.8 + 32 \\
 T_{^\circ\text{C}} &= (T_{^\circ\text{F}} - 32)/1.8
 \end{aligned}$$

Thermal conductivity

$$\begin{aligned}
 1 \text{ Btu}/(\text{h ft } ^\circ\text{F}) &= 1.731 \text{ W}/(\text{m K}) \\
 1 \text{ Btu in}/(\text{ft}^2 \text{ h } ^\circ\text{F}) &= 1.442279 \times 10^{-2} \text{ W}/(\text{m K})
 \end{aligned}$$

Viscosity

$$\begin{aligned}
 1 \text{ lb}_m/(\text{ft h}) &= 0.4134 \text{ cp} \\
 1 \text{ lb}_m/(\text{ft s}) &= 1488.16 \text{ cp} \\
 1 \text{ cp} &= 10^{-2} \text{ g}/(\text{cm s}) = 10^{-2} \text{ poise} \\
 1 \text{ cp} &= 10^{-3} \text{ Pa s} = 10^{-3} \text{ kg}/(\text{m s}) = 10^{-3} \text{ N s/m}^2 \\
 1 \text{ lb}_f \text{ s}/\text{ft}^2 &= 4.7879 \times 10^4 \text{ cp} \\
 1 \text{ N s/m}^2 &= 1 \text{ Pa s} \\
 1 \text{ kg}/(\text{m s}) &= 1 \text{ Pa s}
 \end{aligned}$$

Volume

$$\begin{aligned}
 1 \text{ ft}^3 &= 0.02832 \text{ m}^3 \\
 1 \text{ U.S. gal} &= 3.785 \times 10^{-3} \text{ m}^3 \\
 1 \text{ L} &= 1000 \text{ cm}^3 \\
 1 \text{ m}^3 &= 1000 \text{ L} \\
 1 \text{ U.S. gal} &= 4 \text{ qt} \\
 1 \text{ ft}^3 &= 7.481 \text{ U.S. gal} \\
 1 \text{ British gal} &= 1.20094 \text{ U.S. gal}
 \end{aligned}$$

Work

$$\begin{aligned}
 1 \text{ hp h} &= 0.7457 \text{ kW h} \\
 1 \text{ hp h} &= 2544.5 \text{ Btu} \\
 1 \text{ ft lb}_f &= 1.35582 \text{ J}
 \end{aligned}$$

Table A.1.3 Conversion Factors for Pressure

	lb_f/in²	kPa	kg_f/cm²	in Hg (at 21°C)	mm Hg (at 21°C)	in H₂O (at 21°C)	atm
1 lb _f /in ²	= 1	689.473×10^{-2}	0.07031	2.036	51.715	27.71	0.06805
1 kPa	= 0.1450383	1	101.972×10^{-4}	0.2952997	7.5003	4.0188	986.923×10^{-5}
1 kg _f /cm ²	= 14.2234	980.665×10^{-1}	1	28.959	735.550	394.0918	967.841×10^{-3}
1 in Hg (21°C)	= 0.4912	338.64×10^{-2}	0.03452	1	25.40	13.608	0.03342
1 mm Hg (21°C)	= 0.01934	0.1333273	1.359×10^{-3}	0.03937	1	0.5398	1.315×10^{-3}
1 in H ₂ O (21°C)	= 0.03609	24.883×10^{-2}	2.537×10^{-3}	0.0735	1.8665	1	2.458×10^{-3}
1 atm	= 14.6959	101.3251	1.03323	29.9212	760	406	1

A.2 PHYSICAL PROPERTIES OF FOODS

Table A.2.1 Specific Heat of Foods

Product	Composition (%)					Specific heat	
	Water	Protein	Carbohydrate	Fat	Ash	Eq. (4.4) (kJ/kg K)	Experimental ^a (kJ/[kg K])
Beef (hamburger)	68.3	20.7	0.0	10.0	1.0	3.35	3.52
Fish, canned	70.0	27.1	0.0	0.3	2.6	3.35	
Starch	12.0	0.5	87.0	0.2	0.3	1.754	
Orange juice	87.5	0.8	11.1	0.2	0.4	3.882	
Liver, raw beef	74.9	15.0	0.9	9.1	1.1	3.525	
Dry milk, nonfat	3.5	35.6	52.0	1.0	7.9	1.520	
Butter	15.5	0.6	0.4	81.0	2.5	2.043	2.051–2.135
Milk, whole pasteurized	87.0	3.5	4.9	3.9	0.7	3.831	3.852
Blueberries, syrup pack	73.0	0.4	23.6	0.4	2.6	3.445	
Cod, raw	82.6	15.0	0.0	0.4	2.0	3.697	
Skim milk	90.5	3.5	5.1	0.1	0.8	3.935	3.977–4.019
Tomato soup, concentrate	81.4	1.8	14.6	1.8	0.4	3.676	
Beef, lean	77.0	22.0	–	–	1.0	3.579	
Egg yolk	49.0	13.0	–	11.0	1.0	2.449	2.810
Fish, fresh	76.0	19.0	–	–	1.4	3.500	3.600
Beef, lean	71.7	21.6	0.0	5.7	1.0	3.437	3.433
Potato	79.8	2.1	17.1	0.1	0.9	3.634	3.517
Apple, raw	84.4	0.2	14.5	0.6	0.3	3.759	3.726–4.019
Bacon	49.9	27.6	0.3	17.5	4.7	2.851	2.01
Cucumber	96.1	0.5	1.9	0.1	1.4	4.061	4.103
Blackberry, syrup pack	76.0	0.7	22.9	0.2	0.2	3.521	
Potato	75.0	0.0	23.0	0.0	2.0	3.483	3.517
Veal	68.0	21.0	0.0	10.0	1.0	3.349	3.223
Fish	80.0	15.0	4.0	0.3	0.7	3.651	3.60
Cheese, cottage	65.0	25.0	1.0	2.0	7.0	3.215	3.265
Shrimp	66.2	26.8	0.0	1.4	0.0	3.404	3.014
Sardines	57.4	25.7	1.2	11.0	0.0	3.002	3.014
Beef, roast	60.0	25.0	0.0	13.0	0.0	3.115	3.056
Carrot, fresh	88.2	1.2	9.3	0.3	1.1	3.864	3.81–3.935

Source: Adapted from Heldman and Singh (1981).
^aExperimental specific heat values from Reidy (1968).

Table A.2.2 Thermal Conductivity of Selected Food Products

Product	Moisture content (%)	Temperature (°C)	Thermal conductivity (W/[m °C])
Apple	85.6	2–36	0.393
Applesauce	78.8	2–36	0.516
Beef, freeze dried			
1000 mm Hg pressure	–	0	0.065
0.001 mm Hg pressure	–	0	0.037
Beef, lean			
Perpendicular to fibers	78.9	7	0.476
Perpendicular to fibers	78.9	62	0.485
Parallel to fibers	78.7	8	0.431
Parallel to fibers	78.7	61	0.447
Beef fat	–	24–38	0.19
Butter	15	46	0.197
Cod	83	2.8	0.544
Corn, yellow dust	0.91	8–52	0.141
	30.2	8–52	0.172
Egg, frozen whole	–	–10 to –6	0.97
Egg, white	–	36	0.577
Egg, yolk	–	33	0.338
Fish muscle	–	0–10	0.557
Grapefruit, whole	–	30	0.45
Honey	12.6	2	0.502
	80	2	0.344
	14.8	69	0.623
	80	69	0.415
Juice, apple	87.4	20	0.559
	87.4	80	0.632
	36.0	20	0.389
	36.0	80	0.436
Lamb			
Perpendicular to fiber	71.8	5	0.45
		61	0.478
Parallel to fiber	71.0	5	0.415
		61	0.422
Milk	–	37	0.530
Milk, condensed	90	24	0.571
	–	78	0.641
	50	26	0.329
	–	78	0.364

(Continued)

Table A.2.2 (Continued)

Product	Moisture content (%)	Temperature (°C)	Thermal conductivity (W/[m°C])
Milk, skimmed	–	1.5	0.538
	–	80	0.635
Milk, nonfat dry	4.2	39	0.419
Olive oil	–	15	0.189
	–	100	0.163
Oranges, combined	–	30	0.431
Peas, black-eyed	–	3–17	0.312
Pork			
Perpendicular to fibers	75.1	6	0.488
		60	0.54
Parallel to fibers	75.9	4	0.443
		61	0.489
Pork fat	–	25	0.152
Potato, raw flesh	81.5	1–32	0.554
Potato, starch gel	–	1–67	0.04
Poultry, broiler muscle	69.1–74.9	4–27	0.412
Salmon			
Perpendicular to fibers	73	4	0.502
Salt	–	87	0.247
Sausage mixture	65.72	24	0.407
Soybean oil meal	13.2	7–10	0.069
Strawberries	–	14–25	0.675
Sugars	–	29–62	0.087–0.22
Turkey, breast			
Perpendicular to fibers	74	3	0.502
Parallel to fibers	74	3	0.523
Veal			
Perpendicular to fibers	75	6	0.476
		62	0.489
Parallel to fibers	75	5	0.441
		60	0.452
Vegetable and animal oils	–	4–187	0.169
Wheat flour	8.8	43	0.45
		65.5	0.689
		1.7	0.542
Whey		80	0.641

Source: Reidy (1968).

Table A.2.3 Thermal Diffusivity of Some Foodstuffs

Product	Water content (% wt.)	Temperature ^a (°C)	Thermal diffusivity ($\times 10^{-7} \text{ m}^2/\text{s}$)
Fruits, vegetables, and by-products			
Apples, whole, Red Delicious	85	0–30	1.37
Applesauce	37	5	1.05
	37	65	1.12
	80	5	1.22
	80	65	1.40
	–	26–129	1.67
Avocado, flesh	–	24, 0	1.24
Seed	–	24, 0	1.29
Whole	–	41, 0	1.54
Banana, flesh	76	5	1.18
	76	65	1.42
Beans, baked	–	4–122	1.68
Cherries, tart, flesh	–	30, 0	1.32
Grapefruit, Marsh, flesh	88.8	–	1.27
Grapefruit, Marsh, albedo	72.2	–	1.09
Lemon, whole	–	40, 0	1.07
Lima bean, pureed	–	26–122	1.80
Pea, pureed	–	26–128	1.82
Peach, whole	–	27, 4	1.39
Potato, flesh	–	25	1.70
Potato, mashed, cooked	78	5	1.23
	78	65	1.45
Rutabaga	–	48, 0	1.34
Squash, whole	–	47, 0	1.71
Strawberry, flesh	92	5	1.27
Sugarbeet	–	14, 60	1.26
Sweet potato, whole	–	35	1.06
	–	55	1.39
	–	70	1.91
Tomato, pulp	–	4, 26	1.48
Fish and meat products			
Codfish	81	5	1.22
	81	65	1.42
Corned beef	65	5	1.32
	65	65	1.18
Beef chuck ^b	66	40–65	1.23
Beef, round ^b	71	40–65	1.33
Beef, tongue ^b	68	40–65	1.32
Halibut	76	40–65	1.47
Ham, smoked	64	5	1.18
Ham, smoked	64	40–65	1.38
Water	–	30	1.48
	–	65	1.60
Ice	–	0	11.82

Source: Singh (1982). Reprinted from *Food Technology* 36(2), 87–91. Copyright © Institute of Food Technologists.

^a Where two temperatures separated by a comma are given, the first is the initial temperature of the sample, and the second is that of the surroundings.

^b Data are applicable only where the juices that exuded during the heating remain in the food samples.

Table A.2.4 Viscosity of Liquid Foods

Product	Composition	Temperature (°C)	Viscosity (Pa s)
Cream	10% fat	40	0.00148
	10% fat	60	0.00107
	10% fat	80	0.00083
Cream	20% fat	60	0.00171
	30% fat	60	0.00289
	40% fat	60	0.00510
Homogenized milk	–	20	0.0020
	–	40	0.0015
	–	60	0.000775
	–	80	0.0006
Raw milk	–	0	0.00344
	–	10	0.00264
	–	20	0.00199
	–	30	0.00149
	–	40	0.00123
Corn oil	–	25	0.0565
	–	38	0.0317
Cottonseed oil	–	20	0.0704
	–	38	0.0306
Peanut oil	–	25	0.0656
	–	38	0.0251
Safflower oil	–	25	0.0522
	–	38	0.0286
Soybean oil	–	30	0.04
Honey, buckwheat sage white clover	18.6% T.S.	24.8	3.86
	18.6% T.S.	25.9	8.88
	18.2% T.S.	25.0	4.80
Apple juice	20° Brix	27	0.0021
	60° Brix	27	0.03
Grape juice	20° Brix	27	0.0025
	60° Brix	27	0.11
Corn syrup	48.4% T.S.	27	0.053

Source: Steffe (1983).

Table A.2.5 Properties of Ice as a Function of Temperature

Temperature (°C)	Thermal conductivity (W/m °C)	Specific heat (kJ/kg °C)	Density (kg/m ³)
-101	3.50	1.382	925.8
-73	3.08	1.587	924.2
-45.5	2.72	1.783	922.6
-23	2.41	1.922	919.4
-18	2.37	1.955	919.4
-12	2.32	1.989	919.4
-7	2.27	2.022	917.8
0	2.22	2.050	916.2

Source: Adapted from Dickerson (1969).

Table A.2.6 Approximate Heat Evolution Rates of Fresh Fruits and Vegetables When Stored at Temperatures Shown

Commodity	0°C	Watts per megagram (W/Mg) ^a		
		5°C	10°C	15°C
Apples	10–12	15–21	41–61	41–92
Apricots	15–17	19–27	33–56	63–101
Artichokes, globe	67–133	94–177	161–291	229–429
Asparagus	81–237	161–403	269–902	471–970
Avocados	–	59–89	–	183–464
Bananas, ripening	–	–	65–116	87–164
Beans, green or snap	–	101–103	161–172	251–276
Beans, lima (unshelled)	31–89	58–106	–	296–369
Beets, red (roots)	16–21	27–28	35–40	50–69
Blackberries	46–68	85–135	154–280	208–431
Blueberries	7–31	27–36	69–104	101–183
Broccoli, sprouting	55–63	102–474	–	514–1000
Brussels sprouts	46–71	95–143	186–250	282–316
Cabbage	12–40	28–63	36–86	66–169
Cantaloupes	15–17	26–30	46	100–114
Carrots, topped	46	58	93	117
Cauliflower	53–71	61–81	100–144	136–242
Celery	21	32	58–81	110
Cherries, sour	17–39	38–39	–	81–148
Corn, sweet	125	230	331	482
Cranberries	–	12–14	–	–
Cucumbers	–	–	68–86	71–98
Figs, Mission	–	32–39	65–68	145–187
Garlic	9–32	17–29	27–29	32–81

(Continued)

Table A.2.6 (Continued)

Commodity	0°C	Watts per megagram (W/Mg) ^a		
		5°C	10°C	15°C
Gooseberries	20–26	36–40	–	64–95
Grapefruit	–	–	20–27	35–38
Grapes, American	8	16	23	47
Grapes, European	4–7	9–17	24	30–35
Honeydew melons	–	9–15	24	35–47
Horseradish	24	32	78	97
Kohlrabi	30	48	93	145
Leeks	28–48	58–86	158–201	245–346
Lemons	9	15	33	47
Lettuce, head	27–50	39–59	64–118	114–121
Lettuce, leaf	68	87	116	186
Mushrooms	83–129	210	297	–
Nuts, kind not specified	2	5	10	10
Okra	–	163	258	431
Onions	7–9	10–20	21	33
Onions, green	31–66	51–201	107–174	195–288
Olives	–	–	–	64–115
Oranges	9	14–19	35–40	38–67
Peaches	11–19	19–27	46	98–125
Pears	8–20	15–46	23–63	45–159
Peas, green (in pod)	90–138	163–226	–	529–599
Peppers, sweet	–	–	43	68
Plums, Wickson	6–9	12–27	27–34	35–37
Potatoes, immature	–	35	42–62	42–92
Potatoes, mature	–	17–20	20–30	20–35
Radishes, with tops	43–51	57–62	92–108	207–230
Radishes, topped	16–17	23–24	45–47	82–97
Raspberries	52–74	92–114	82–164	243–300
Rhubarb, topped	24–39	32–54	–	92–134
Spinach	–	136	327	529
Squash, yellow	35–38	42–55	103–108	222–269
Strawberries	36–52	48–98	145–280	210–273
Sweet potatoes	–	–	39–95	47–85
Tomatoes, mature green	–	21	45	61
Tomatoes, ripening	–	–	42	79
Turnips, roots	26	28–30	–	63–71
Watermelons	–	9–12	22	–

^a Conversion factor: (watts per megagram) \times (74.12898) = Btu per ton per 24 hr. From American Society of Heating, Refrigerating and Air-Conditioning Engineers; with permission of the American Society of Heating, Refrigerating, and Air-Conditioning Engineers, Atlanta, Georgia (1978).

Table A.2.7 Enthalpy of Frozen Foods

Temperature (°C)	Beef (kJ/kg)	Lamb (kJ/kg)	Poultry (kJ/kg)	Fish (kJ/kg)	Beans (kJ/kg)	Broccoli (kJ/kg)	Peas (kJ/kg)	Mashed potatoes (kJ/kg)	Cooked rice (kJ/kg)
−28.9	14.7	19.3	11.2	9.1	4.4	4.2	11.2	9.1	18.1
−23.3	27.7	31.4	23.5	21.6	16.5	16.3	23.5	21.6	31.9
−17.8	42.6	45.4	37.7	35.6	29.3	28.8	37.7	35.6	47.7
−12.2	62.8	67.2	55.6	52.1	43.7	42.8	55.6	52.1	70.0
−9.4	77.7	84.2	68.1	63.9	52.1	51.2	68.1	63.9	87.5
−6.7	101.2	112.6	87.5	80.7	63.3	62.1	87.5	80.7	115.1
−5.6	115.8	130.9	99.1	91.2	69.8	67.9	99.1	91.2	133.0
−4.4	136.9	157.7	104.4	105.1	77.9	75.6	104.4	105.1	158.9
−3.9	151.6	176.8	126.8	115.1	83.0	80.7	126.8	115.1	176.9
−3.3	170.9	201.6	141.6	128.2	90.2	87.2	141.6	128.2	177.9
−2.8	197.2	228.2	142.3	145.1	99.1	95.6	142.3	145.1	233.5
−2.2	236.5	229.8	191.7	170.7	112.1	107.7	191.7	170.7	242.3
−1.7	278.2	231.2	240.9	212.1	132.8	126.9	240.9	212.1	243.9
−1.1	280.0	232.8	295.4	295.1	173.7	165.1	295.4	295.1	245.6
1.7	288.4	240.7	304.5	317.7	361.9	366.8	304.5	317.7	254.9
4.4	297.9	248.4	313.8	327.2	372.6	377.5	313.8	327.2	261.4
7.2	306.8	256.3	323.1	336.5	383.3	388.2	323.1	336.5	269.3
10.0	315.8	263.9	332.1	346.3	393.8	398.9	332.1	346.3	277.2
15.6	333.5	279.6	350.5	365.4	414.7	420.3	350.5	365.4	292.8

Source: Mott (1964), by permission of H.G. Goldstein, editor, Aust. Refrig. Air Cond. Heat.

Table A.2.8 Composition Values of Selected Foods

Food	Water (%)	Protein (%)	Fat (%)	Carbohydrate (%)	Ash (%)
Apples, fresh	84.4	0.2	0.6	14.5	0.3
Applesauce	88.5	0.2	0.2	10.8	0.6
Asparagus	91.7	2.5	0.2	5.0	0.6
Beans, lima	67.5	8.4	0.5	22.1	1.5
Beef, hamburger, raw	68.3	20.7	10.0	0.0	1.0
Bread, white	35.8	8.7	3.2	50.4	1.9
Butter	15.5	0.6	81.0	0.4	2.5
Cod	81.2	17.6	0.3	0.0	1.2
Corn, sweet, raw	72.7	3.5	1.0	22.1	0.7
Cream, half-and-half	79.7	3.2	11.7	4.6	0.6
Eggs	73.7	12.9	11.5	0.9	1.0
Garlic	61.3	6.2	0.2	30.8	1.5
Lettuce, Iceburg	95.5	0.9	0.1	2.9	0.6
Milk, whole	87.4	3.5	3.5	4.9	0.7
Orange juice	88.3	0.7	0.2	10.4	0.4
Peaches	89.1	0.6	0.1	9.7	0.5
Peanuts, raw	5.6	26.0	47.5	18.6	2.3
Peas, raw	78.0	6.3	0.4	14.4	0.9
Pineapple, raw	85.3	0.4	0.2	13.7	0.4
Potatoes, raw	79.8	2.1	0.1	17.1	0.9
Rice, white	12.0	6.7	0.4	80.4	0.5
Spinach	90.7	3.2	0.3	4.3	1.5
Tomatoes	93.5	1.1	0.2	4.7	0.5
Turkey	64.2	20.1	14.7	0.0	1.0
Turnips	91.5	1.0	0.2	6.6	0.7
Yogurt (whole milk)	88.0	3.0	3.4	4.9	0.7

Table A.2.9 Coefficients to Estimate Food Properties

Property	Component	Temperature function	Standard error	Standard % error
k (W/m°C)	Protein	$k = 1.7881 \times 10^{-1} + 1.1958 \times 10^{-3}T - 2.7178 \times 10^{-6}T^2$	0.012	5.91
	Fat	$k = 1.8071 \times 10^{-1} - 2.7604 \times 10^{-3}T - 1.7749 \times 10^{-7}T^2$	0.0032	1.95
	Carbohydrate	$k = 2.0141 \times 10^{-1} + 1.3874 \times 10^{-3}T - 4.3312 \times 10^{-6}T^2$	0.0134	5.42
	Fiber	$k = 1.8331 \times 10^{-1} + 1.2497 \times 10^{-3}T - 3.1683 \times 10^{-6}T^2$	0.0127	5.55
	Ash	$k = 3.2962 \times 10^{-1} + 1.4011 \times 10^{-3}T - 2.9069 \times 10^{-6}T^2$	0.0083	2.15
	Water	$k = 5.7109 \times 10^{-1} + 1.7625 \times 10^{-3}T - 6.7036 \times 10^{-6}T^2$	0.0028	0.45
	Ice	$k = 2.2196 - 6.2489 \times 10^{-3}T + 1.0154 \times 10^{-4}T^2$	0.0079	0.79
α (mm ² /s)	Protein	$\alpha = 6.8714 \times 10^{-2} + 4.7578 \times 10^{-4}T - 1.4646 \times 10^{-6}T^2$	0.0038	4.50
	Fat	$\alpha = 9.8777 \times 10^{-2} - 1.2569 \times 10^{-4}T - 3.8286 \times 10^{-8}T^2$	0.0020	2.15
	Carbohydrate	$\alpha = 8.0842 \times 10^{-2} + 5.3052 \times 10^{-4}T - 2.3218 \times 10^{-6}T^2$	0.0058	5.84
	Fiber	$\alpha = 7.3976 \times 10^{-2} + 5.1902 \times 10^{-4}T - 2.2202 \times 10^{-6}T^2$	0.0026	3.14
	Ash	$\alpha = 1.2461 \times 10^{-1} + 3.7321 \times 10^{-4}T - 1.2244 \times 10^{-6}T^2$	0.0022	1.61
	Water	$\alpha = 1.3168 \times 10^{-1} + 6.2477 \times 10^{-4}T - 2.4022 \times 10^{-6}T^2$	0.0022×10^{-6}	1.44
	Ice	$\alpha = 1.1756 - 6.0833 \times 10^{-3}T + 9.5037 \times 10^{-5}T^2$	0.0044×10^{-6}	0.33
ρ (kg/m ³)	Protein	$\rho = 1.3299 \times 10^3 - 5.1840 \times 10^{-1}T$	39.9501	3.07
	Fat	$\rho = 9.2559 \times 10^2 - 4.1757 \times 10^{-1}T$	4.2554	0.47
	Carbohydrate	$\rho = 1.5991 \times 10^3 - 3.1046 \times 10^{-1}T$	93.1249	5.98
	Fiber	$\rho = 1.3115 \times 10^3 - 3.6589 \times 10^{-1}T$	8.2687	0.64
	Ash	$\rho = 2.4238 \times 10^3 - 2.8063 \times 10^{-1}T$	2.2315	0.09
	Water	$\rho = 9.9718 \times 10^2 + 3.1439 \times 10^{-3}T - 3.7574 \times 10^{-3}T^2$	2.1044	0.22
	Ice	$\rho = 9.1689 \times 10^2 - 1.3071 \times 10^{-1}T$	0.5382	0.06
c_p (kJ/kg°C)	Protein	$c_p = 2.0082 + 1.2089 \times 10^{-3}T - 1.3129 \times 10^{-6}T^2$	0.1147	5.57
	Fat	$c_p = 1.9842 + 1.4733 \times 10^{-3}T - 4.8008 \times 10^{-6}T^2$	0.0236	1.16
	Carbohydrate	$c_p = 1.5488 + 1.9625 \times 10^{-3}T - 5.9399 \times 10^{-6}T^2$	0.0986	5.96
	Fiber	$c_p = 1.8459 + 1.8306 \times 10^{-3}T - 4.6509 \times 10^{-6}T^2$	0.0293	1.66
	Ash	$c_p = 1.0926 + 1.8896 \times 10^{-3}T - 3.6817 \times 10^{-6}T^2$	0.0296	2.47
	Water ^a	$c_p = 4.0817 - 5.3062 \times 10^{-3}T + 9.9516 \times 10^{-4}T^2$	0.0988	2.15
	Water ^b	$c_p = 4.1762 - 9.0864 \times 10^{-5}T + 5.4731 \times 10^{-6}T^2$	0.0159	0.38
	Ice	$c_p = 2.0623 + 6.0769 \times 10^{-3}T$	0.0014	0.07

^a For the temperature range of -40 to 0°C.^b For the temperature range of 0 to 150°C.

A.3 PHYSICAL PROPERTIES OF NONFOOD MATERIALS

Table A.3.1 Physical Properties of Metals

Metal	Properties at 20°C			
	ρ (kg/m ³)	c_p (kJ/kg °C)	k (W/m °C)	α ($\times 10^{-5}$ m ² /s)
Aluminum				
Pure	2707	0.896	204	8.418
Al-Cu (Duralumin, 94–96% Al, 3–5% Cu, trace Mg)	2787	0.883	164	6.676
Al-Si (Silumin, copper-bearing: 86.5% Al, 1% Cu)	2659	0.867	137	5.933
Al-Si (Alusil, 78–80% Al, 20–22% Si)	2627	0.854	161	7.172
Al-Mg-Si, 97% Al, 1%Mg, 1% Si, 1% Mn	2707	0.892	177	7.311
Lead	11,373	0.130	35	2.343
Iron				
Pure	7897	0.452	73	2.034
Steel				
(C max = 1.5%):				
Carbon steel				
C = 0.5%	7833	0.465	54	1.474
1.00%	7801	0.473	43	1.712
1.50%	7753	0.486	36	0.970
Nickel steel				
Ni = 0%	7897	0.452	73	2.026
20%	7933	0.46	19	0.526
40%	8169	0.46	10	0.279
80%	8618	0.46	35	0.872
Invar 36% Ni	8137	0.46	10.7	0.286
Chrome steel				
Cr = 0%	7897	0.452	73	2.026
1%	7865	0.46	61	1.665
5%	7833	0.46	40	1.110
20%	7689	0.46	22	0.635
Cr-Ni (chrome-nickel)				
15% Cr, 10% Ni	7865	0.46	19	0.526
18% Cr, 8% Ni (V2A)	7817	0.46	16.3	0.444
20% Cr, 15% Ni	7833	0.46	15.1	0.415
25% Cr, 20% Ni	7865	0.46	12.8	0.361
Tungsten steel				
W = 0%	7897	0.452	73	2.026
W = 1%	7913	0.448	66	1.858
W = 5%	8073	0.435	54	1.525
W = 10%	8314	0.419	48	1.391
Copper				
Pure	8954	0.3831	386	11.234
Aluminum bronze (95% Cu, 5% Al)	8666	0.410	83	2.330
Bronze (75%, 25% Sn)	8666	0.343	26	0.859

(Continued)

Table A.3.1 (Continued)

Metal	Properties at 20°C			
	ρ (kg/m ³)	c_p (kJ/kg °C)	k (W/m °C)	α ($\times 10^{-5}$ m ² /s)
Red brass (85% Cu, 9% Sn, 6% Zn)	8714	0.385	61	1.804
Brass (70% Cu, 30% Zn)	8522	0.385	111	3.412
German silver (62% Cu, 15% Ni, 22% Zn)	8618	0.394	24.9	0.733
Constantan (60% Cu, 40% Ni)	8922	0.410	22.7	0.612
Magnesium				
Pure	1746	1.013	171	9.708
Mg-Al (electrolytic), 6–8% Al, 1–2% Zn	1810	1.00	66	3.605
Molybdenum	10,220	0.251	123	4.790
Nickel				
Pure (99.9%)	8906	0.4459	90	2.266
Ni-Cr (90% Ni, 10% Cr)	8666	0.444	17	0.444
80% Ni, 20% Cr	8314	0.444	12.6	0.343
Silver				
Purest	10,524	0.2340	419	17.004
Pure (99.9%)	10,524	0.2340	407	16.563
Tin, pure	7304	0.2265	64	3.884
Tungsten	19,350	0.1344	163	6.271
Zinc, pure	7144	0.3843	112.2	4.106

Source: Adapted from Holman (2002). Reproduced with permission from the publisher.

Table A.3.2 Physical Properties of Nonmetals

Substance	Temperature (°C)	k (W/m °C)	ρ (kg/m ³)	c (kJ/kg °C)	α ($\times 10^{-7}$ m ² /s)
Asphalt	20–55	0.74–0.76			
Brick					
Building brick, common	20	0.69	1600	0.84	5.2
Fireclay brick, burnt					
133°C	500	1.04	2000	0.96	5.4
	800	1.07			
	1100	1.09			
Cement, Portland		0.29	1500		
Mortar	23	1.16			
Concrete, cinder	23	0.76			
Glass, window	20	0.78 (avg)	2700	0.84	3.4

(Continued)

Table A.3.2 (Continued)

Substance	Temperature (°C)	k (W/m °C)	ρ (kg/m ³)	c (kJ/kg °C)	α ($\times 10^{-7}$ m ² /s)
Plaster, gypsum	20	0.48	1440	0.84	4.0
Metal lath	20	0.47			
Wood lath	20	0.28			
Stone					
Granite		1.73–3.98	2640	0.82	8–18
Limestone	100–300	1.26–1.33	2500	0.90	5.6–5.9
Marble		2.07–2.94	2500–2700	0.80	10–13.6
Sandstone	40	1.83	2160–2300	0.71	11.2–11.9
Wood (across the grain)					
Cypress	30	0.097	460		
Fir	23	0.11	420	2.72	0.96
Maple or Oak	30	0.166	540	2.4	1.28
Yellow pine	23	0.147	640	2.8	0.82
White pine	30	0.112	430		
Asbestos					
Loosely packed	–45	0.149			
	0	0.154	470–570	0.816	3.3–4
	100	0.161			
Sheets	51	0.166			
Cardboard, corrugated	—	0.064			
Corkboard, 160 kg/m ³	30	0.043	160		
Cork, regranulated	32	0.045	45–120	1.88	2–5.3
Ground	32	0.043	150		
Diatomaceous earth (Sil-o-cel)	0	0.061	320		
Fiber, insulating board	20	0.048	240		
Glass wool, 24 kg/m ³	23	0.038	24	0.7	22.6
Magnesia, 85%	38	0.067	270		
	93	0.071			
	150	0.074			
	204	0.080			
Rock wool, 24 kg/m ³	32	0.040	160		
Loosely packed	150	0.067	64		
	260	0.087			
Sawdust	23	0.059			
Wood shavings	23	0.059			

Source: Adapted from Holman (2002). Reproduced with the permission of the publisher.

Table A.3.3 Emissivity of Various Surfaces

Material	Wavelength and average temperatures				
	9.3 μm 38°C	5.4 μm 260°C	3.6 μm 540°C	1.8 μm 1370°C	0.6 μm Solar
Metals					
Aluminum					
Polished	0.04	0.05	0.08	0.19	~0.3
Oxidized	0.11	0.12	0.18		
24-ST weathered	0.4	0.32	0.27		
Surface roofing	0.22				
Anodized (at 1000°F)	0.94	0.42	0.60	0.34	
Brass					
Polished	0.10	0.10			
Oxidized	0.61				
Chromium, polished	0.08	0.17	0.26	0.40	0.49
Copper					
Polished	0.04	0.05	0.18	0.17	
Oxidized	0.87	0.83	0.77		
Iron					
Polished	0.06	0.08	0.13	0.25	0.45
Cast, oxidized	0.63	0.66	0.76		
Galvanized, new	0.23	–	–	0.42	0.66
Galvanized, dirty	0.28	–	–	0.90	0.89
Steel plate, rough	0.94	0.97	0.98		
Oxide	0.96	–	0.85	–	0.74
Magnesium	0.07	0.13	0.18	0.24	0.30
Silver, polished	0.01	0.02	0.03	–	0.11
Stainless steel					
18-8, polished	0.15	0.18	0.22		
18-8, weathered	0.85	0.85	0.85		
Steel tube					
Oxidized	–	0.80			
Tungsten filament	0.03	–	–	~0.18	0.36 ^a
Zinc					
Polished	0.02	0.03	0.04	0.06	0.46
Galvanized sheet	~0.25				
Building and insulating materials					
Asphalt	0.93	–	0.9	–	0.93
Brick					
Red	0.93	–	–	–	0.7
Fire clay	0.9	–	~0.7	~0.75	
Silica	0.9	–	~0.75	0.84	
Magnesite refractory	0.9	–	–	~0.4	
Enamel, white	0.9				
Paper, white	0.95	–	0.82	0.25	0.28
Plaster	0.91				
Roofing board	0.93				
ENAMELED steel, white	–	–	–	0.65	0.47

(Continued)

Table A.3.3 (Continued)

Material	Wavelength and average temperatures				
	9.3 μm 38°C	5.4 μm 260°C	3.6 μm 540°C	1.8 μm 1370°C	0.6 μm Solar
Paints					
Aluminized lacquer	0.65	0.65			
Lacquer, black	0.96	0.98			
Lampblack paint	0.96	0.97	–	0.97	0.97
Red paint	0.96	–	–	–	0.74
Yellow paint	0.95	–	0.5	–	0.30
Oil paints (all colors)	~0.94	~0.9			
White (ZnO)	0.95	–	0.91	–	0.18
Miscellaneous					
Ice	~0.97 ^b				
Water	~0.96				
Carbon, T-carbon, 0.9% ash	0.82	0.80	0.79		
Wood	~0.93				
Glass	0.90	–	–	–	(Low)

Source: Adapted from Kreith (1973). Copyright © 1973 Harper and Row Publishers, Inc. Reprinted by permission of the publisher.

^a At 3315°C

^b At 0°C

A.4 PHYSICAL PROPERTIES OF WATER AND AIR

Table A.4.1 Physical Properties of **Water** at the Saturation Pressure

Temperature		Density ρ (kg/m ³)	Coefficient of volumetric thermal expansion β ($\times 10^{-4}$ K ⁻¹)	Specific heat c_p (kJ/ [kg °C])	Thermal conductivity k (W/[m °C])	Thermal diffusivity α ($\times 10^{-6}$ m ² /s)	Absolute viscosity μ ($\times 10^{-6}$ Pa s)	Kinematic viscosity ν ($\times 10^{-6}$ m ² /s)	Prandtl number N_{Pr}
T (°C)	T (K)								
0	273.15	999.9	-0.7	4.226	0.558	0.131	1793.636	1.789	13.7
5	278.15	1000.0	-	4.206	0.568	0.135	1534.741	1.535	11.4
10	283.15	999.7	0.95	4.195	0.577	0.137	1296.439	1.300	9.5
15	288.15	999.1	-	4.187	0.587	0.141	1135.610	1.146	8.1
20	293.15	998.2	2.1	4.182	0.597	0.143	993.414	1.006	7.0
25	298.15	997.1	-	4.178	0.606	0.146	880.637	0.884	6.1
30	303.15	995.7	3.0	4.176	0.615	0.149	792.377	0.805	5.4
35	308.15	994.1	-	4.175	0.624	0.150	719.808	0.725	4.8
40	313.15	992.2	3.9	4.175	0.633	0.151	658.026	0.658	4.3
45	318.15	990.2	-	4.176	0.640	0.155	605.070	0.611	3.9
50	323.15	988.1	4.6	4.178	0.647	0.157	555.056	0.556	3.55
55	328.15	985.7	-	4.179	0.652	0.158	509.946	0.517	3.27
60	333.15	983.2	5.3	4.181	0.658	0.159	471.650	0.478	3.00
65	338.15	980.6	-	4.184	0.663	0.161	435.415	0.444	2.76
70	343.15	977.8	5.8	4.187	0.668	0.163	404.034	0.415	2.55
75	348.15	974.9	-	4.190	0.671	0.164	376.575	0.366	2.23
80	353.15	971.8	6.3	4.194	0.673	0.165	352.059	0.364	2.25
85	358.15	968.7	-	4.198	0.676	0.166	328.523	0.339	2.04
90	363.15	965.3	7.0	4.202	0.678	0.167	308.909	0.326	1.95
95	368.15	961.9	-	4.206	0.680	0.168	292.238	0.310	1.84
100	373.15	958.4	7.5	4.211	0.682	0.169	277.528	0.294	1.75
110	383.15	951.0	8.0	4.224	0.684	0.170	254.973	0.268	1.57
120	393.15	943.5	8.5	4.232	0.684	0.171	235.360	0.244	1.43
130	403.15	934.8	9.1	4.250	0.685	0.172	211.824	0.226	1.32
140	413.15	926.3	9.7	4.257	0.686	0.172	201.036	0.212	1.23
150	423.15	916.9	10.3	4.270	0.684	0.173	185.346	0.201	1.17
160	433.15	907.6	10.8	4.285	0.680	0.173	171.616	0.191	1.10
170	443.15	897.3	11.5	4.396	0.679	0.172	162.290	0.181	1.05

(Continued)

Table A.4.1 (Continued)

Temperature		Density ρ (kg/m ³)	Coefficient of volumetric thermal expansion β ($\times 10^{-4}$ K ⁻¹)	Specific heat c_p (kJ/ [kg °C])	Thermal conductivity k (W/[m °C])	Thermal diffusivity α ($\times 10^{-6}$ m ² /s)	Absolute viscosity μ ($\times 10^{-6}$ Pa s)	Kinematic viscosity ν ($\times 10^{-6}$ m ² /s)	Prandtl number N_{Pr}
T (°C)	T (K)								
180	453.15	886.6	12.1	4.396	0.673	0.172	152.003	0.173	1.01
190	463.15	876.0	12.8	4.480	0.670	0.171	145.138	0.166	0.97
200	473.15	862.8	13.5	4.501	0.665	0.170	139.254	0.160	0.95
210	483.15	852.8	14.3	4.560	0.655	0.168	131.409	0.154	0.92
220	493.15	837.0	15.2	4.605	0.652	0.167	124.544	0.149	0.90
230	503.15	827.3	16.2	4.690	0.637	0.164	119.641	0.145	0.88
240	513.15	809.0	17.2	4.731	0.634	0.162	113.757	0.141	0.86
250	523.15	799.2	18.6	4.857	0.618	0.160	109.834	0.137	0.86

Source: Adapted from Raznjevic (1978)

Table A.4.2 Properties of Saturated Steam

Temperature (°C)	Vapor pressure (kPa)	Specific volume (m ³ /kg)		Enthalpy (kJ/kg)		Entropy (kJ/[kg °C])	
		Liquid	Saturated vapor	Liquid (H _f)	Saturated vapor (H _g)	Liquid	Saturated vapor
0.01	0.6113	0.0010002	206.136	0.00	2501.4	0.0000	9.1562
3	0.7577	0.0010001	168.132	12.57	2506.9	0.0457	9.0773
6	0.9349	0.0010001	137.734	25.20	2512.4	0.0912	9.0003
9	1.1477	0.0010003	113.386	37.80	2517.9	0.1362	8.9253
12	1.4022	0.0010005	93.784	50.41	2523.4	0.1806	8.8524
15	1.7051	0.0010009	77.926	62.99	2528.9	0.2245	8.7814
18	2.0640	0.0010014	65.038	75.58	2534.4	0.2679	8.7123
21	2.487	0.0010020	54.514	88.14	2539.9	0.3109	8.6450
24	2.985	0.0010027	45.883	100.70	2545.4	0.3534	8.5794
27	3.567	0.0010035	38.774	113.25	2550.8	0.3954	8.5156
30	4.246	0.0010043	32.894	125.79	2556.3	0.4369	8.4533
33	5.034	0.0010053	28.011	138.33	2561.7	0.4781	8.3927
36	5.947	0.0010063	23.940	150.86	2567.1	0.5188	8.3336
40	7.384	0.0010078	19.523	167.57	2574.3	0.5725	8.2570
45	9.593	0.0010099	15.258	188.45	2583.2	0.6387	8.1648
50	12.349	0.0010121	12.032	209.33	2592.1	0.7038	8.0763

(Continued)

Table A.4.2 (Continued)

Temperature (°C)	Vapor pressure (kPa)	Specific volume (m ³ /kg)		Enthalpy (kJ/kg)		Entropy (kJ/[kg °C])	
		Liquid	Saturated vapor	Liquid (H _l)	Saturated vapor (H _v)	Liquid	Saturated vapor
55	15.758	0.0010146	9.568	230.23	2600.9	0.7679	7.9913
60	19.940	0.0010172	7.671	251.13	2609.6	0.8312	7.9096
65	25.03	0.0010199	6.197	272.06	2618.3	0.8935	7.8310
70	31.19	0.0010228	5.042	292.98	2626.8	0.9549	7.7553
75	38.58	0.0010259	4.131	313.93	2635.3	1.0155	7.6824
80	47.39	0.0010291	3.407	334.91	2643.7	1.0753	7.6122
85	57.83	0.0010325	2.828	355.90	2651.9	1.1343	7.5445
90	70.14	0.0010360	2.361	376.92	2660.1	1.1925	7.4791
95	84.55	0.0010397	1.9819	397.96	2668.1	1.2500	7.4159
100	101.35	0.0010435	1.6729	419.04	2676.1	1.3069	7.3549
105	120.82	0.0010475	1.4194	440.15	2683.8	1.3630	7.2958
110	143.27	0.0010516	1.2102	461.30	2691.5	1.4185	7.2387
115	169.06	0.0010559	1.0366	482.48	2699.0	1.4734	7.1833
120	198.53	0.0010603	0.8919	503.71	2706.3	1.5276	7.1296
125	232.1	0.0010649	0.7706	524.99	2713.5	1.5813	7.0775
130	270.1	0.0010697	0.6685	546.31	2720.5	1.6344	7.0269
135	313.0	0.0010746	0.5822	567.69	2727.3	1.6870	6.9777
140	361.3	0.0010797	0.5089	589.13	2733.9	1.7391	6.9299
145	415.4	0.0010850	0.4463	610.63	2740.3	1.7907	6.8833
150	475.8	0.0010905	0.3928	632.20	2746.5	1.8418	6.8379
155	543.1	0.0010961	0.3468	653.84	2752.4	1.8925	6.7935
160	617.8	0.0011020	0.3071	675.55	2758.1	1.9427	6.7502
165	700.5	0.0011080	0.2727	697.34	2763.5	1.9925	6.7078
170	791.7	0.0011143	0.2428	719.21	2768.7	2.0419	6.6663
175	892.0	0.0011207	0.2168	741.17	2773.6	2.0909	6.6256
180	1002.1	0.0011274	0.19405	763.22	2778.2	2.1396	6.5857
190	1254.4	0.0011414	0.15654	807.62	2786.4	2.2359	6.5079
200	1553.8	0.0011565	0.12736	852.45	2793.2	2.3309	6.4323
225	2548	0.0011992	0.07849	966.78	2803.3	2.5639	6.2503
250	3973	0.0012512	0.05013	1085.36	2801.5	2.7927	6.0730
275	5942	0.0013168	0.03279	1210.07	2785.0	3.0208	5.8938
300	8581	0.0010436	0.02167	1344.0	2749.0	3.2534	5.7045

Source: Abridged from Keenan et al. (1969). Copyright © 1969 by John Wiley and Sons. Reprinted by permission of John Wiley and Sons, Inc.

Table A.4.3 Properties of Superheated Steam

Absolute pressure (kPa, with sat. temperature, °C) ^a		Temperature (°C)							
		100	150	200	250	300	360	420	500
10 (45.81)	V	17.196	19.512	21.825	24.136	26.445	29.216	31.986	35.679
	H	2687.5	2783.0	2879.5	2977.3	3076.5	3197.6	3320.9	3489.1
	s	8.4479	8.6882	8.9038	9.1002	9.2813	9.4821	9.6682	9.8978
50 (81.33)	V	3.418	3.889	4.356	4.820	5.284	5.839	6.394	7.134
	H	2682.5	2780.1	2877.7	2976.0	3075.5	3196.8	3320.4	3488.7
	s	7.6947	7.9401	8.1580	8.3556	8.5373	8.7385	8.9249	9.1546
75 (91.78)	V	2.270	2.587	2.900	3.211	3.520	3.891	4.262	4.755
	H	2679.4	2778.2	2876.5	2975.2	3074.9	3196.4	3320.0	3488.4
	s	7.5009	7.7496	7.9690	8.1673	8.3493	8.5508	8.7374	8.9672
100 (99.63)	V	1.6958	1.9364	2.172	2.406	2.639	2.917	3.195	3.565
	H	2676.2	2776.4	2875.3	2974.3	3074.3	3195.9	3319.6	3488.1
	s	7.3614	7.6134	7.8343	8.0333	8.2158	8.4175	8.6042	8.8342
150 (111.37)	V		1.2853	1.4443	1.6012	1.7570	1.9432	2.129	2.376
	H		2772.6	2872.9	2972.7	3073.1	3195.0	3318.9	3487.6
	s		7.4193	7.6433	7.8438	8.0720	8.2293	8.4163	8.6466
400 (143.63)	V		0.4708	0.5342	0.5951	0.6458	0.7257	0.7960	0.8893
	H		2752.8	2860.5	2964.2	3066.8	3190.3	3315.3	3484.9
	s		6.9299	7.1706	7.3789	7.5662	7.7712	7.9598	8.1913
700 (164.97)	V			0.2999	0.3363	0.3714	0.4126	0.4533	0.5070
	H			2844.8	2953.6	3059.1	3184.7	3310.9	3481.7
	s			6.8865	7.1053	7.2979	7.5063	7.6968	7.9299
1000 (179.91)	V			0.2060	0.2327	0.2579	0.2873	0.3162	0.3541
	H			2827.9	2942.6	3051.2	3178.9	3306.5	3478.5
	s			6.6940	6.9247	7.1229	7.3349	7.5275	7.7622
1500 (198.32)	V			0.13248	0.15195	0.16966	0.18988	0.2095	0.2352
	H			2796.8	2923.3	3037.6	31692	3299.1	3473.1
	s			6.4546	6.7090	6.9179	7.1363	7.3323	7.5698
2000 (212.42)	V				0.11144	0.12547	0.14113	0.15616	0.17568
	H				2902.5	3023.5	3159.3	3291.6	3467.6
	s				6.5453	6.7664	6.9917	7.1915	7.4317
2500 (223.99)	V				0.08700	0.09890	0.11186	0.12414	0.13998
	H				2880.1	3008.8	3149.1	3284.0	3462.1
	s				6.4085	6.6438	6.8767	7.0803	7.3234
3000 (233.90)	V				0.07058	0.08114	0.09233	0.10279	0.11619
	H				2855.8	2993.5	3138.7	3276.3	3456.5
	s				6.2872	6.5390	6.7801	6.9878	7.2338

Source: Abridged from Keenan et al. (1969). Copyright © 1969 by John Wiley and Sons. Reprinted by permission of John Wiley and Sons, Inc.

^aV, specific volume, m³/kg; H, enthalpy, kJ/kg; s, entropy, kJ/kg K.

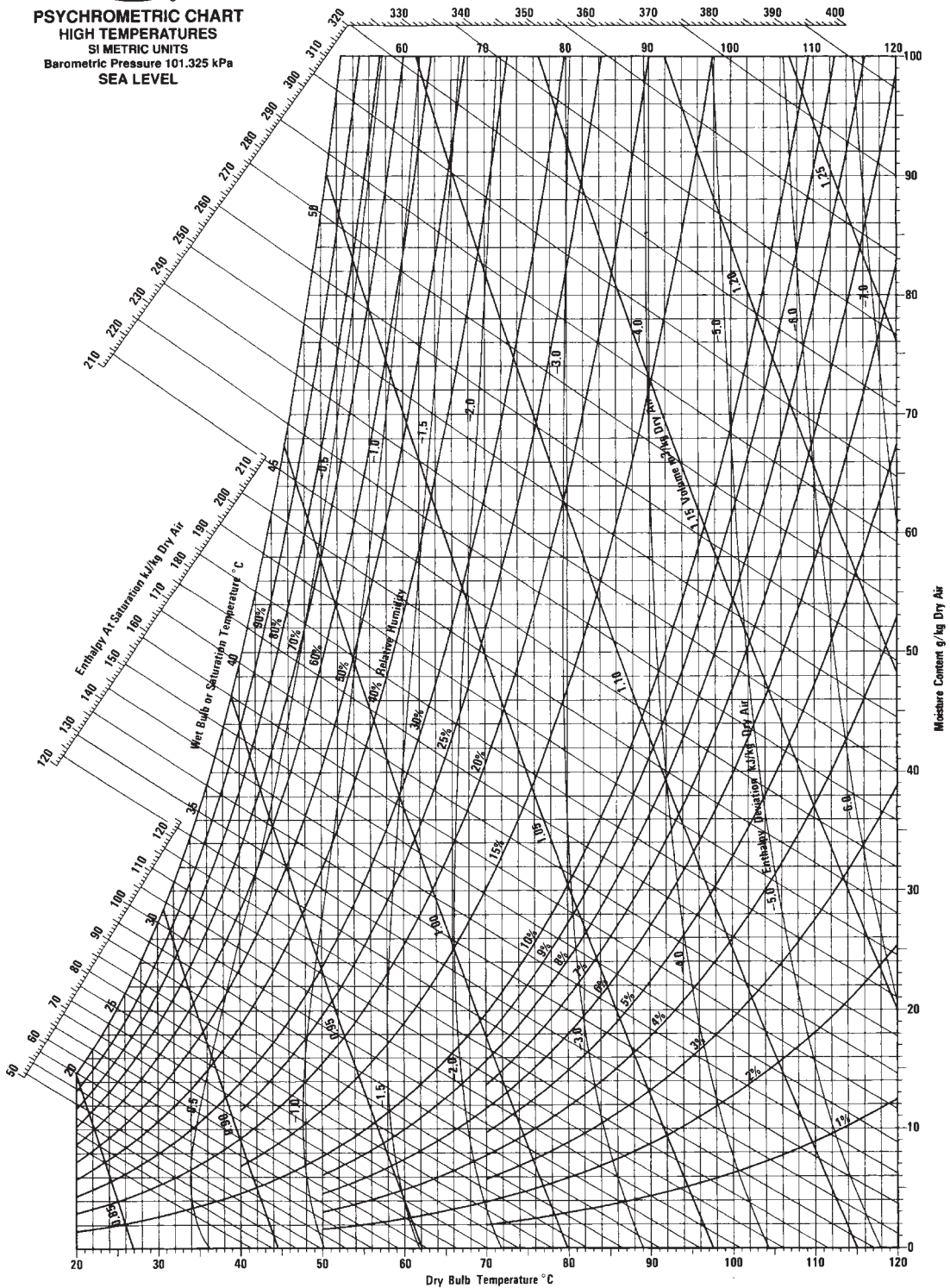
Table A.4.4 Physical Properties of Dry Air at Atmospheric Pressure

Temperature		Density (ρ) (kg/m ³)	Volumetric coefficient of expansion (β) ($\times 10^{-3} \text{ K}^{-1}$)	Specific heat (c_p) (kJ/[kg K])	Thermal conductivity (k) (W/[m K])	Thermal diffusivity (α) ($\times 10^{-6} \text{ m}^2/\text{s}$)	Viscosity (μ) ($\times 10^{-6} \text{ N s/m}^2$)	Kinematic viscosity (ν) ($\times 10^{-6} \text{ m}^2/\text{s}$)	Prandtl number (N_{Pr})
t (°C)	T (K)								
-20	253.15	1.365	3.97	1.005	0.0226	16.8	16.279	12.0	0.71
0	273.15	1.252	3.65	1.011	0.0237	19.2	17.456	13.9	0.71
10	283.15	1.206	3.53	1.010	0.0244	20.7	17.848	14.66	0.71
20	293.15	1.164	3.41	1.012	0.0251	22.0	18.240	15.7	0.71
30	303.15	1.127	3.30	1.013	0.0258	23.4	18.682	16.58	0.71
40	313.15	1.092	3.20	1.014	0.0265	24.8	19.123	17.6	0.71
50	323.15	1.057	3.10	1.016	0.0272	26.2	19.515	18.58	0.71
60	333.15	1.025	3.00	1.017	0.0279	27.6	19.907	19.4	0.71
70	343.15	0.996	2.91	1.018	0.0286	29.2	20.398	20.65	0.71
80	353.15	0.968	2.83	1.019	0.0293	30.6	20.790	21.5	0.71
90	363.15	0.942	2.76	1.021	0.0300	32.2	21.231	22.82	0.71
100	373.15	0.916	2.69	1.022	0.0307	33.6	21.673	23.6	0.71
120	393.15	0.870	2.55	1.025	0.0320	37.0	22.555	25.9	0.71
140	413.15	0.827	2.43	1.027	0.0333	40.0	23.340	28.2	0.71
150	423.15	0.810	2.37	1.028	0.0336	41.2	23.732	29.4	0.71
160	433.15	0.789	2.31	1.030	0.0344	43.3	24.124	30.6	0.71
180	453.15	0.755	2.20	1.032	0.0357	47.0	24.909	33.0	0.71
200	473.15	0.723	2.11	1.035	0.0370	49.7	25.693	35.5	0.71
250	523.15	0.653	1.89	1.043	0.0400	60.0	27.557	42.2	0.71

Source: Adapted from Raznjevic (1978).

A.5 PSYCHROMETRIC CHARTS

Carrier
PSYCHROMETRIC CHART
HIGH TEMPERATURES
 SI METRIC UNITS
 Barometric Pressure 101.325 kPa
 SEA LEVEL



■ **Figure A.5.1** Psychrometric chart for high temperatures.



Carrier

A United Technologies Company

PSYCHROMETRIC CHART NORMAL TEMPERATURES SI METRIC UNITS Barometric Pressure 101.325 kPa SEA LEVEL

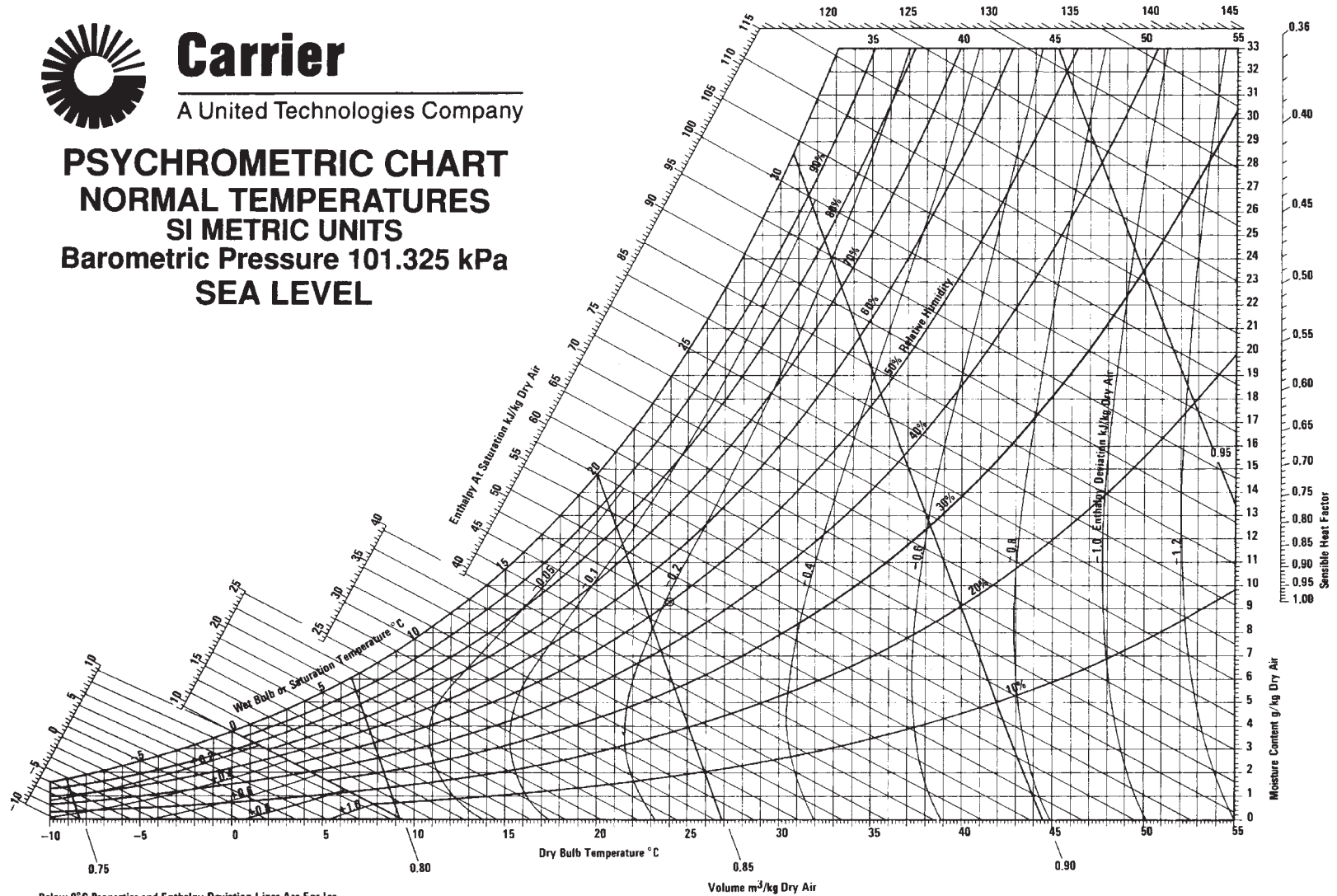
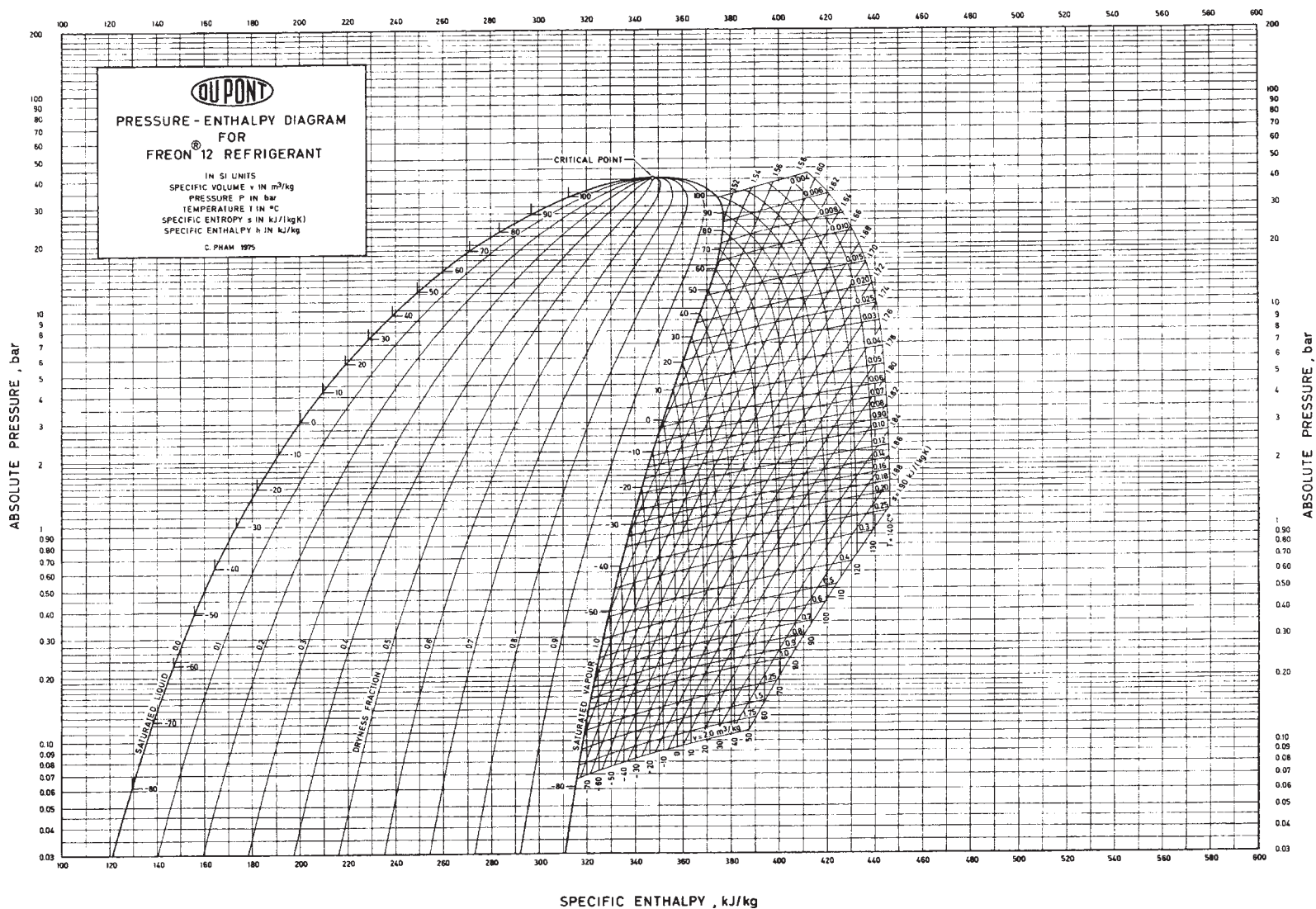


Figure A.5.2 Psychrometric chart for low temperatures.



■ Figure A.6.1 Pressure-enthalpy diagram for Refrigerant 12. (Reproduced by permission of Du Pont de Nemours International S.A.)

Table A.6.1 Properties of Saturated Liquid and Vapor R-12^a

Temp (°C)	Absolute pressure (kPa)	Enthalpy (kJ/kg)		Entropy (kJ/kg K)		Specific volume (L/kg)	
		h_f	h_g	s_f	s_g	v_f	v_g
-60	22.62	146.463	324.236	0.77977	1.61373	0.63689	637.911
-55	29.98	150.808	326.567	0.79990	1.60552	0.64226	491.000
-50	39.15	155.169	328.897	0.81964	1.59810	0.64782	383.105
-45	50.44	159.549	331.223	0.83901	1.59142	0.65355	302.683
-40	64.17	163.948	333.541	0.85805	1.58539	0.65949	241.910
-35	80.71	168.396	335.849	0.86776	1.57996	0.66563	195.398
-30	100.41	172.810	338.143	0.89516	1.57507	0.67200	159.375
-28	109.27	174.593	339.057	0.90244	1.57326	0.67461	147.275
-26	118.72	176.380	339.968	0.90967	1.57152	0.67726	136.284
-24	128.80	178.171	340.876	0.91686	1.56985	0.67996	126.282
-22	139.53	179.965	341.780	0.92400	1.56825	0.68269	117.167
-20	150.93	181.764	342.682	0.93110	1.56672	0.68547	108.847
-18	163.04	183.567	343.580	0.93816	1.56526	0.68829	101.242
-16	175.89	185.374	344.474	0.94518	1.56385	0.69115	94.2788
-14	189.50	187.185	345.365	0.95216	1.56250	0.69407	87.8951
-12	203.90	189.001	346.252	0.95910	1.56121	0.60703	82.0344
-10	219.12	190.822	347.134	0.96601	1.55997	0.70004	76.6464
-9	227.04	191.734	347.574	0.96945	1.55938	0.70157	74.1155
-8	235.19	192.647	348.012	0.97287	1.55897	0.70310	71.6864
-7	243.55	193.562	348.450	0.97629	1.55822	0.70465	69.3543
-6	252.14	194.477	348.886	0.97971	1.55765	0.70622	67.1146
-5	260.96	195.395	349.321	0.98311	1.55710	0.70780	64.9629
-4	270.01	196.313	349.755	0.98650	1.55657	0.70939	62.8952
-3	279.30	197.233	350.187	0.98989	1.55604	0.71099	60.9075
-2	288.82	198.154	350.619	0.99327	1.55552	0.71261	58.9963
-1	298.59	199.076	351.049	0.99664	1.55502	0.71425	57.1579
0	308.61	200.000	351.477	1.00000	1.55452	0.71590	55.3892
1	318.88	200.925	351.905	1.00355	1.55404	0.71756	53.6869
2	329.40	201.852	352.331	1.00670	1.55356	0.71324	52.0481
3	340.19	202.780	352.755	1.01004	1.55310	0.72094	50.4700
4	351.24	203.710	353.179	1.01337	1.55264	0.72265	48.9499
5	363.55	204.642	353.600	1.01670	1.55220	0.72438	47.4853
6	374.14	205.575	354.020	1.02001	1.55176	0.72612	46.0737

(Continued)

Table A.6.1 (Continued)

Temp (°C)	Absolute pressure (kPa)	Enthalpy (kJ/kg)		Entropy (kJ/kg K)		Specific volume (L/kg)	
		h_f	h_g	s_f	s_g	v_f	v_g
7	386.01	206.509	354.439	1.02333	1.55133	0.72788	44.7129
8	398.15	207.445	354.856	1.02663	1.55091	0.72966	43.4006
9	410.58	208.383	355.272	1.02993	1.55050	0.73146	42.1349
10	423.30	209.323	355.686	1.03322	1.55010	0.73326	40.9137
11	436.31	210.264	356.098	1.03650	1.54970	0.73510	39.7352
12	449.62	211.207	356.509	1.03978	1.54931	0.73695	38.5975
13	463.23	212.152	356.918	1.04305	1.54893	0.73882	37.4991
14	477.14	213.099	357.325	1.04632	1.54856	0.74071	36.4382
15	491.37	214.048	357.730	1.04958	1.54819	0.74262	35.4133
16	505.91	214.998	358.134	1.05284	1.54783	0.74455	34.4230
17	520.76	215.951	358.535	1.05609	1.54748	0.74649	33.4658
18	535.94	216.906	358.935	1.05933	1.54713	0.74846	32.5405
19	551.45	217.863	359.333	1.06258	1.54679	0.75045	31.6457
20	567.29	218.821	359.729	1.06581	1.54645	0.75246	30.7802
21	583.47	219.783	360.122	1.06904	1.54612	0.75449	29.9429
22	599.98	220.746	360.514	1.07227	1.54579	0.75655	29.1327
23	616.84	221.712	360.904	1.07549	1.54547	0.75863	28.3485
24	634.05	222.680	361.291	1.07871	1.54515	0.76073	27.5894
25	651.62	223.650	361.676	1.08193	1.54484	0.76286	26.8542
26	669.54	224.623	362.059	1.08514	1.54453	0.76501	26.1442
27	687.82	225.598	362.439	1.08835	1.54423	0.76718	25.4524
28	706.47	226.576	362.817	1.09155	1.54393	0.76938	24.7840
29	725.50	227.557	363.193	1.09475	1.54363	0.77161	24.1362
30	744.90	228.540	363.566	1.09795	1.54334	0.77386	23.5082
31	764.68	229.526	363.937	1.10115	1.54305	0.77614	22.8993
32	784.85	230.515	364.305	1.10434	1.54276	0.77845	22.3088
33	805.41	231.506	364.670	1.10753	1.54247	0.78079	21.7359
34	826.36	232.501	365.033	1.11072	1.54219	0.78316	21.1802
35	847.72	233.498	365.392	1.11391	1.54191	0.78556	20.6408
36	869.48	234.499	365.749	1.11710	1.54163	0.78799	20.1173
37	891.64	235.503	366.103	1.12028	1.54135	0.79045	19.6091
38	914.23	236.510	366.454	1.12347	1.54107	0.79294	19.1156
39	937.23	237.521	366.802	1.12665	1.54079	0.79546	18.6362

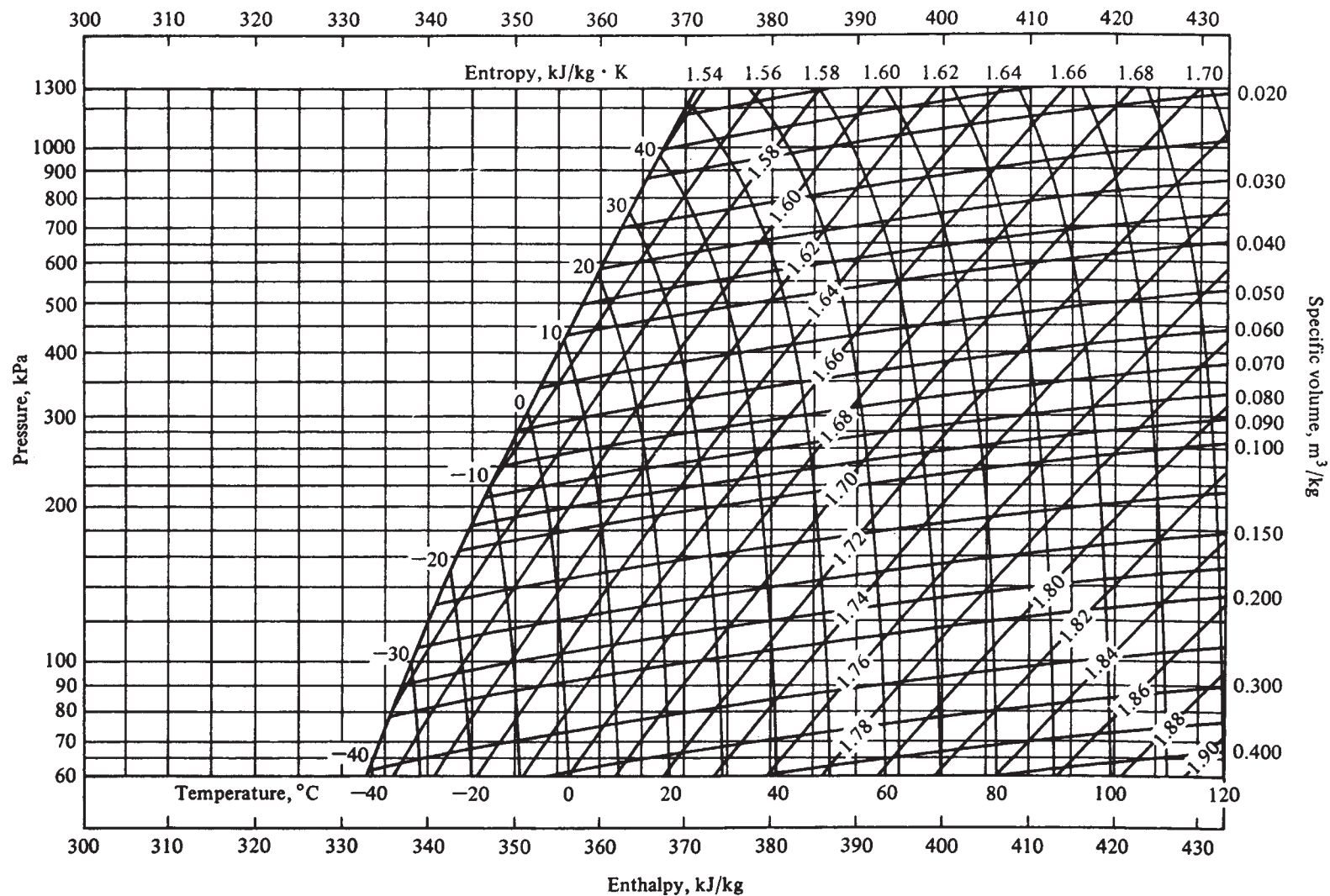
(Continued)

Table A.6.1 (Continued)

Temp (°C)	Absolute pressure (kPa)	Enthalpy (kJ/kg)		Entropy (kJ/kg K)		Specific volume (L/kg)	
		h_f	h_g	s_f	s_g	v_f	v_g
40	960.65	238.535	367.146	1.12984	1.54051	0.79802	18.1706
41	984.51	239.552	267.487	1.13302	1.54024	0.80062	17.7182
42	1008.8	240.574	367.825	1.13620	1.53996	0.80325	17.2785
43	1033.5	241.598	368.160	1.13938	1.53968	0.80592	16.8511
44	1058.7	242.627	368.491	1.14257	1.53941	0.80863	16.4356
45	1084.3	243.659	368.818	1.14575	1.53913	0.81137	16.0316
46	1110.4	244.696	369.141	1.14894	1.53885	0.81416	15.6386
47	1136.9	245.736	369.461	1.15213	1.53856	0.81698	15.2563
48	1163.9	246.781	369.777	1.15532	1.53828	0.81985	14.8844
49	1191.4	247.830	370.088	1.15851	1.53799	0.82277	14.5224
50	1219.3	248.884	370.396	1.16170	1.53770	0.82573	14.1701
52	1276.6	251.004	370.997	1.16810	1.53712	0.83179	13.4931
54	1335.9	253.144	371.581	1.17451	1.53651	0.83804	12.8509
56	1397.2	255.304	372.145	1.18093	1.53589	0.84451	12.2412
58	1460.5	257.486	372.688	1.18738	1.53524	0.85121	11.6620
60	1525.9	259.690	373.210	1.19384	1.53457	0.85814	11.1113
62	1593.5	261.918	373.707	1.20034	1.53387	0.86534	10.5872
64	1663.2	264.172	374.810	1.20686	1.53313	0.87282	10.0881
66	1735.1	266.452	374.625	1.21342	1.53235	0.88059	9.61234
68	1809.3	268.762	375.042	1.22001	1.53153	0.88870	9.15844
70	1885.8	271.102	375.427	1.22665	1.53066	0.89716	8.72502
75	2087.5	277.100	376.234	1.24347	1.52821	0.92009	7.72258
80	2304.6	283.341	376.777	1.26069	1.52526	0.94612	6.82143
85	2538.0	289.879	376.985	1.27845	1.52164	0.97621	6.00494
90	2788.5	296.788	376.748	1.29691	1.51708	1.01190	5.25759
95	3056.9	304.181	375.887	1.31637	1.51113	1.05581	4.56341
100	3344.1	312.261	374.070	1.33732	1.50296	1.11311	3.90280

Source: Stoecker (1988).

^aSubscripts: f = liquid, g = gas.



■ **Figure A.6.2** Pressure–enthalpy diagram of superheated R-12 vapor. (Courtesy, Technical University of Denmark.)

Table A.6.2 Properties of Saturated Liquid and Vapor R-717 (Ammonia)^a

Temp (°C)	Absolute pressure (kPa)	Enthalpy (kJ/kg)		Entropy (kJ/[kg K])		Specific volume (L/kg)	
		h_f	h_g	s_f	s_g	v_f	v_g
−60	21.99	−69.5330	1373.19	−0.10909	6.6592	1.4010	4685.08
−55	30.29	−47.5062	1382.01	−0.00717	6.5454	1.4126	3474.22
−50	41.03	−25.4342	1390.64	−0.09264	6.4382	1.4245	2616.51
−45	54.74	−3.3020	1399.07	−0.19049	6.3369	1.4367	1998.91
−40	72.01	18.9024	1407.26	0.28651	6.2410	1.4493	1547.36
−35	93.49	41.1883	1415.20	0.38082	6.1501	1.4623	1212.49
−30	119.90	63.5629	1422.86	0.47351	6.0636	1.4757	960.867
−28	132.02	72.5387	1425.84	0.51015	6.0302	1.4811	878.100
−26	145.11	81.5300	1428.76	0.54655	5.9974	1.4867	803.761
−24	159.22	90.5370	1431.64	0.58272	5.9652	1.4923	736.868
−22	174.41	99.5600	1434.46	0.61865	5.9336	1.4980	676.570
−20	190.74	108.599	1437.23	0.65436	5.9025	1.5037	622.122
−18	208.26	117.656	1439.94	0.68984	5.8720	1.5096	572.875
−16	227.04	126.729	1442.60	0.72511	5.8420	1.5155	528.257
−14	247.14	135.820	1445.20	0.76016	5.8125	1.5215	487.769
−12	268.63	144.929	1447.74	0.79501	5.7835	1.5276	450.971
−10	291.57	154.056	1450.22	0.82965	5.7550	1.5338	417.477
−9	303.60	158.628	1451.44	0.84690	5.7409	1.5369	401.860
−8	316.02	163.204	1452.64	0.86410	5.7269	1.5400	386.944
−7	328.84	167.785	1453.83	0.88125	5.7131	1.5432	372.692
−6	342.07	172.371	1455.00	0.89835	5.6993	1.5464	359.071
−5	355.71	176.962	1456.15	0.91541	5.6856	1.5496	346.046
−4	369.77	181.559	1457.29	0.93242	5.6721	1.5528	333.589
−3	384.26	186.161	1458.42	0.94938	5.6586	1.5561	321.670
−2	399.20	190.768	1459.53	0.96630	5.6453	1.5594	310.263
−1	414.58	195.381	1460.62	0.98317	5.6320	1.5627	299.340
0	430.43	200.000	1461.70	1.00000	5.6189	1.5660	288.880
1	446.74	204.625	1462.76	1.01679	5.6058	1.5694	278.858
2	463.53	209.256	1463.80	1.03354	5.5929	1.5727	269.253
3	480.81	213.892	1464.83	1.05024	5.5800	1.5762	260.046
4	498.59	218.535	1465.84	1.06691	5.5672	1.5796	251.216
5	516.87	223.185	1466.84	1.08353	5.5545	1.5831	242.745
6	535.67	227.841	1467.82	1.10012	5.5419	1.5866	234.618

(Continued)

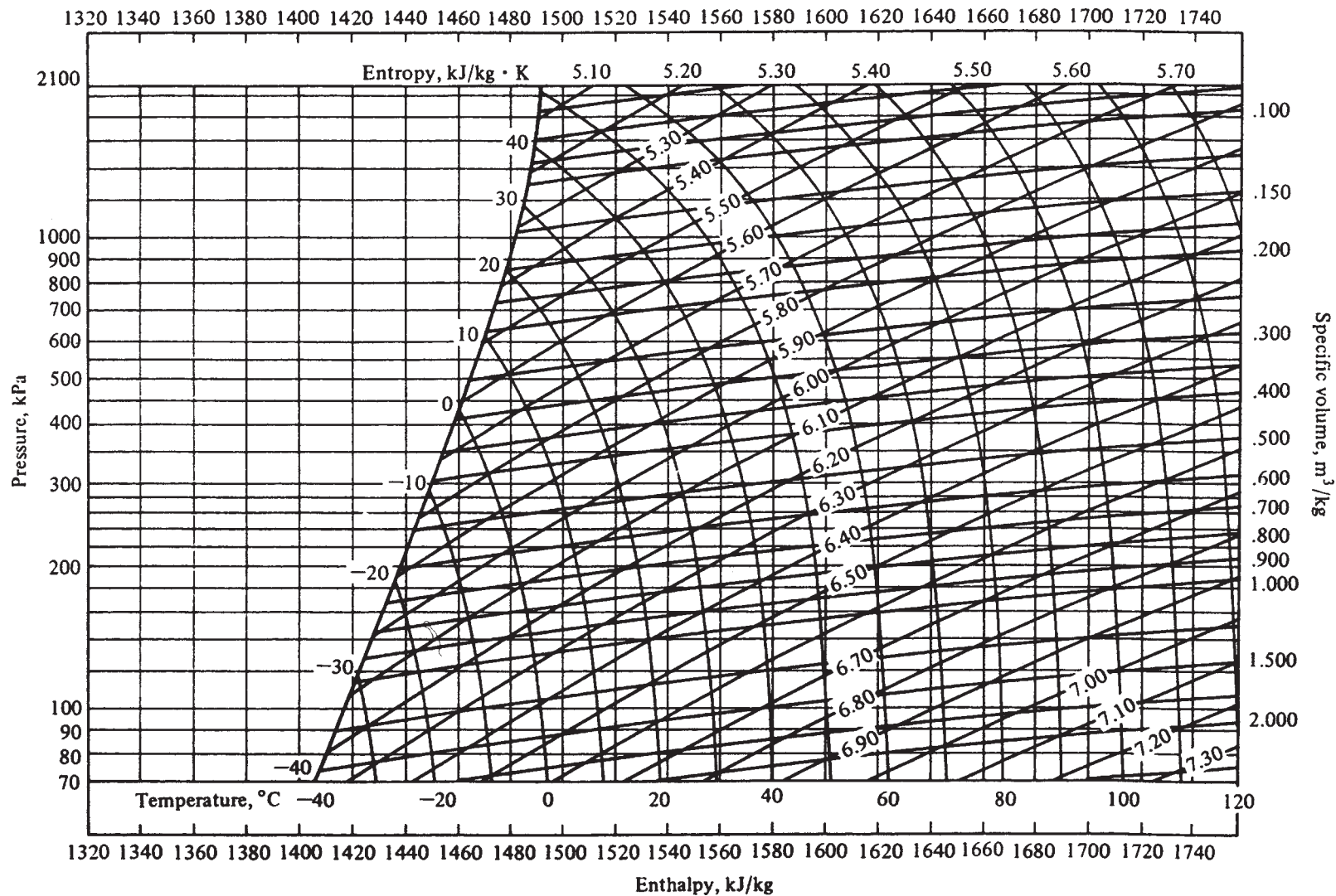
Table A.6.2 (Continued)

Temp (°C)	Absolute pressure (kPa)	Enthalpy (kJ/kg)		Entropy (kJ/[kg K])		Specific volume (L/kg)	
		h_f	h_g	s_f	s_g	v_f	v_g
7	555.00	232.503	1468.78	1.11667	5.5294	1.5901	226.817
8	574.87	237.172	1469.72	1.13317	5.5170	1.5936	219.326
9	595.28	241.848	1470.64	1.14964	5.5046	1.5972	212.132
10	616.25	246.531	1471.57	1.16607	5.4924	1.6008	205.221
11	637.78	251.221	1472.46	1.18246	5.4802	1.6045	198.580
12	659.89	255.918	1473.34	1.19882	5.4681	1.6081	192.196
13	682.59	260.622	1474.20	1.21515	5.4561	1.6118	186.058
14	705.88	265.334	1475.05	1.23144	5.4441	1.6156	180.154
15	729.29	270.053	1475.88	1.24769	5.4322	1.6193	174.475
16	754.31	274.779	1476.69	1.26391	5.4204	1.6231	169.009
17	779.46	279.513	1477.48	1.28010	5.4087	1.6269	163.748
18	805.25	284.255	1478.25	1.29626	5.3971	1.6308	158.683
19	831.69	289.005	1479.01	1.31238	5.3855	1.6347	153.804
20	858.79	293.762	1479.75	1.32847	5.3740	1.6386	149.106
21	886.57	298.527	1480.48	1.34452	5.3626	1.6426	144.578
22	915.03	303.300	1481.18	1.36055	5.3512	1.6466	140.214
23	944.18	308.081	1481.87	1.37654	5.3399	1.6507	136.006
24	974.03	312.870	1482.53	1.39250	5.3286	1.6547	131.950
25	1004.6	316.667	1483.18	1.40843	5.3175	1.6588	128.037
26	1035.9	322.471	1483.81	1.42433	4.3063	1.6630	124.261
27	1068.0	327.284	1484.42	1.44020	5.2953	1.6672	120.619
28	1100.7	332.104	1485.01	1.45064	5.2843	1.6714	117.103
29	1134.3	336.933	1485.59	1.47185	5.2733	1.6757	113.708
30	1168.6	341.769	1486.14	1.48762	5.2624	1.6800	110.430
31	1203.7	346.614	1486.67	1.50337	5.2516	1.6844	107.263
32	1239.6	351.466	1487.18	1.51908	5.2408	1.6888	104.205
33	1276.3	356.326	1487.66	1.53477	5.2300	1.6932	101.248
34	1313.9	361.195	1488.13	1.55042	5.2193	1.6977	98.3913
35	1352.2	366.072	1488.57	1.56605	5.2086	1.7023	95.6290
36	1391.5	370.957	1488.99	1.58165	5.1980	1.7069	92.9579
37	1431.5	375.851	1489.39	1.59722	5.1874	1.7115	90.3743
38	1472.4	380.754	1489.76	1.61276	5.1768	1.7162	87.8748
39	1514.3	385.666	1490.10	1.62828	5.1663	1.7209	85.4561

(Continued)

Table A.6.2 (Continued)

Temp (°C)	Absolute pressure (kPa)	Enthalpy (kJ/kg)		Entropy (kJ/[kg K])		Specific volume (L/kg)	
		h_f	h_g	s_f	s_g	v_f	v_g
40	1557.0	390.587	1490.42	1.64377	5.1558	1.7257	83.1150
41	1600.6	395.519	1490.71	1.65924	5.1453	1.7305	80.8484
42	1645.1	400.462	1490.98	1.67470	5.1349	1.7354	78.6536
43	1690.6	405.416	1491.21	1.69013	5.1244	1.7404	76.5276
44	1737.0	410.382	1491.41	1.70554	5.1140	1.7454	74.4678
45	1784.3	415.362	1491.58	1.72095	5.1036	1.7504	72.4716
46	1832.6	420.358	1491.72	1.73635	5.0932	1.7555	70.5365
47	1881.9	425.369	1491.83	1.75174	5.0827	1.7607	68.6602
48	1932.2	430.399	1491.88	1.76714	5.0723	1.7659	66.8403
49	1983.5	435.450	1491.91	1.78255	5.0618	1.7712	65.0746
50	2035.9	440.523	1491.89	1.79798	5.0514	1.7766	63.3608
51	2089.2	445.623	1491.83	1.81343	5.0409	1.7820	61.6971
52	2143.6	450.751	1491.73	1.82891	5.0303	1.7875	60.0813
53	2199.1	455.913	1491.58	1.84445	5.0198	1.7931	58.5114
54	2255.6	461.112	1491.38	1.86004	5.0092	1.7987	56.9855
55	2313.2	466.353	1491.12	1.87571	4.9985	1.8044	55.5019
Source: Stoecker (1988). ^a Subscripts: f = liquid, g = gas.							



■ **Figure A.6.3** Pressure–enthalpy diagram of superheated R-717 (ammonia) vapor. (Courtesy, Technical University of Denmark.)

Table A.6.3 Properties of Saturated Liquid and Vapor R-134a

Temp °C	Absolute pressure bar	Density		Enthalpy		Entropy	
		kg/m ³ Liquid	kg/m ³ Vapor	kJ/kg Liquid	kJ/kg Vapor	kJ/ (kg K) Liquid	kJ/ (kg K) Vapor
−60	0.15935	1472.0	0.9291	24.109	261.491	0.68772	1.8014
−55	0.21856	1458.5	1.2489	30.191	264.633	0.7159	1.79059
−50	0.29477	1444.9	1.6526	36.302	267.779	0.74358	1.7809
−45	0.39139	1431.0	2.1552	42.448	270.926	0.77078	1.77222
−40	0.51225	1417.0	2.7733	48.631	274.068	0.79756	1.76448
−35	0.66153	1402.7	3.5252	54.857	277.203	0.82393	1.75757
−30	0.84379	1388.2	4.4307	61.130	280.324	0.84995	1.75142
−28	0.92701	1382.3	4.8406	63.653	281.569	0.86026	1.74916
−26	1.01662	1376.4	5.2800	66.185	282.81	0.87051	1.74701
−24	1.11295	1370.5	5.7504	68.725	284.048	0.88072	1.74495
−22	1.21636	1364.4	6.2533	71.274	285.282	0.89088	1.743
−20	1.32719	1358.4	6.7903	73.833	286.513	0.901	1.74113
−18	1.44582	1352.3	7.3630	76.401	287.739	0.91107	1.73936
−16	1.57260	1346.2	7.9733	78.980	288.961	0.9211	1.73767
−14	1.70793	1340.0	8.6228	81.568	290.179	0.93109	1.73607
−12	1.85218	1333.7	9.3135	84.167	291.391	0.94104	1.73454
−10	2.00575	1327.4	10.047	86.777	292.598	0.95095	1.73309
−9	2.08615	1324.3	10.431	88.086	293.199	0.95589	1.73239
−8	2.16904	1321.1	10.826	89.398	293.798	0.96082	1.73171
−7	2.25446	1317.9	11.233	90.713	294.396	0.96575	1.73105
−6	2.34246	1314.7	11.652	92.031	294.993	0.97067	1.7304
−5	2.43310	1311.5	12.083	93.351	295.588	0.97557	1.72977
−4	2.52643	1308.2	12.526	94.675	296.181	0.98047	1.72915
−3	2.62250	1305.0	12.983	96.002	296.772	0.98537	1.72855
−2	2.72136	1301.7	13.453	97.331	297.362	0.99025	1.72796
−1	2.82307	1298.4	13.936	98.664	297.95	0.99513	1.72739
0	2.92769	1295.1	14.433	100.00	298.536	1	1.72684
1	3.03526	1291.8	14.944	101.339	299.12	1.00486	1.72629
2	3.14584	1288.5	15.469	102.681	299.701	1.00972	1.72577
3	3.25950	1285.1	16.009	104.027	300.281	1.01457	1.72525
4	3.37627	1281.8	16.564	105.376	300.859	1.01941	1.72474
5	3.49623	1278.4	17.134	106.728	301.434	1.02425	1.72425
6	3.61942	1275.0	17.719	108.083	302.008	1.02908	1.72377

(Continued)

Table A.6.3 (Continued)

Temp °C	Absolute pressure bar	Density		Enthalpy		Entropy	
		kg/m ³ Liquid	kg/m ³ Vapor	kJ/kg Liquid	kJ/kg Vapor	kJ/(kg K) Liquid	kJ/(kg K) Vapor
7	3.74591	1271.6	18.321	109.442	302.578	1.0339	1.7233
8	3.87575	1268.2	18.939	110.805	303.147	1.03872	1.72285
9	4.00900	1264.7	19.574	112.171	303.713	1.04353	1.7224
10	4.14571	1261.2	20.226	113.540	304.276	1.04834	1.72196
11	4.28595	1257.8	20.895	114.913	304.837	1.05314	1.72153
12	4.42978	1254.3	21.583	116.290	305.396	1.05793	1.72112
13	4.57725	1250.7	22.288	117.670	305.951	1.06273	1.72071
14	4.72842	1247.2	23.012	119.054	306.504	1.06751	1.72031
15	4.88336	1243.6	23.755	120.441	307.054	1.07229	1.71991
16	5.04212	1240.0	24.518	121.833	307.6	1.07707	1.71953
17	5.20477	1236.4	25.301	123.228	308.144	1.08184	1.71915
18	5.37137	1232.8	26.104	124.627	308.685	1.08661	1.71878
19	5.54197	1229.2	26.928	126.030	309.222	1.09137	1.71842
20	5.71665	1225.5	27.773	127.437	309.756	1.09613	1.71806
21	5.89546	1221.8	28.640	128.848	310.287	1.10089	1.71771
22	6.07846	1218.1	29.529	130.263	310.814	1.10564	1.71736
23	6.26573	1214.3	30.422	131.683	311.337	1.11039	1.71702
24	6.45732	1210.6	31.378	133.106	311.857	1.11513	1.71668
25	6.65330	1206.8	32.337	134.533	312.373	1.11987	1.71635
26	6.85374	1203.0	33.322	135.965	312.885	1.12461	1.71602
27	7.05869	1199.2	34.331	137.401	313.393	1.12935	1.71569
28	7.26823	1195.3	35.367	138.842	313.897	1.13408	1.71537
29	7.48241	1191.4	36.428	140.287	314.397	1.13881	1.71505
30	7.70132	1187.5	37.517	141.736	314.892	1.14354	1.71473
31	7.92501	1183.5	38.634	143.190	315.383	1.14826	1.71441
32	8.15355	1179.6	39.779	144.649	315.869	1.15299	1.71409
33	8.38701	1175.6	40.953	146.112	316.351	1.15771	1.71377
34	8.62545	1171.5	42.157	147.580	316.827	1.16243	1.71346
35	8.86896	1167.5	43.391	149.053	317.299	1.16715	1.71314
36	9.11759	1163.4	44.658	150.530	317.765	1.17187	1.71282
37	9.37142	1159.2	45.956	152.013	318.226	1.17659	1.7125
38	9.63052	1155.1	47.288	153.500	318.681	1.1813	1.71217
39	9.89496	1150.9	48.654	154.993	319.131	1.18602	1.71185

(Continued)

Table A.6.3 (Continued)

Temp °C	Absolute pressure bar	Density		Enthalpy		Entropy	
		kg/m ³ Liquid	kg/m ³ Vapor	kJ/kg Liquid	kJ/kg Vapor	kJ/ (kg K) Liquid	kJ/ (kg K) Vapor
40	10.1648	1146.7	50.055	156.491	319.575	1.19073	1.71152
41	10.4401	1142.4	51.492	157.994	320.013	1.19545	1.71119
42	10.7210	1138.1	52.967	159.503	320.445	1.20017	1.71085
43	11.0076	1133.7	54.479	161.017	320.87	1.20488	1.71051
44	11.2998	1129.4	56.031	162.537	321.289	1.2096	1.71016
45	11.5978	1124.9	57.623	164.062	321.701	1.21432	1.70981
46	11.9017	1120.5	59.256	165.593	322.106	1.21904	1.70945
47	12.2115	1116.0	60.933	167.130	322.504	1.22376	1.70908
48	12.5273	1111.4	62.645	168.673	322.894	1.22848	1.7087
49	12.8492	1106.8	64.421	170.222	323.277	1.23321	1.70832
50	13.1773	1102.2	66.234	171.778	323.652	1.23794	1.70792
52	13.8523	1092.8	70.009	174.908	324.376	1.24741	1.7071
54	14.5529	1083.1	73.992	178.065	325.066	1.25689	1.70623
56	15.2799	1073.3	78.198	181.251	325.717	1.26639	1.7053
58	16.0339	1063.2	82.643	184.467	326.329	1.27592	1.70431
60	16.8156	1052.9	87.346	187.715	326.896	1.28548	1.70325
62	17.6258	1042.2	92.328	190.996	327.417	1.29507	1.70211
64	18.4653	1031.3	97.611	194.314	327.886	1.30469	1.70087
66	19.3347	1020.1	103.223	197.671	328.3	1.31437	1.69954
68	20.2349	1008.5	109.196	201.070	328.654	1.3241	1.69808
70	21.1668	996.49	115.564	204.515	328.941	1.3339	1.6965
75	23.6409	964.48	133.511	213.359	329.321	1.35876	1.69184
80	26.3336	928.78	155.130	222.616	329.095	1.38434	1.68585
85	29.2625	887.82	181.955	232.448	328.023	1.41108	1.67794
90	32.4489	838.51	216.936	243.168	325.655	1.43978	1.66692
95	35.9210	773.06	267.322	255.551	320.915	1.47246	1.65001
100	39.7254	649.71	367.064	273.641	309.037	1.5198	1.61466

Source: ICI Chemicals and Polymers Ltd. (KLEA 134a); Reference enthalpy 100 kJ/kg at 0°C.

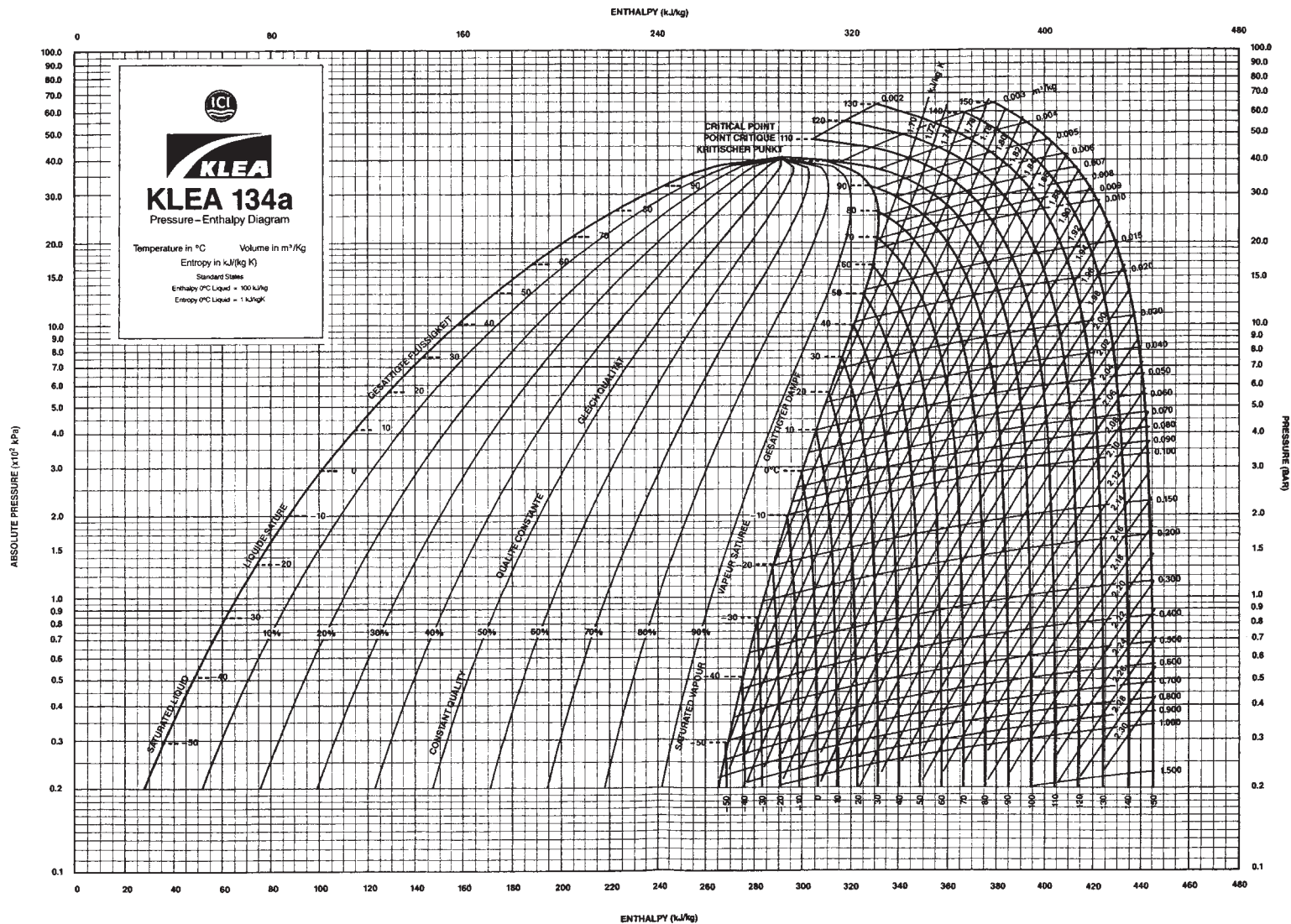
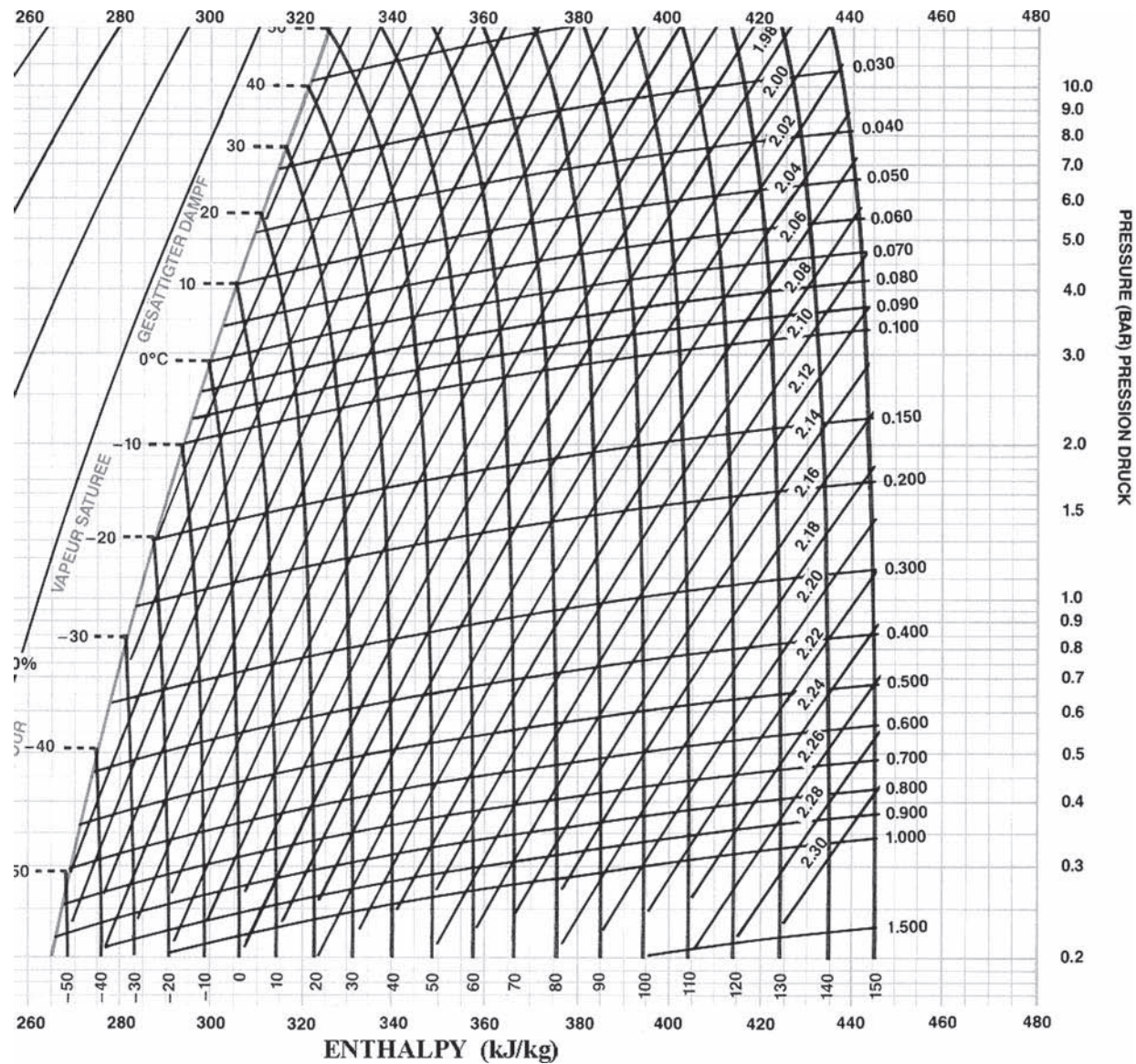


Figure A.6.4 Pressure–enthalpy diagram of R-134a. (Alternate P-H diagram with a datum of 200 kJ/kg AT 0°C is available from DuPont Fluorochemicals, Wilmington, Delaware, USA.)

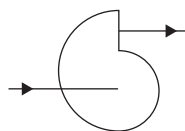


■ Figure A.6.5 Pressure–enthalpy diagram of R-134a (expanded scale). (Courtesy, ICI Co.)

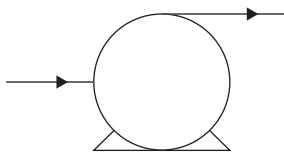
A.7 SYMBOLS FOR USE IN DRAWING FOOD ENGINEERING PROCESS EQUIPMENT



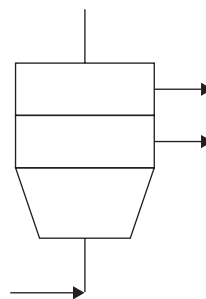
Belt conveyor



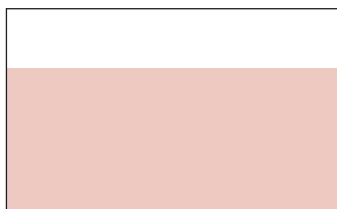
Blower



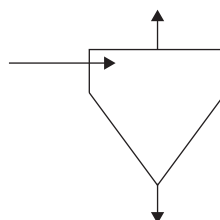
Centrifugal pump



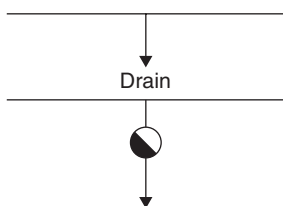
Centrifuge



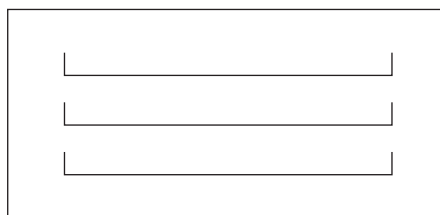
Closed tank



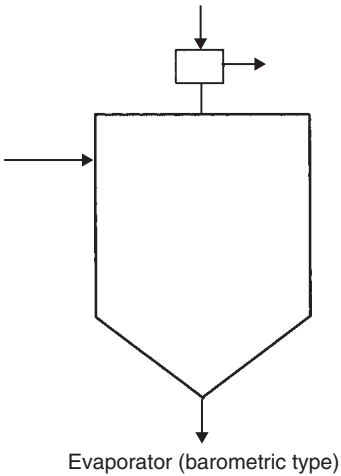
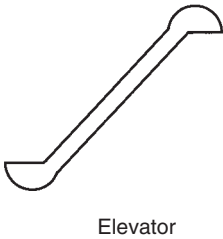
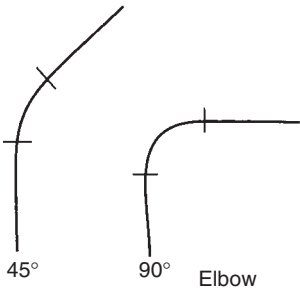
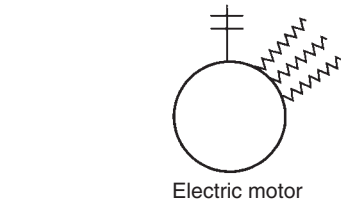
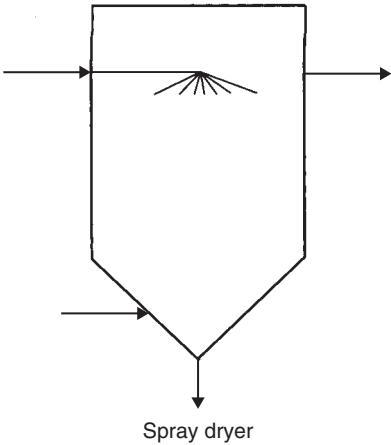
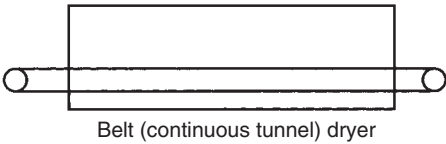
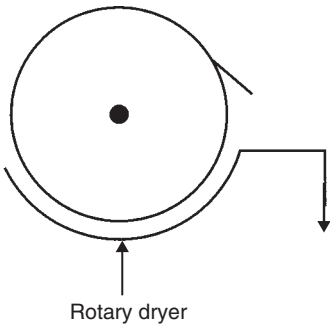
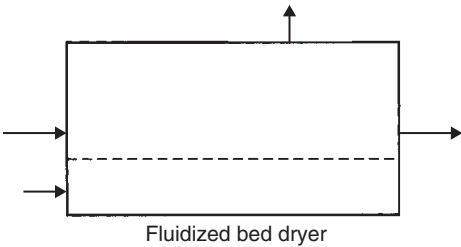
Cyclone

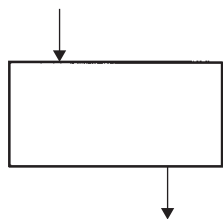


Trap (e.g., condensate release)

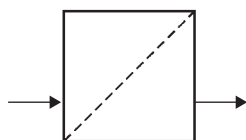


Batch dryer

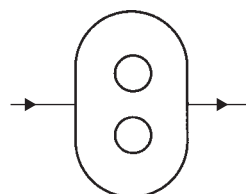




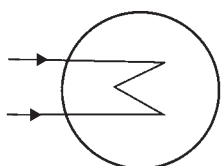
Feeder



Filter



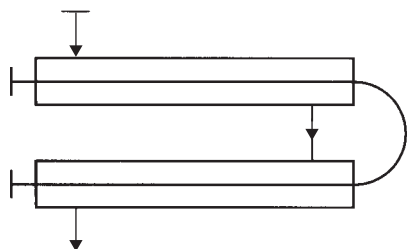
Gear pump



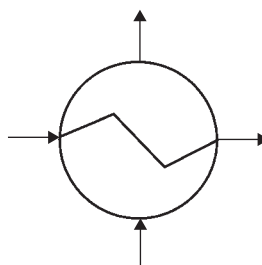
Basic heat exchanger



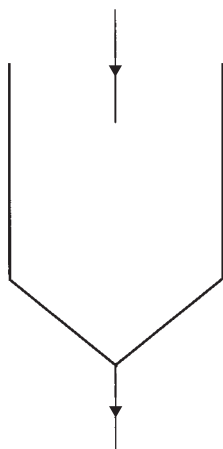
Plate heat exchanger



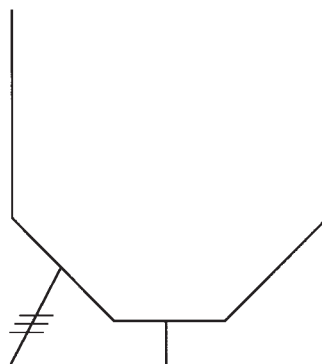
Double pipe type heat exchanger



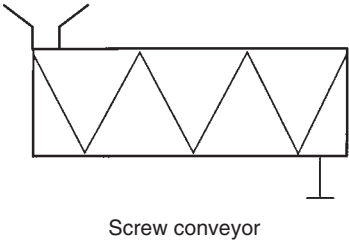
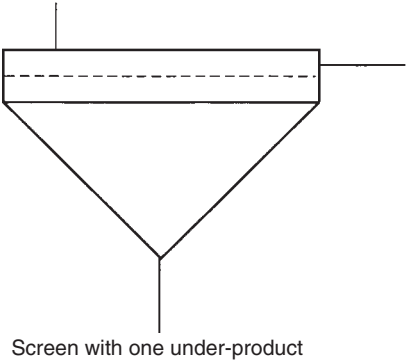
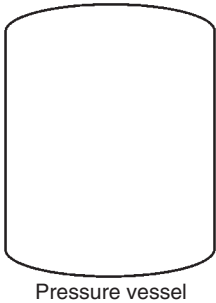
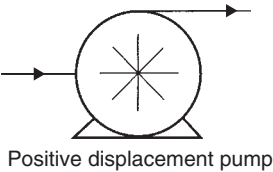
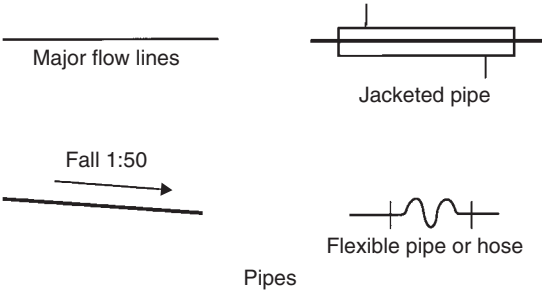
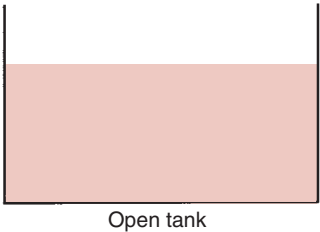
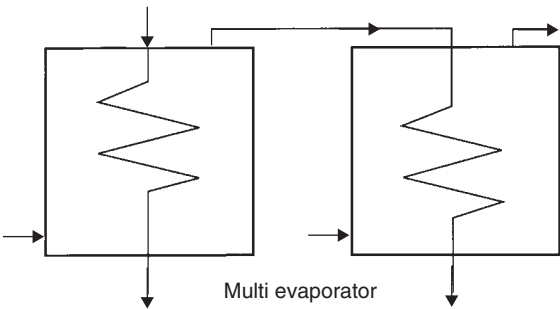
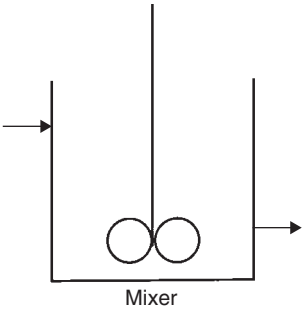
Shell and tube heat exchanger

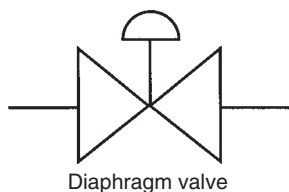
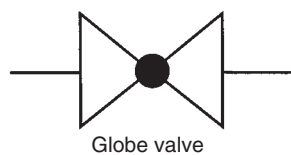
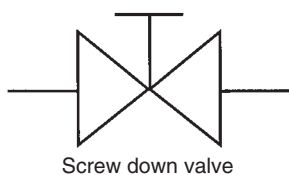
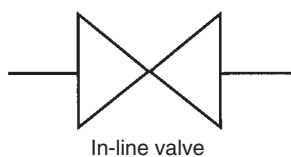
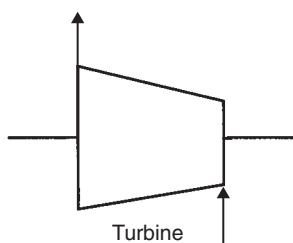
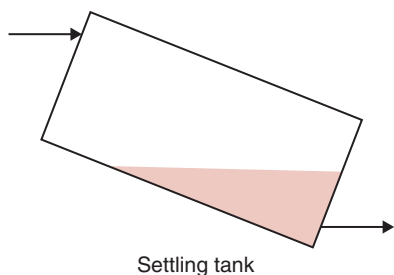


Hopper

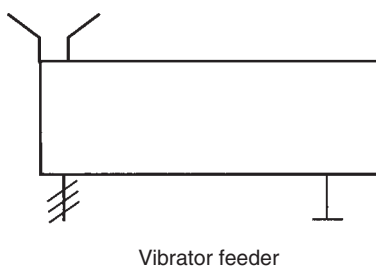
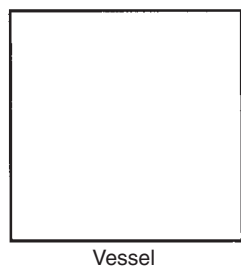


Hopper with vibrator

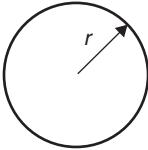
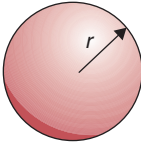
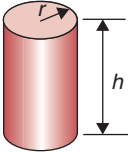
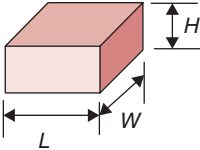


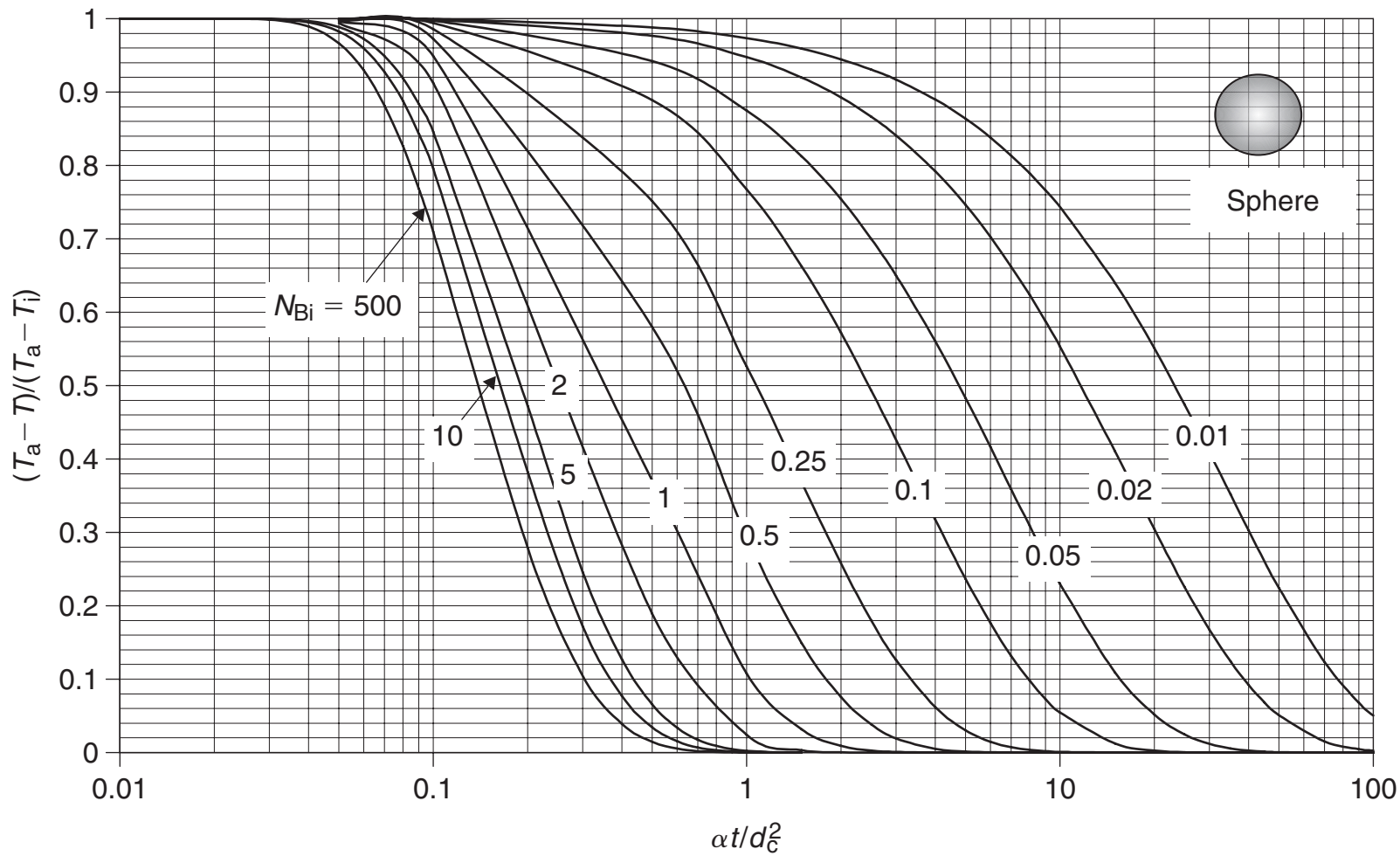


Valves

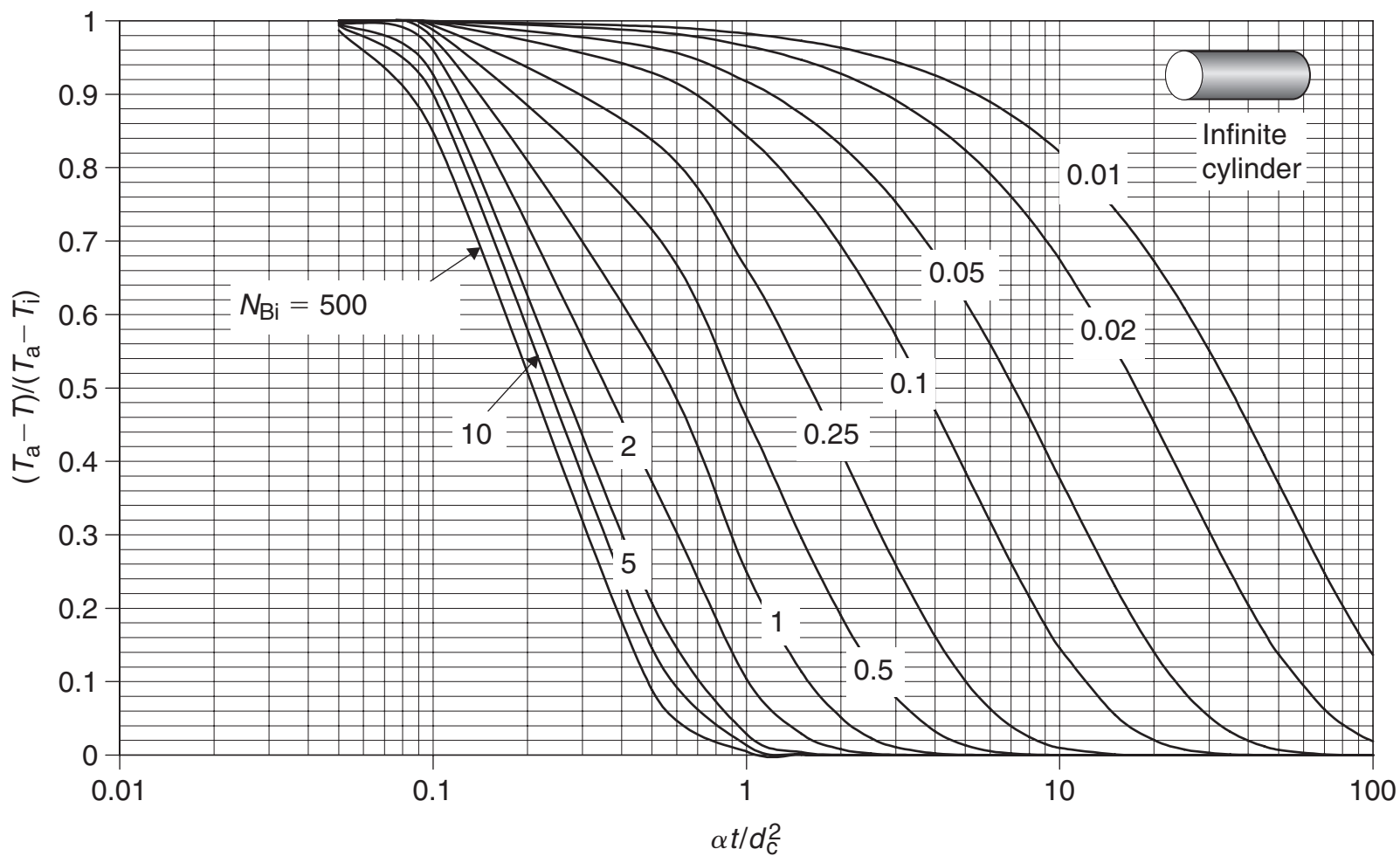


A.8 MISCELLANEOUS

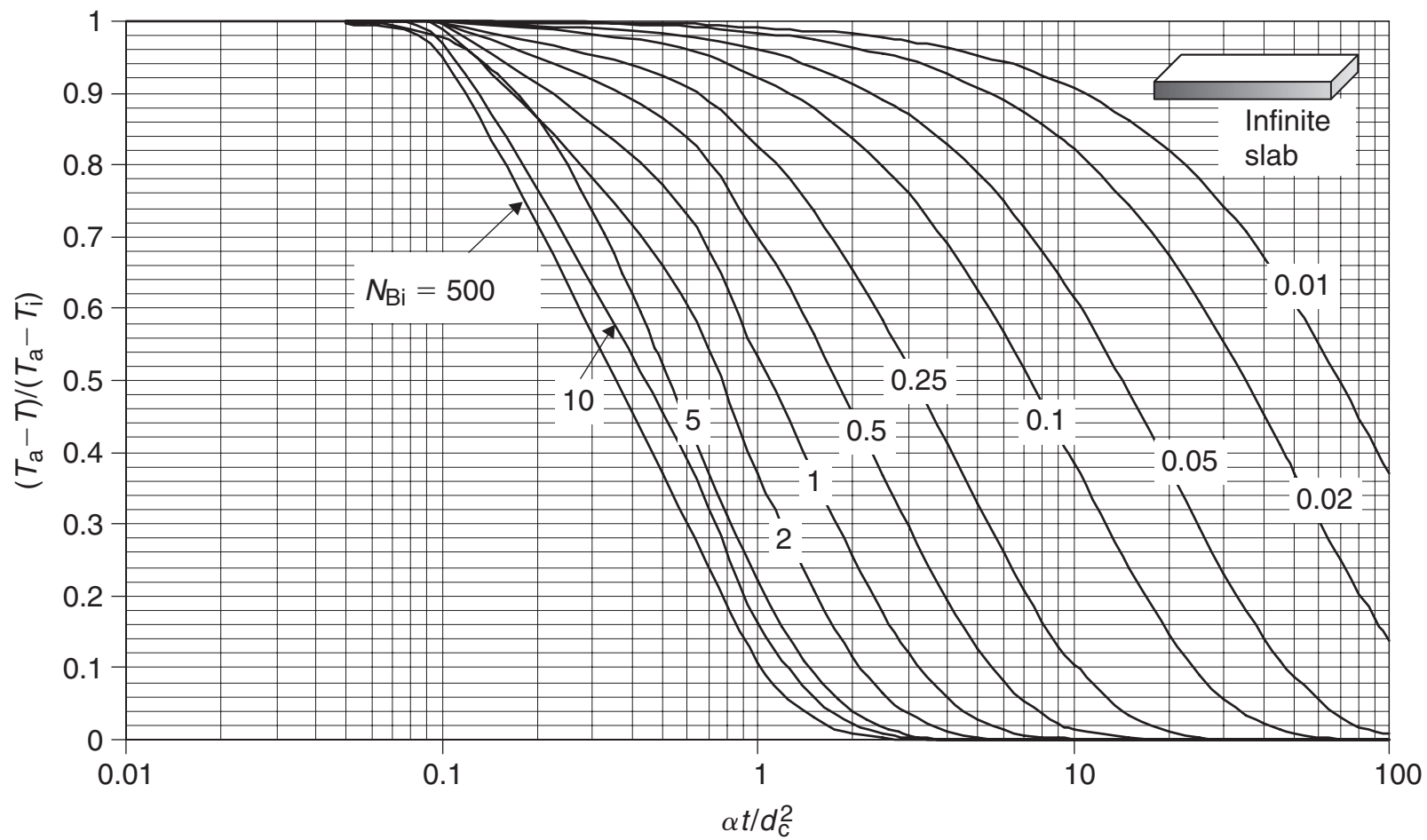
Table A.8.1 Numerical Data and Area/Volume of Objects		
Numerical data		
$\pi = 3.142$ $e = 2.718$ $\log_e 2 = 0.6931$ $\log_e 10 = 2.303$ $\log_{10} e = 0.4343$		
Areas and Volumes		
Object	Area/surface area	Volume
Circle, radius r 	πr^2	– (Circumference = $2\pi r$)
Sphere, radius r 	$4\pi r^2$	$\frac{4}{3}\pi r^3$
Cylinder, radius r , height h 	$2\pi r^2 + 2\pi rh$	$\pi r^2 h$
Brick 	$2(L \times W + W \times H + L \times H)$	$L \times W \times H$



■ **Figure A.8.1** Temperature at the geometric center of a sphere (expanded scale).



■ **Figure A.8.2** Temperature at the axis of an infinitely long cylinder (expanded scale).



■ **Figure A.8.3** Temperature at the midplane of an infinite slab (expanded scale).

A.9 DIMENSIONAL ANALYSIS

In engineering analysis, it is not uncommon to encounter problems that cannot be solved by using standard analytical procedures. For example, in the case of fluid flow, the highly complex nature of fluid flow in the immediate vicinity of a solid surface prevents us from developing a straightforward analytical solution. Similarly, heat transfer from a solid surface into a fluid is complicated, and analytical procedures to determine the convective heat transfer coefficient are possible only for much simplified situations. To solve these types of problems, we resort to experimental studies.

An experimental approach requires that we first clearly define the given physical system. Experiments are then conducted to investigate the contribution of various factors that may influence a parameter of interest. It is quite possible that, once all the important factors are identified, the list of such factors may become quite large. The experimental procedure then becomes laborious. For example, consider a scenario where seven variables are identified to influence the convective heat transfer coefficient: fluid velocity, viscosity, density, thermal conductivity, specific heat, characteristic dimension, and axial distance. If we design an experiment that involves conducting trials holding all but one variable constant, and the trials are repeated at four levels of each variable, the number of trials required for this experimental plan will be 4^7 or 16,384 experiments! This will be a daunting task. To substantially reduce the number of experiments, and yet obtain all the necessary information, we use dimensional analysis. As we will see later in this section, with dimensional analysis, the same amount of information is obtained from a significantly reduced number of experiments, namely 64.

A.9.1 Buckingham π Theorem

A mathematically rigorous procedure used in dimensional analysis is the Buckingham π theorem. According to this theorem, the number of independent dimensional groups π_i , associated with a physical phenomenon, are equal to the total number of significant variables, A , minus the number of fundamental dimensions, J , required to define the dimensions of all variables. The relationship among various dimensionless groups is written as:

$$\pi_1 = \text{functions}(\pi_2, \pi_3 \dots \pi_N) \quad (\text{A.91})$$

Table A.9.1 Dimensions of Selected Experimental Variables

Factors	Symbol	Units (S.I.)	Dimensions
Convective heat transfer coefficient	h	$\text{Js}^{-1}\text{m}^{-2}\text{K}^{-1}$ $\text{kg s}^{-3}\text{K}^{-1}$	$[M/(t^3T)]$
Pipe diameter	D	m	$[L]$
Thermal conductivity	k	$\text{Js}^{-1}\text{m}^{-1}\text{K}^{-1}$ $\text{kg m s}^{-3}\text{K}^{-1}$	$[ML/(t^3T)]$
Density	ρ	kg m^{-3}	$[M/L^3]$
Viscosity	μ	$\text{kg m}^{-1}\text{s}^{-1}$	$[M/(Lt)]$
Velocity	u	m s^{-1}	$[L/t]$
Specific heat	c_p	$\text{J kg}^{-1}\text{K}^{-1}$ $\text{m}^2 \text{s}^{-2}\text{K}^{-1}$	$[L^2/(t^2T)]$
Entrance length	X	m	$[L]$

Let us use dimensional analysis to develop a correlation useful for estimating the convective heat transfer coefficient for a liquid flowing in a pipe. Assume that the liquid flow is turbulent. From previous knowledge of this system, we can list seven variables that are important in terms of their influence on the convective heat transfer coefficient.

From Table A.9.1, we note that there are eight variables, namely h , D , k , ρ , μ , u , c_p , and X . And, there are four fundamental dimensions, mass $[M]$, length $[L]$, temperature $[T]$, and time $[t]$. According to the Buckingham π theorem, $A = 8$ and $J = 4$, therefore,

$$\begin{aligned} N &= A - J \\ N &= 8 - 4 = 4 \end{aligned} \quad (\text{A.9.2})$$

Thus, there are four dimensionless variables. We will call them π_1 , π_2 , π_3 , and π_4 .

Next, we will select groups of variables in such a way that in each case the selected group will contain all four fundamental dimensions. Variables D , k , ρ , μ are selected to be common for each group, and the remaining variables h , u , c_p , and X will be added as the last variable in each case. The dimensionless groups are selected as follows:

$$\pi_1 = D^a k^b \rho^c \mu^d h^e \quad (\text{A.9.3})$$

$$\pi_2 = D^a k^b \rho^c \mu^d u^e \quad (\text{A.9.4})$$

$$\pi_3 = D^a k^b \rho^c \mu^d c_p^e \quad (\text{A.9.5})$$

$$\pi_4 = D^a k^b \rho^c \mu^d X^e \quad (\text{A.9.6})$$

Next, we will substitute dimensions for each variable in Equations (A.9.3) through (A.9.6):

$$\pi_1 = [L]^a [M]^b [L]^b [t]^{-3b} [T]^{-b} [M]^c [L]^{-3c} [M]^d [L]^{-d} [t]^{-d} [M]^e [t]^{-3e} [T]^{-e} \quad (\text{A.9.7})$$

For π_1 to be dimensionless, each fundamental dimension must have a power of zero, therefore

$$\text{For dimension } L: \quad a + b - 3c - d = 0 \quad (\text{A.9.8})$$

$$\text{for } M: \quad b + c + d + e = 0 \quad (\text{A.9.9})$$

$$\text{for } t: \quad -3b - d - 3e = 0 \quad (\text{A.9.10})$$

$$\text{for } T: \quad -b - e = 0 \quad (\text{A.9.11})$$

solving the preceding equations in terms of e

$$b = -e$$

$$d = 0$$

$$c = 0$$

$$a = e$$

Using the calculated values for a , b , c , and d in Equation (A.9.3),

$$\pi_1 = (D)^e (k)^{-e} (h)^e \quad (\text{A.9.12})$$

$$\pi_1 = \frac{(h)^e (D)^e}{(k)^e} = (N_{\text{Nu}})^e \quad (\text{A.9.13})$$

where π_1 is Nusselt number, N_{Nu} .

Equation (A.9.4) written in terms of dimensions

$$\pi_2 = [L]^a [M]^b [L]^b [t]^{-3b} [T]^{-b} [M]^c [L]^{-3c} [M]^d [L]^{-d} [t]^{-d} [L]^e [t]^{-e} \quad (\text{A.9.14})$$

$$\text{for } L: \quad a + b - 3c - d + e = 0 \quad (\text{A.9.15})$$

$$\text{for } M: \quad b + c + d = 0 \quad (\text{A.9.16})$$

$$\text{for } t: \quad -3b - d - e = 0 \quad (\text{A.9.17})$$

$$\text{for } T: \quad -b = 0 \quad (\text{A.9.18})$$

Again solving the previous equations in terms of e

$$\begin{aligned}b &= 0 \\d &= -e \\c &= e \\a &= e\end{aligned}$$

$$\text{Therefore} \quad \pi_2 = (D)^e (\rho)^e (\mu)^{-e} (u)^e \quad (\text{A.9.19})$$

$$\pi_2 = \left(\frac{D\rho u}{\mu} \right)^e = (N_{\text{Re}})^e \quad (\text{A.9.20})$$

Equation (A.9.5) written in terms of its dimensions:

$$\pi_3 = [L]^a [M]^b [L]^b [t]^{-3b} [T]^{-b} [M]^c [L]^{-3c} [M]^d [L]^{-d} [t]^{-d} [L]^{2e} [t]^{-2e} [T]^{-e} \quad (\text{A.9.21})$$

To make Equation (A.9.21) dimensionless:

$$L: \quad a + b - 3c - d + 2e = 0 \quad (\text{A.9.22})$$

$$\text{for } M: \quad b + c + d = 0 \quad (\text{A.9.23})$$

$$\text{for } t: \quad -3b - d - 2e = 0 \quad (\text{A.9.24})$$

$$\text{for } T: \quad -b - e = 0 \quad (\text{A.9.25})$$

Solving the previous equations in terms of e

$$\begin{aligned}b &= -e \\d &= e \\c &= 0 \\a &= 0\end{aligned}$$

Therefore,

$$\pi_3 = (k)^{-e} (\mu)^e (c_p)^e \quad (\text{A.9.26})$$

or,

$$\pi_3 = \left(\frac{\mu c_p}{k} \right)^e = N_{\text{Pr}}^e \quad (\text{A.9.27})$$

Equation (A.9.6) written in terms of dimensions:

$$\pi_4 = [L]^a [M]^b [L]^b [t]^{-3b} [T]^{-b} [M]^c [L]^{-3c} [M]^d [L]^{-d} [t]^{-d} [L]^e \quad (\text{A.9.28})$$

To make Equation (A.9.28) dimensionless,

$$\text{for } L: a + b - 3c - d + e = 0 \quad (\text{A.9.29})$$

$$\text{for } M: b + c + d = 0 \quad (\text{A.9.30})$$

$$\text{for } t: -3b - d = 0 \quad (\text{A.9.31})$$

$$\text{for } T: -b = 0 \quad (\text{A.9.32})$$

Then solving the preceding equations in terms of e :

$$b = 0 \quad (\text{A.9.33})$$

$$d = 0 \quad (\text{A.9.34})$$

$$c = 0 \quad (\text{A.9.35})$$

$$a = -e \quad (\text{A.9.36})$$

Therefore,

$$\pi_4 = (D)^{-e}(k)^0(\rho)^0(\mu)^0(X)^e \quad (\text{A.9.37})$$

or,

$$\pi_4 = \left(\frac{X}{D} \right)^e \quad (\text{A.9.38})$$

From Equations (A.9.1), (A.9.13), (A.9.20), (A.9.27), and (A.9.38), we obtain

$$N_{\text{Nu}} = \text{function} (N_{\text{Re}}, N_{\text{Pr}}, X/D) \quad (\text{A.9.39})$$

To obtain the functional relationship as suggested in Equation (A.9.39), experiments must be conducted varying each of the three dimensionless numbers. The number of experiments required to obtain the functional correlation, assuming that each number is varied four times, while holding others constant, is $4^3 = 64$; certainly more manageable than our original estimate of 16,400 measurements.

■ BIBLIOGRAPHY

- American Society of Agricultural Engineers (1982). *Agricultural Engineers Yearbook*, ASAE, St. Joseph, Michigan.
- American Society of Heating, Refrigerating and Air-Conditioning Engineers, Inc. (1978). *Handbook and Product Directory. 1978 Applications*. ASHRAE, Atlanta, Georgia.
- Choi, Y. and Okos, M. R. (1986). Effects of temperature and composition on the thermal properties of foods. In *Food Engineering*

- and Process Applications*, Volume 1: Transport Phenomena. M. Le Maguer and P. Jelen, eds., 93–101. Elsevier Applied Science Publishers, London.
- Dickerson, R. W., Jr. (1969). Thermal properties of foods. In *The Freezing Preservation of Foods 4th ed*, D. K. Tressler, W. B. Van Arsdel, and M. J. Copley, eds., Volume. 2, 26–51. AVI Publ. Co., Westport, Connecticut.
- Heldman, D. R. and Singh, R. P. (1981). *Food Process Engineering*, 2nd ed. AVI Publ. Co., Westport, Connecticut.
- Holman, J. P. (2002). *Heat Transfer*, 9th ed. McGraw-Hill, New York.
- Keenan, J. H., Keyes, F. G., Hill, P. G., and Moore, J. G. (1969). *Steam Tables—Metric Units*. Wiley, New York.
- Raznjevic, K. (1978). *Handbook of Thermodynamic Tables and Charts*. Hemisphere Publ. Corp, Washington, D.C.
- Reidy, G.A. (1968). Thermal properties of foods and methods of their determination. M.S. Thesis, Food Science Department, Michigan State University, East Lansing.
- Singh, R. P. (1982). Thermal diffusivity in food processing. *Food Technol.* 36(2): 87–91.
- Steffe, J.F. (1983). Rheological properties of liquid foods. ASAE Paper No. 83-6512. ASAE, St. Joseph, Michigan.
- Stoecker, W. F. (1988). *Industrial Refrigeration*. Business News Publishing Company, Troy, Michigan.

This page intentionally left blank

Index

A

Absolute pressure, 23
 Accuracy, 237
 Activation energy, 418
 Active packaging
 simple active packaging, 755
 advanced active packaging, 755
 Adiabatic saturation, air, 577, 578, 578f
 Adiabatic system, 11
 Affinity laws, 135–136
 Agitated thin-film evaporator, 551–554, 552f
 Agitation, see Mixing
 Air, see also Psychrometrics
 adiabatic saturation, 577, 578, 578f
 composition, 571, 572t
 dry bulb temperature, 573
 enthalpy, 572
 physical properties at atmospheric pressure, 796t
 specific heat, 572
 specific volume, 572
 Air-blast freezer
 direct contact system, 508, 509f
 indirect contact system, 505–506, 505f
 Alloy, thermal conductivity, 260
 Alternating current, 212
 American Society of Heating, Refrigeration, and Air Conditioning Engineers (ASHRAE), 457
 Ammonia
 diffusion coefficient, 599t
 refrigerant properties, 457, 458t, 804–806t
 Ampere, 2–3, 212
 Angle of internal friction, 174–175
 Angle of repose, 174
 Apparent specific heat, frozen food, 513, 513f
 Apparent thermal diffusivity, frozen food, 513, 514f
 Apparent viscosity, 156
 Area, see also Surface area
 equations, 818t
 overview, 59–60
 Arrhenius equation, 763
 Aseptic processing and packaging

 General Method for Process Calculation, 432–440, 435f, 435t
 systems, 409–410, 410f
 Ash
 coefficients to estimate food properties, 786t
 composition of selected foods, 785t
 ASHRAE, see American Society of Heating, Refrigeration, and Air Conditioning Engineers
 Atmosphere, 23
 Automatic expansion valve, 470, 470f
 Automatic high-pressure float valve, 469–470, 469f
 Automatic low-pressure float valve, 469, 469f

B

Ball Method, see Formula Method
 Bar, 22
 Batch-type pan evaporator, 547–548, 547f
 Bernoulli equation, 100–106
 Bingham plastic, 159
 Biot number, 340
 Blackbody radiation, 333
 Blanching, processing systems, 405–406, 406f
 Boiling point elevation, 545–547, 546f
 Boundary, system, 10, 11f
 Bourdon tube pressure sensor, 25, 25f
 Buckingham π theorem, 822, 823t
 Building materials, physical properties, 788–789t
 Bulk density, 13–15, 14t, 170–171
 Burners
 efficiencies, 209–210
 systems, 206–207, 206f

C

Cabinet drier, 660, 660f, 661f
 Candela, 3
 Cannon–Fenske viscometer, 149, 69f
 Capillary tube viscometer, 81, 148–150, 148f, 149f
 Carbohydrate
 coefficients to estimate food properties, 786t

 composition of selected foods, 785t
 Celsius scale, 21, 22
 Centrifugal pumps, 68–69, 70f, 119–120, 120f, 128–129
 Centrifugation
 basic equations, 705, 705f
 liquid–liquid separation, 707–709, 709f
 particle–gas separation, 709
 rate of separation, 705–709
 CFCs, see Chlorofluorocarbons
 Chemical equilibrium, 11–12
 Chlorofluorocarbons (CFCs), 459
 Classical thermodynamics, 41
 Closed system
 conservation of mass, 32
 energy balance
 heat transfer, 45–46
 work
 energy balance calculations, 51–55
 frictional forces, 57
 gravitational forces, 49
 moving boundary-associated work, 47–49, 47f, 48f
 shaft rotation, 50–51, 50f
 units, 46–55
 velocity change, 49–50
 overview, 10–11, 11f
 Coefficient of performance (C.O.P.), refrigeration, 481, 482–487
 Cold extrusion, 729–735, 730f
 Combustion
 mass and energy balance analysis, 207–209
 systems, 206–207, 206f
 Compressible fluids, 72
 Compressor, refrigeration, 463–466, 463f, 465f, 480
 Concentration
 calculations, 16
 expression, 35–36
 Concentration polarization, 639, 639f, 641f, 642, 644
 Condenser, refrigeration, 466–468, 467f, 468f
 Condensing pressure, refrigerant, 457
 Conductive heat transfer
 overview, 264, 265f, 266, 266f

- Conductive heat transfer (*continued*)
 - steady-state heat transfer
 - pipe, 274, 275f, 276, 276f
 - rectangular slab, 271
- Conductor, 213
- Conservation of energy, 42
- Conservation of mass
 - closed system, 32
 - open system, 30–32
 - principles, 29–32
- Constant-pressure filtration, 693–695
- Constant-rate filtration, 691–693
- Continuity equation, 81–84
- Continuous retort systems, 408, 409f
- Controlled variable, 223
- Convective heat transfer
 - overview, 267, 267f, 268, 268t
 - steady-state heat transfer
 - coefficient estimation, 285, 285f, 286f, 288f, 292, 293f
 - forced convection, 290, 290f, 292f, 294, 295, 296
 - free convection, 297, 297f, 299, 299t, 300f
 - overall heat transfer coefficient
 - estimation, 302, 302f, 304, 304f
 - thermal resistance, 301
- Convective mass transfer, 600–604, 602f
- Cooling load, refrigeration, 478–480
- C.O.P., see Coefficient of performance
- Coulomb, 4
- Crateless retort, 408
- Critical temperature, refrigerant, 457
- D**
- Darcy friction factor, 97–100, 181
- Dehydration, 653–688
 - drying processes
 - drying rate curves, 658, 658f, 659–660
 - heat and mass transfer, 658
 - moisture diffusion, 657
 - water activity, 654, 654f, 655, 655f
 - symbols, 685
 - systems
 - cabinet-type tray drier, 660, 660f, 661f
 - design
 - drying-time prediction, 670, 672–680
 - mass and energy balance, 665–669
 - fluidized-bed dryer, 663, 663f, 667–669
 - freeze-drying system, 664, 664f
 - puff-drying, 662
 - spray dryer, 663, 664f
 - tunnel dryer, 661, 661f, 662f
- Density
 - air as function of temperature, 796t
 - bulk density, 13–15, 14t, 170–171
 - frozen food, 510–511, 511f
 - ice properties as function of temperature, 782t
 - particle density, 13, 171–172
 - principles, 13–15, 72–73
 - solid density, 13, 14t
- Dew-point temperature, 574
- Diameter to avoid arching, 178
- Diffusion, see also Mass transfer
 - coefficients, 599t
 - moisture diffusion in dehydration, 657
 - process, 596–610, 597f
 - steady-state diffusion through solids, 610
 - unsteady-state mass transfer
 - diffusion of gases, 616–619
 - transient-state diffusion, 611–616, 612f
- Diffusion rate equation, 614
- Diffusivity, 598
- Dilatant liquid, 158–159
- Dimensional analysis
 - Buckingham π theorem, 822, 823t
 - overview, 822
- Dimensions, 1–2
- Direct current, 212
- Discharge head, 121, 122f
- Displacement
 - piston displacement in compressor, 464
 - volumetric, 148
- Disturbances in variables, 223
- Drag, 75, 75f
- Drift, 237
- Dry bulb temperature, air, 573
- Drying, see Dehydration
- Dühring rule, 545–547, 546f
- Dynamic viscosity, 78–79
- E**
- Elastic solid, 72
- Electric power utilization
 - circuits, 214–216, 214f, 215f
 - controls, 217–218
 - energy use by industry, 205t
 - lighting, 218–220
 - motor, 216–217
 - Ohm's law, 213–214
 - symbols, 244–245
 - terms and units, 212–213
 - tomato processing, 211f
- Electrical conductivity, foods, 366, 366f, 367t, 368
- Electricity, 212
- Electrodialysis, 625, 626f, 628t
- Emissivity, values for surfaces, 790–791t
- Energy, 43–44
- Energy balance
 - closed system
 - heat transfer, 45–46
 - work
 - energy balance calculations, 51–55
 - frictional forces, 57
 - gravitational forces, 49
 - moving boundary-associated work, 47–49, 47f, 48f
 - shaft rotation, 50–51, 50f
 - units, 46–55
 - velocity change, 49–50
 - combustion analysis, 207–209
 - expression, 45
 - open system, 55–56
 - steady flow system, 56
 - total energy balance, 56–59
- Energy use, see Electric power utilization;
- Fuel utilization
- Engineering units, see Units
- Enthalpy
 - air, 572
 - frozen foods, 511–512, 512f, 784t
 - principles, 26, 29f, 53–55
 - water vapor, 574
- Entrance region, 88–90
- Equation of state, 26–27
- Error signal, 237
- Evaporation, 543–570
 - boiling point elevation, 545–547, 546f
 - symbols, 569
 - vapor recompression
 - mechanical vapor recompression system, 566, 566f

- thermal recompression system, 565–566, 565f
- Evaporator
 - agitated thin-film evaporator, 551–554, 552f
 - batch-type pan evaporator, 547–548, 547f
 - falling-film evaporator, 549–550, 549f
 - forced-circulation evaporator, 551, 551f
 - natural circulation evaporator, 548, 548f
 - refrigeration, 461–463, 462f, 481
 - rising-film evaporator, 548, 549f
 - rising/falling-film evaporator, 550–551, 550f
 - single-effect evaporator
 - design, 554–558, 554f, 557f
 - overview, 544f
 - triple-effect evaporator
 - design, 559–564, 559f
 - overview, 544f
 - types and properties, 553t
- Expansion valve, refrigeration, 468–470, 468f, 469f, 470f
- Extrusion, 721–744
 - applications, 722
 - flow rates, 725, 726–727
 - power law models for extrudates, 724t
 - pressure equations, 727, 728, 729
 - principles, 722–729
 - symbols, 742
 - systems
 - cold extrusion, 729–735, 730f
 - components, 721–722
 - cooking process, 731–732
 - design, 735–741, 736f
 - single screw extruder, 732–734, 731f, 732f, 733f
 - twin screw extruder, 734–735, 735f
- F**
- Falling-film evaporator, 549–550, 549f
- Fanning friction factor, 96–97, 98f, 181
- Farad, 4
- Fat
 - coefficients to estimate food properties, 786t
 - composition of selected foods, 785t
- Feedback control system, 225–226, 226f, 227f
- Feedforward control system, 226–227
- fh factor, temperature prediction in transient heat transfer, 358, 360f, 361f, 362f, 363, 364, 364f
- Fiber, coefficients to estimate food properties, 786t
- Fick's law, 597, 749
- Filtration
 - mechanisms, 695–696
 - operating equations
 - constant-pressure filtration, 693–695
 - constant-rate filtration, 691–693
 - rate, 690
 - resistance, 690
 - system design, 696–698, 698f
- Fire-tube steam generator, 188–189, 188f
- First Law of Thermodynamics, 42
- First-order reaction, shelf life, 760, 761f
- Flash gas removal system, refrigeration, 491–495, 491f, 492f, 493f
- Flow, sensors, 236
- Flow measurement
 - miscellaneous techniques, 147–148
 - orifice meter, 142–145, 143f
 - overview, 136–148
 - Pitot tube, 140–142, 140f, 141f
 - variable flow meter, 146–147, 146f
 - venturi meter, 146, 146f
- Flow rate, refrigerant, 481–490
- Flue gas, energy loss, 208f, 209–210, 209t
- Fluid flow, 65–186
- Fluidized-bed dryer, 663, 663f, 667–669
- Food dehydration, see Dehydration
- Food freezing, see Freezing
- Force, units, 9
- Force balance, fluid in pipe, 100–106, 101f
- Forced-circulation evaporator, 551, 551f
- Formula Method, 440–447, 442f
- Fouling, heat transfer surfaces, 306, 307t, 308f, 310, 310f, 311f
- Freeze-drying system, 664, 664f
- Freezing, 501–542
 - freezing rate, 529
 - freezing time
 - experimental measurement, 528
 - factors affecting, 528–529
 - finite objects, 524–527, 524f, 525t, 528f
 - overview, 514–530
 - Pham equation for determination, 520–524, 521f
 - Planck's equation in
 - determination, 516–520, 516f
 - frozen food properties
 - apparent specific heat, 513, 513f
 - apparent thermal diffusivity, 513, 514f
 - density, 510–511, 511f
 - enthalpy, 511–512, 512f
 - thermal conductivity, 511, 512f
 - preservation mechanisms, 501
 - quality changes in foods, 530–534, 533f, 534t
 - symbols, 538–539
 - systems
 - direct contact systems
 - air-blast freezers, 508, 509f
 - immersion freezing system, 509–510, 509f, 510f
 - principles, 508f
 - indirect contact systems
 - air-blast freezers, 505–506, 505f
 - liquid food freezers, 506–507, 507f
 - plate freezers, 502–504, 503f, 504f
 - thawing time, 529–530
- Freezing temperature, refrigerant, 457
- Freon, 458t
- Friction
 - energy loss
 - major losses, 112
 - minor losses, 112
 - pipe fittings, 113–115, 114t
 - sudden contraction, 112–113
 - sudden expansion, 113
 - fluid flow, 96–100
 - pressure loss calculation, 97–100
- Friction factor, 96, 98f, 163–165
- Froude number, 716
- Frozen food, see Freezing
- Fuel utilization
 - burner efficiency, 209–210
 - energy use by industry, 205t
 - mass and energy balance analysis, 207–209
 - symbols, 244–245
 - systems, 206–207, 206f
- Fully developed flow, 88–95

G

GAB model, see Guggenheim–Anderson–DeBoer model
 Gas constant
 universal gas constant, 598
 water vapor, 573
 Gauge pressure, 23
 General Method for Process Calculation
 aseptic processing and packaging, 432–440, 434f, 435t, 435f
 overview, 424–440, 425f
 pasteurization, 426–429, 426f, 427f
 sterilization, 429–432, 430f, 431f
 Gibbs–Dalton law, 574
 Gravitational force, sedimentation, 699
 Guggenheim–Anderson–DeBoer (GAB) model, 654, 655

H

Head
 fluids, 24, 24f, 121
 pump head, 83–84, 124, 132f, 135f
 system head curves, 130–132, 131f
 Heat capacity rate ratio, 320
 Heat evolution rates, fresh fruits and vegetables, 782–783t
 Heat exchanger
 classification, 248f
 design
 effectiveness and number of transfer units approach
 heat capacity rate ratio, 320
 heat exchanger effectiveness, 321
 number of transfer units, 322, 322t, 323, 323t, 324f
 plate heat exchanger, 325, 329
 tubular heat exchanger, 312, 313f, 316, 318, 318f
 fouling of heat transfer surfaces, 306, 307t, 308f, 310, 310f, 311f
 plate heat exchanger, 248, 249f, 250f, 251f, 251f
 scraped-surface heat exchanger, 253, 254f
 steam-infusion heat exchanger, 255, 255f
 tube dimensions and pump power requirement calculations, 116–119, 116t
 tubular heat exchanger, 252, 252f, 253f, 254f

Heat transfer, 247
 conductive heat transfer, 264, 265f, 266, 266f
 convective heat transfer, 267, 267f, 268, 268t
 dehydration, 658
 fouling of heat transfer surfaces, 306, 307t, 308f, 310, 310f, 311f
 overview, 45–46
 overview, 264
 radiation heat transfer
 between two objects, 334, 335f, 336, 336f, 337f
 overview, 269, 270
 surface characteristics importance, 332, 332f, 333
 steady-state heat transfer
 conductive heat transfer in pipe, 274, 275f, 276, 276f
 conductive heat transfer in rectangular slab, 271
 convective heat transfer
 coefficient estimation, 285, 285f, 286f, 288f, 292, 293f
 forced convection, 290, 290f, 292f, 294, 295, 296
 free convection, 297, 297f, 299, 299t, 300f
 thermal resistance, 301
 multilayered systems
 composite cylindrical tube in series, 280, 281f, 282, 283, 284f, 377f
 composite rectangular wall in series, 277, 278f, 279
 overall heat transfer coefficient estimation, 302, 302f, 304, 304f
 principles, 270, 270f
 thermal resistance, 272, 273, 274f
 symbols, 381
 unsteady-state heat transfer
 external versus internal resistance to heat transfer, 339, 340f
 finite internal and surface resistance to heat transfer, 345, 347f, 348f, 349f
 finite objects, 348, 349f
 lumped system analysis of negligible internal resistance to heat transfer, 340, 342, 343, 343f
 negligible surface resistance to heat transfer, 348
 overview, 337, 339f

 temperature prediction with *fh* and *j* factors, 358, 360f, 361f, 362f, 363, 364, 364f
 temperature–time charts, 350, 351, 352, 355, 356f, 357f, 358f
 Henry, 4
 Henry's law, 749
 Herschel–Bulkley fluid, 159
 Herschel–Bulkley model, 159, 160t
 High-pressure float valve, 469–470, 469f
 High-quality life (HQL), frozen foods, 531
 Hollow-fiber membrane system, 648f, 649
 HQL, see High-quality life
 Humid heat, 576
 Humidity ratio, 575
 Hysteresis, 237

I

Ice, see also Freezing
 coefficients to estimate food properties, 786t
 properties as function of temperature, 782t
 Ice box, 455, 455f
 Ideal gas law, 597
 Illumination, 219
 Immersion freezing system, 509–510, 509f, 510f
 Impact pressure, 25
 Impeller
 geometric ratios, 712t
 marine-type propeller impeller, 712–713, 712f
 paddle impeller, 713–714, 713f
 power requirements, 714–718
 schematic, 711f
 viscosity and type selection, 715t
 Incompressible fluids, 72
 Individual quick freezing (IQF), 510, 510f
 Intelligent packaging
 interactive intelligent packaging, 758
 objectives, 756
 simple intelligent packaging, 757
 Interparticle porosity, 15
 IQF, see Individual quick freezing
 Isothermal system, 11

J

Jenike's flow function, 176t
 j factor, temperature prediction in
 transient heat transfer, 358, 360f, 361f,
 362f, 363, 364, 364f
 Joule, 4

K

Kelvin scale, 3, 21, 22
 Kilogram, 2
 Kinematic viscosity, 78–81
 Kinetic energy, 44, 110–111
 Kirchhoff's law, 333
 Laminar flow, 84, 84f, 87–88, 95, 291,
 604–608

L

Lamps, 218–220
 Latent heat of vaporization, refrigerant,
 456–457
 Lewis number, 603
 Lighting, 218–220
 Liquid enthalpy, refrigerant, 476
 Liquid food freezers, 506–507, 507f
 Liquid level, sensors, 234–235
 Liquid properties
 density, 72–73
 stress response, 72
 viscosity, 73–81, 74f
 Liquid transport systems, 66–71
 LMTD, see Log-mean-temperature-
 difference
 Local freezing rate, 529
 Log-mean-temperature-difference
 (LMTD), heat exchanger design, 312,
 313f, 316, 318, 318f
 Low-pressure float valve, 469, 469f
 Lumen, 4
 Lumped system, 271, 340

M

Manipulated variable, 223
 Manometer, 136–148, 136f, 138f
 Marine-type propeller impeller,
 712–713, 712f
 Mass diffusivity, 598
 Mass transfer, 595–622
 convective mass transfer, 600–604,
 602f
 dehydration, 658
 diffusion

 coefficients, 599t
 process, 596–610, 597f
 steady-state diffusion through
 solids, 599–600
 flow over spherical objects, 609–610
 laminar flow
 flat plate, 604–608
 pipe, 608
 overview, 595, 596
 packaging materials
 fixed gas permeability, 751, 752t,
 753
 permeability coefficient, 750, 750t
 steps, 749, 749f
 symbols, 621
 turbulent flow
 flat plate, 608
 pipe, 609
 unsteady-state mass transfer
 diffusion of gases, 616–619
 transient-state diffusion, 611–616,
 612f
 Material balance
 calculations, 34–40
 overview, 32–40, 33f
 Mechanical equilibrium, 11–12
 Mechanical vapor recompression system,
 566, 566f
 Membrane separation, 623–652
 concentration polarization, 639,
 639f, 641f, 642, 644
 electrodialysis, 625, 626f, 628t
 overview, 623, 623f, 624–625
 performance of membranes, 636
 reverse osmosis, 629, 629f, 630f, 631,
 633, 635t, 645
 spectrum of separation, 624f
 structure of membrane, 625f
 symbols, 650
 system types
 comparison, 645t
 hollow-fiber system, 648f, 649
 plate and frame system, 646, 646f
 spiral-wound system, 631, 647f
 tubular system, 646, 647f
 ultrafiltration membrane systems,
 637, 638, 645
 Metals, physical properties, 787–788t
 Meter, 2
 Microbial survivor curves, 413–421, 414f,
 415f, 416f, 418f
 Microwave heating

 dielectric properties, 373f
 electromagnetic frequencies, 371
 energy conversion to heat, 374
 food composition effects, 379
 frozen foods, 378, 378t
 mechanisms, 372, 373, 373f
 oven features, 377, 377f
 penetration depth, 375, 376
 shape, density, and uniform heating,
 379
 speed, 378
 Milk processing, production line, 66f
 Mixing
 impellers in agitation equipment
 geometric ratios, 712t
 marine-type propeller impeller,
 712–713, 712f
 paddle impeller, 713–714, 713f
 power requirements, 714–718
 schematic, 711f
 viscosity and type selection,
 715t
 overview, 709–718
 symbols, 719–720
 turbine agitator, 714, 714f
 Moisture content
 calculations, 18–19, 37–38
 expression, 17–19
 Moisture content, see Humidity ratio
 Molality, 16
 Molarity, 15
 Mole, 3
 Mole fraction, 15
 Montreal Protocol, 459–460
 Moody chart, 97, 98f

N

Natural circulation evaporator, 548,
 548f
 Net positive suction head (NPSH),
 126–129, 128f
 Newton, 3
 Non-Newtonian fluids, see also Power
 law liquid
 calculations, 165
 classification, 156f
 properties, 155–161
 pumping requirement computation,
 166–168
 Normal stress, 24, 72
 NPSH, see Net positive suction head
 NTU, see Number of transfer units

Number of transfer units (NTU), heat exchanger design, 322, 322t, 323, 323t, 324f
Nusselt number, 824

O

Offset, 237
Ohm, 4
Ohm's law, 213–214, 366
Ohmic heating, 369, 370
Open system
 conservation of mass, 30–32
 energy balance, 55–56
 overview, 10–11
Orifice meter, 142–145, 143f
Osmotic pressure, 631, 632, 632t, 633

P

Packaging, 745–770
 active packaging
 advanced active packaging, 755
 simple active packaging, 755
 functions
 food protection, 746, 746f
 overview, 745
 product communication, 748
 product containment, 747
 product convenience, 748
 intelligent packaging
 interactive intelligent packaging, 758
 objectives, 756
 simple intelligent packaging, 757
 mass transfer
 fixed gas permeability, 751, 752t, 753
 permeability coefficient, 750, 750t
 steps, 749, 749f
 passive packaging, 754
 shelf life
 ascorbic acid degradation
 example, 763
 first-order reaction, 760, 761f
 general rate equation, 758–759
 zero-order reaction, 759
 symbols, 767
Paddle impeller, 713–714, 713f
Particle density, 13, 171–172
Particle flow, 174–175
Particle size distribution, 172–174, 173t
Pascal, 22
Pascal-second, 77, 78
Passive packaging, 754
Pasteurization
 General Method for Process
 Calculation, 426–429, 426f, 427f
 processing systems, 404–405, 405f
 Path, process, 12, 12f
 Perfect gas law, 27
 Performance, control system, 223
 Permeability coefficient, packaging materials, 750, 750t, 752t
 Pham method, freezing time determination, 520–524, 521f
 Phase diagram, water, 27–28, 28f
 Phase equilibrium, 11–12
 PI controller, see Proportional integral controller
 PID controller, see Proportional–integral–derivative controller
 Pipe
 force balance, 100–106, 101f
 friction energy loss from fittings, 113–115, 114t
 laminar flow, 608
 pump power requirement calculations, 116–119, 116t
 steady-state heat transfer, 274, 275f, 276, 276f
 turbulent flow, 609
 Pipeline system, 67–68, 68f
 Piston displacement, compressor, 464
 Pitot tube, 140–142, 140f, 141f
 Planck's equation, freezing time determination, 516–520, 516f
 Plastic material, 72
 Plate and frame membrane system, 646, 646f
 Plate freezer, 502–504, 503f, 504f
 Plate heat exchanger
 design, 325, 329
 principles, 248, 249f, 250f, 251f
 Pneumatic valve, 231f
 Poise, 78
 Porosity, 15
 Positive displacement pumps, 70–71, 71f
 Potential energy, 44, 112
 Pouch processing
 mathematical methods for process calculation, 444–447
 systems, 409
 Powder flow, 70f, 176t, 177–178
 Power, 59
 Power factors, 213

Power law liquid
 average velocity, 163
 definition, 157–158
 friction factor, 163–165
 generalized Reynolds number, 164–165
 velocity profile, 161–162
 volumetric flow rate, 162–163
Power number, 716, 717f
Practical storage life (PSL), frozen foods, 530–531, 532–533t
Prandtl number, 603, 792–793t, 796t
Precision, 237
Preservation, 403–454, see also Dehydration, Freezing, Refrigeration
 General Method for Process
 Calculation
 aseptic processing and packaging, 432–440, 434f, 435f, 435t
 overview, 424–440, 425f
 pasteurization, 426–429, 426f, 427f
 sterilization, 429–432, 430f, 431f
 mathematical methods for process calculation
 Formula Method, 440–447, 442f
 pouch processing, 444–447
 microbial survivor curves, 413–421, 414f, 415f, 416f, 418f
 processing systems
 blanching, 405–406, 406f
 pasteurization, 404–405, 405f
 pulsed electric field processing systems, 412–413, 413f
 radiofrequency approaches, 413
 sterilization systems
 aseptic processing systems, 409–410, 410f
 batch systems, 406–408, 407f
 continuous retort systems, 408, 409f
 pouch processing systems, 409
 ultra-high pressure processing systems, 410–412, 411f
 spoilage probability, 423–424
 symbols, 450–451
 temperature and microbial survival, 418–421, 419f, 421f, 422f
 thermal death time, 422, 447
Pressure, 22–25, 23f, 72
Pressure energy, 110

- Pressure–enthalpy charts, refrigeration, 470–478, 471f, 472f, 473f, 486f, 799f
- Pressure–enthalpy tables, refrigeration, 474–475, 484
- Pressure sensors, 235–236, 235f
- Process controls
- design of control system
 - control strategy, 224–225
 - feedback control system, 225–226, 226f, 227f
 - feedforward control system, 226–227
 - final control element, 230–232, 231t
 - on-off control, 228–229, 229f
 - proportional controller, 229
 - proportional integral controller, 230
 - proportional–integral–derivative controller, 230
 - stability and modes of control functions, 227–228, 227f
 - transmission lines, 230
 - input and output signals, 224, 224f
 - manual, 221, 222f
 - overview, 220–232
 - sensors, *see* Sensors
 - symbols, 244–245
 - tomato canning, 220f
 - variables and performance indicators, 222–223
- Proportional controller, 229
- Proportional integral (PI) controller, 230
- Proportional–integral–derivative (PID) controller, 230
- Protein
- coefficients to estimate food properties, 786t
 - composition of selected foods, 785t
- Pseudoplastic liquid, 157–158
- PSL, *see* Practical storage life
- Psychrometrics, 571
- air
 - adiabatic saturation, 577, 578, 578f
 - composition, 571, 572t
 - dry bulb temperature, 573
 - enthalpy, 572
 - specific heat, 572
 - specific volume, 572
 - charts
 - air-conditioning process evaluation
 - drying, 588, 589f
 - heating or cooling, 584, 585, 585f
 - mixing of air, 586, 586f, 587, 588f
 - construction, 582, 582f, 583, 584f
 - high-temperature chart, 797f
 - low-temperature chart, 798f
 - definition, 571
 - dew-point temperature, 574
 - Gibbs–Dalton law, 574
 - humid heat, 576
 - humidity ratio, 575
 - relative humidity, 576
 - specific volume of air–water vapor mixture, 559–564
 - symbols, 592
 - water vapor
 - enthalpy, 574
 - gas constant equation, 573
 - specific heat, 573
 - specific volume, 573
 - wet bulb temperature, 579, 580, 581, 581f
 - Puff-drying, 662
 - Pulsed electric field processing systems, 412–413, 413f
 - Pump
 - affinity laws, 135–136
 - centrifugal pumps, 68–69, 70f, 119–120, 120f, 128–129
 - classification, 68–71, 69f
 - net positive suction head, 126–129, 128f
 - performance characteristics
 - calculations, 133–136
 - curves, 125–126, 126f
 - parameters, 121–125, 123f
 - positive displacement pumps, 70–71, 71f
 - power requirements, 115–119, 116t, 179
 - selection, 129–134, 131f
 - Pump head, 83–84, 124, 132f, 135f
- R**
- R-12, 800–802t
 - R-134A, 808–810t
 - R-717, *see* Ammonia
 - Radian, 4
 - Radiation
 - absorbed, 332, 332f
 - reflected, 332, 332f
 - transmitted, 332, 332f
 - Radiation heat transfer
 - between two objects, 334, 335f, 336, 336f, 337f
 - overview, 269, 270
 - surface characteristics importance, 332, 332f, 333
 - Range, 237
 - Reciprocating pump, 71
 - Refrigeration, 455–500
 - coefficient of performance, 481, 482–487
 - components of system
 - compressor, 463–466, 463f, 465f, 480
 - condenser, 466–468, 467f, 468f
 - evaporator, 461–463, 462f, 481
 - expansion valve, 468–470, 468f, 469f, 470f
 - overview, 460–470, 460f
 - cooling load, 478–480
 - multistage systems
 - flash gas removal system, 491–495, 491f, 492f, 493f
 - overview, 490–495
 - pressure–enthalpy charts, 470–478, 471f, 472f, 473f, 486f, 799f, 803f, 807f, 811f, 812f
 - pressure–enthalpy tables, 474–475, 484
 - refrigerant
 - characteristics in selection, 456–460, 458t
 - computer-aided determination of thermodynamic properties, 475–478, 479t
 - designations, 459t
 - flow rate, 481–490
 - principles, 455–456, 456f
 - properties of saturated liquid and vapor refrigerants
 - R-12, 800–802t
 - R-134A, 808–810t
 - R-717, 804–806t
 - symbols, 498
 - Relative humidity, 576
 - Repeatability, 237

- Residence time
 - evaporators, 547–548, 550
 - freezers, 503, 505
- Resistance
 - electrical, 212
 - filtration, 690, 690
- Resolution, 237
- Reverse osmosis, 629, 629f, 630f, 631, 633, 635t, 645
- Reynolds number, 84–88, 164–165, 178, 700–702, 700f, 715, 717f
- Rising/falling-film evaporator, 550–551, 550f
- Rising-film evaporator, 548, 549f
- Robustness, 223
- Rotary pump, 71
- Rotational viscometer, 150–153, 151f
- Rotor
 - motor, 217f
 - scraped-surface heat exchanger, 255
- S**
- Saturated liquid, 27, 194
- Saturated vapor, 27, 194, 243, 244
- Saturated vapor enthalpy, refrigerant, 477, 488–490
- Saturated vapor specific volume, refrigerant, 477
- Saturation pressure, 27
- Saturation temperature, refrigerant, 476
- Schmidt number, 603
- Scraped-surface heat exchanger, 253, 254f
- Second, 2
- Second Law of Thermodynamics, 42–43
- Sedimentation
 - high-concentration suspensions, 702–704
 - low-concentration suspensions, 699–702, 700f
 - symbols, 719–720
- Sensitivity, 237
- Sensors
 - data acquisition terminology, 237
 - dynamic response characteristics, 237–240, 238f
 - flow, 236
 - liquid level, 234–235
 - pressure, 235–236, 235f
 - temperature, 232–234, 232f, 233f, 233t, 234t, 235f
- Shear rate, 156f, 157f, 158f
- Shear stress
 - Newton's equation for strain relationship, 597
 - principles, 72, 77, 156f, 157f, 175f
 - Shear-thickening liquid, 158–159
 - Shear-thinning liquid, 156–157
- Shelf life
 - ascorbic acid degradation example, 763
 - first-order reaction, 760, 761f
 - general rate equation, 758–759
 - zero-order reaction, 759
- Sherwood number, 604
- Single screw extruder, 731f, 732–734, 732f, 733f
- Single-effect evaporator
 - design, 554–558, 554f, 557f
 - overview, 544f
- Single-phase electricity, 212
- SI units, see Units
- Slab
 - conductive steady-state heat transfer, 271
 - temperature of infinite slab plane, 821f
- Solid density, 13, 14t
- Solid food transport
 - granular food flow, 175–178
 - properties of granular materials and powders
 - bulk density, 170–171
 - particle density, 171–172
 - particle flow, 174–175, 176t
 - particle size and size distribution, 172–174, 173t
- Specific heat
 - air, 572, 796t
 - foods, 777t
 - ice properties as function of temperature, 782t
 - principles, 257, 259–260
 - water, 792–793t
 - water vapor, 573
- Specific volume
 - air, 572
 - air–water vapor mixture, 545–547, 559–564
 - water vapor, 573
- Spiral-wound membrane system, 631, 647f
- Spoilage probability, 423–424
- Spray dryer, 663, 664f
- Stagnation pressure, 139
- State, system, 11–13
- Static pressure, 25, 138
- Statistical thermodynamics, 41
- Stator, motor, 217f
- Steady flow
 - device, 107f
 - energy equations
 - frictional energy loss
 - major losses, 112
 - minor losses, 112
 - pipe fittings, 113–115, 114t
 - sudden contraction, 112–113
 - sudden expansion, 113
 - kinetic energy, 110–111
 - overview, 107–119
 - potential energy, 112
 - pressure energy, 110
 - pump power requirements, 115–119, 116t
- Steady-state heat transfer
 - conductive heat transfer
 - pipe, 274, 275f, 276, 276f
 - rectangular slab, 271
 - convective heat transfer
 - coefficient estimation, 285, 285f, 286f, 288f, 292, 293f
 - forced convection, 290, 290f, 292f, 294, 295, 296
 - free convection, 297, 297f, 299, 299t, 300f
 - overall heat transfer coefficient estimation, 302, 302f, 304, 304f
 - thermal resistance, 301
 - multilayered systems
 - composite cylindrical tube in series, 280, 281f, 282, 283, 284f, 377f
 - composite rectangular wall in series, 277, 278f, 279
 - principles, 270, 270f
 - thermal resistance, 272, 273, 274f
- Steam
 - generation systems, 188–190, 188f, 189f, 190f
 - heating calculations, 196–197, 202–204, 241
 - phase change thermodynamics, 190–197, 192f, 193f
 - saturated steam properties, 793–794t
 - superheated steam properties, 795t
 - transport, 200–204
- Steam-infusion heat exchanger, 255, 255f
- Steam quality, 194

Steam tables, 194–197
 Steradian, 6
 Sterilization systems
 aseptic processing systems, 409–410, 410f
 batch systems, 406–408, 407f
 continuous retort systems, 408, 409f
 General Method for Process
 Calculation, 429–432, 430f, 431f
 pouch processing systems, 409
 Stress, 72
 Subcooled liquid, 27
 Suction head, 121, 122f
 Superheated vapor, 27, 194
 Superheated vapor enthalpy, refrigerant, 477
 Superheated vapor specific volume, refrigerant, 477
 Surface area, foods, 59–60, 60t
 Symbols
 centrifugation, mixing, and sedimentation, 719–720
 dehydration, 685
 drawing symbols for engineering process equipment, 756
 evaporation, 569
 extrusion, 742
 fluid flow, 183–184
 freezing of food, 538–539
 heat transfer, 381
 mass transfer, 621
 membrane separation, 650
 packaging, 767
 preservation processes, 450–451
 psychrometrics, 592
 refrigeration, 498
 units, 60
 System
 extensive properties, 12–13
 intensive properties, 13
 overview, 10–11, 10f
 state, 11–13

T

Temperature
 infinite slab plane, 821f
 infinitely long cylinder axis, 820f
 microbial survival, 418–421, 419f, 420, 421, 421f, 422f
 principles, 20–22
 sphere geometric center, 819f
 sensors, 232–234, 232f, 233f, 233t, 234t, 235f, 238f

Temperature–time charts, transient heat transfer calculations, 350, 351, 352, 355, 356f, 357f, 358f
 Thawing time, 529–530
 Thermal conductivity, see also Conductive heat transfer
 air as function of temperature, 796t
 foods, 778–779t
 frozen food, 511, 512f
 ice properties as function of temperature, 782t
 principles, 260, 263
 water, 792–793t
 Thermal death time, 422, 447
 Thermal diffusivity
 air, 796t
 foods, 780t
 principles, 262
 water, 792–793t
 Thermal equilibrium, 11–12
 Thermal recompression system, 565–566, 565f
 Thermal resistance, 272, 273, 274f
 Thermocouple, 232–234, 232f, 233f, 233t, 234t
 Thermodynamics
 First Law of Thermodynamics, 42
 overview, 41
 phase change thermodynamics, 190–194, 192f, 193f
 Second Law of Thermodynamics, 42–43
 Zeroth Law of Thermodynamics, 21
 Thermostatic expansion valve, 470, 470f
 Three-phase electricity, 212
 Total energy, 44, 45
 Total energy balance, 56–59
 Transient heat transfer, see Unsteady-state heat transfer
 Transitional flow, 84, 84f, 87–88, 291
 Tray drier, 660, 660f, 661f
 Triple-effect evaporator
 design, 559–564, 559f
 overview, 544f
 Tubular heat exchanger
 design, 312, 313f, 316, 318, 318f
 overview, 252, 252f, 253f, 254f
 Tubular membrane system, 646, 647f
 Tunnel dryer, 661, 661f, 662f
 Turbine agitator, 714, 714f
 Turbulent flow, 84, 84f, 291, 608, 609
 Twin screw extruder, 734–735, 735f

U

Uncontrolled variable, 223
 UHP processing systems, see Ultra-high pressure processing systems
 Ultrafiltration membrane systems, 637, 638, 645
 Ultra-high pressure (UHP) processing systems, 410–412, 411f
 Units
 base units, 2–3, 3t
 capitalization rules, 772
 derived units, 3–4, 5t, 6t, 773
 English unit conversion
 factors, 774–775t, 776t
 problems, 7–8
 plural expression, 773
 prefixes, 771, 771t
 punctuation rules, 773
 supplementary units, 4–10, 6t
 Universal gas constant, 598
 Unsteady-state heat transfer
 external versus internal resistance to heat transfer, 339, 340f
 finite internal and surface resistance to heat transfer, 345, 347f, 348f, 349f
 finite objects, 348, 349f
 lumped system analysis of negligible internal resistance to heat transfer, 340, 342, 343, 343f
 negligible surface resistance to heat transfer, 348
 overview, 337, 339f
 temperature prediction with fh and j factors, 358, 360f, 361f, 362f, 363, 364, 364f
 temperature–time charts, 350, 351, 352, 355, 356f, 357f, 358f
 Unsteady-state mass transfer
 diffusion of gases, 616–619
 transient-state diffusion, 611–616, 612f

V

Vacuum, 23–24
 Vapor, see Water vapor
 Vapor pressure, refrigerant, 476
 Variable flow meter, 146–147, 146f
 Velocity profile
 fully developed flow, 90–95
 power law fluid, 161–162
 Venturi meter, 146, 146f
 Viscosity

Viscosity (*continued*)

- air as function of temperature, 796t
 - calculations, 79–81
 - foods, 781t
 - impeller type selection, 715t
 - kinematic viscosity, 78–79
 - materials at room temperature, 77t
 - measurement
 - capillary tube viscometer, 148–150, 148f, 149f
 - rotational viscometer, 150–153, 151f
 - temperature effects, 153–155
 - overview, 73–81, 74f
 - water
 - absolute viscosity, 792–793t
 - kinematic viscosity, 792–793t
- Volt, 4
- Voltage, 212
- Volume, equations, 818t
- Volumetric coefficient of expansion, air as function of temperature, 796t

W

- Water
- coefficients to estimate food properties, 786t
 - composition of selected foods, 785t
 - density as function of temperature, 73f
 - freezing diagram, 515f
 - ice properties as function of temperature, 782t
 - phase change thermodynamics, 190–196, 192f, 193f
 - phase diagram, 27–28, 28f
 - saturation pressure, 792–793t
- Water activity, 654, 654f, 655, 655f
- Water-tube steam generator, 189, 189f
- Water vapor, see also Psychrometrics, Steam
- enthalpy, 574
 - gas constant equation, 573
 - specific heat, 573
 - specific volume, 573

Watt, 4, 213

Weber, 4

Weight, units, 10

Wet bulb temperature, 579, 580, 581, 581f

Work

- energy balance calculations, 51–55
- frictional forces, 57
- gravitational forces, 49
- moving boundary-associated work, 47–49, 47f, 48f
- shaft rotation, 50–51, 50f
- units, 46–55
- velocity change, 49–50

Y

Yield stress, 159, 160–161

Z

Zero-order reaction, shelf life, 759

Zeroth Law of Thermodynamics, 21

Food Science and Technology

International Series

- Maynard A. Amerine, Rose Marie Pangborn, and Edward B. Roessler, *Principles of Sensory Evaluation of Food*. 1965.
- Martin Glicksman, *Gum Technology in the Food Industry*. 1970.
- Maynard A. Joslyn, *Methods in Food Analysis*, second edition. 1970.
- C. R. Stumbo, *Thermobacteriology in Food Processing*, second edition. 1973.
- Aaron M. Altschul (ed.), *New Protein Foods*: Volume 1, *Technology, Part A*—1974. Volume 2, *Technology, Part B*—1976. Volume 3, *Animal Protein Supplies, Part A*—1978. Volume 4, *Animal Protein Supplies, Part B*—1981. Volume 5, *Seed Storage Proteins*—1985.
- S. A. Goldblith, L. Rey, and W. W. Rothmayr, *Freeze Drying and Advanced Food Technology*. 1975.
- R. B. Duckworth (ed.), *Water Relations of Food*. 1975.
- John A. Troller and J. H. B. Christian, *Water Activity and Food*. 1978.
- A. E. Bender, *Food Processing and Nutrition*. 1978.
- D. R. Osborne and P. Voegt, *The Analysis of Nutrients in Foods*. 1978.
- Marcel Loncin and R. L. Merson, *Food Engineering: Principles and Selected Applications*. 1979.
- J. G. Vaughan (ed.), *Food Microscopy*. 1979.
- J. R. A. Pollock (ed.), *Brewing Science*, Volume 1—1979. Volume 2—1980. Volume 3—1987.
- J. Christopher Bauernfeind (ed.), *Carotenoids as Colorants and Vitamin A Precursors: Technological and Nutritional Applications*. 1981.
- Pericles Markakis (ed.), *Anthocyanins as Food Colors*. 1982.
- George F. Stewart and Maynard A. Amerine (eds), *Introduction to Food Science and Technology*, second edition. 1982.
- Hector A. Iglesias and Jorge Chirife, *Handbook of Food Isotherms: Water Sorption Parameters for Food and Food Components*. 1982.
- Colin Dennis (ed.), *Post-Harvest Pathology of Fruits and Vegetables*. 1983.
- P. J. Barnes (ed.), *Lipids in Cereal Technology*. 1983.
- David Pimentel and Carl W. Hall (eds), *Food and Energy Resources*. 1984.

- Joe M. Regenstein and Carrie E. Regenstein, *Food Protein Chemistry: An Introduction for Food Scientists*. 1984.
- Maximo C. Gacula, Jr. and Jagbir Singh, *Statistical Methods in Food and Consumer Research*. 1984.
- Fergus M. Clydesdale and Kathryn L. Wiemer (eds), *Iron Fortification of Foods*. 1985.
- Robert V. Decareau, *Microwaves in the Food Processing Industry*. 1985.
- S. M. Herschdoerfer (ed.), *Quality Control in the Food Industry*, second edition. Volume 1—1985. Volume 2—1985. Volume 3—1986. Volume 4—1987.
- F. E. Cunningham and N. A. Cox (eds), *Microbiology of Poultry Meat Products*. 1987.
- Walter M. Urbain, *Food Irradiation*. 1986.
- Peter J. Bechtel, *Muscle as Food*. 1986. H. W.-S. Chan, *Autoxidation of Unsaturated Lipids*. 1986.
- Chester O. McCorkle, Jr., *Economics of Food Processing in the United States*. 1987.
- Jethro Japtiani, Harvey T. Chan, Jr., and William S. Sakai, *Tropical Fruit Processing*. 1987.
- J. Solms, D. A. Booth, R. M. Dangborn, and O. Raunhardt, *Food Acceptance and Nutrition*. 1987.
- R. Macrae, *HPLC in Food Analysis*, second edition. 1988.
- A. M. Pearson and R. B. Young, *Muscle and Meat Biochemistry*. 1989.
- Marjorie P. Penfield and Ada Marie Campbell, *Experimental Food Science*, third edition. 1990.
- Leroy C. Blankenship, *Colonization Control of Human Bacterial Enteropathogens in Poultry*. 1991.
- Yeshajahu Pomeranz, *Functional Properties of Food Components*, second edition. 1991.
- Reginald H. Walter, *The Chemistry and Technology of Pectin*. 1991.
- Herbert Stone and Joel L. Sidel, *Sensory Evaluation Practices*, second edition. 1993.
- Robert L. Shewfelt and Stanley E. Prussia, *Postharvest Handling: A Systems Approach*. 1993.
- Tilak Nagodawithana and Gerald Reed, *Enzymes in Food Processing*, third edition. 1993.
- Dallas G. Hoover and Larry R. Steenson, *Bacteriocins*. 1993.
- Takayaki Shibamoto and Leonard Bjeldanes, *Introduction to Food Toxicology*. 1993.
- John A. Troller, *Sanitation in Food Processing*, second edition. 1993.
- Harold D. Hafs and Robert G. Zimbelman, *Low-fat Meats*. 1994.

- Lance G. Phillips, Dana M. Whitehead, and John Kinsella, *Structure-Function Properties of Food Proteins*. 1994.
- Robert G. Jensen, *Handbook of Milk Composition*. 1995.
- Yrjö H. Roos, *Phase Transitions in Foods*. 1995.
- Reginald H. Walter, *Polysaccharide Dispersions*. 1997.
- Gustavo V. Barbosa-Cánovas, M. Marcela Góngora-Nieto, Usha R. Pothakamury, and Barry G. Swanson, *Preservation of Foods with Pulsed Electric Fields*. 1999.
- Ronald S. Jackson, *Wine Tasting: A Professional Handbook*. 2002.
- Malcolm C. Bourne, *Food Texture and Viscosity: Concept and Measurement*, second edition. 2002.
- Benjamin Caballero and Barry M. Popkin (eds), *The Nutrition Transition: Diet and Disease in the Developing World*. 2002.
- Dean O. Cliver and Hans P. Riemann (eds), *Foodborne Diseases*, second edition. 2002.
- Martin Kohlmeier, *Nutrient Metabolism*, 2003.
- Herbert Stone and Joel L. Sidel, *Sensory Evaluation Practices*, third edition. 2004.
- Jung H. Han, *Innovations in Food Packaging*. 2005.
- Da-Wen Sun, *Emerging Technologies for Food Processing*. 2005.
- Hans Riemann and Dean Cliver (eds) *Foodborne Infections and Intoxications*, third edition. 2006.
- Ioannis S. Arvanitoyannis, *Waste Management for the Food Industries*. 2008.
- Ronald S. Jackson, *Wine Science: Principles and Applications*, third edition. 2008.
- Da-Wen Sun, *Computer Vision Technology for Food Quality Evaluation*. 2008.
- Kenneth David and Paul Thompson, *What Can Nanotechnology Learn From Biotechnology?* 2008.
- Elke K. Arendt and Fabio Dal Bello, *Gluten-Free Cereal Products and Beverages*. 2008.
- Debasis Bagchi, *Nutraceutical and Functional Food Regulations in the United States and Around the World*, 2008.
- R. Paul Singh and Dennis R. Heldman, *Introduction to Food Engineering*, fourth edition. 2008.
- Zeki Berk, *Food Process Engineering and Technology*. 2009.
- Abby Thompson, Mike Boland and Harjinder Singh, *Milk Proteins: From Expression to Food*. 2009.
- Wojciech J. Florkowski, Stanley E. Prussia, Robert L. Shewfelt and Bernhard Brueckner (eds) *Postharvest Handling*, second edition. 2009.